The University of Nottingham

UNITED KINGDOM · CHINA · MALAYSIA

BEHAVIOUR OF FIBRE REINFORCED CEMENTED SAND AT HIGH PRESSURES

by

SALAH-UD-DIN, M. Eng.

Thesis submitted to The University of Nottingham
for the degree of Doctor of Philosophy
Department of Civil Engineering
January, 2012

ABSTRACT

Several well established techniques of soil stabilisation and soil reinforcement are available to improve properties of geotechnical materials. However, the addition of fibre into soils has its unique potential as a reinforcing agent. This is because a friction between fibre and soil particles increases the bonding between the particles of soils and this can improve the plasticity, stress-strain behaviour and failure characteristics of both cemented and uncemented soils. It also reduces the brittleness of the cemented sand. Numerous experiments on fibre-reinforced granular materials have been carried out by several researchers. However, the behaviour of fibre-reinforced cemented granular soils has not been fully understood yet. Furthermore, most experimental studies of fibre reinforced cemented materials have been carried out at relatively low confining pressures. As a result, more experiments are still needed to understand complicated behaviour of soil-cement-fibre composite materials. The main objective of this thesis is to analyse the behaviour of fibre reinforced cemented sand under wide range of confining pressures.

For this GDS high pressure triaxial cell apparatus and Bishop and Wesley conventional triaxial cell apparatus have been used to carry out the tests at wide range of confining pressures from 50kPa to 20MPa. Drained and undrained tests have been carried out on polypropylene fibre reinforced sand with and without the addition of cement. Samples with varying fibre and cement content were prepared by the method of undercompaction and were cured for 28 days prior to testing.

The experimental results indicate that there is a significant effect from the addition of fibre and/or cement contents and confining pressures on the mechanical behaviour of Portaway sand. Particularly, these effects were noted in drained and undrained triaxial tests, particularly peak strength, strength parameters, shear banding, particle crushing, yielding, and stress-dilatancy relationships. The addition of fibres increases the peak, yield, and ultimate strengths. Increase in confining pressure also increases the strength but the individual effect of the addition of fibres was more pronounced at low confining pressures. Progressive suppression in the dilation by the gradual increase in confining pressures as well as an increase in dilation with the addition of fibres during triaxial compression was also worth noticeable. Although, no noticeable affect was observed in isotropic compression due to the addition of fibre in both cemented and uncemented sand. An extensive series of tests were carried out but due to time constraint only one type and length of fibre was used. Therefore, more research needs to be carried out at different fibre lengths and types in order to see that whether these change the behaviour observed in this research.

ACKNOWLEDGEMENTS

I would like to express my greatest gratitude and appreciation to my supervisor, Dr. Dariusz Wanatowski, for his valuable guidance, support, and assistance during the course of my present research work. Without his encouragement and guidance throughout the length of this research, its completion would not have been possible. I am also thankful to my second supervisor, Dr. Matthew Hall for his help and guidance.

I would like to thank Ian Richardson for his assistance on matters relating to laboratory experimentation. Thanks are also due to Dr. Amanullah Marri, for providing me the data for comparison and his presence here really helped me and provided the impetus for this research.

I would also like to show appreciation to the financial support of Balochistan University of Engineering and Technology, Khuzdar. Special thanks to my mother, I can feel how difficult this whole time would have been for her in my absence. Lots of love to my wife and children who stood with me in all the difficult time in Nottingham. Finally, I would like to dedicate this thesis to my late father.

CONTENTS

LIST OF FIGURES

LIST OF TABLES

NOMENCLATURE

D_r = Relative density = $(e_{max}-e_{min})/(e_{max}-e)$

e_0 = Initial void ratio

e_c = Void ratio at the end of consolidation

e_{cr} = Critical state void ratio

e_{max} = Maximum void ratio

e_{min} = Minimum void ratio

E = Young's modulus

I_B = Brittleness index = q_f/q_u-1

p' = Cambridge mean effective stress = $(\sigma'_1+2\sigma'_3)/3$

q = Deviator stress= $\sigma_1-\sigma_3$

p'_f = Cambridge mean effective stress at failure/peak

q_f = Deviator stress at failure/peak

q_y = Deviator stress at primary yield point

q_u = Unconfined compressive strength

ν = Poisson's ratio

ε_a = Axial strain

ε_r = Radial strain

ε_v = Volumetric strain

ε_q = ε_s = Deviator/shear strain = $2/3(\varepsilon_a+\varepsilon_r)$

σ_1 = Major principal stress

σ_3 = Minor principal stress

ϕ_f = Peak/failure friction angle

ϕ_{cr} = Critical friction angle

ψ = Dilatancy angle

λ = Gradient of normal compression line

γ_d = Dry unit weight

γ = Bulk unit weight

Δu = Excess pore water pressure

l_c = Critical length of fibre

G_s = Specific gravity

C =Cement content

F =Fibre content

M =Effective stress ratio at critical state

Γ =Specific volume of critical state at which p' is unit

λ =slope of critical state line in v-ln(p') space

D =Dilatancy= $-\varepsilon_v/\varepsilon_q$

ACRONYMS

CD =Isotropically consolidated drained test

CU = Isotropically consolidated undrained test

CSL = Critical state line

DPVC = Digital pressure volume controller

FL = Failure state line

IC = isotropic compression/consolidation

GDS = Global Digital Systems Ltd.

LVDT = Linear variable differential transformer

NCL = Normal compression line

RDFS = Randomly distributed fibre in soil

SEM = Scanning electron microscope

UCS = Unconfined compressive strength

SS = Steady state

VIS = Virtual infinite stiffness

CP = Confining pressure

PT = Phase transformation

CHAPTER 1

INTRODUCTION

1.1 Background

Different techniques such as cementation, grouting, compaction, fibre reinforcement etc. have been used to improve soil capability against deformation. Fibre reinforcement of soil has been an interesting and innovative area of modern soil reinforcing techniques and is becoming a viable soil improvement method for geotechnical engineering problems (Chen, 2008).

Due to the constructions of massive structures and the excessive land utilization, some areas, which are not considered feasible for any safe engineering constructions, become dynamic zones for engineering development to fulfil the needs of growing population in terms of multi-story buildings for accommodation, commercial and recreational purposes. Construction of buildings and other civil engineering structures on weak soil is highly risky because such a soil is susceptible to excessive settlements due to its poor shear strength and high compressibility. There are also some advantages in using randomly distributed fibres as these are added and mixed randomly in much the same way as cement or other additives, also randomly distributed fibres limit potentials planes of weakness that can develop parallel to oriented reinforcement.

Although several researchers have worked on fibre reinforced materials, a review of literature reveals that there are important areas which have not been addressed in detail, for instance compressibility, dilatancy, and critical state of fibre reinforced cemented and uncemented sand. There is also very limited information available on fibre reinforced cemented sand for varying fibre/cement contents and confining pressures. The Confining pressure in most of the reported work has been limited within the range of 20-600kPa (Consoli et al., 1998, Prabakar and Sridhar, 2002, Li and Ding, 2002, Consoli et al., 2002, Michalowski and Cermak, 2003, Consoli et al., 2003a, Mofiz et al., 2004, Latha and Murthy, 2007, Michalowski, 2008).

However, under massive structures, the confining pressure is significantly above the conventional pressures. Normally pressures of the buildings reach 500-1000kPa, and occasionally much more. For instance, the design load of the Santiago Calatrava tower reached 32MPa (Ukhov, 2003). Therefore, it becomes imperative to consider the ground improvement techniques at a wide range of confining pressures.

The stress-strain analysis reveals that there is significant difference of the soil response at a wide range of confining pressures. For example dense and cemented materials have the tendency for dilation during shear at conventional pressures. However, at high pressures they become purely compressive in nature. This example gives a clear message that soil behaviour at conventional and high pressures may be different.

It is quite interesting to find out how fibre reinforcement in cemented soil behaves at a wide range of confining pressures with the ultimate effect on the mechanical

behaviour of soil. For example looking at Figure 1.1, it can be seen that there is trend of decrease in the effect of fibre content on the strength of composite. Whether these responses continue or disappear at further high pressures still needs to be investigated.

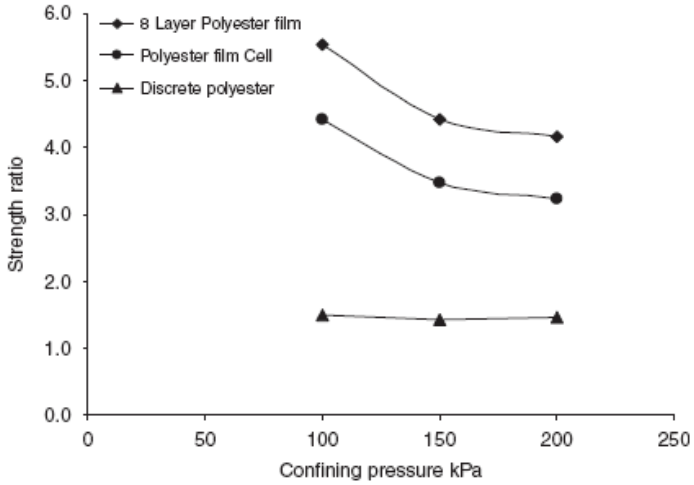

Figure 1.1 Variation of strength ratio with confining pressure for sand reinforced with different forms of polyester film (after Latha and Murthy, 2007).

1.2 Objective

The objective of this study was to investigate the mechanics of fibre reinforced cemented and uncemented Portaway sand at a wide range of confining pressures to give a reasonable qualitative assessment of the effect of cement and fibre content on the compressibility, stress strain, stress-dilatancy, yielding and critical state behaviour of sand.

As a result, the motivations behind this study were as follows:

1) To evaluate and extend the capabilities of the triaxial systems at the University of Nottingham to include the testing of fibre reinforced cemented and uncemented sand.

2) To gain better understanding and broaden the chain of previous studies on Portaway sand by incorporating the effect of fibre content.
3) To investigate experimentally the effect of a wide range of confining pressures on fibre reinforced cemented materials with varying degrees of fibre and cement contents and densities.
4) To compare, validate and bridge the gap in the literature by the incorporating varying fibre and cement content on the isotropic compression behaviour.
5) To compare and validate the existing reported work on general stress strain behaviour of fibre reinforced cemented and uncemented sand and to extend the findings for increasing range of confining pressures.
6) To explore the stress dilatancy behaviour of fibre reinforced cemented materials at varying fibre and cement contents as well as on low to high confining pressures.
7) To investigate the effect of addition of fibre, cement at wide range of confining pressures on deformation, yielding and failure modes.

1.3 Scope

This study presents a review of laboratory testing of Portaway sand reinforced with fibre and/or cement. Despite a significant progress in the high-pressure triaxial testing and incorporation of investigating the mechanical behaviour of fibre reinforced cemented materials, there were certain limitations of this study, such as:

1) The triaxial cell of a high-pressure triaxial system is made of non-transparent steel; therefore, the specimens cannot be seen inside the cell. Therefore,

the real-time analysis of the specimens during different stages of shearing could not be undertaken.

2) There were no LVDTs installed for local strain measurements; therefore, the stress-strain measurements were made through internal load cell and displacement transducers. Moreover, the load cell capacity limit was 100kN, therefore, the tests were only run within this loading range.
3) The isotropic compression tests were run up to the confining pressure of 50MPa. However, the drained and undrained shearing tests were limited up to 20MPa of effective confining pressure, to avoid exceeding the maximum load cell capacity.
4) Due to the time constraints, the scope of the work was limited to one type and length of fibre (i.e., Polypropylene fibre) and therefore, the effects of different types of fibre were not investigated.

1.4 Thesis structure

The thesis is organized as follows:

Chapter 1 gives the background, objectives, scope, limitations, and motivations of the research.

Chapter 2 provides an overview of the literature on behaviour of sand reinforced with fibre and cement and its effects on isotropic compression behaviour, stress dilatancy, yielding and critical state in high pressure triaxial testing, and review of the existing related work on the mechanical behaviour of cemented materials.

Chapter 3 discusses the methodology. It describes the materials and index properties, sample preparation, test setup, testing procedures, high-pressure triaxial

testing. It also describes the microstructure of uncemented and cemented fibre reinforced sands, as well as the consistency and homogeneity of the sand-cement-fibre mix.

Chapter 4 discusses the isotropic compression characteristics of cemented and uncemented fibre reinforced sands. The effect of the initial relative density, cement content, and confining pressures were investigated over the cement bond breakage, particle crushing during compression and the microstructure of the material after compression.

Chapter 5 explores the drained and undrained behaviour of fibre reinforced cemented sand. The effect of the addition of fibre content, cement content and confining pressure on the stress-strain behaviour, volumetric strain-axial strain, and a comparison of the drained and undrained response were investigated.

Chapter 6 is focused on the stress-dilatancy relation of fibre reinforced cemented materials. Inclusion of fibre and cement into stress-dilatancy, volumetric dilation, and progressive suppression of dilation by the gradual increase in confining pressure were studied.

Chapter 7 is about strength characteristics of fibre reinforced cemented sand behaviour. Yielding, pre-failure deformation, and critical state mechanism of the material were addressed. Stiffness degradation and problems in identifying critical state parameters for cemented sand at high pressures were mainly focused.

Chapter 8 draws the conclusions of the research work, potential applications, and future recommendations.

CHAPTER 2

LITERATURE REVIEW

2.1 Introduction

Different reinforcements e.g. cement, geotextiles, fibres etc. can be used to increase bearing capacity, shear strength of soil and to sustain the loads applied. Fibre reinforcement has its unique advantages. For instance, friction between fibre and soil particles increases the bonding between the particles of soils and this can improve the plasticity, failure stress, failure strain, the peak and ultimate strength of both cemented and uncemented soils. Fibres reduce the brittleness of the cemented sand, whereas, the initial stiffness is not appreciably changed by the inclusion of fibres (Consoli et al., 1998). Fibre reinforcement is cost effective, easy in adaptability and reproducibility (Prabakar and Sridhar, 2002). In general fibres are resistant to tensile failure, cracking and are characterized by remarkable improvement in ductility.

Different fibre reinforcement can be used in lieu of the failure mechanism in the soil. Fibres can be broadly classified as natural fibres and synthetic fibres. Synthetic fibres are generally preferred than the natural fibres because of their properties. For example polypropylenes are resistant to acids, alkaline and chemicals. They have high tensile strength and also have high melting point. Glass, carbon fibres have also found to be resistant to alkalis and other chemical hazards. Fibre orientation also affects the response, as randomly oriented fibres improve strength

by friction and coiling around the soil particles. Fibres are most influential when orientated in the same direction as tensile strains for any particular loading condition.

This literature review focuses on the behaviour of fibre reinforced cemented sand over a wide range of confining pressures, varying fibre and cement contents. The review covers isotropic compression behaviour, general stress-strain behaviour, stress dilatancy, critical/ultimate state behaviour, yielding and failure mechanisms.

2.1.1 Reinforcement by cement

Cemented soils can be found naturally, or induced artificially for the purpose of improving the bearing capacity of weak soils. Cementation plays a significant role in the engineering behaviour of soils, and has been investigated extensively around the world. The beneficial effects of cement treatment on the performance of a broad range of soils have been widely documented.

Cement stabilization is a quick process and can be used for stabilization of a wide range of soils. Cement addition has showed significant improvement in workability, unconfined compressive strength and shear strength of soils (Sariosseiri and Muhunthan, 2009). Abdulla and Kiousis, (1997) reported that increase of cement content results in a stronger, stiffer and more brittle material whereas increase of confining pressure reduces the softening tendencies, and generally results in a more ductile response. Increasing confining pressures cause a more ductile shear deformation, with larger initial volumetric compression and reduced ultimate dilation rate. Abdulla and Kiousis, (1997) concluded that most of the experimental

reports agree that an increase of cement content results in increase of cohesion. However, there is no general agreement regarding the effects of cement content on the peak friction angle. The post-peak behaviour of cemented sand is in general characterized by some softening which is diminished as the confinement pressure increases. Saxena and Lastrico, (1978) suggested that at low axial strains (<1%), the cohesion caused by the cement bonding between particles is the major component of the strength. The cohesive shear strength vanishes around 1% strain and at the same time the frictional strength becomes dominant. They reported that a very high confining stress could break the cementation bonds as well. For the cemented sand larger stresses are necessary to yield the cementitious bonds between the particles (dos Santos et al., 2010a). Lee et al., (2010) reported distinctive yielding for cemented sand due to the damage of cementation bondage, while only a monotonic increase in the deformation without yielding for uncemented sand. For cemented sand, yield is approached when the bond created by the cementing agent gradually breaks, after which the stresses will be carried by the new destructed (uncemented) matrix of the host grains and broken cement (Coop and Atkinson, 1993, Hamidi and Haeri, 2008). Marri, (2010) reported that no detailed investigations have been carried out to determine the yield locus of cemented granular materials at high pressures.

Sariosseiri and Muhunthan, (2009) reported that addition of cement improves shear strength however the type of failure varied greatly. Uncemented, 5% and 10% cement treated soils displayed ductile, planar, and splitting type of failure, respectively. Cement content, confining pressure, initial density, moisture content etc. are the key parameters dictating the strength of cemented sand. The affect of

addition of cement on sand and fibre reinforced sand and its effects on the parameter studied in this research are being reviewed.

2.1.2 Reinforcement by fibre

Fibre inclusions within a soil mass can provide a reinforcement function by developing tensile forces which contribute to the stability of the soil-fibres composite (a reinforced soil structure). The use of inclusions to improve the mechanical properties of soils dates to ancient times. However, it is only within the last quarter of century or so (Vidal, 1969) that analytical and experimental studies have led to the current soil reinforcement techniques. Soil reinforcement is now a highly attractive technique and its acceptance has also been triggered by a number of factors, which include aesthetics, reliability, simple construction techniques, good seismic performance, and the ability to tolerate large deformations without structural distress. Reinforcement can vary greatly according to form; strips, sheets, grids, bars or fibres, by texture; rough or smooth and relative stiffness; high stiffness as steel or low as polymeric fibrics (Gray and Ohashi, 1983). Fibres can also be differentiated by ideally inextensible for example high modulus metal strips and bars or ideally extensible inclusions such as natural and synthetic fibres. The reinforced soil in the former case was termed as reinforced earth while the later as plysoil (Gray and Ohashi, 1983). Fibres are also commonly differentiated as natural fibres e.g. coconut fibre, sisal fibre, jute fibre, cotton fibre etc. and synthetic fibre e.g. polypropylene fibre, nylon fibre, polyester fibre, rubber fibre, plastic glass etc.

Fibre reinofrced sand has often been investigated experimentally and theoritically in literature e.g.(Consoli et al., 1998, Prabakar and Sridhar, 2002, Consoli et al.,

2002, Consoli et al., 2003a, Michalowski and Cermak, 2003, Mofiz et al., 2004, Latha and Murthy, 2007, Michalowski, 2008, Consoli et al., 2009a, Consoli et al., 2010, Dos Santos et al., 2010a).

Swami, (2005) reported that there is a maximum limit of fibre content (usually 2%-3%) in soil beyond which mixing of fibres in soil becomes very difficult. The laboratory studies on fibre reinforced sand were mostly done by using the following tests:

1) Triaxial test: (Gray and Alrefeai, 1986, Maher and Gray, 1990, Maher and Ho, 1993, Michalowski and Zhao, 1996, Consoli et al., 1998, Consoli et al., 2004, Consoli et al., 2005a, Consoli et al., 2009c, Consoli et al., 2010, Dos Santos et al., 2010a).
2) Unconfined compression test: (Frietag, 1986, Maher and Ho, 1994, Santoni et al., 2002, Kumar and Tabor, 2003).
3) Direct shear test: (Gray and Ohashi, 1983, Fatani et al., 1991, Bauer and Fatani, 1991, Ibraim and Fourmont, 2006).
4) Tensile test: (Setty and Rao, 1987, Ranjan et al., 1996, Consoli, 2002 etc.
5) Flexural test: Maher and Ho (1994).

Consoli et al., (2005a) reported that isotropic compression behaviour of sand changes by the random insertion of fibres as two distinct and parallel normal compression lines can be seen for the fibre reinforced and nonreinforced sand. For the fibre reinforced sample, the fibres after testing were found to have been both extended and broken, indicating that the fibres act in tension even when the sample is undergoing large compressive volumetric strains and that the fibres suffer

large plastic tensile deformations before breaking. Consoli et al., (2009a) reported that dilatancy is kept practically unchanged with the introduction of fibres in the sand. However, the stress ratio (q/p') is reduced with increasing confining stress.

2.1.3 Reinforcement by fibre and cement

Combined usage of fibre and cement has also gained importance as use of cement alone results in the material being brittle. However, with the addition of fibre this problem can be avoided.

The addition of cement increases the shear strength and stiffness of fibre reinforced sand and also amplifies the effect of fibre on residual strength (Consoli et al., 1998) as shown in Figure 2.1.

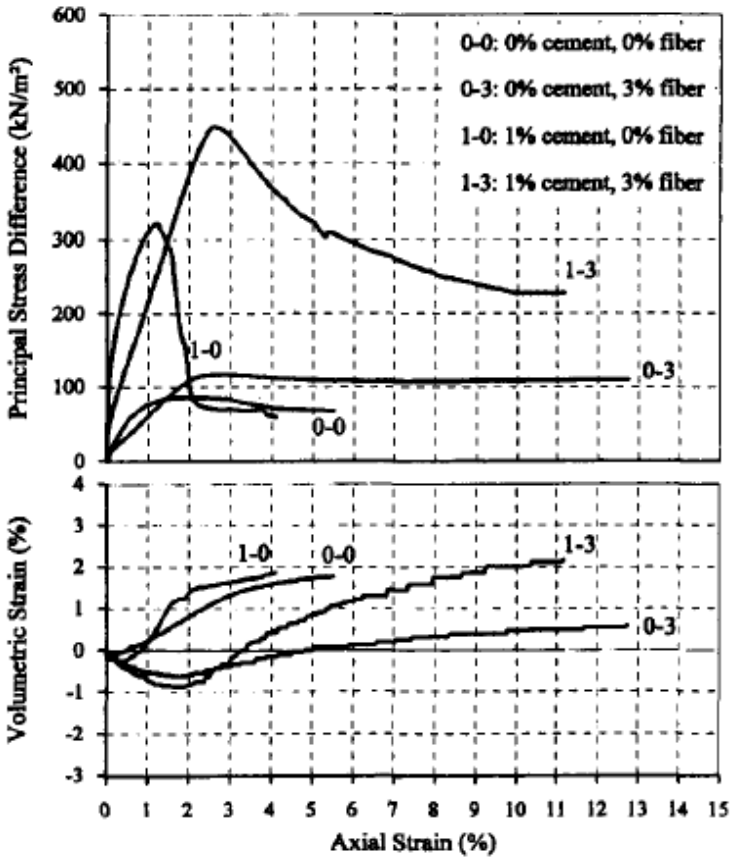

Figure 2.1 Stress-strain-volumetric response for fibre-reinforced and non reinforced soils at confining pressure of 20kPa (after Consoli et al. 1998).

Kaniraj and Havanagi, (2001) investigated the behaviour of cement stabilized fibre reinforced fly ash-soil mixtures and concluded that fibre inclusions increase the strength of the raw fly ash-soil specimens as well as that of the cement-stabilized specimens and change their brittle behaviour to ductile behaviour. Depending on the type of fly ash-soil mixture and curing period, the increase in strength caused by the combined action of cement and fibres is either more than or nearly equal to the sum of the increase caused by them individually. Consoli et al., (2002) verified the affects of fibres of different nature, length and percentage, as well as the influence of cement content and confining pressures up to 100kPa by carrying out drained triaxial tests. They showed that the peak strength, initial stiffness and brittleness are strongly increased with increase in cement content. Inclusion of fibre has also increased the peak strength and ultimate strength. Tang et al., (2007) have studied the effect of fibre and cement inclusion, effect of interfacial interaction and effect of fibre content by unconfined compression tests and direct shear tests and have concluded that the combination of discrete fibre and cement has the virtues of both fibre reinforced soil and cement-stabilized soil. Therefore the addition of fibre-cement to soil can be considered as an efficient method for soil reinforcement.

2.1.4 Overview of previous published literature

The detailed review of literature is presented in following section regarding the parameters and materials studied. However, an overview of the previous reported literature is presented in Table 2.1

Table 2.1 Past researches on fibre reinforced soil

Author	Fibre type	Fibre length(mm)	Cement	Fibre	Pressure
Maher and Ho (1993)	Chopped glass fibre	0.75in	4wt%	Up to 3%	Up to 300kPa
Michalowski and Zhao (1996)	Galvanized or stainless tell and polyamide monofilament	25mm		Up to 1.25% by Volume	Up to 600 kPa
Consoli et al (1998)	Chopped Fibreglass	12.8mm	1 wt%. of soil	0% & 3%	Up to 100 kPa
Consoli et al (2002)	Plastic waste (Chopped PET)	12, 24, 36 mm long	0- 7wt%	Up to 0.9 wt%	Up to 100 kPa
Prabakar & Sridhar (2002)	Sisal fibre	10,15, 20 & 25mm	---	0.25%- 1%	---
Li and Ding (2002)	Geofibre	Not Given	Nil	0, 0.2 and 0.5%	Up to 150 kPa
Consoli et al. (2003)	Polypropylene	24 mm	7%	0.5%	Up to 200 kPa
Michalowski & Cermark (2003)	polyamide monofilament, steel galvanized wire and polypropylene fibrillated fibres	25.4 mm	Nil	Up to 2% by Volume	up to 600kPa
Mofiz et al (2004)	Fabric	300 ×200 mm	---	---	Shear Box
Consoli et al. (2004)	Polyester, polypropylene and glass fibres	12 &36mm (polyester; polypropylene) and 6.4,25.4mm (glass)	0 & 7%	0 & 0.5%	Up to 100kPa
Consoli et al. (2005)	Polypropylene	24 mm long	--	0.5%	Isotropic Compression up to 50MPa
Park and Tan (2005)	Short polypropylene fibre	60 mm	Nil	0.2% by weight of the soil	
Cai et al (2006)	Polypropylene	12 mm	0-8% Lime Content	0 to 0.2wt% of Soil	Upto 300KPa
Zhang et al (2006)	Plastic Sheet & Galvanized Iron Sheet	3D	--	---	
Cheng-Wei Cheng (2006)	Fibrillated polypropylene fibres	50 mm	--	0.4%	Upto 414kPa
Consoli et al. (2007)	Polypropylene fibres	24mm	Nil	0.5wt%	20-680 kPa

Table 2.1 Past researches on Fibre Reinforced Soil

Author	Fibre type	Fibre length (mm)	Cement	Fibre	Pressure
Latha & Murthy (2007)	Polyster Film	11mm long & 2mm wide	Nil	Quantity in terms of area is 9073mm^2	Up to 200 kPa
Concoli et al (2007)	Polypropylene fibres	6, 12 or 24 mm length and 0.023 mm diameter,	Nil	Up to 30%	Ring shear Test
Rimouldi and Intra (2008)	Calcium stabilization, geogrid reinforcement	---	---	---	
Consoli et al. (2009a)	Polypropylene fibres	24mm long & 0.023mm dia	0-10wt%.	0% & 0.5 %	Upto 100 kPa
Consoli et al. (2009b)	Polypropylene fibres	12,24,36 & 50mm	Nil	0.5%	550 kPa
Consoli et al. (2009c)	Polypropylene fibres	24mm & 0.023mm diameter	0% to 10%	0.5%	Upto 100 kPa
Dos Santos et al. (2010a)	Polypropylene fibres	24mm & 0.023mm diameter	3%	0.5%	Direct shear tests
Dos Santos et al. (2010b)	Polypropylene fibres	24mm & 0.023mm diameter	Nil	0.5%	Upto 7MPa

2.2 Effect of reinforcement on isotropic compression of sand

When the soil is loaded isotropically or anisotropically, a decrease in its volume takes place. The decrease in the volume of a soil mass under stress is known as compression and the property of the soil mass pertaining to its tendency to decrease in volume under pressure is known as compressibility. In a saturated soil mass decrease in volume or compression can take place when water is expelled out of the voids.

Sand under isotropic compression loading is relatively incompressible at low stress and large volume changes can only occur at high stress level (Sheng et al., 2008).

Mesri and Vardhanabhuti, (2009) reported that particle rearrangement into a more compact configuration is achieved by overcoming interparticle friction through interparticle slip and rotation. In granular soils, particle rearrangement is also facilitated by overcoming particle strength through particle damage. Particle damage may be quantified as level 1 damage (abrasion or grinding of particle surface asperities), level 2 damage (breaking or crushing of particle surface protrusions and sharp particle corners and edges), and level 3 damage (fracturing, splitting, or shattering of particles). During compression of granular materials, both unlocking and locking mechanisms operate simultaneously. The net effect determines the shape of the void ratio or volumetric strain versus effective stress relationship. Bopp and Lade, (2005) reported that the materials with different initial void ratios consolidated at high pressures eventually converge to a unique void ratio as shown in Figure 2.2.

Wood, (1990) reported that large volumetric strains can occur during isotropic compression as a result of the collapse of the arrays of particles. Each such collapse causes rolling and sliding between particles and as a result tangential forces average out to zero over a surface passed through many contact points. Thus the shear forces exist at individual contacts. Smith, (1990) reported that compression curves obtained from isotropic compression in a triaxial cell are more or less the same as those obtained from one-dimensional consolidation in an oedometer. Similar conclusion was made by (Atkinson, 2007).

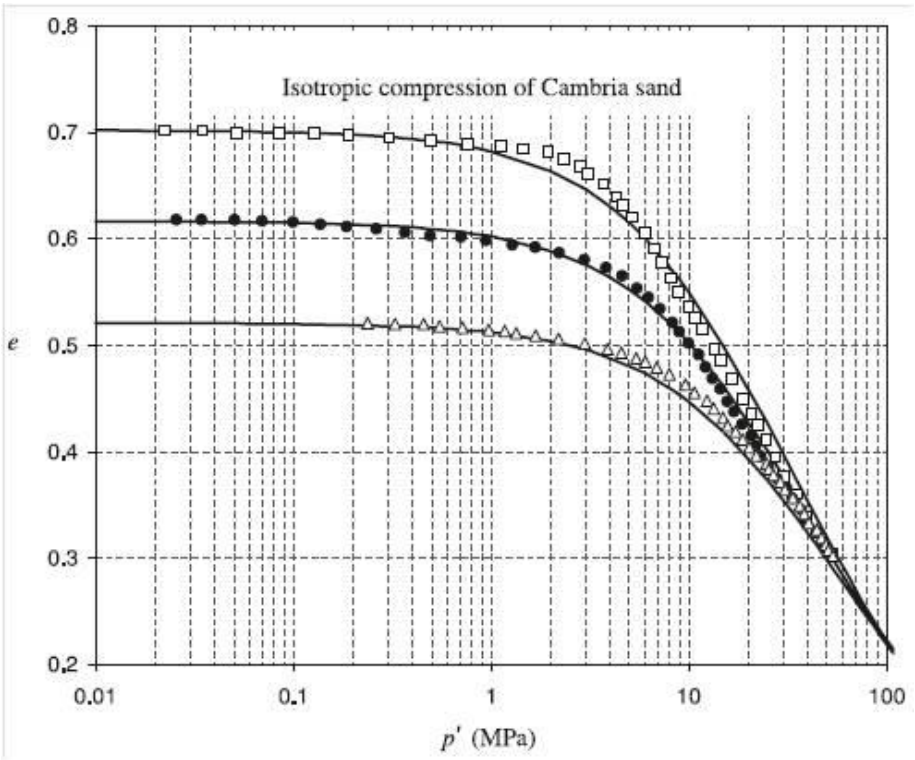

Figure 2.2 Isotropic compression curves of Cambria sand at different initial void ratios (after Bopp and Lade 2005).

2.2.1 Cemented sand

The pattern of the compression behaviour of the cemented sands is representative of carbonate soils and similar to that of other compressive soils. In isotropic

compression, the specimens show a stiff response up to a fairly well-defined apparent pre-consolidation pressure and then follow a unique normal compression line (NCL) (Huang and Airey, 1998). A linear normal compression line was proposed as given in Eq. 2.1

$$\upsilon = \mathrm{N} - \lambda \ln p' \tag{2.1}$$

Where N=volume intercept of isotropic normal compression line at p'=1 kPa; λ = gradient of normal compression line.

The slopes of the compression lines are practically independent of the amount of cement added. At confining pressures greater than 20MPa, departures from the linear v-In(p') responses occurred and the λ values decreased for all cement contents. As the cement content increases, the normal consolidation line shifts to the right in a v-In(p') plot, indicated by the increasing values of N shown in Table 2.2. As the bonding appears to be substantially broken down once the NCL is reached, the shift of the line is believed to reflect the changing grading of the soil.

Table 2.2 Influence of cement contents on compression parameters (after Huang and Airey, 1998)

Cement content (%)	λ	κ	N
0	0.209	0.0075	3.55
5	0.209	0.0071	3.56
20	0.213	0.0072	3.62

Huang and Airey, (1998) further reported that the idealized isotropic compression behaviour of calcarenite of various degrees of bonding indicates that stronger bonding results in higher specific volume. The relative contribution of cementation to the soil behaviour in isotropic compression reduces with decreasing void ratio.

Rotta et al., (2003) reported that isotropic compression curves obtained for the cemented specimens are similar in shape to those reported in the literature for structured and naturally/artificially cemented soils. The cemented specimens are initially much stiffer than the soil in its destructured state, then becoming gradually softer as the isotropic stress increases, as shown in Figure 2.3.

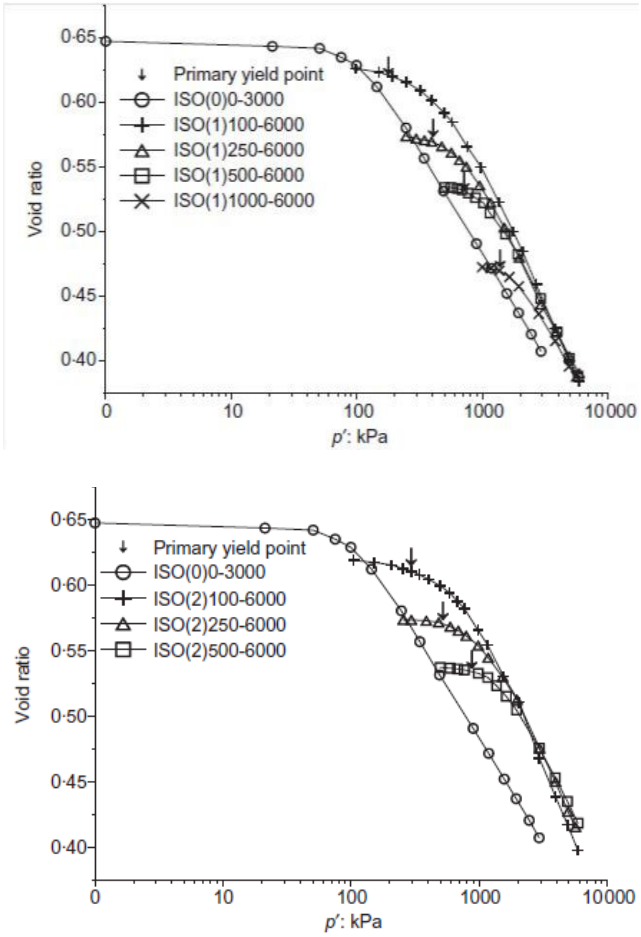

Figure 2.3 Isotropic compression curves for 1% and 2% cement content (after Rotta et al. 2003).

2.2.2 Fibre reinforced sand

Consoli et al., (2005b) studied the effect of fibre reinforcement on isotropic compression behaviour of sand and reported that the key feature to observe is that both the loose and dense fibre-reinforced sand specimens tend toward a unique

NCL when plotted in specific volume v-ln(p') space. It was also observed that insertion of fibres into the sand changes its behaviour as it can be seen that there are two distinct and parallel normal compression lines for the fibre reinforced and non reinforced sand as shown in Figure 2.4

The authors argued that the location of the NCL of the fibres reinforced sand above the NCL of the sand might be due to a lock-in effect of the fibres, therefore allowing a larger void ratio to exist in the composite material, which is not removed at large compressive stresses and large volumetric strains. Dos Santos et al., (2010a) reported similar results as that of (Consoli et al., 2005b) as shown in Figure 2.5 from isotropic compression tests on sand only and sand reinforced with fibres but used curved equation to the NCLs for sand and fibre reinforced sand. They argued that as the shearing tests were performed at confining stresses ranging from very low 20kPa to very high 5400kPa, it was decided to fit a curved equation.

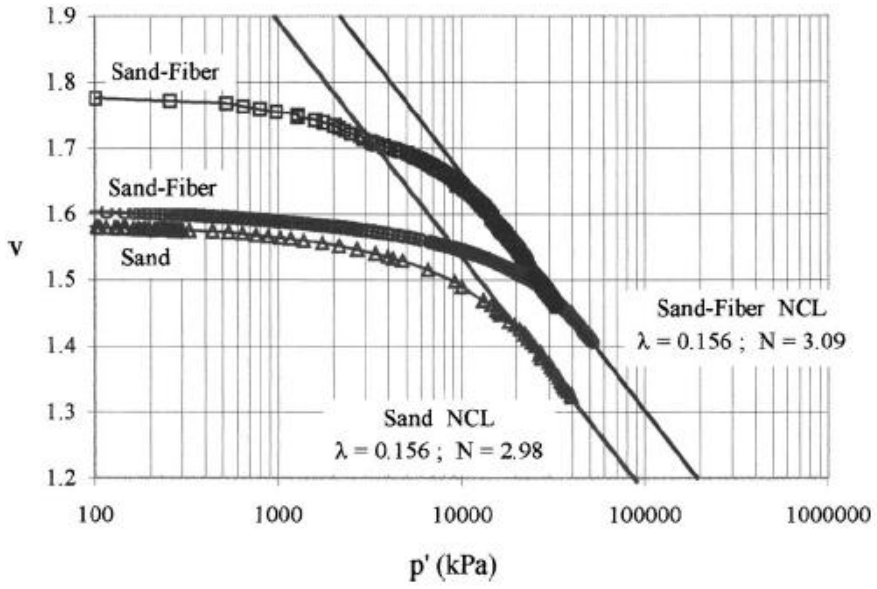

Figure 2.4 Isotropic compression data for sand and fibre-reinforced sand (after Consoli et al. 2005).

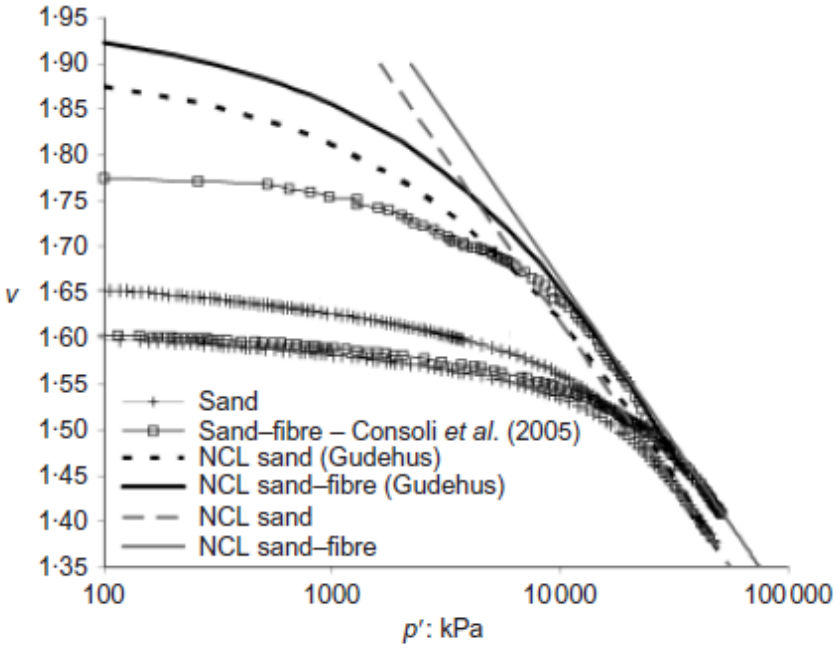

Figure 2.5 Isotropic compression curves for sand and fibre-reinforced sand (after dos Santos et al. 2010b).

2.2.3 Fibre reinforced cemented sand

Dos Santos et al., (2010b) reported the results of high pressure isotropic compression tests carried at confining pressures up to 50MPa on sand, fibre reinforced sand and fibre reinforced cemented sand samples. The authors reported that each type of material tend toward a unique normal compression line when plotted in v-log (p') space for both loose and dense specimens. They further concluded that the cementation modified the isotropic compression behaviour of the sand amplifying the range of stresses reached for a given specific volume. The inclusion of randomly distributed fibres in the uncemented sand also has a beneficial effect on the location of the NCL, but the insertion of both the cement and fibres is much more effective perhaps due to the control of crack propagation in the cemented sand after the inclusion of fibres, increasing even more yield stress at a given density. Distinct NCLs were identified for each material.

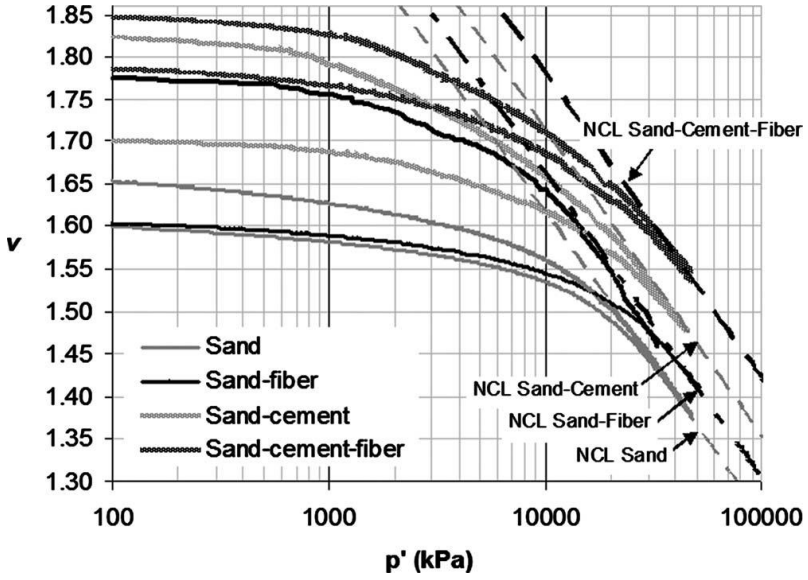

Figure 2.6 Isotropic compression data for various types of sand (after Dos Santos et al. 2010b).

Therefore, more work is needed to investigate and validate the behaviour of sand reinforced with fibre and/or cement under isotropic compression at high pressures in exploring the effect of the inclusion of fibre alone or the combined effect of the inclusion of fibre and cement. Moreover, comparison with uncemented sands including the effects of varying fibre and cement contents, dry density, and void ratio can give a reasonable framework. Scanning Electron Microscopy (SEM) analysis is also becoming a popular and emerging technique for the microscopic study of the granular materials, and can be better used for the microscopic study of the exhumed specimens after compression.

2.3 Effect of reinforcement on triaxial compression behaviour of sand

Soil stress strain behaviour can be investigated by deviator stress or stress ratio versus axial strain and volumetric strain or shear strain versus axial stress. The soil characteristics usually needed for most of the design, exploration and construction works can be investigated through triaxial testing.

Yamamuro and Lade, (1996) presented an experimental study of the stress-strain, volume change, and strength behaviour of dense Cambria sand at high pressures in drained triaxial compression and extension tests. The authors reported that particle crushing is the single most important factor affecting the behaviour of granular soil at high pressures. Increase in confining pressure causes a measured increase in the amount of particle crushing. Initially, this causes the volumetric strains at failure to become more contractive, the friction angles to decrease, and the major principal strains at failure to increase. The increase in particle crushing also affected the overall shape of the normalized stress-strain curve, creating a flattened middle section, reflecting the large amounts of particle crushing.

Marri, (2010) reported that increase in confining pressure increases the peak deviatoric stress, the axial strain to the peak and the amount of contraction during shearing. The stress-strain behaviour becomes increasingly ductile with increasing confining pressure. It was also reported that both the deviatoric stress and the volumetric strain increased gradually with the axial strain and approached (or were approaching) a constant ultimate value at the end of each test.

Boukpeti and Drescher, (2000) reported that in a drained triaxial test the volumetric-shear strain response is initially contractive and then dilatant, with the rate of dilation decreasing with increasing shear strains. With increasing confining pressure, the peak in the stress-strain curve becomes less visible, and the dilative response becomes more and more suppressed as shown in Figure 2.7.

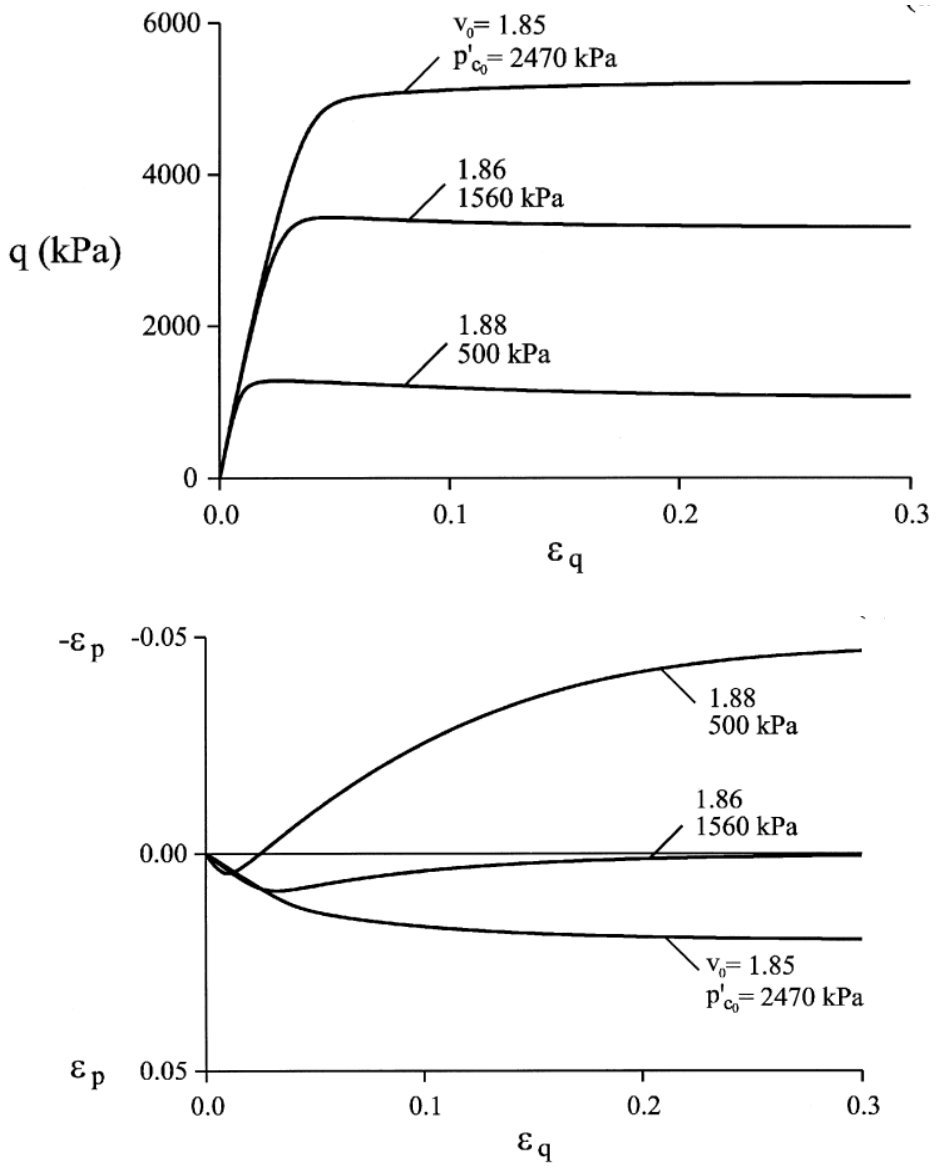

Figure 2.7 Influence of confining pressure on drained response of sand; (a) stress-strain response; (b) volumetric response (after Boukpeti and Drescher, 2000).

When an undrained test is carried out on dense sand under a high confining pressure, the stress-strain behaviour will change from strain hardening to strain softening and will be similar to the strain softening of loose sand under lower confining pressures. Typical stress-strain behaviour of sand in an undrained triaxial test is presented in Figure 2.8. It is seen that sand depicts a more pronounced peak in the stress strain curve when the consolidation pressure increases.

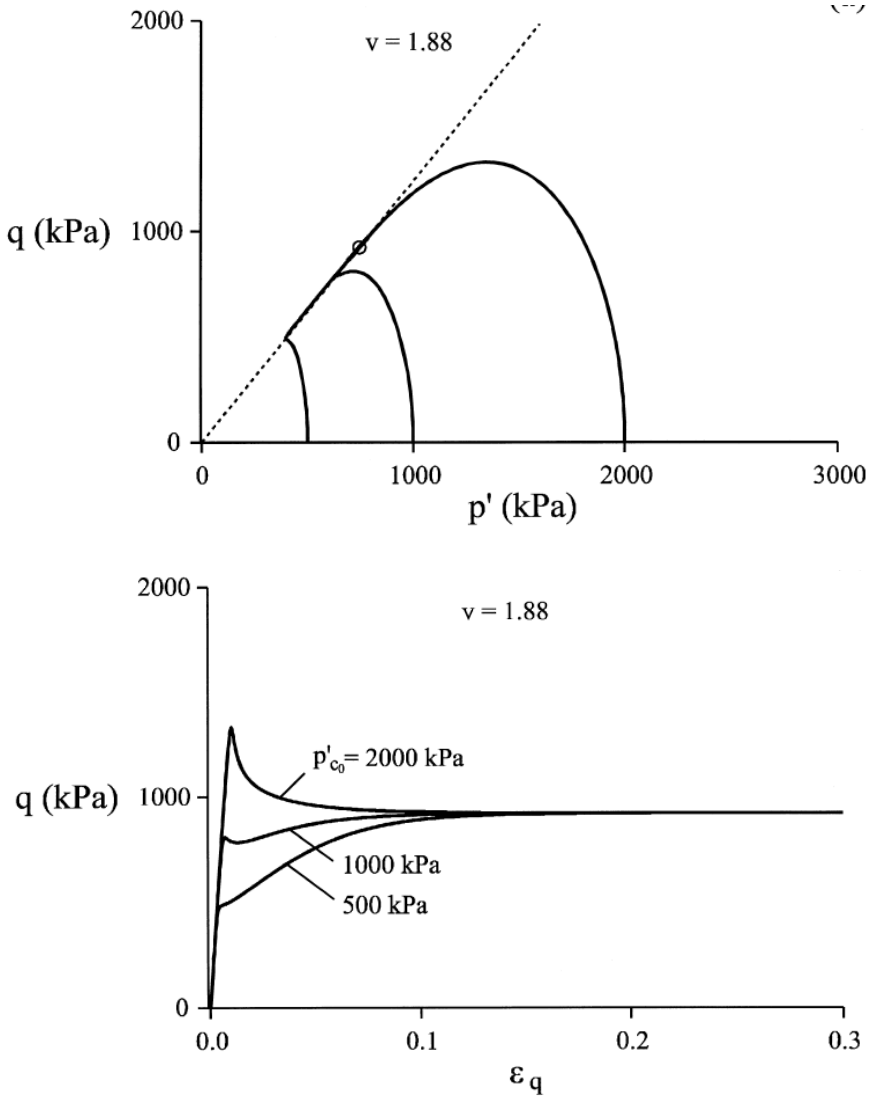

Figure 2.8 Influence of confining pressure on undrained response of sand; (a) stress path; (b) stress strain respone (after Boukpeti and Drescher, 2000).

An experimental study of the behaviour of dense Cambria sand in undrained triaxial compression and extension at high pressures was presented by Lade and Yamamuro, (1996). They reported that at confining pressures great enough to suppress dilatant volume change tendencies in the soil, the stress-strain curves indicated that peak deviatoric stress occurred at very low major principal strain values (ε_1 < 2%) as shown in Figure 2.9, and well inside the effective stress failure envelope, as defined by the maximum effective principal stress ratio (σ'_1 / σ'_3). This was caused by large, rapidly developing pore pressures, which quickly decreased

the effective confining pressure. As strains levels increased, stress differences continued to decline, until eventually effective stress failure was achieved. Lower confining pressure tests indicated volumetric dilation tendencies allowing the maximum deviatoric stress to approximately coincide with effective stress failure. High pressure effective stress paths tended to exhibit very similar shapes regardless of confining pressure. Lower pressure undrained tests exhibited effective stress paths that either rise to a peak near failure or to a second peak before effective stress failure as shown in Figure 2.10

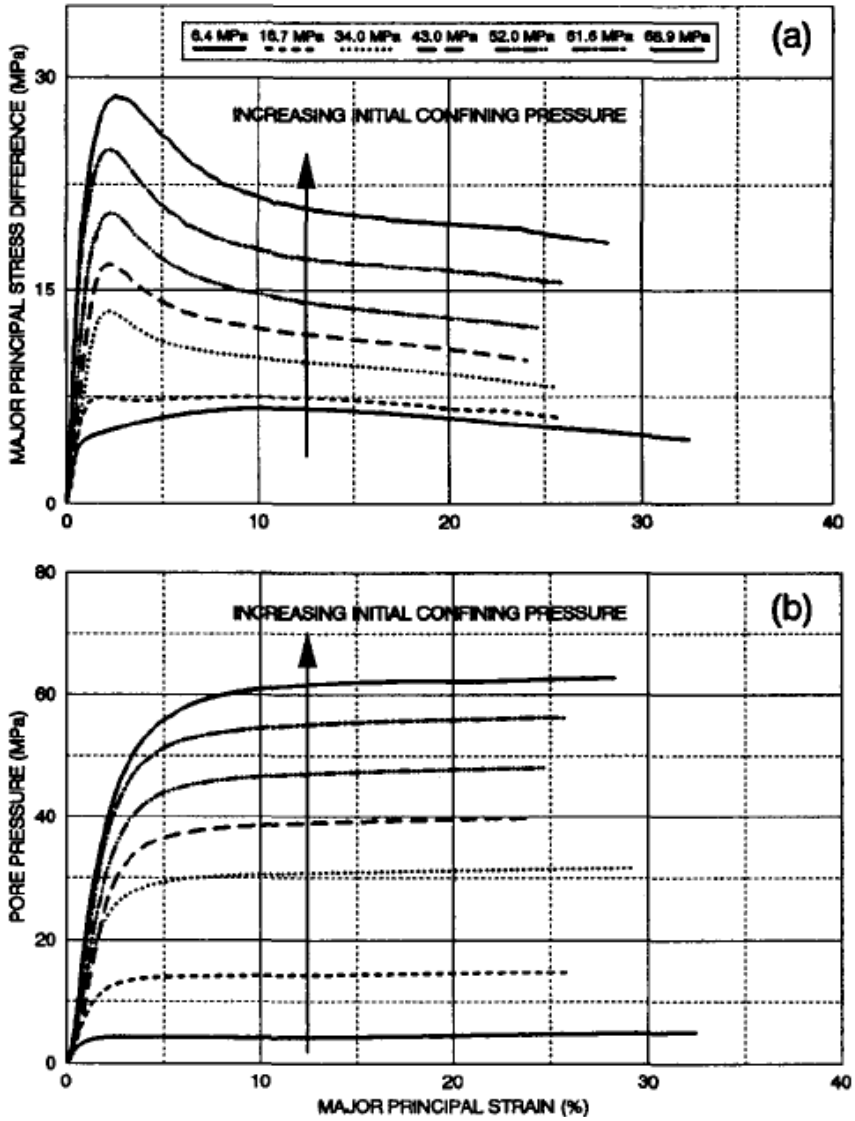

Figure 2.9 Influence of confining pressure on undrained response of sand; (a) stress ration vs. strain; (b) pore pressure variation (after Lade and Yamamuro, 1996).

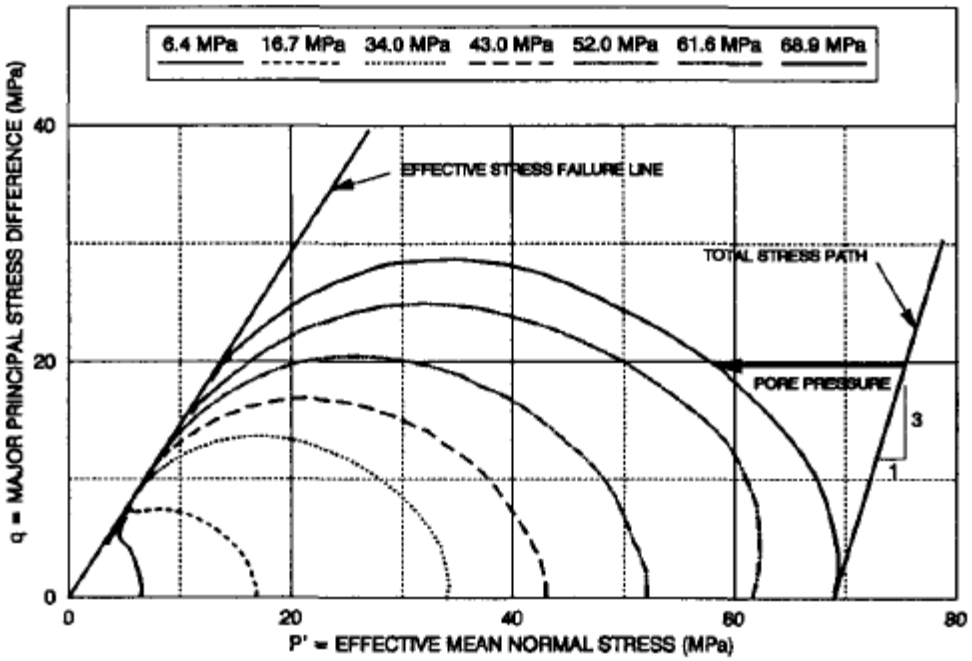

Figure 2.10 Influence of confining pressure on effective stress path (after Lade and Yamamuro, 1996).

A brief review has been presented here for cemented sand, fibre reinforced sand and fibre reinforced cemented sand.

2.3.1 Cemented sand

The overall stress–strain and volumetric behaviour of the cemented soil is governed by the relative magnitudes of the gross yield stress and confining pressure, which mainly depend on the nature of the soil particles, the void ratio, the cement content and the strength of the cement.

Schnaid et al., (2001) reported the results of drained triaxial tests on varying cement content and increasing confining pressure as shown in Figure 2.11. They reported that the stress-strain behaviour of the cemented soil can be described as initially stiff, apparently linear up to a well-defined yield point, beyond which the soil suffers increasingly plastic deformation until failure. As the cement content increases, both peak strength and initial stiffness increase. The brittle response of cemented sand

and axial strain at failure decreases as the mean effective stress increases and increases with increasing cement content. As for the volumetric response, the cemented specimens show an initial compression followed by a strong expansion with the maximum dilation rate taking place right after the peak strength. Subsequently, the dilation rate decreases as the soil approaches an ultimate stable condition. There is general consensus that the brittle behaviour changes to a ductile soil response as the stress level changes from low to high.

Marri et al., (2010) reported the drained triaxial behaviour of cemented sand at high pressure up to 12MPa as shown in Figure 2.12 and reported that with increasing confining pressure above 1MPa the peak deviatoric stress could not be clearly defined and there was no strain softening observed. The deviatoric stress in the tests conducted at 4 to 12MPa increased gradually to maximum value and remained constant until the end of test. It was also observed that, the higher the p_c', the more contractive behaviour of the specimen was obtained and that the volumetric strain curves were approaching a constant value at the end of each test. Therefore, the ultimate state obtained from the q-ε_a and q/p'-ε_a curves could also be considered to be very close to the critical state for the cemented sand tested. Similar behaviour was also obtained for the specimens with 10% and 15% cement contents.

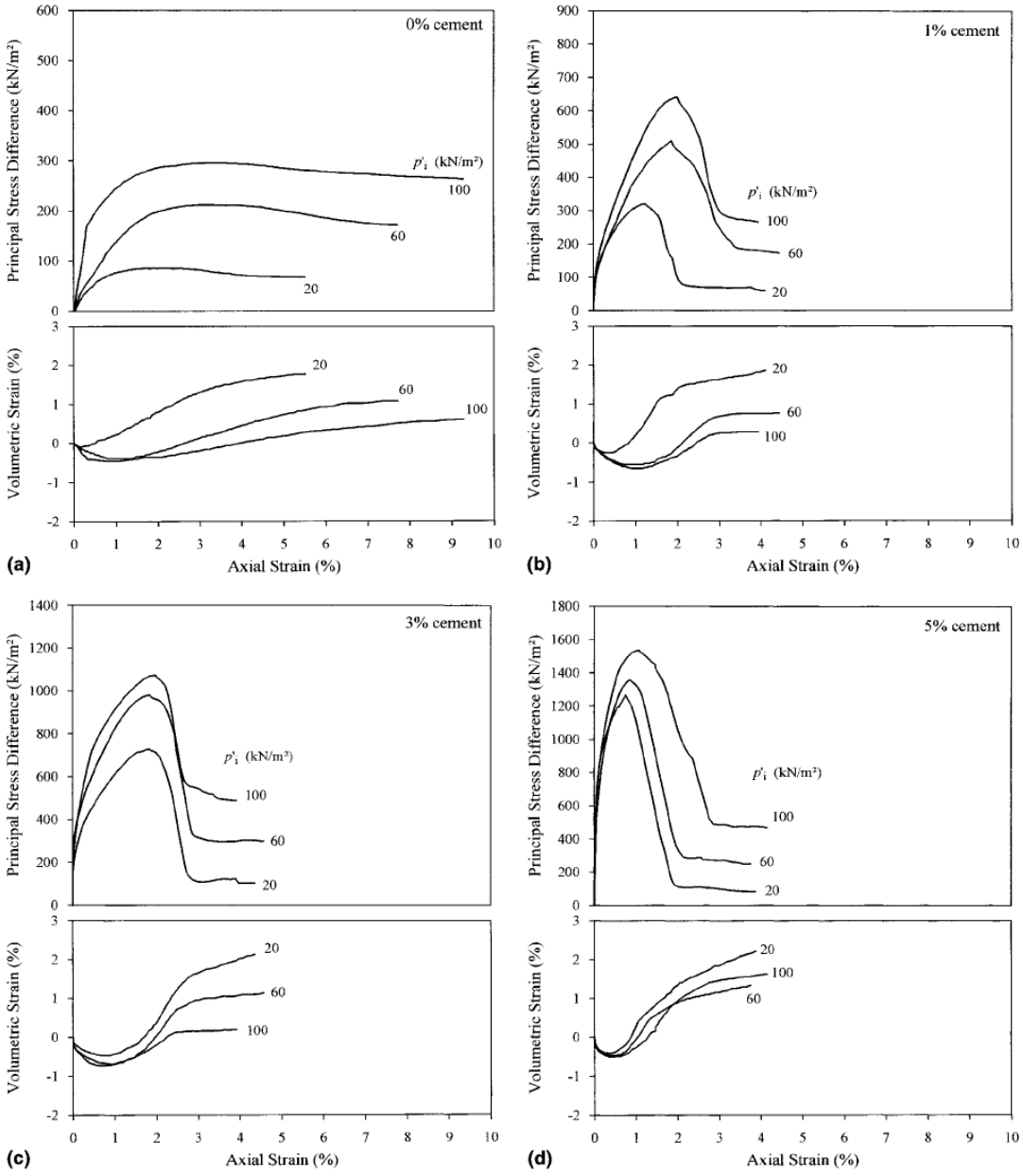

Figure 2.11 Stress-strain-volumetric response for a) 0% cement b) 1% cement c) 3% cement d) 5% cement (after Schnaid et al. 2001).

Sariosseiri and Muhunthan, (2009) reported the results of undrained triaxial tests conducted on three different soils with varying cement content up to confining pressures of 600kPa and concluded that deviator stress increased with the increase in confining pressure. The increase was significant with the addition of cement. The addition of 5% cement resulted in the soils attaining a peak deviator stress at about 2% strain increment followed by progressive softening. Slightly negative pore

pressure developed during shearing of non-treated and 5% cement treated at low confining pressures as shown in Figure 2.13. It was noted that in the case of 10% cement treated soil, pore pressures raised up to almost confining pressure at very low strain (1%). As a result, the effective confining pressure dropped to near zero suggesting a split type failure of the specimen with cracks transferring pressures immediately to the pore water resulting in such dramatic increase.

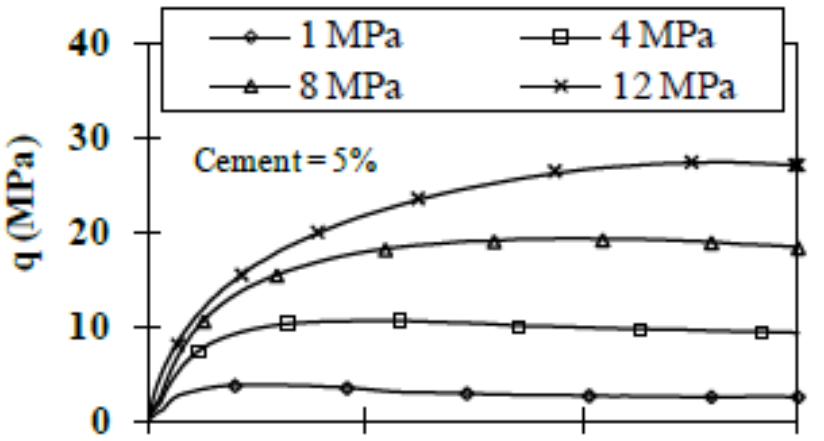

(a)

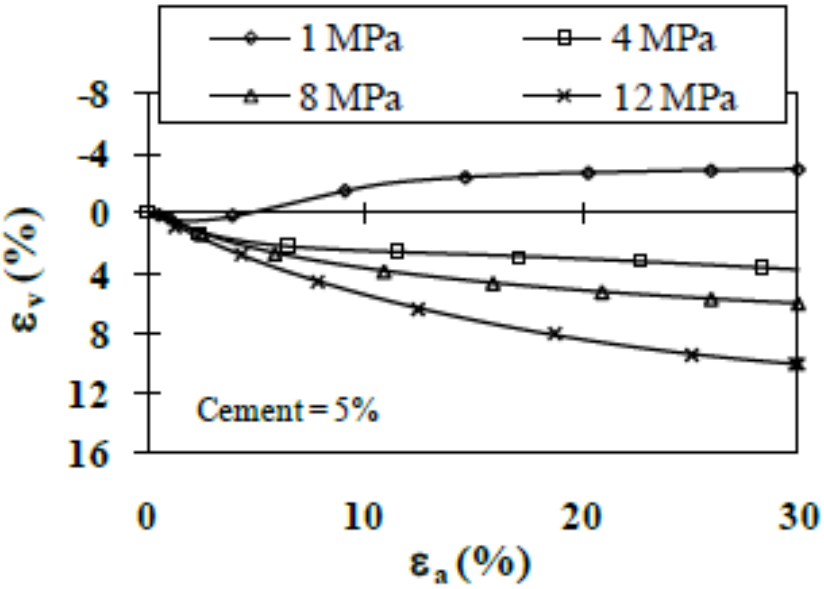

(b)

Figure 2.12 Effect of confining pressure on (a) stress-strain behaviour; and (b) vlumetric behaviour of sand with 5% cement content (after Marri et al., 2010).

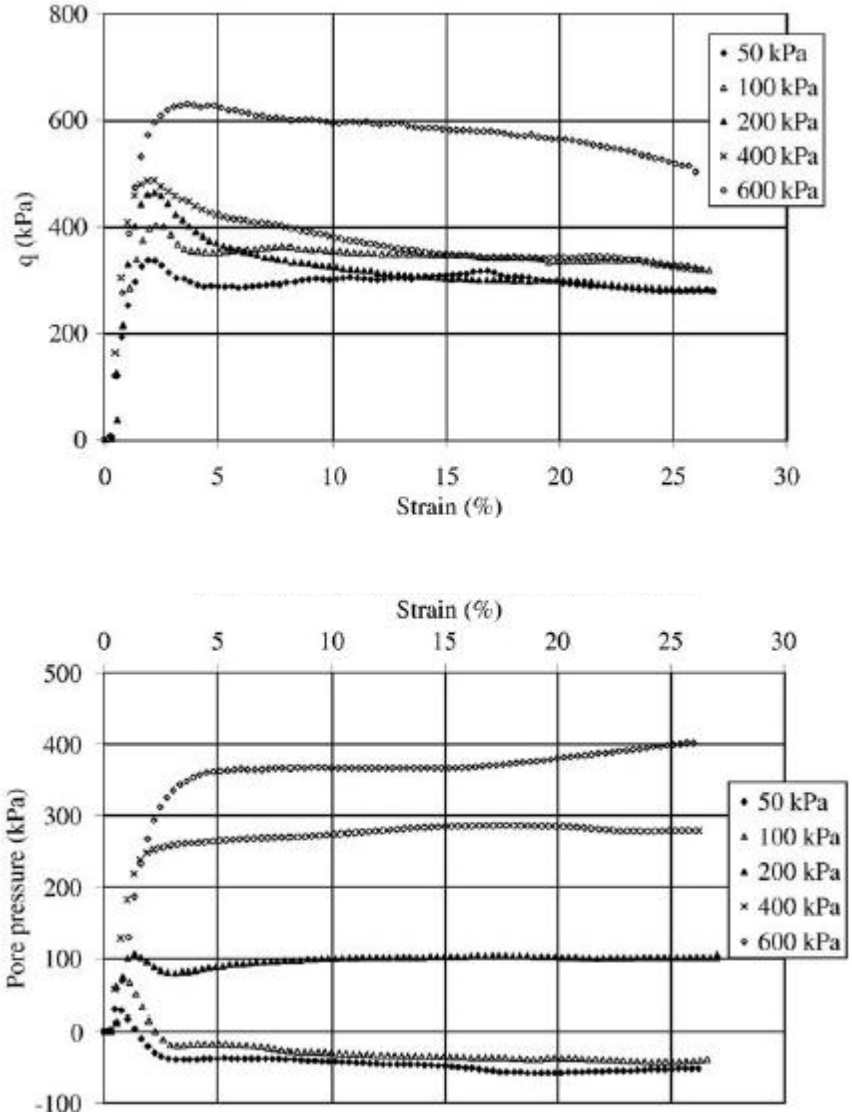

Figure 2.13 Effect of confining pressure on undrained triaxial behaviour with 5% cement content (a) variation of devaitor stress; and (b) variation of pore pressure. (after Sariosseiri and Muhunthan, 2009).

The undrained triaxial behaviour of cemented sand at high pressure above 1MPa was reported by Marri, (2010) and is shown in Figure 2.14. The author reported that the undrained response of dense cemented sand at high pressures is similar to loose sand at high pressure. However, the post peak softening of cemented sand is mild as compared to sharp post peak softening of loose sand at conventional pressure. The stress path of cemented sand at higher pressure shows a sharp turn at peak stress point as compared to the smoother stress path of loose sand. The

cemented sand is not reaching to the state of liquefaction as compared to loose sand. These differences might be due to the cement bonding.

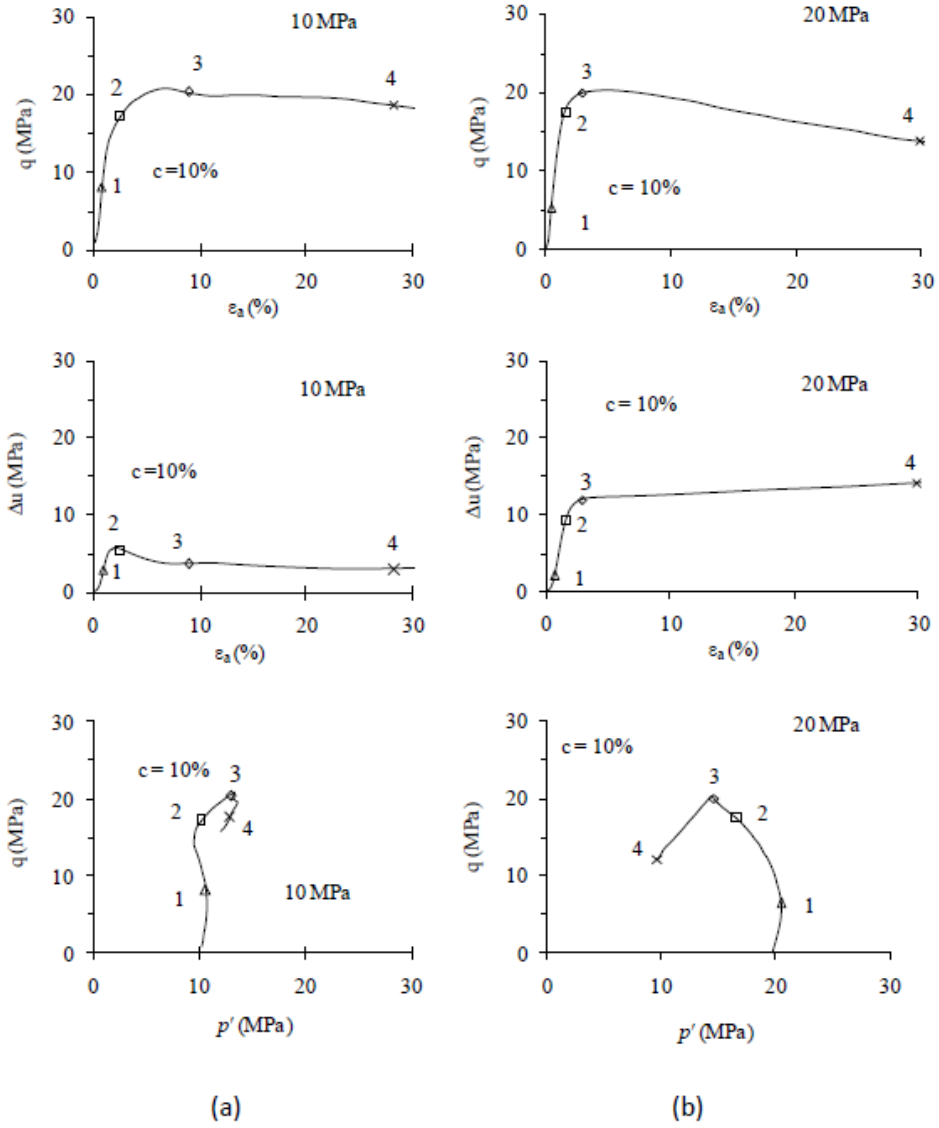

Figure 2.14 Typical undrained response of cemented sand at: (a) 10 MPa; and (b) 20 MPa (after Marri et al. 2010).

2.3.2 Fibre reinforced sand

The influence and the contribution of fibre reinforcement to the shear strength of sand have been examined by various investigators (e.g. Consoli et al., 1998, Prabakar and Sridhar, 2002, Consoli et al., 2002, Consoli et al., 2003, Michalowski and Cermak, 2003, Mofiz et al., 2004, Latha and Murthy, 2007, Michalowski, 2008,

Consoli et al., 2009a, Consoli et al., 2010, Dos Santos et al., 2010a etc). Several parameters such as confining stress, fibre type (natural and synthetic), volume fraction, density, length, aspect ratio, modulus of elasticity, orientation, and soil characteristics including particle size, shape, gradation have been studied. It has been established that the addition of fibres can significantly increase the peak shear strength and limit the post peak strength loss of both cohesive and granular soil. An increase in fibre content leads to increasing strain at failure and, consequently, to a more ductile behaviour. The peak shear strength and the strain at peak deviator stress also increases with increasing aspect ratio i.e. ratio of fibre length to fibre diameter. In addition Diambra et al., (2007a) have reported that fibres are most influential when orientated in the same direction as tensile strains. Therefore, for any particular loading condition, the effectiveness of fibre inclusions depends on their orientation, which in turn depends on the sample mixing and formation procedure. The composite behaviour is governed by the content and mechanical and geometrical properties of the fibres.

Gray and Alrefeai, (1986) reported the results of triaxial compression tests on fibre reinforced sand and stated that increasing amount of fibre increased peak strength and reduced post peak loss in strength of dense sand at high strains. They also reported that strength increase with fibre content was also affected by the ratio of fibre length to fibre diameter, aspect ratio. Most of the previous publication reported similar results e.g. (Gray and Ohashi, 1983, Gray and Alrefeai, 1986, Michalowski and Cermak, 2003, Consoli et al., 1998). A typical stress-strain

relationship of fibre reinforced soil obtained from consolidated drained tests is shown in Figure 2.15

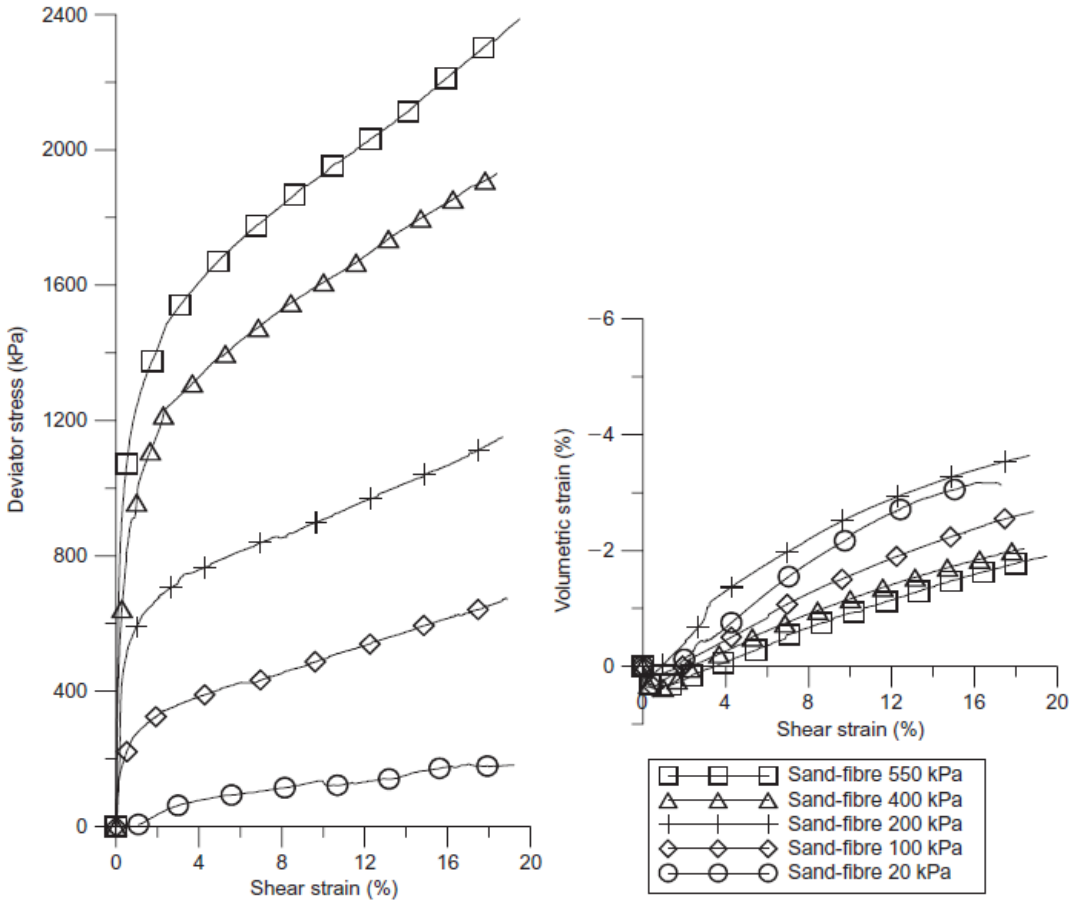

Figure 2.15 Stress-strain-volumetric response of fibre reinforced sand drained triaxial tests with 0.5% fibre content, 0.1mm diameter and 50mm length (after Consoli et al. 2009b).

2.3.3 Fibre reinforced cemented sand

The review of literature on stress-strain response of fibre reinforced cemented sand yields that peak strength, stiffness, brittleness, and residual response are changed as a result of the joined effects of fibre and cement inclusions. Shear strength and stiffness are both increased while residual strength remains practically the same as that of sand only. The dilation rate increases and the post peak behaviour becomes

brittle (Consoli et al., 1998). Consoli et al., (2009c) also reported that the fibre-reinforced cemented specimens demonstrate a ductile behaviour up to about 4% of cement content and a rather less pronounced brittle behaviour for higher cement contents up to 10%. Nevertheless, the axial strain corresponding to failure and post peak response is dependent on fibre content. In general, both the failure axial strain and the ultimate strength are greater for the fibre-reinforced material. The authors further reported that polypropylene fibres caused a significant reduction in the initial stiffness of the cemented matrix. It was believed that this reduction is due to the large volume occupied by the polypropylene fibres. This fact, allied to the hypothesis of losing continuity of the cementitious links, is the probable explanation for the decrease in stiffness modulus, E_s of the cemented matrix (Consoli et al., 2004).

Consoli et al., (1998) investigated the effect of fibre and cement inclusion on the stress-strain behaviour of the composites and reported that overall behaviour is significantly influenced by the inclusion of fibre and cement. Peak strength, stiffness, brittleness, and residual response are changed as a consequence of either separate or the joined effects of fibre and cement inclusions as shown in Figure 2.16. It can be seen that the effect of fibre inclusion as related to uncemented soil is shown to be less pronounced but consistent. A moderate increase in shear strength is accompanied by a rigidity loss; the residual strength is increased and the volumetric response becomes more compressive in the early stages of loading and less expansive afterwards. Finally, the coupled effect of fibre and cement inclusions is pointed out. The shear strength is greater than those produced separately by

cementation and fibre inclusion. The fibre-reinforced cemented soil is stiffer as compared to uncemented, but a consistent rigidity loss is observed as related to cemented soil, which is fully compensated by a behaviour that is far more ductile.

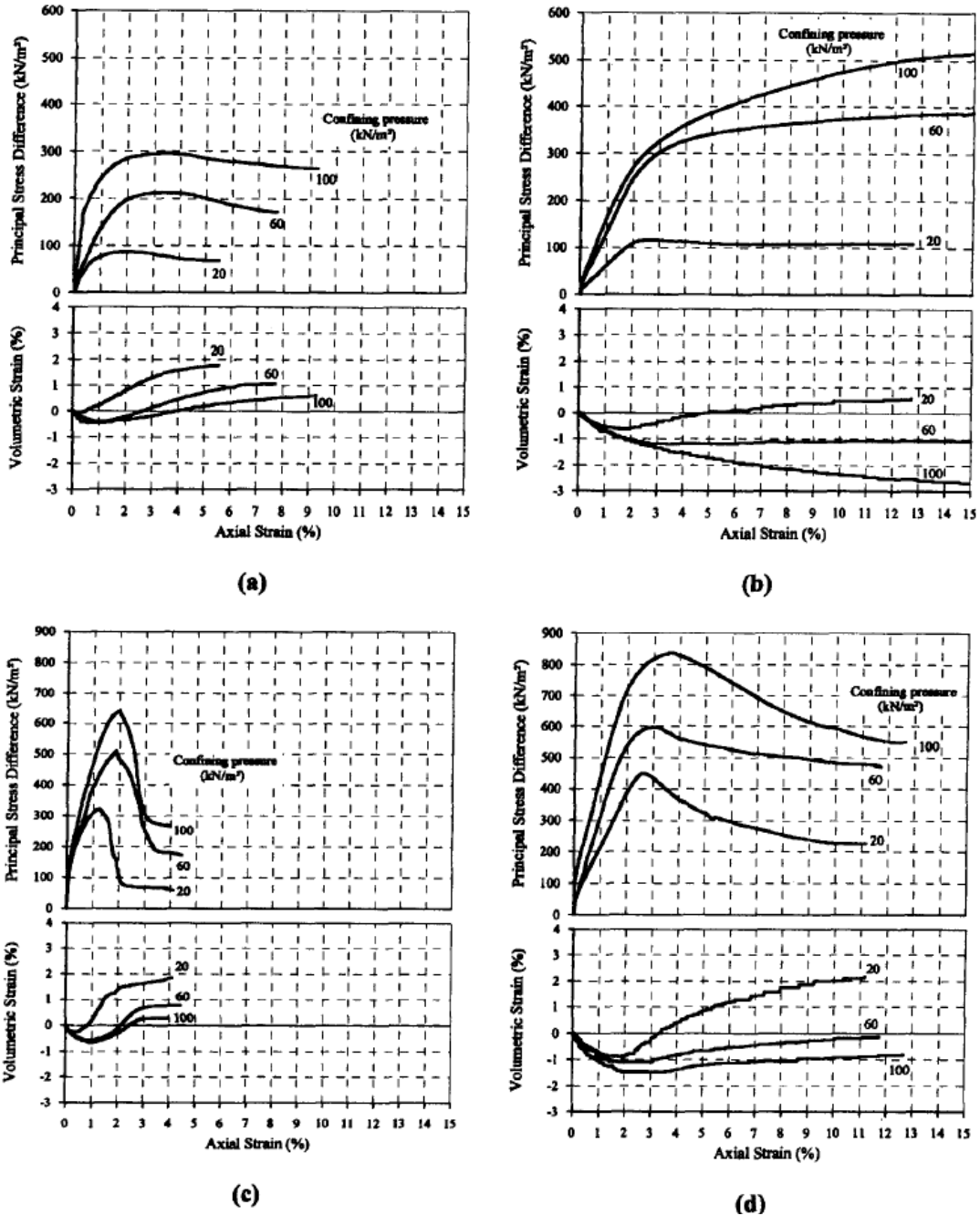

Figure 2.16 Stress- strain response of (a) sand; (b) fibre reinforced sand; (c) cemented sand; and (d) fibre reinforced cemented sand (after Consoli et al. 1998).

Also, the residual strength is greater than that produced only by fibre inclusion, indicating that the fibre effect on the residual strength is amplified by the cement

addition, even though, as stated previously; the cementation itself does not have a direct influence on the residual behaviour of the soil.

How fibre reinforced cemented sand behaves at increasing pressures has not yet been explored, therefore it will be interesting to know how the composite will behave when sheared at high confining pressures.

2.4 Effect of reinforcement on failure characteristics

Shear failure occurs when loading creates shear stresses that exceed the shear strength. Failure parameters are the most important in describing the failure characteristics. The purpose of failure criteria is to predict or estimate the failure/yield of soils. The Strength Parameters only allow the definition of the failure (strength) criterion for a material. For an elastic material, that returns to its original shape after the stress is removed, the failure criterion parameters will only be used for the calculation and plotting of the strength factor within the material. Although an elastic material cannot "fail", the failure envelope allows a degree of overstress to be calculated.

For plastic material, which describes the deformation of a material undergoing non-reversible change of shape in response to applied forces the strength parameters will be used in the analysis if yielding occurs. This is unlike elastic materials, where the strength parameters are only used to obtain values of strength factor, but do not affect the analysis results (i.e. stresses and displacements are not affected). For a plastic material depending on the strength criterion, residual strength parameters and a dilation parameter also need to be defined.

Mohr–Coulomb theory is a mathematical model, in geotechnical engineering; it is used to define shear strength of soils and rocks at different effective stresses. The Mohr–Coulomb failure criterion represents the linear envelope that is obtained from a plot of the shear strength of a material versus the applied normal stress. This relation is expressed as:

$$\tau = c + \sigma \tan(\phi') \quad (2.2)$$

Where, τ is the shear strength, σ is the normal stress, c is the intercept of the failure envelope with the τ axis, and ϕ' is the slope of the failure envelope. The quantity c is often called the cohesion and the angle ϕ' is called the angle of internal friction.

In addition to the failure parameters, modes of failure are also important. Generally, three types of failure modes reported in literature are (1) peak failure, indicated by a gradual degradation of the average strength after the peak is reached; (2) localized failure, indicated by the development of the shear bands and is often indicated by a rapid reduction in the average strength and finally (3) bulging failure which is caused by friction on top and bottom faces of the specimen (Huang et al., 2007). The deformation can be brittle or ductile depending on the properties of the material and the effective confining stress level. Brittle failure is a sudden failure characterised by a dilative response whereas ductile failure is a gradual deformation at peak shear strength. Suzuki and Yamada, (2006) reported the mechanism of progressive failure by carrying out a series of drained triaxial tests on Toyoura sand shown in Figure 2.17. The failure process is described as follows:

a. The initial condition of stress and strain is assumed to be the same throughout the specimen;

b. Tiny compressive and dilative strain areas occur at various locations, but the uniformity and homogeneity of stress and strain are maintained;
c. The dilative strain areas begin to link continuously to form a shear band. The start of this process coincides with the peak strength. Part of the specimen then slides gradually along the developing shear band. The deformation is mostly absorbed by sliding at the shear band, so that the dilative strain increment areas of the specimen gradually decrease as the shear band progresses from being weakly developed to fully developed, and the dilatancy index becomes smaller;
d. The volumetric strain increment becomes zero even within shear bands. At this point the dilatancy index is zero, and a new equilibrium is reached;
e. If a further fully developed shear band can arise, dilative strain areas develop in the specimen again, but only a small stress ratio increment is now required;
f. The dilative strain areas begin to link continuously to make up a further fully developed shear band. “Diagonally crossing shear bands” are liable to form; and
g. The dilatancy index becomes zero again, and a further equilibrium is reached.

The degree of cement content, fibre content and confining pressures affect the mechanism of failure in fibre reinforced cemented sand. A review of these effects is presented in the following sections.

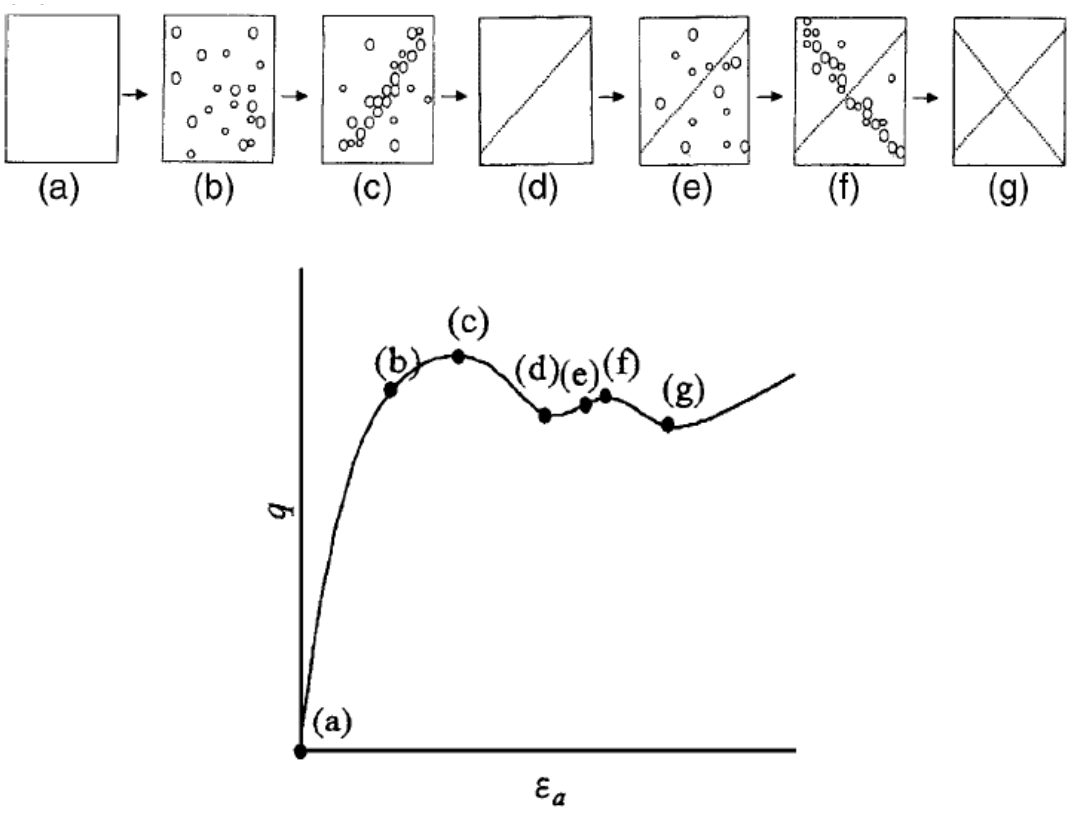

Figure 2.17 Illustration of progressive failure of sands in drained triaxial tests: (a) initial condition; (b) occurrence of dilative strain areas; (c) continuous linking of dilative strain areas; (d) fully developed shear band; (e) further occurrence of dilative strain areas; (f) continuous link of dilative strain areas; (g) "diagonally crossing shear bands" and (h) q versus ε_a. (after Suzuki and Yamada, 2006).

2.4.1 Cemented sand

Peak strength and mode of failure are the two most important aspects in considering the failure mechanism. Different failure criteria have been used in literature, for instance q_{max}, $(q/p')_{max}$ and also the limiting strain criteria. Abdulla and Kiousis, (1997) reported that although failure criteria of cemented soils are often discussed, complete constitutive models are rather rare and are direct extensions of established soil models, with an added cohesion component. Schnaid et al., (2001) reported that due to the cohesive-frictional nature of the cemented soil, the shear strength can be expressed as a function of the internal friction angle

and the cohesion intercept. It is difficult to establish a clear correlation between cement content and the friction angle due to lack of a defined pattern. They showed that the deviatoric stress at failure, q_f, obtained in drained triaxial tests, can be expressed as a linear function of the degree of cementation and the initial mean effective stress. It was suggested that the triaxial shear strength of artificially cemented sand can be conveniently expressed as a function of the unconfined compressive strength and the uncemented friction angle as shown in Figure 2.18. In this plot, the degree of cementation is directly represented by the unconfined compressive strength since a linear relationship between the two was observed.

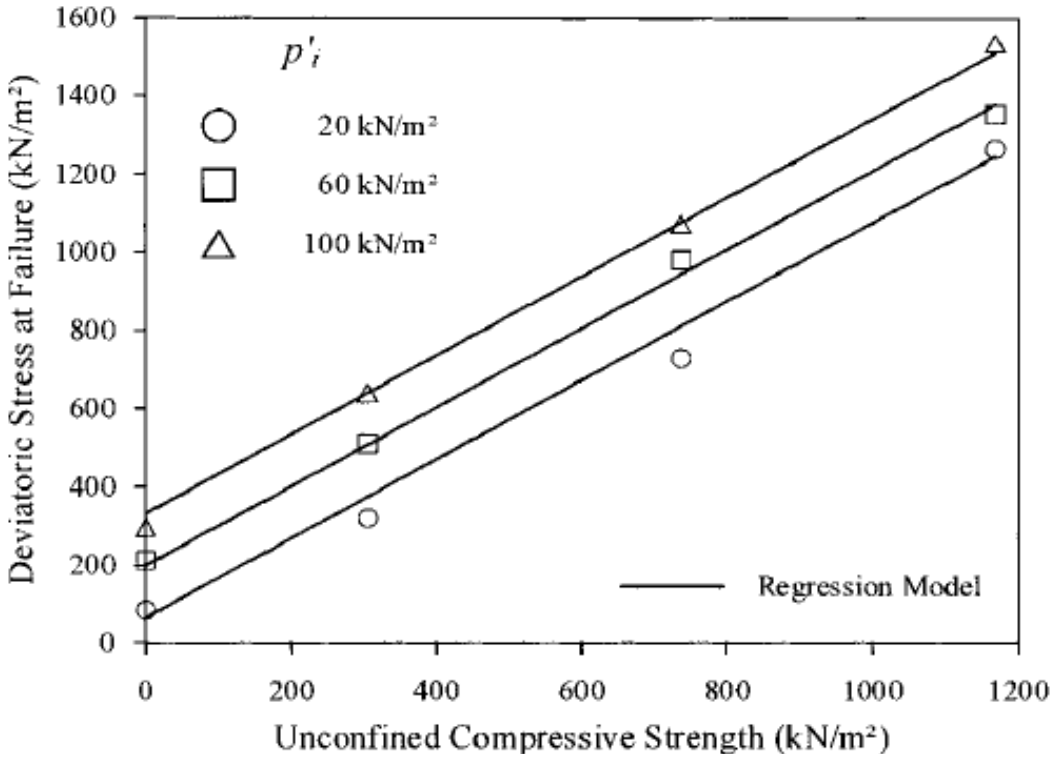

Figure 2.18 Effect of cementation and initial mean effective stress on deviatoric stress at failure (after Schnaid et al. 2001).

Sariosseiri and Muhunthan, (2009) reported the results of undrained triaxial tests and showed that while cement treatment improved shear strength significantly, the

type of failure behaviour varied greatly. Non-treated, 5%, and 10% cement treated soils displayed ductile, planar, and splitting types of failure, as shown in Figure 2.19. For 10% cement treated soils, pore pressures raised rapidly to confining pressures resulting in zero effective confining pressure at failure. Consequently, specimens split vertically (Figure 2.19 c).

(a)

(b)

(c)

Figure 2.19 Failure types of Aberdeen soils; (a) Non treated soil, (b) 5% cement treated soil, and (c) 10% cement treated soil. (after Sariosseiri and Muhunthan, 2009).

2.4.2 Fibre reinforced sand

The failure mechanism in fibre reinforced soil is such that below a certain confining or normal pressure, called critical confining pressure, failure occurs by slipping of the fibres and lack of adhesion within the soil mass. At confining pressure above the critical level, the soil normally fails before the fibre (Maher and Ho, 1993). Shear stress that develops in the sand mobilises tensile resistance in the fibres via friction at the sand-fibre interface. Shearing action in the sand causes the fibres to distort; as a result the tensile resistance in the fibres is directed into the normal component, which increases the confining stress on the failure plane and a tangential component that directly opposes shear. The most probable orientation of randomly distributed fibres with respect to a shear failure surface is 90° (Gray and Alrefeai, 1986). Diambra et al., (2009) reported that addition of fibres results in a significant increase of the friction angle and cohesion intercept. A loose specimen reinforced with 0.6% fibre content has the same deviatoric strength as a denser specimen with 0.3% fibre content strength. This particular characteristic is related to the deformation patterns of the specimens. Dense specimens tend to dilate more than loose ones, inducing a greater desire for radial strain and therefore greater potential tensile stresses in the fibres which create an increased confinement on the sand in the dense specimens and hence a much larger increase in strength than observed for loose specimens.

Ibraim et al., (2010) reported that at increasing confining stresses, the compressive strength of the reinforced sand appears to increase linearly with the concentration of fibres. For low values of the confining stress, this increase approaches an

asymptotic upper limit. Also, for a given fibre concentration, strength, as expressed by the major principal stress at failure, increases linearly with fibre aspect ratio i.e. fibre length over fibre diameter. It has also been noted that for a given confining stress, the strength of the reinforced sand increases with reducing average grain size D_{50}.

Prabakar and Sridhar, (2002) mentioned that one of the main advantages of randomly distributed fibres is the maintenance of strength isotropy and absence of potential failure plane, which can develop parallel to the oriented reinforcement. However, Latha and Murthy, (2007) reported that sand reinforced with randomly oriented discrete fibres failed along classic planar shear plane as shown in Figure 2.20. The authors further stated that the beneficial effect of geosynthetic material is largely dependent on the form in which it is used as reinforcement. For example, the same geosynthetic material, when used in planar layers or geocells or discrete fibres, comprising exactly the same quantity of material will give different strength improvements. This difference in strengths is mainly achieved due to the difference in the mechanism of failure in the soil reinforced with different forms of geosynthetic material.

Figure 2.20 Failure mode in fibre reinforced sand. (after Latha and Murthy, 2007).

2.4.3 Fibre reinforced cemented sand

As stated before, the peak strength and the mode of failure are two relevant aspects of soil behaviour. It was observed by Consoli et al., (2004) that depending on the nature of the fibre, the introduction of fibres into the cemented composite may reduce the strength at failure, and this effect is increased for longer fibres as shown in Figure 2.21. A possible explanation for this situation is that increasing the fibre length in a soil results in an increased contact surface area and consequently a higher strength resulting from friction between the fibre and the soil. On the other hand, the introduction of certain extensible fibres (such as polypropylene fibres), when compared with the cemented matrix stiffness, causes a reduction in the cementitious bonds formed between soil particles, once part of the voids is filled by the fibres and not cement, and such fibres only will work after certain deformation.

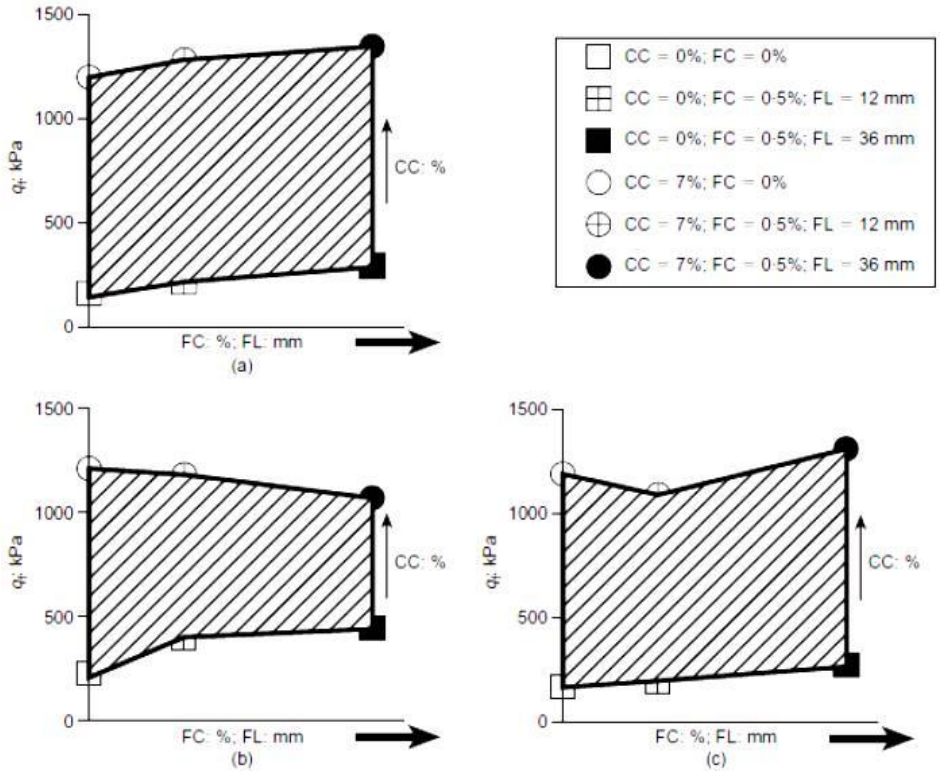

Figure 2.21 Effect of cement content, fibre content and fibre length on q_f: (a) polyster; (b) polypropylene; and (c) glass. (after Consoli et al. 2004).

The axial strain corresponding to failure and post peak response is dependent on fibre insertion to the composite. In general, both the failure axial strain and the ultimate strength are greater for the fibre-reinforced material (Consoli et al., 2009c). They further observed that fibres are more effective for uncemented sand. As the cement content increases, the proportional gain in strength due to fibre inclusion decreases, that is, the fibre reinforcement becomes less effective. In order to explain reducing fibre reinforcement effectiveness with increasing cement content, it was recalled that the tensile strength of the reinforcing elements would be mobilized only after deformation of the soil around the fibres. The portion of tensile strength to be mobilized depends on the magnitude of the soil deformation and also on the stiffness of the fibres. Polypropylene fibres are extensible fibres. For the uncemented matrix, polypropylene fibres can fully produce their effects, increasing deviatoric stress at failure q_f, at higher deformations, once large deformations are needed to develop all soil strength. For the cemented matrix with reduced cement contents (up to about 4%), increasing cement content increases both strength and stiffness characteristics, but mobilization of tensile strength of polypropylene fibres still occurs at strains before peak of such cemented soils, and so fibres do contribute to an increase of q_f. The less stiff the cemented matrix (consequently the smaller the cement content) the larger the effect of mobilization of tensile strength of the fibres and the larger is its contribution to an increase of q_f. However, for higher cement contents the stiffness of the cement governs strength and stiffness characteristics. Polypropylene fibres, being less stiff, are not able to mobilize tensile strength before peak of such cemented soils is reached at very low deformations, and so do not contribute to an increase of q_f.

Consoli et al., (2004) reported that geotechnical parameter that better represents the mode of failure is the brittleness index,

$$I_B = \left({}^{q_f}/_{q_{ult}} \right) - 1 \qquad (2.3)$$

Where q_f is peak stress at failure and q_{ult} is the ultimate deviator stress. The cement confers a brittle behaviour to the composite. The effect of fibre inclusion on the ductile/brittle characteristics of the composites differs according to the nature of the fibres. Polyester fibres insertion caused a decrease of I_B of the cemented matrix, although the changes were not sufficient for the post-peak behaviour of the composite to be characterised as ductile. Polypropylene fibres, on the other hand, changed the mode of failure of the cemented matrix from brittle to ductile. Glass fibres did not interfere in the mode of failure of the cemented composites.

2.5 Effect of reinforcement on stress-dilatancy of sand

Dilatancy is the observed tendency of a compacted granular material to dilate (expand in volume) as it is sheared. This occurs because the grains in a compacted state are interlocked and therefore do not have the freedom to move around one another. When stressed, a lever motion occurs between neighbouring grains, which produces a bulk expansion of the material. On the other hand, when a granular material starts in a very loose state it may initially compact instead of dilating under shear. This property distinguishes granular materials from most other engineering materials.

One of the parameters used to quantify the dilation is the angle of dilation. It is defined by the ratio between the rate of volumetric strain and the rate of shear strain and expressed as in Eq 2.4

$$\Psi = \tan^{-1}\left(\frac{-d\varepsilon_v}{d\varepsilon_q}\right) \quad (2.4)$$

Where ε_v is the volumetric strain and ε_q is the shear strain. More formally, ψ is defined as the negative of the rate of increase of volumetric strain with shear strain. The negative sign is required so that a negative (i.e. expansive) change in volume corresponds to a positive rate of dilation.

This dilative behaviour is found to have great influence on the apparent strength behaviour of granular soils. Ignorance of such dilative behaviour can lead to significant error in predicting ultimate bearing stresses, deformation or stability of geotechnical structures. Vermeer and de Borst, (1984) first reported the typical values of dilation angles of various geological materials based on the empirical data. For instance, a 15° dilatancy angle for very dense sand whereas loose sands were reported to have dilatancy angle of few degrees and normally consolidated clays show no dilatancy at all. It was concluded that all values for dilatancy angles range between 0° and 20° for soils, concrete and rocks. After intense shearing the dilatancy angle gradually vanishes and any subsequent shearing causes no more volume change. Bolton, (1986) proposed a theoretical solution of the maximum dilation angle in the plane strain condition, suggesting the typical dilation angle of granular soil is in the range of 10 to 20 degrees.

Bolton, (1986) indicated that both effective stress and soil density affect the dilative behaviour of soils and their strength parameters. It has also been demonstrated (Bishop, 1972; Billam, 1972; Vesic & Clough, 1968) by tests on granular soils at elevated pressures that particle crushing occurs, thereby reducing the observed maximum angles of dilation and shearing, ψ_{max} and ϕ'_{max}, for a given initial density. Lancelot et al., (2006) reported the results of triaxial tests data on loose and dense sand and reported similar results as shown in Figure 2.22.

At high stresses, the suppression of dilatancy plays an important role in controlling the shear behaviour. The influence of the confining pressure on the plastic properties of sand, mainly for friction and dilatancy angles are of significant importance. Moreover, it would be interesting to elaborate that how the addition of cement and/or fibres affect this progressive suppression of dilation with gradual increase in confining pressures.

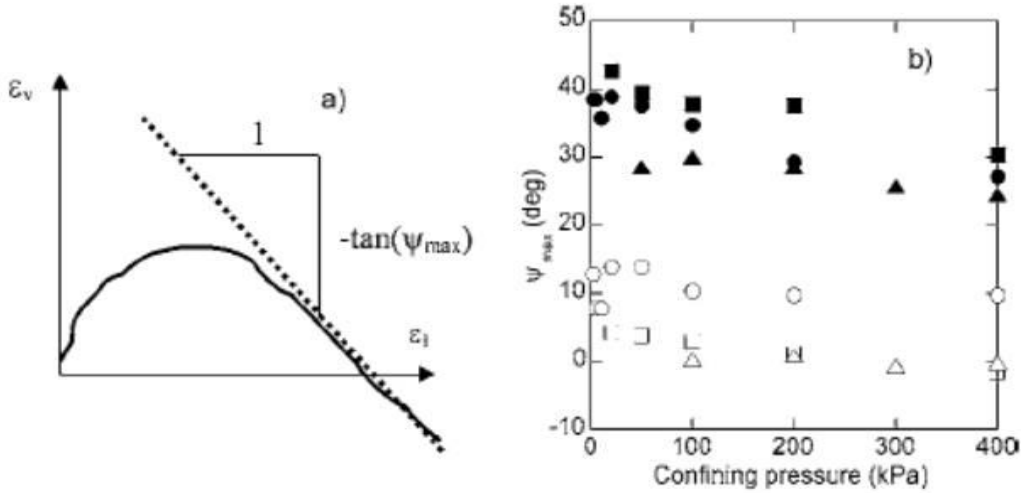

Figure 2.22 Influence of confining pressure on ψ_{max} for Hostun sand (open square=loose, close square=dense, Karlsruhe sand (open triangle=loose, close triangle= dense) (after Lancelot et al., 2006).

2.5.1 Cemented sand

Following the work of (Rowe 1962), the following stress-dilatancy relationship can be used to describe the plastic flow of a bonded geomaterial:

$$\frac{\sigma`_1}{\sigma`_3}\times\frac{1}{1-\frac{d\varepsilon_v}{d\varepsilon_a}}=\tan^2\left(\frac{\pi}{4}+\frac{\phi`_f}{2}\right)+\frac{2c}{\sigma`_3}\tan\left(\frac{\pi}{4}+\frac{\phi`_f}{2}\right) \qquad (2.5)$$

Where, $\sigma`_1$ and $\sigma`_3$ are the major and minor principal stresses, respectively, $d\varepsilon_v$ and $d\varepsilon_a$ are the increments of volumetric and major principal strains, respectively, c is the inter-particle cohesion, and $\phi`_f$ is the friction angle. It is more commonly expressed as $R=K_cD$, where R is the ratio of principal stresses, K_c is a constant, and D is the rate of dilatancy. By rearranging the equation, the rate of dilatancy can be expressed as:

$$D=\frac{\frac{\sigma`_1}{\sigma`_3}}{\tan^2\left(\frac{\pi}{4}+\frac{\phi`_f}{2}\right)+\frac{2c}{\sigma`_3}\tan\left(\frac{\pi}{4}+\frac{\phi`_f}{2}\right)} \qquad (2.6)$$

It is clear from Eq 2.6 that the dilatancy of a bonded geomaterial is influenced by both the inter-particle cohesion c and the angle of friction $\phi`_f$, showing that dilatancy is inhibited by the presence of cohesion or bonding between the particles. Wang and Leung (2008) reported that the Portland cement exhibit volumetric dilation upon shearing even with 1% cement content, whereas the uncemented sample shows volumetric contraction as shown in Figure 2.23. This shows that the volumetric dilation is completely due to the cementation effect and not to the density effect. This dilative feature has been hypothetically attributed to cemented

particles forming highly interlocked clusters. The dilative response, as expected, is suppressed by confinement and encouraged by cohesion as shown in Figure 2.24.

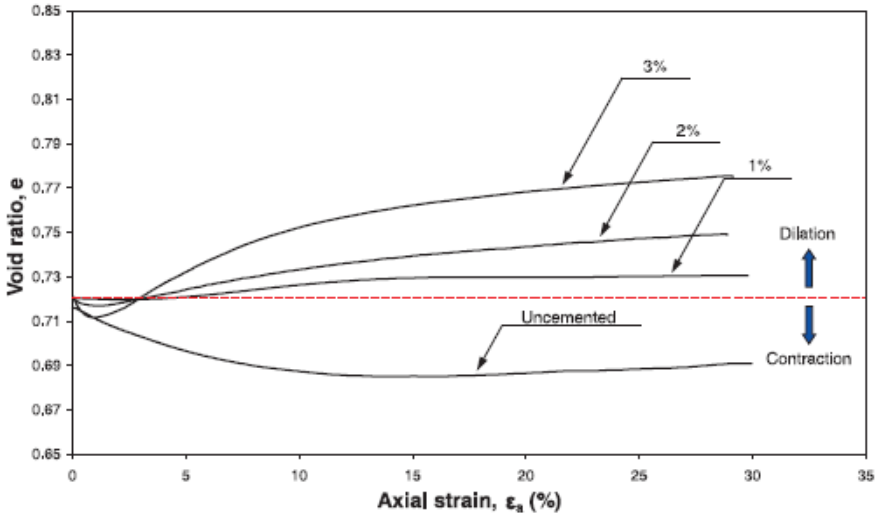

Figure 2.23 Void-ratio variations of Portland cement sand samples in response to shearing (50 kPa confining pressure) (after Wang and Leung 2008).

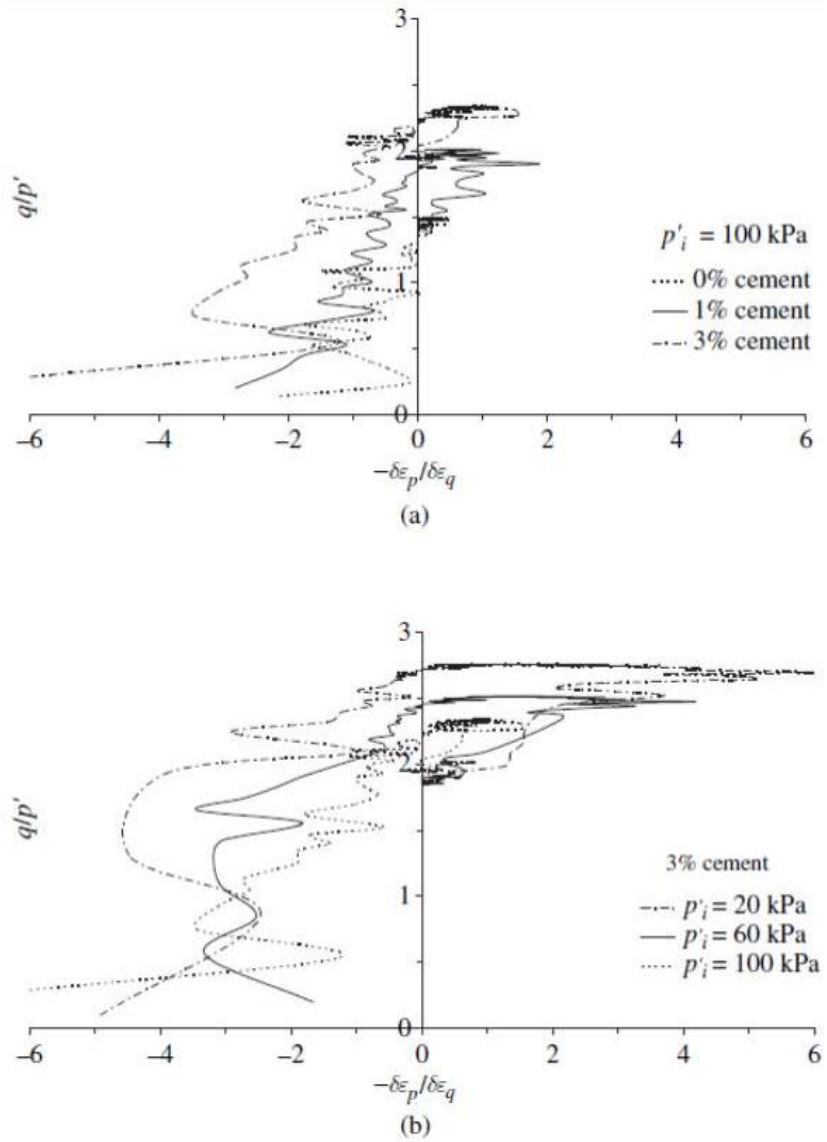

Figure 2.24 Stress-dilatancy behaviour of cemented sand: (a) effect of cement content; (b) effect of initial mean effective stress (after Yu et al. 2003)

Marri, (2010) reported the dilative behaviour of cemented sand at high pressures and concluded that cement content can effectively alter the volumetric response from contraction to dilation, and such a change is enhanced with increasing cement content. The dilative response, as expected, is suppressed by high confining pressure and this is obvious as shown in Figure 2.25

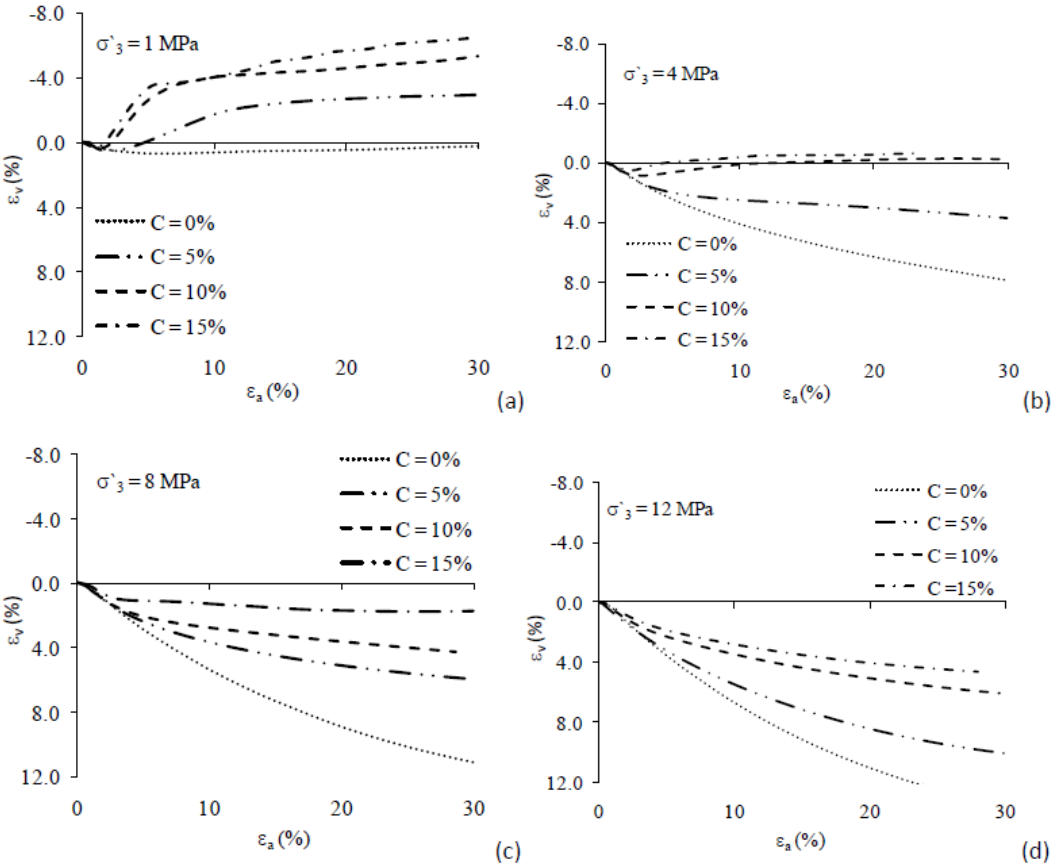

Figure 2.25 Volumetric responses of cemented sand at high pressures with cement contents 0 to 15 % at effective confining pressures of: (a) 1MPa; (b) 4MPa; (c) 8MPa; and (d) 12MPa (after Marri 2010).

2.5.2 Fibre reinforced sand

As it has been reported that the addition of cement increases dilation and an increase in pressure reduces dilation, it would be intresting to see how the addition of fibre affect the dilative behaviour of sand. Consoli et al. (1998) investigated the influence of fibre on the behaviour of sandy soil by carrying out the drained triaxial compression tests and reported that an increase in confining pressure reduces volumetric expansion as shown in Figure 2.26.

Consoli et al., (2003b) reported the results of varying fibre length, diameter, confining pressure and fibre content by carrying out drained triaxial tests. The

results showed that varying fibre length and diameter had very little effect on volumetric behaviour of fibre reinforced sand, while increasing confining pressure and fibre content reduced the dilation.

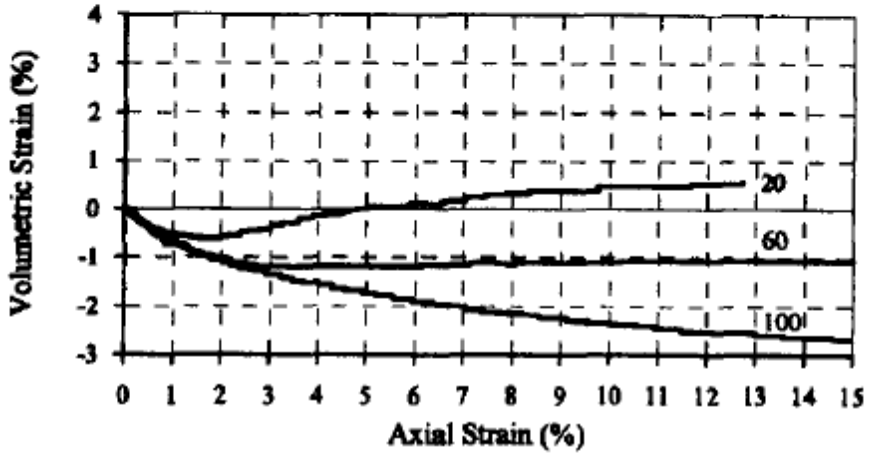

Figure 2.26 Effect of confining pressure on volumetric response for Fibre-reinforced sand (after Consoli et al. 1998).

Contrary to the above reported work which shows that increasing confining pressure reduces the dilatancy of fibre reinforced sand, (Consoli et al., 2009b) reported that the effects of fibre reinforcement (fibre length of 50 mm) on the stress–dilatancy response of the sand at confining pressures of 100kPa and 550kPa. In this range of confining stress the dilatancy is kept unchanged as shown in Figure 2.27, but the final stress ratio is reduced with increasing confining stress.

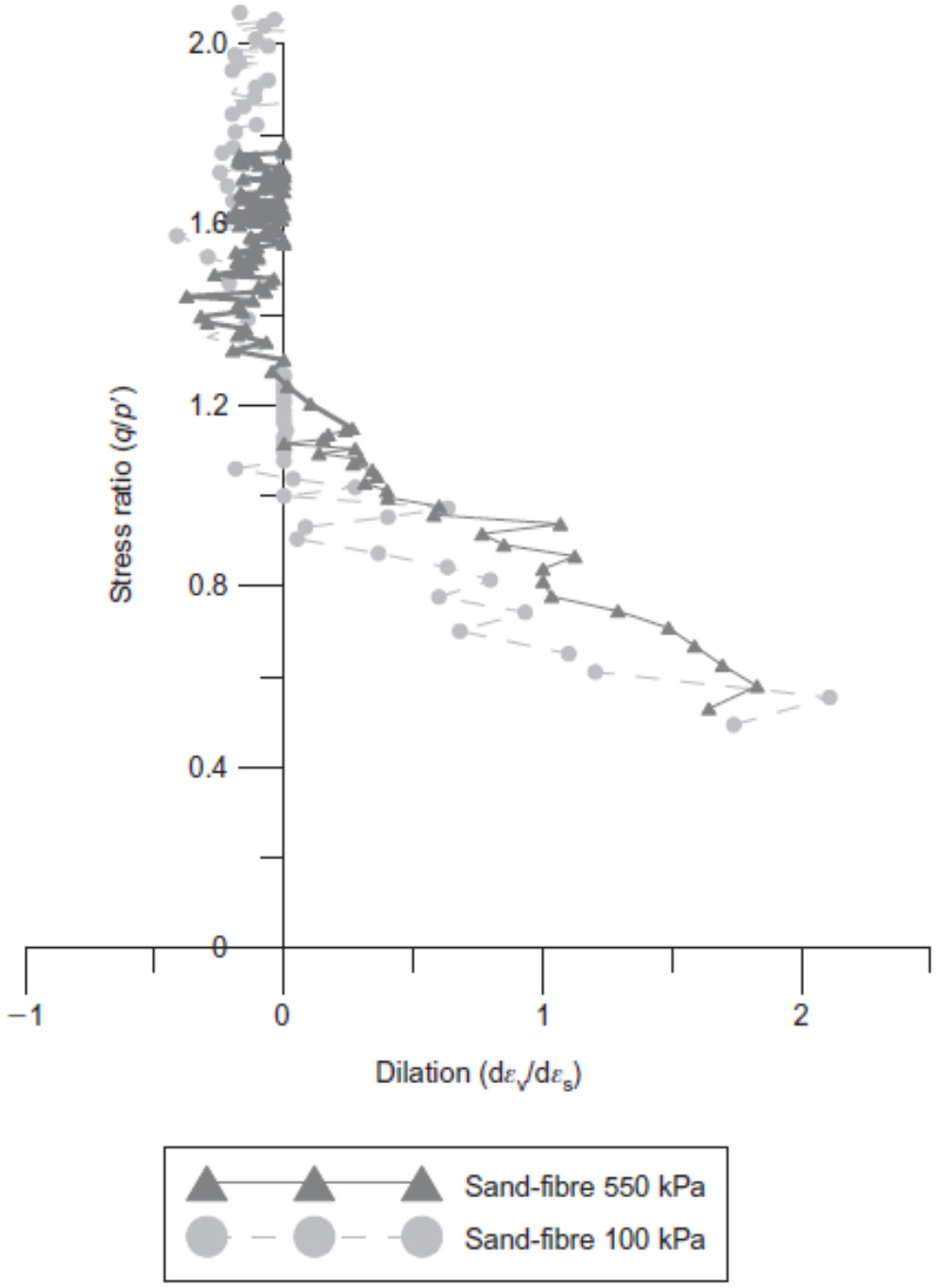

Figure 2.27 Stress ratio-dilatancy response of fibre reinforced sand with 0.5% fibre, 0.1mm diameter and 50mm length (after Consoli et al. 2009b).

Dos Santos et al., (2010a) reported that confining pressure seems to influence the dilatancy behaviour as at lower confining stress levels, the compression does not stop at reaching a rate of zero volumetric change, but is followed by a small dilation, which then reduces to reach a stress ratio equal to 2.4 as shown in Figure 2.28. Thus

at lower confining stresses, the inclusion of fibres increases the peak stress ratio, but this peak stress ratio does not correspond to the maximum rate of dilation, and rather seems to be reached at the end of dilation. At higher confining pressures, this dilation behaviour disappears so the sand–fibre composite only compresses to a stress state ratio equal to 1.33–1.6 that seems to be increasingly independent of stress level. However, the compressive part of the stress–dilatancy curve does not depend on stress level, with approach paths forming a narrow band.

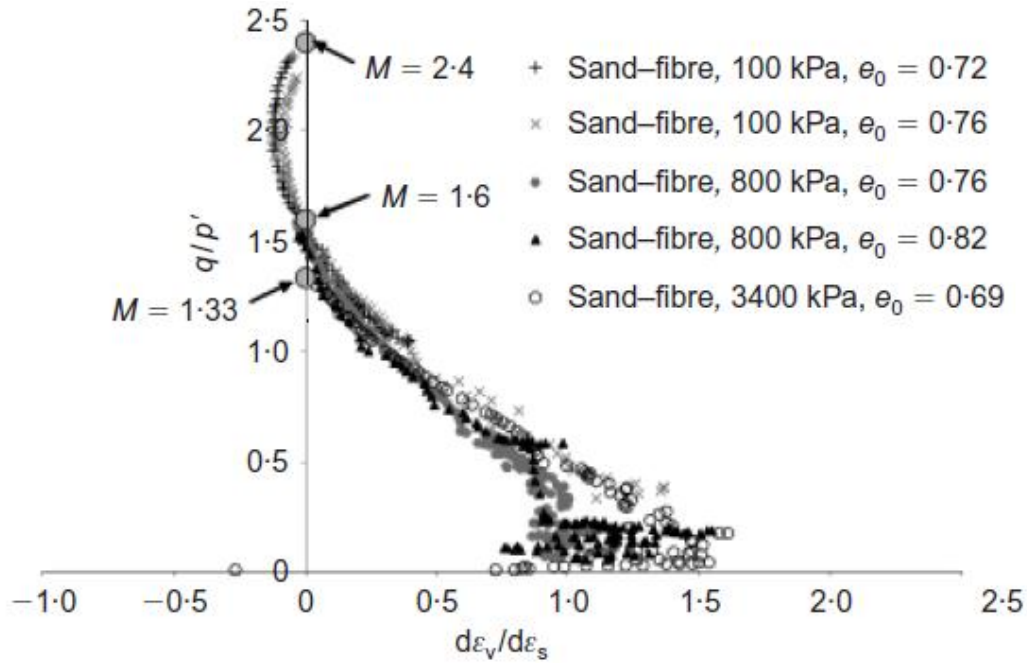

Figure 2.28 Stress-dilatancy response of fibre reinforced sand (after Dos Santos et al., 2010a).

Despite recent research in the area of fibre reinforced sands (e.g. Consoli et al. 2005, 2007a, 2007b, 2009a), there are some points that still need to be clarified, such as the outcome of using very thin to thin monofilament extensible polypropylene fibres (lengths up to 50mm) on the effective stress–strain–strength behaviour of fibre-reinforced sands under a range of confining stresses; the effect of large aspect ratios on the effective stress–strain–strength behaviour of fibre-

reinforced sands; and the effect of fibres on stress–dilatancy behaviour (Consoli et al., 2009b).

2.5.3 Fibre reinforced cemented sand

Figure 2.29 shows the stress–dilatancy response of fibre reinforced sand, as well as fibre-reinforced cemented sand (1% cement) obtained by carrying out tests on fibre reinforced cemented sand by Consoli et al., (2009c). The mechanisms of behaviour were investigated using a (q/p')–$(d\varepsilon_v/d\varepsilon_s)$ graph as shown in Figure 2.29 where the dilatancy was based on the total strains rather than the plastic component. According to Consoli et al., (2009c) a pure sand sample displayed an initially compressive behaviour, followed by a dilatant behaviour until reaching a maximum dilatancy of about -0.25, after which the rate of dilation started reducing to reach zero at the critical state (at a stress ratio of about 1.3) on the vertical axis. The fibre reinforced sand sample showed a similar maximum dilatancy, which is reached at a higher stress ratio of about 2.0. In addition, after reaching the maximum dilatancy, the value of the maximum stress ratio is seen to continuously increase with decreasing dilatancy until reaching zero at critical state, the stress ratio of about 2.4 on the vertical axis. Looking at the behaviour of the fibre reinforced cemented sand, it can be observed that it was first dominated by the bonds, with smaller compression that the uncemented fibre reinforced sand up to a stress ratio of about 1.2 as shown in Figure 2.29. After such stress ratio, the cemented sample starts to dilate reaching a maximum dilation of about -0.9 (about three times of the uncemented specimens). The change in volume associated with dilation implies that bond breakage must have occurred. Finally, the behaviour of the fibre-reinforced

cemented sand degenerated to that of the fibre reinforced uncemented sand, which must coincide with complete bond breakage.

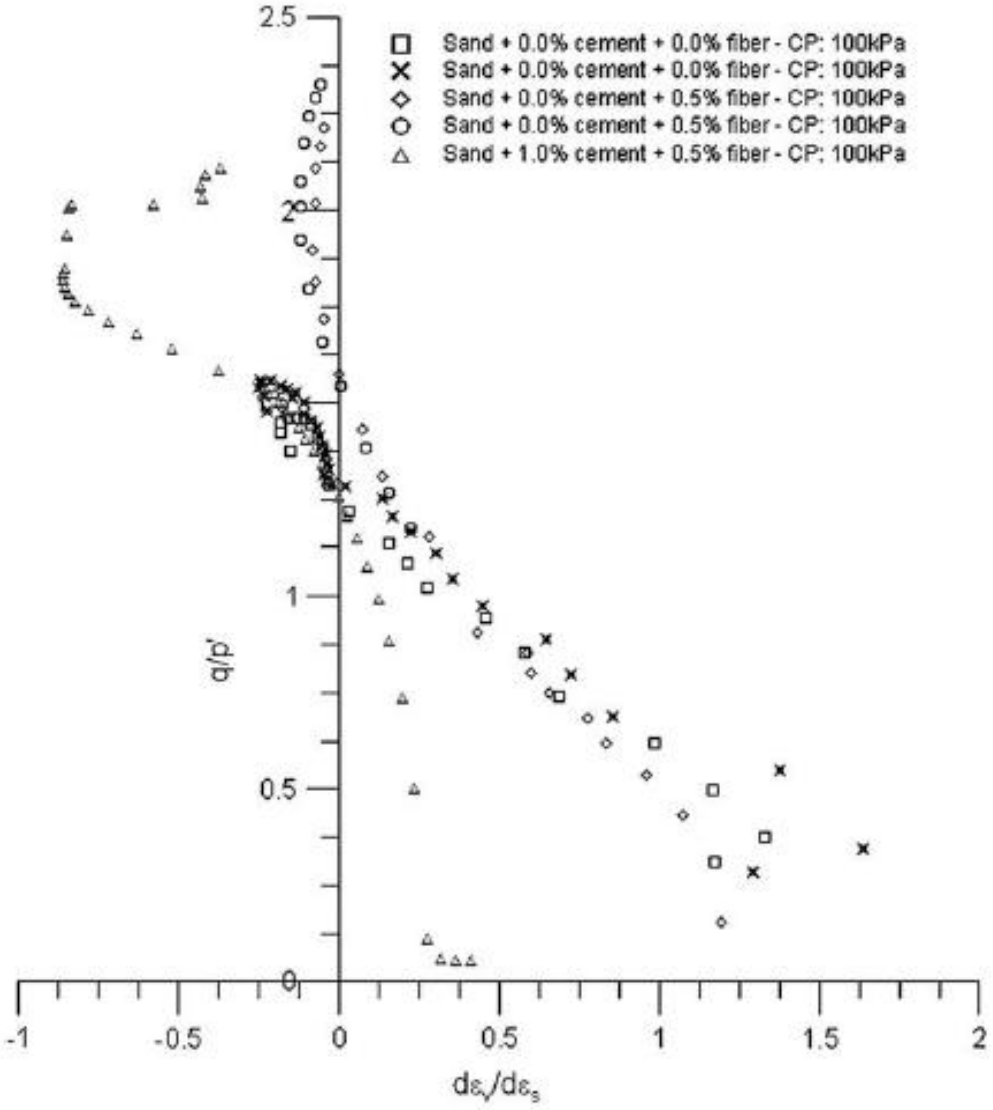

Figure 2.29 Stress–dilatancy response of sand, fibre reinforced cemented and uncemented sand sheared at confining pressures of 100 kPa after (after Consoli et al., 2009c).

A review of the literature reveals that there is very limited work available on the behaviour of fibre reinforced cemented sand particularly on the dilative behaviour. Therefore, more experimental work is needed to elaborate the dilative behaviour of fibre reinforced cemented sand with varying cement and fibre content and under a

wide range of confining pressures, as it would be interesting to see how fibre reinforced cemented sand behaves under increasing confining pressures.

2.6 Effect of reinforcement on critical state of sand

The state of the soil at which axial deformation occurs without any change in volumetric strain (constant volume strain) is known as the critical state. If several samples of the same soil are tested at different initial densities it is found that, if p` is constant, all the samples fail at the same void ratio. If the deformation is allowed to continue the sample will remain at the same void ratio and only deform by distortion. All critical states, for a given soil, form a unique line called the Critical State Line (CSL) defined by the following equations in q-p' and v-p' planes:

$$q = Mp' \tag{2.7}$$

$$v = \Gamma - \lambda \ln (p') \tag{2.8}$$

where,

M = the effective stress ratio at critical state

Γ = specific volume v, of critical state at which p' is a unit pressure

λ = it is the slope of critical state v-p' plane

M and Γ are constant for a particular soil. They determine the slope of the CSL in the q-p' and the location of the CSL in the v-ln(p') plot as shown in Figure 2.30. The constant volume (or critical state) shear strength is said to be intrinsic to the soil, and independent of the initial density or packing arrangement of the soil grains.

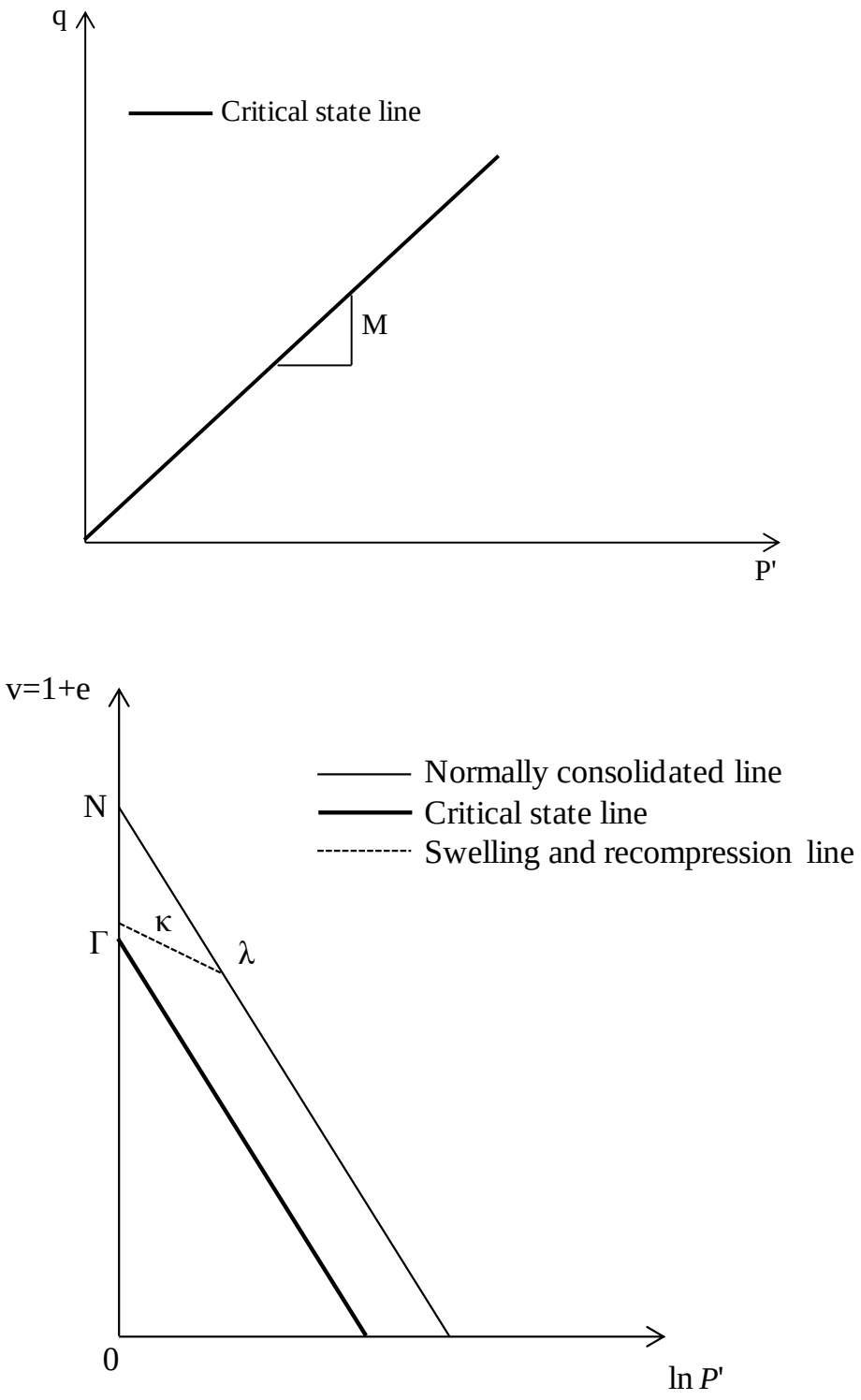

Figure 2.30 Critical state lines parameter in q-p’ and v-p’ planes.

The notion of critical state in granular materials was introduced in connection with observations that granular materials tend to reach the same void ratio in the course

of shear deformations, irrespective of the initial void ratio. Dense granular materials reach the critical state as a result of dilation, while loose materials tend to reach the same state after volumetric contraction (Kruyt and Rothenburg 2006).

In triaxial tests, soils reach critical states where they continue to distort at a constant state i.e. with constant effective stresses and constant volume. The critical state line represents the final state of soil samples in triaxial tests when it is possible to continue to shear the sample with no change in imposed stresses or volume of the soil. If several samples of the same soil are tested at different initial densities it is found that, if p' is constant, the samples all fail at the same void ratio, giving a unique shearing stress *q*. Thus for plotting CSL at one relative density different samples of the same soil should be tested at different confining pressures, so that different critical state values for the same soil. A plot of these critical states will be the critical state line.

Mooney et al., (1998) reported that characterizing the behaviour of soil near and beyond peak stress levels has proven to be quite challenging due to the development of shear banding making experimental data difficult to reduce. As a consequence, the existence of a critical state to which a soil deforms irrespective of initial state, remains unclear. Many aspects related to critical state are presently not well understood, even empirically. A micromechanical theory of the critical state is not even in its infancy yet (Rothenburg and Kruyt, 2004).

2.6.1 Cemented sand

Coop and Atkinson (1993) defined the critical state line for cemented sand in a double logarithmic scale i.e. ln(q)-ln(p'). They showed that the critical state line for cemented sand is a little lower than that of uncemented sand. They argued that lower critical state parameters of cemented soil may be due to the cement adhering to the sand particles after yield. However Cuccovillo (1999) reported that structure does not affect the critical state characteristics of the sandy soil at the q-p' space. The difference between these researches was attributed to the different soil fabric, soil structure and cement type (Hamidi, 2005). Hamidi (2005) also reported in their study that a unique line can be assigned to the points associated with the uncemented soil with a very low scatter in contrast to the large scatter in cemented soil, as shown in Figure 2.31.

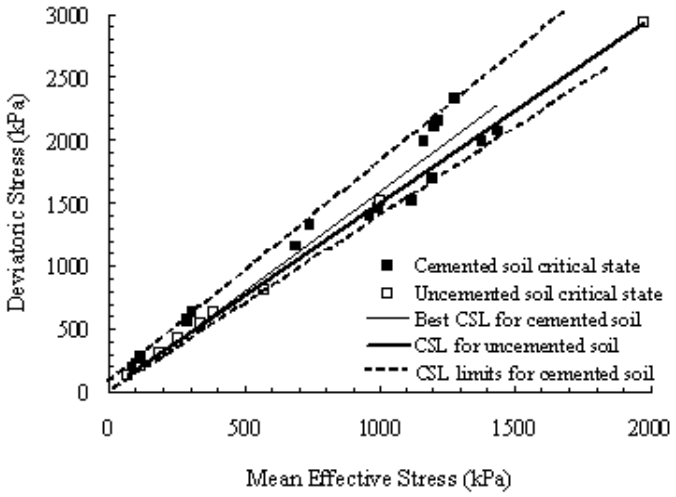

(a)

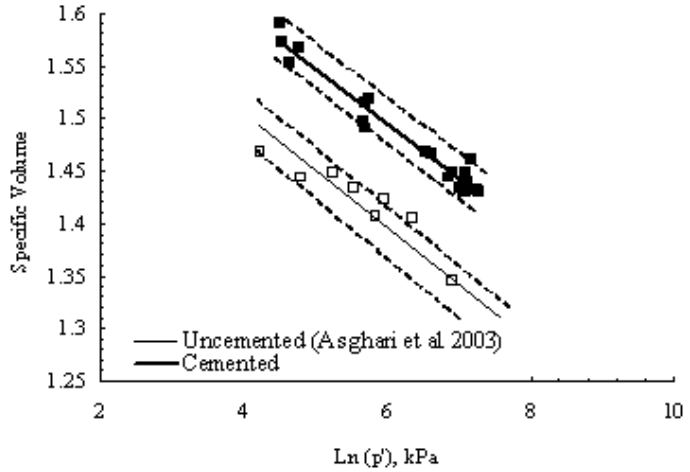

(b)

Figure 2.31 Critical state lines and its limits for cemented and uncemented soils; (a)q-p' plane, (b) v-ln(p') plane (after Hamidi, 2005).

Kasama et al., (1998) reported that when the soil is normally consolidated the critical state of geomaterial can be considered as a failure state. In the failure state of a geomaterial with cementation, the effect of cementation ought to make the strength of soil increase and extend the domain in which it can exist as shown in Figure 2.32.

Futai et al. (2004) stated that sometimes critical state conditions could not be achieved, thus large strain data close to critical state should be used. Also, Schnaid et al., (2001) reported that it must be recognized that the complete determination of the ultimate or critical state in a p'-q-e space presents some experimental difficulties, given the brittle behaviour and the strain localization observed for cemented specimens. This problem is commonly reported in the literature, especially for conventional triaxial tests.

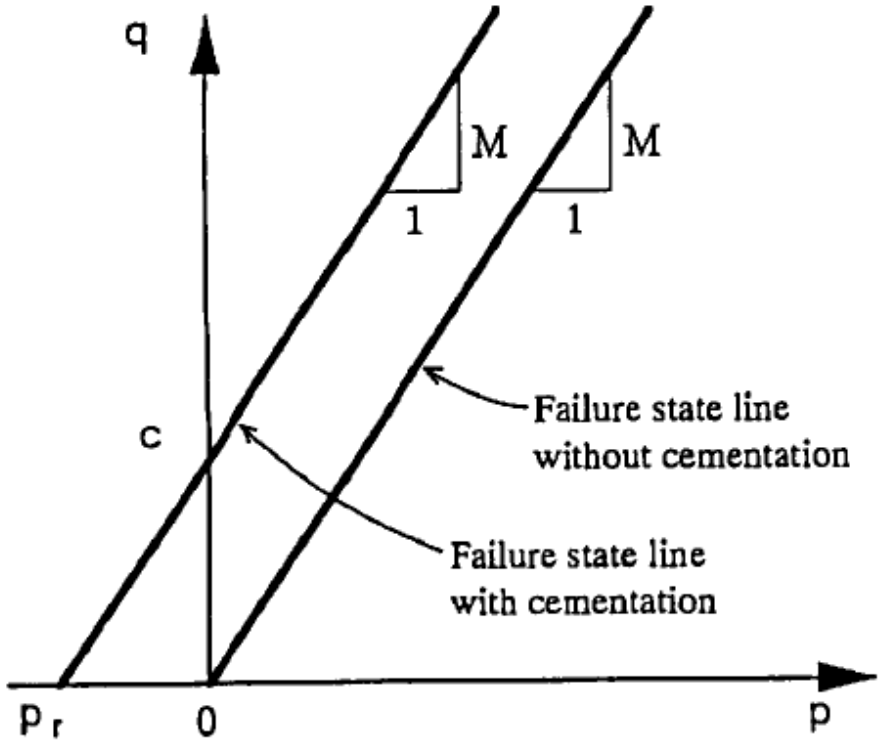

Figure 2.32 A schematic diagram of failure state line with cementation effect (after Kasama et al., 1998).

2.6.2 Fibre reinforced sand

Dos Santos et al., (2010a) mentioned that studies reported in the literature have generally been conducted independently and have not always been consistent, with the consequence that for a topic so wide it has been difficult to build a unified framework that could be linked to the critical state framework. In fibre reinforced sand, there is the additional difficulty that the fibres can deform and break. A 'true' critical state will be reached when sand particles and fibres cease to deform and break. For the purpose of developing a useful critical state framework, it has been necessary to identify representative lines at large strains, where reasonably constant stress and volume were found with continuous shearing. It is clear that the volumetric strain had not stabilised at the end of all tests. The deviatoric stress was, however, found to be constant at the end of nearly all tests, and the end points for

these tests provided reliable points to derive a critical state line in the stress plane. The end points of the stress-strain curves were used to plot the critical state line as shown Figure 2.33. Gray & Ohashi (1983), Gray & Al-Refeai (1986) and Maher & Gray (1990) reported the bilinear failure envelope for other sand-fibre combinations, although steady states were less identifiable from their data. A simple exponential equation was proposed for the variation of the gradient M of the CSL of fibre reinforced sand. In kPa units, the expression for M is

$$M = 1.22\,[1 + \mathrm{e}^{-(\mathrm{p}'/2600)}] \tag{2.9}$$

According to Eq 2.9, M=2.4 at p'=0 kPa, M=1.33 at p'= 6000 kPa, and converges to the value of M for the pure sand (M=1.22) at larger stresses.

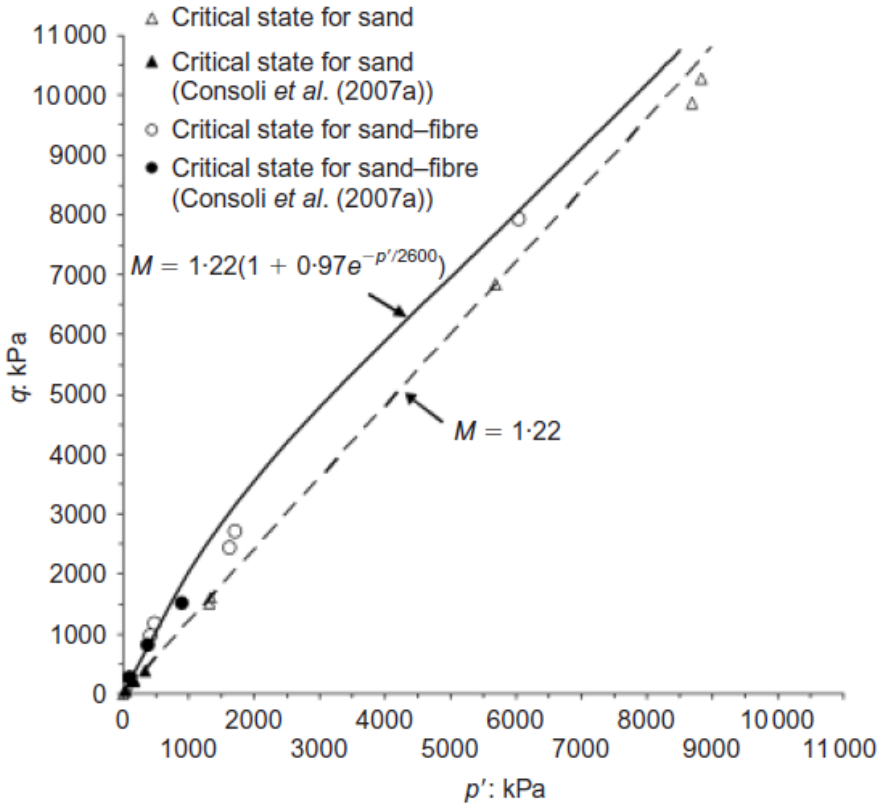

Figure 2.33 Critical state lines for sand and fibre reinforced sand in q-p' plane (after Dos Santos et al., 2010a).

From the review of literature it can be concluded that there is either scarcity or lack of reported literature on the framework of critical state particularly on the behaviour of fibre reinforced cemented and uncemented sand. Therefore it would be interesting to see how varying the fibre and/or cement content in the sand effect the critical state framework at low to high confining pressures.

2.7 Effect of reinforcement on yielding of sand

The yield strength or yield point of a material is defined in engineering and materials science as the stress at which a material begins to deform plastically. Prior to the yield point the material will deform elastically and will return to its original shape when the applied stress is removed. Once the yield point is passed some of the deformation will be permanent and non-reversible. In the three-dimensional space of the principal stresses (σ_1, σ_2, σ_3), an infinite number of yield points form together a yield surface. Classically, the term 'yielding' refers to the transition from elastic to plastic behaviour, and is associated with sharp curvature developing in a stress-strain relationship that had been linear up to that point (Kuwano and Jardine 2007). Leroueil and Vaughan (1990) defined yield stress as a stress state at which a material shows a discontinuity in stress-strain behaviour. They also suggested that yield is best identified from the stress-strain curve when plotted on a natural or log-log scale. Karner et al. (2003) described yielding as a four stage scheme. In the first stage, soils exhibit linear elastic behaviour with completely reversible strain up to a 'yield' stress level analogous to an elastic limit. In the second stage, strains are still recoverable but the loading path becomes nonlinear providing an apparent decrease in material stiffness. The third stage is marked by the onset of non

recoverable strain, a feature considered to define material yield. Permanent strains increase in magnitude during this stage as the applied stresses become greater. This third stage is limited by the failure envelope for the soil which, in turn, corresponds to an abrupt and significant change in volumetric strain rates. The fourth, and final, stage is marked by deformation in what can be considered as a 'post failure' region.

2.7.1 Cemented sand

The primary yield is the point at which breakage of the cement bonds commences and is considered to be when, in the linear scale, the stress-strain curve deviates from the initial linear behaviour. This definition is consistent with that used in other work e.g. (Wang and leung, 2008). Maccarini (1987) in his study of an artificially bonded soil identified a first yield at the end of the linear part of the deviator stress versus axial strain and a second yield as the point of maximum curvature on the same graph plotted at natural scale. Bressani (1990) used the same plot on a log-log scale in an attempt to identify a clearer change in behaviour. Coop and Atkinson (1993) studied the behaviour of an artificially cemented carbonate sand and identified yield from a discontinuity in the stress-strain curve, at an axial strain ε_a = 0.3-0.7%. Airey (1993) carried out conventional and stress path triaxial tests to examine the behaviour of natural calcarenite soils. He suggested that the cementation increases the shear modulus and the size of the yield locus; however, its effects on the volumetric response are negligible. Malandraki (1996) identified four zones of behaviour for an artificially bonded soil under shear in triaxial compression. In the first zone the bond entirely control the soil behaviour at failure. In the second transitional zone the bonds only partially control the soil's behaviour.

In the third and fourth zone the soil's behaviour at failure is independent of bonding and its behaviour is governed by that of the destructed material. However the second yield occurs under shear in the third zone and under isotropic compression in the fourth zone. Malandraki (1996) further states that identifying second yield has proved to be rather important as it better clarifies the behaviour of bonded soils under shear. If the final yield alone is identified, the second transitional zone of behaviour is masked. It is suggested that yield should be defined based on changes in stiffness from the tangential stiffness versus axial strain graph.

2.7.2 Fibre reinforced sand

Consoli et al. (2003b) conducted triaxial tests and reported the effect of fibre content, length and diameter on the behaviour of fibre reinforced sand. They concluded that under loading-unloading conditions, strains were predominantly irreversible or plastic. Reloading strains were basically reversible or elastic. After reloading when stresses reached once again the yield locus, the material hardened at the same rate observed previously to unloading.

There are no published work covering the yielding behaviour of fibre reinforced cemented and uncemented sand. Therefore it would be important to investigate how varying the fibre and/or cement content in the sand effect the yielding at low to high confining pressures.

2.8 Summary

This literature review explores the work carried out on investigating and understanding the behaviour of sand, cement, fibre composites. The behaviour of

sand, cemented sand and fibre reinforced cemented sand was reviewed regarding the compressibility, shear behaviour, failure characteristics, stress dilatancy, critical state and yielding. It can be concluded that

1) A lot of work has been done on uncemented and cemented sand covering a wide range of parameters, cement content and confining pressures. There is also some reported work on fibre reinforced sand but very little has been reported on fibre reinforced cemented sand.
2) The effect of the addition of fibre in sand and cemented sand on isotropic compression behaviour of sand is that there are two distinct and parallel normal compression lines for sand and fibre reinforced sand. Both linear and curved normal compression lines were reported. However, later (dos Santos et al., 2010b) reported that normal compression lines for fibre reinforced cemented and uncemented sands tend toward a unique normal compression line rather than two distinct and parallel line for each material. Furthermore, there is limited date available for fibre reinforced cemented or uncemented sand for isotropic compression behaviour. Therefore, more experiments are needed to understand the fundamental mechanism and to validate or modify existing theories for varying fibre and cement content.
3) It was noted that there is general consensus that the addition of fibre into sand or cemented sand increases the peak deviatoric stress. Peak strength, stiffness, brittleness, and residual response are changed as a consequence of either separate or the joined effects of fibre and cement inclusions. An increase in fibre content leads to increasing strain at failure and,

consequently, to a more ductile behaviour. The composite behaviour is governed by the fibres and cement content, mechanical and geometrical properties of fibres and confining pressure.

4) Addition of fibres result in an increase of the friction angle and cohesion intercept of sand. The failure mechanism in fibre reinforced soil is such that below a certain confining or normal pressure, called critical confining pressure, failure occurs by slipping of the fibres and lack of adhesion within the soil mass. At confining pressure above the critical level, the soil normally fails before the fibre. One of the main advantages of randomly distributed fibres is the maintenance of strength isotropy and absence of potential failure plane, which can develop parallel to the oriented reinforcement. For higher cement contents the stiffness of the cement governs strength and stiffness characteristics.

5) Varying fibre length and diameter had very little effect on volumetric behaviour of fibre reinforced sand, while increasing confining pressure and fibre content reduced the dilation. A review of the literature reveals that there is very limited work available on the behaviour of fibre reinforced cemented sand particularly on the stress-dilatancy. Therefore, more experimental work is needed to elaborate the dilative behaviour of fibre reinforced cemented sand with varying cement and fibre content and under wide range of confining pressures as it would be interesting to see how fibre reinforced cemented sand behaves under increasing confining pressures.

6) From the review of literature it can be concluded that there is either scarcity or lack of reported literature on framework of critical state particularly on

the behaviour of fibre reinforced cemented and uncemented sand. Therefore it would be interesting to see how varying the fibre and/or cement content in the sand effect the critical state framework at low to high confining pressures.

7) There are very few published pages covering the yielding behaviour of fibre reinforced cemented and uncemented sand. Therefore it would be interesting to investigate how varying the fibre and/or cement content in the sand effects the yielding at low to high confining pressures.

CHAPTER 3

METHODOLOGY

3.1 Introduction

The advantage of the triaxial test is its replication of real conditions: the failure plane is no longer conditioned by the apparatus itself but develops along the plane of lesser resistance within the sample. The control of drainage and pore pressure allows the study of the effect fluids have on the mechanical properties of the material in the sample. The triaxial test also allows measurement of radial strain of the sample under load, a feature not present in consolidation tests performed with oedometers. Different types of loading conditions can be tested and many different soil properties can be found, for instance shear strength and internal friction angle.

The basic requirements for reliable triaxial testing are controlled specimen preparation to ensure reproducible initial state, complete saturation of the specimen, well centred axial load, negligible friction on the loading ram, well-controlled cell and pore pressures, and accurate measurements of axial load, axial deformation, and volumetric change.

3.2 Materials

3.2.1 Sand

On the basis of previous investigations carried out in University of Nottingham for both uncemented and cemented sand, Portaway sand from Sheffield, England;

consisting of subangular and sub rounded grains as shown in Figure 3.1 has been taken as the base material for the preparation of the specimens.

Figure 3.1 Scanning electron microgtaph of Portaway sand.

The washed, oven dried and sieved sand, passing through 2.0 mm and retaining on 63 μm, is the fraction of the material that was selected for subsequent investigation. Table 3.1 and Figure 3.2 indicate the gradation and index properties of the material respectively.

Table 3.1 Index properties of Portaway sand (after Marri 2010)

Characteristic	**Value**
Effective grain size $D_{10:}$ mm	0.19
D_{30}: mm	0.295
Mean grain size D_{50}: mm	0.393
D_{60}: mm	0.42
Uniformity Coefficient D_{60} / D_{10}	2.21
Specific Gravity, G_s	2.65
e_{max}	0.79
e_{min}	0.46

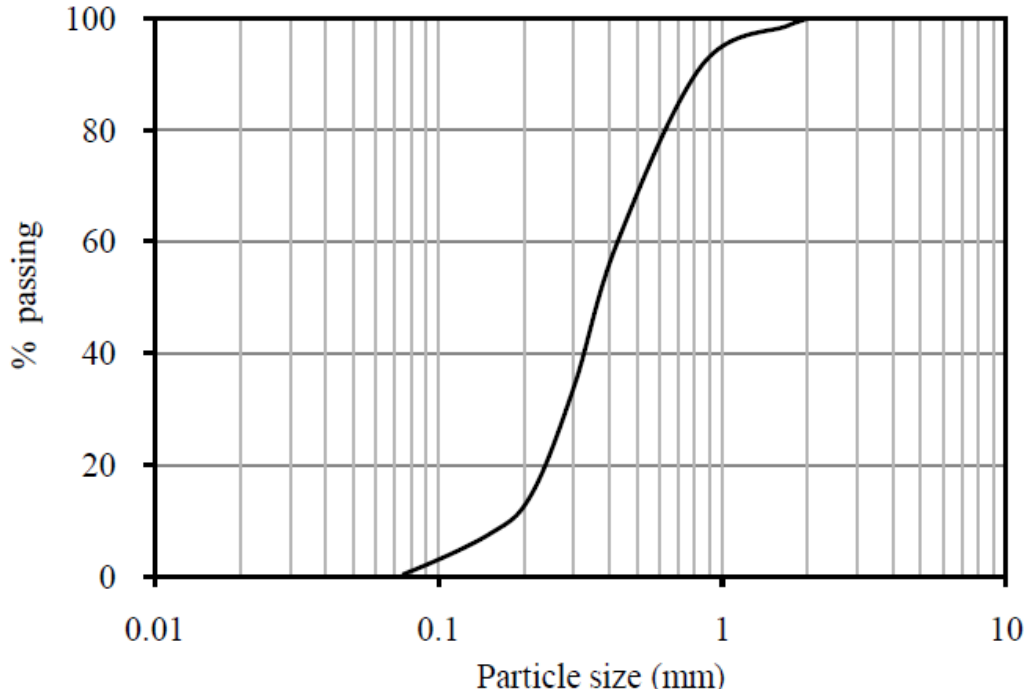

Figure 3.2 Gradation curve of sand

3.2.2 Cement

Ordinary Portland cement has been used throughout this study, as it has been used frequently in the previous researches. The specific gravity of Portland cement is generally around 3.15

3.2.3 Fibres

Polypropylene fibres shown in Figure 3.3, are used as the reinforcing material throughout the study. The length and diameter of the polypropylene fibres used in current investigations are 22mm and 0.023mm, respectively.

Polypropylene fibre is one of the most widely used inclusion in the laboratory testing of soil reinforcement e.g. (Consoli et al., 2003b, Consoli et al., 2003a, Michalowski and Cermak, 2003, Consoli et al., 2004, Consoli et al., 2005, Park and Tan, 2005, Cai et al., 2006, Consoli et al., 2007, Consoli et al., 2009).

Figure 3.3 Polypropylene fibres

Polypropylene is one of those most versatile polymers available with applications, both as a plastic and as a fibre, in virtually all of the plastics end-use markets. Polypropylene is a plastic polymer, of the chemical designation C_3H_6. It is used in many different settings, both in industry and in consumer goods. The general properties of the fibre used is given in Table 3.2

Table 3.2 Physical and mechanical characteristic of fibre

Characteristic	**Value**
Specific gravity: G_s	0.91
Elastic modulus: GPa	8
Tensile strength: MPa	300
Diameter: μm	23
Length: mm	22
Failure strain: %	80

3.3 Sample preparation

The quantity of sand and cement required for sample was mixed thoroughly in 10% water content; the exact weight of fibre was than mixed into the sand cement paste in four equal proportions to get the homogenous mixing of fibre. The targeted dry unit weight of the material for a standard size specimen was maintained.

The method of undercompaction proposed by Ladd (1978), in which each layer is compacted to a selected percentage of the required dry unit weight of the specimen, has been used throughout this study. The method has the following advantages

1) It results in a relatively uniform stress-strain response
2) It reduces the chances of particle segregation
3) It is useful for most types of soil

The total weight of material required for sample preparation was calculated by following equation

$$W_T = \gamma_d (1+ \omega) \times V/g \qquad (3.1)$$

Where

W_T = total dry weight in grams

γ_d = dry unit weight of soil in kN/m^3

V = volume of the mould in mm^3

ω = water content in %

g=9800mm/s^2

The total material required for each layer was

$$W = \frac{W_T}{n_t} \tag{3.2}$$

The percentage undercompaction for the 1st layer, U_{ni} was chosen as 0%. The correct value of U_{ni} can be determined by measuring the dry unit weight of the prepared test specimen as a function of its height. A dry unit weight not uniform with height indicates an inappropriate value of U_{ni}.

Each subsequent layer received a lesser percentage of undercompaction calculated from the relationship

$$U_n = U_{ni} - \left[\frac{(U_{ni} - U_{nt})}{n_t - 1} \times (n-1)\right] \tag{3.3}$$

U_{ni} = percent under compaction selected for 1st layer

U_{nt} = percent under compaction for final layer usually zero

n = number of layers being considered

n_i = first layer

n_t = total number of layer (final layer)

The required height of the specimen at the top of the nth layer

$$h_n = \frac{h_t}{n_t}\left[(n-1) + \left(1 + \frac{U_n}{100}\right)\right] \tag{3.4}$$

Where,

h_n = Height of compacted material at the top of the layer being considered

h_t = Final (total) height of the specimen

n_t = Total number of layers, n = Number of the layer being considered

U_n = Percent undercompaction for layer being considered, for dense specimen the Uni is taken as 0%.

Latex and neoprene membranes were used to enclose the specimens. The thickness of the latex and neoprene membrane is 0.25 mm and 0.5 mm respectively. The elastic modulus E for latex is reported as 1100kPa (Donaghe et al. 1988).

3.3.1 Fibre reinforced sand sample

1) Conventional pressure

In Figure 3.4, the photographs of various stages of sample preparation for fibre reinforced uncemented sand for conventional triaxial testing system are given. The pedestal base as shown in (a) was lubricated with silicon grease to provide an airtight connection with the latex membrane. The latex membrane was then provided on the pedestal base as shown in (b). With the help of an o-ring stretcher, the o-rings were mounted to provide an airtight grip as shown in (c) and (d). The split mould was then mounted and tightened with clamping ring as show in (e) and (f). Top o-rings were slipped over the split mould with the help of the o-ring stretcher and then the membrane was stretched carefully to release crease from inside to provide smoother inner surface as shown in (g), (h) and (i). Prior to pouring the sand fibre mix into the mould, the bottom porous stone and filter paper were placed and vacuum suction was applied to keep the membrane stretched and crease free as shown in (j). The mixture was then filled in three layers and each layer was tamped to a required number of blows as per the procedure of undercompaction. Prior to the placement of the next layer, the surface was well scratched to avoid layering. After the final layer, the surface was levelled prior the placement of the top porous stone as shown in (k). Filter paper and the top porous stone were put on the top as shown in (l). The top cap was lubricated with silicon

grease and placed on the top as shown in (m). The folded membrane was then stretched over the top cap carefully and then the o-rings were glided over the top cap and membrane to create a watertight connection as shown in (n). The top drainage wall was closed and a slight suction was applied through bottom drainage wall to keep the sample intact prior to the removal of the split mould and then the mould was removed as shown in (o). The triaxial cell was mounted over the cell base and was provided with necessary connections.

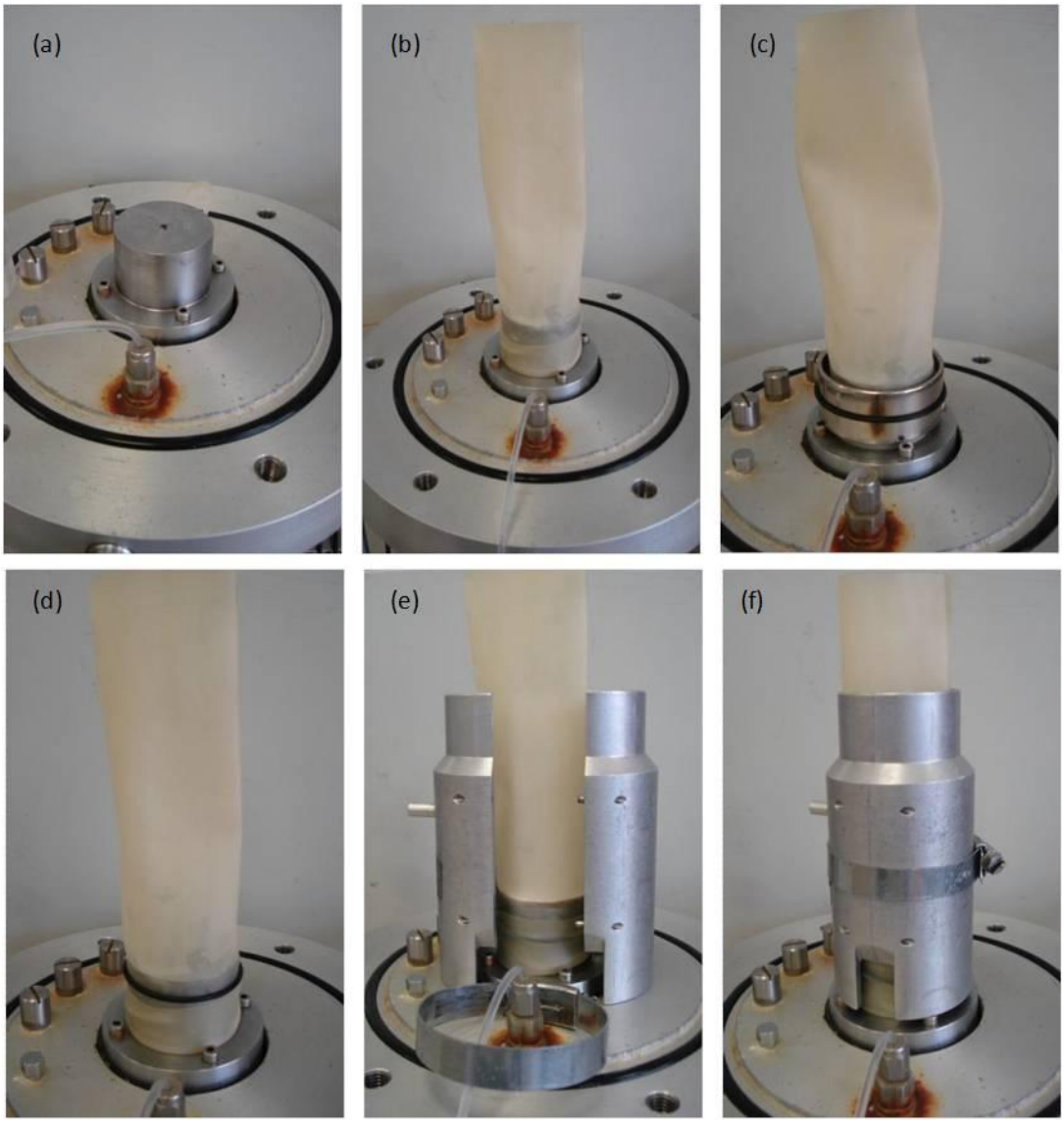

Figure 3.4 The sequential steps for the preparation of uncemented samples for conventional triaxial testing from: (a) to (o).

2) High pressure

In Figure 3.5, the photographs of various stages of sample preparation for uncemented fibre reinforced sand for high pressure triaxial testing system are given. Most of the steps of high pressure test setup were similar to that of conventional pressure triaxial testing system. A further brief description is given here. The pedestal base was lubricated with silicon grease to provide an airtight connection with the neoprene membrane. The neoprene membrane was then mounted on the pedestal base as shown in (a). A split mould was then provided and tightened with clamping ring and the top extended portion of the membrane was stretched and rolled over the top portion of split mould as show in (b). Prior to pouring the sand-fibre mix into the mould, the bottom porous stone and filter paper were placed and vacuum suction was applied to keep the membrane stretched and crease free. The fibre reinforced sand was then filled in layers and each layer was tamped to a required number of blows as per the procedure of undercompaction. Prior to the placement of the next layer, the surface was well scratched to avoid layering. Prior to the placement of filter paper and top porous stone, the surface was levelled.

In order to avoid testing failures due to membrane damage and puncture at high pressures, double membranes were provided to the specimens. The top and bottom edges were covered with thin strips of membrane as shown in Figure 3.6. In the case of providing a double membrane the split mould was re-moved and the second membrane was put on the first membrane with the help of membrane stretcher as shown in (d). Bottom o-rings were put with the help of o-ring stretcher.

The top o-rings were left on the o-ring stretcher at the bottom of the sample. The mould was mounted again. The extended membrane was folded over the split mould. Filter paper and top porous stone were put on the top and the top cap was lubricated with silicon grease and placed on the top porous stone. Folded membrane was then stretched over the top cap carefully as shown in (e). The split mould was then removed as shown in (f) and then the o-rings were glided over the top cap and membrane to create a water tight connection as shown in (g), (h) and (i). The specimen ready to put into the cell is shown in (j).

Figure 3.5 The sequential steps of the preparation of uncemented samples for high-pressure testing from: (a) to (j).

For high pressure triaxial tests the cured sample was set on the base pedestal of a standard triaxial cell. With the cell base on a flat and level surface the cell top assembly was lowered slowly into place, taking care to manually guide it over the seal and to ensure it descends vertically. Once the cell top was in place, the three clamp ring parts and retaining ring were placed as shown in Figure 3.7 . Care was taken not to damage the parts on assembly.

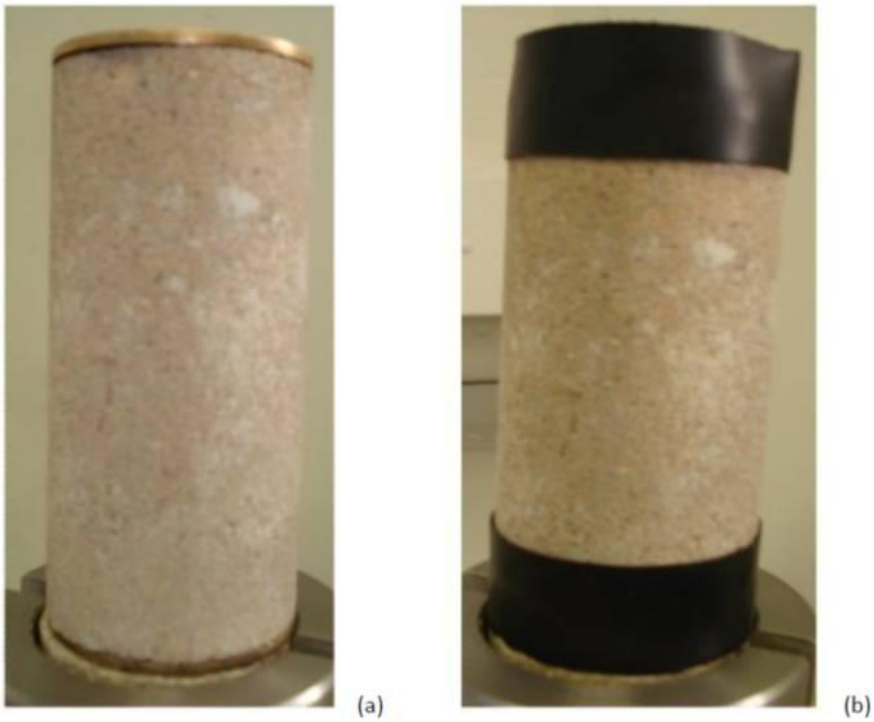

Figure 3.6 Avoiding membrane puncture: (a) the top and bottom edges of the specimen; (b) Membrane strip provided to avoid penetration and puncture at sharp edges.

Figure 3.7 Placement of clamp rings and retaining ring

The cell was then moved and placed on to the loading frame and was connected to the base. Once all of the connections were made, the cell was filled with water.

3.3.2 Fibre reinforced cemented sand

Washed and oven dried Portaway sand passing 2.0 mm and retaining on 63 μm was taken in a predetermined quantity needed for sample preparation. The proposed

proportion of cement content i.e. 2%, 5% and 10%, by weight of dry sand was taken and mixed until a uniform consistency was achieved. Water was added in accordance with optimum moisture content (10%) and mixed until a homogeneous paste was created. The mixture was stored in a covered container to avoid moisture loss before subsequent placement and compaction. Two small portions of the mixture were also taken for moisture content determination.

A cylindrical PVC split mould 5 cm in diameter and 10 cm in height and the method of undercompaction as described above was used for pouring and compaction. The time it took to prepare mix and compact was within the initial setting time of Portland cement. The sample was allowed to cure inside the mould for 24 h at 20^{o}C. After removal from the mould, the samples were cured for a further two weeks in a humid room at 23 °C ±2 °C and relative humidity above 95%.

During the mixing process, water was added to the cement-sand mix prior to adding the fibres, to prevent floating of the fibres. Fibre was mixed in four equal parts to get a consistent and uniform mix. The same method of undercompaction described above was used for placing and compaction of the mix. Visual examination of prepared specimens showed the mixtures to be satisfactorily uniform.

As the specific gravity of sand (G_{sand}), cement (G_{cement}) and fibre (G_{fibre}) and also the mass of solid (M_{solid}) are already known. The average specific gravity of the specimen G (taking cement content = C % and fibre content = F %) was calculated from the equation below. The average specific gravity of the specimen

$$G = \frac{100 - C - F}{100} \times G_{sand} + \frac{C}{100} \times G_{cement} + \frac{F}{100} \times G_{fibre} \qquad (3.5)$$

The volume of solid (i.e., sand + cement+ fibre) V_{solid}

$$V_{solid} = \frac{M_{solid}}{G \times \rho_w} \tag{3.6}$$

The total volume of the specimen V_{total} can be calculated from following equation by knowing height H and diameter D of the specimen

$$V_{total} = \frac{\pi}{4} D^2 \mathrm{H} \tag{3.7}$$

The volume of voids V_{voids}

$$V_{voids} = V_{total} - V_{solid} \tag{3.8}$$

The initial void ratio of the specimen e

$$e = \frac{V_{voids}}{V_{solids}} \tag{3.9}$$

As the volume of the mould is the same, let's suppose V; therefore, to get a fixed dry density, γ_d , the dry mass should also be a fixed value for different percentages of cement. If M_{total} is the total mass of sand + cement+ fibre and C & F are the percent of cement and fibre by dry weight of sand then:

The mass of sand M_{sand}, mass of cement M_{cement} and mass of fibre M_{fibre} can be calculated as follow:

$$M_{sand} = \left(\frac{100}{100 + C + F}\right) M_{total} \tag{3.10}$$

$$M_{cement} = \left(\frac{C}{100 + C + F}\right) M_{total} \tag{3.11}$$

$$M_{fibre} = \left(\frac{F}{100 + C + F}\right) M_{total} \quad (3.12)$$

Where C and F are taken in percentage

3.3.3 Specimen preparation for SEM analysis

Reduced size samples of 50 mm diameter and 20 mm high with constant dry density at cement content of 5% and 0.5% fibre content were prepared following the similar procedure as was adopted for the specimens prepared for triaxial testing. Fibres and cement of required percent by dry weight of sand was mixed. The prepared specimens were then kept covered to avoid the moisture loss. The specimens were then prepared in a mould of known volume provided with a transparent sheet inside to avoid sticking of the material once cured. The dry unit weight was assured by taking the known moist weight of the material and known moisture content. The material was compacted applying the method of undercompaction. The specimens were left in the mould covered with moisture tight plastic bags overnight and then taken out and kept in the moisture control room for curing up to 14 days.

The dried middle parts of the isotropically consolidated and consolidated drained and undrained sheared specimens of 50mm diameter were taken for subsequent investigation for their micromechanical analysis and were analysed uncoated. The surface was cleaned and loose particles were blown away before mounting the specimen. 20kV accelerating voltage was used and working distances were varied accordingly.

3.4 Test setup

A GDS Bishop-Wesley conventional pressure and GDS high-pressure triaxial apparatus were used for triaxial testing. The detail features, working mechanism and test setup of these apparatus are described here in detail.

3.4.1 Bishop-Wesley triaxial system

The GDS Bishop-Wesley triaxial testing system is as shown in Figure 3.8 and schematically in Figure 3.9. The system uses GDSLAB Windows software, the Bishop & Wesley triaxial cell, and is based on Standard 3MPa pressure/volume controller. Three of these pressure controllers link the computer to the test cell as follows:

1) One for axial stress and axial displacement control.
2) One for cell pressure control.
3) One for setting back pressure and measuring volume change.

All control and data logging is built into the system via GDSLAB software.

This system comprises the classic Bishop-Wesley stress path triaxial cell with 38 mm and 50 mm diameter pedestals and top caps, one internal submersible load cell, 2000kPa range pore pressure transducer and ±20 mm range displacement transducer. It has three standard 3MPa pressure/volume controllers configured with volume change measurement and a data acquisition device for accurate measurement of all transducers.

Figure 3.8 GDS Standard triaxial testing system

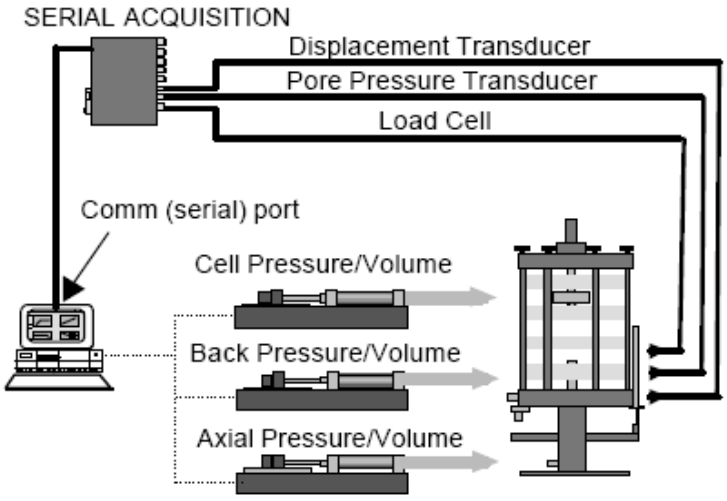

Figure 3.9 A schematic diagram of GDS Bishop-Wesly triaxial System (after GDS)

3.4.2 High pressure triaxial testing system

The GDS high pressure triaxial cell is designed to accept specimens with a diameter of up to 100 mm and a height of 200 mm without local strain transducers and up to a diameter of 70 mm and a height of 140 mm with local instrumentation. The

parameters that can be controlled/measured are cell pressure, back pressure, specimen volume change, pore pressure, axial stress and axial displacement. The technical specification of the system is given in Table 3.3.

Table 3.3 Technical specification of GDS high-pressure triaxial apparatus.

Parameters	**Values**
Nominal size	2.3m x 1.0m x 0.96m
Computer interface	IEEE-488 standard
Load range	100kPa (10 ton)
Load resolution	±1 in 10,000
Load cell accuracy	±0.03%
Displacement range	100mm
Displacement resolution	0.1 µm
Displacement accuracy	0.05%
Max. Displacement rate	3.75mm/min
Ramp	1.2mm/mm
Ramp target load control	1.0mm/min

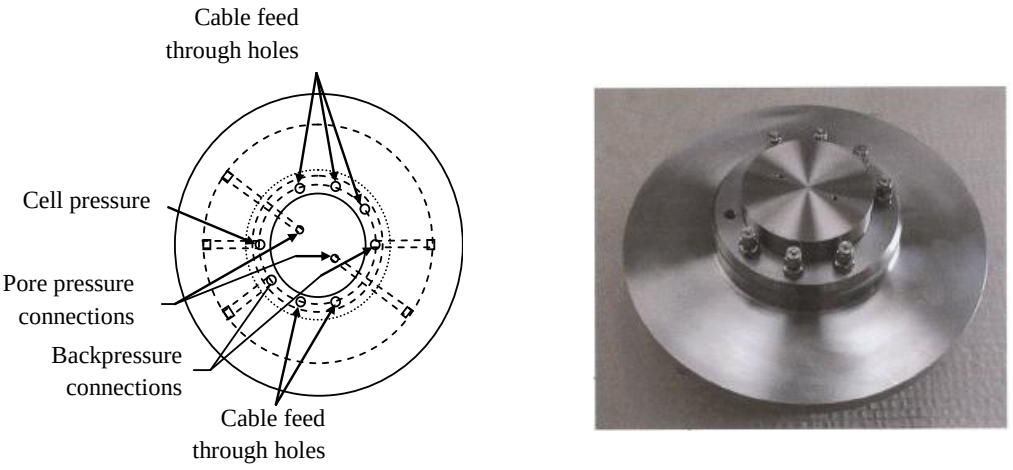

Figure 3.10 High pressure triaxial cell base schematic diagram and cell base photograph

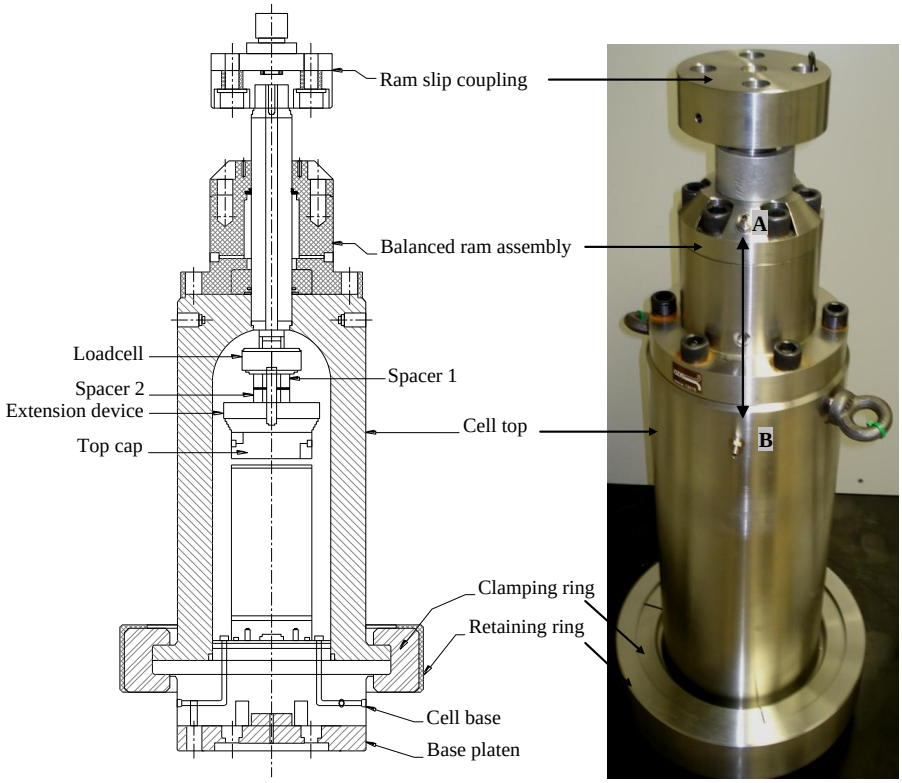

Figure 3.11 High pressure triaxial schematic cross-section and cell photograph

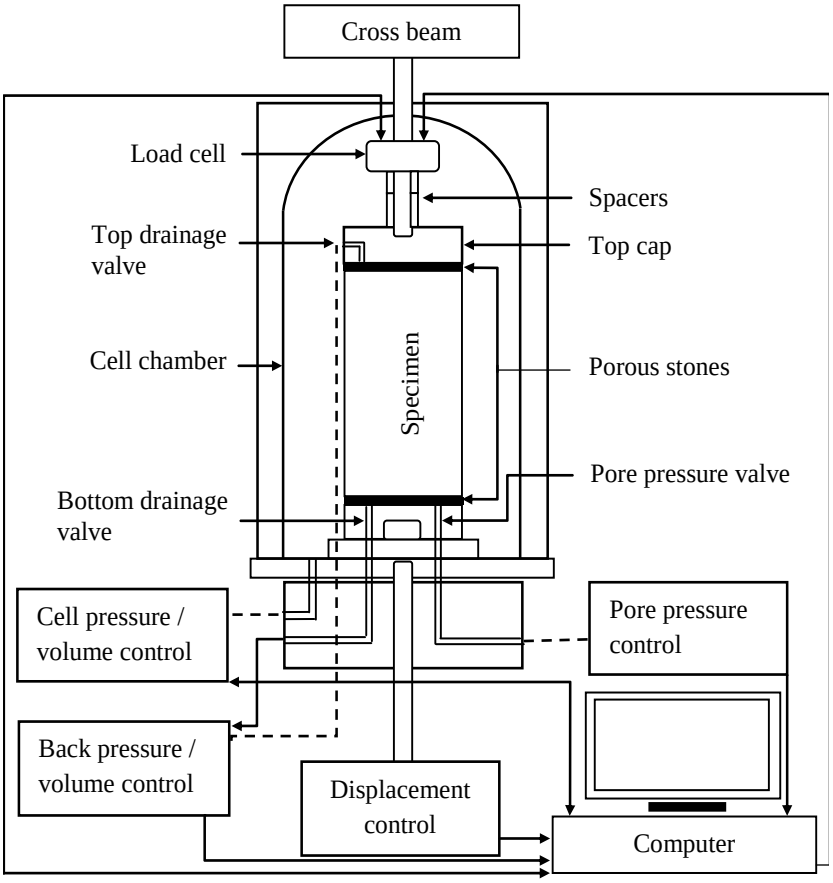

Figure 3.12 Schematic diagram of the high pressure triaxial test setup.

3.4.3 Scanning Electron Microscope

Micromechanical analysis can offer an insight into the nature of a soil and the way in which the structure changes in response to the stress and strain imposed on the soil mass.

Attention in the current study has been extended to the effects of fibre and cement content on the microstructure i.e., soil mineralogy, cement bonding, uniformity of the mix, bond breakage and particle crushing. Fibre reinforced cemented and uncemented sand sections at wide range of confining pressure were examined. The specimens with varying density cement and fibre contents after isotropic compression, drained shearing and undrained shearing were examined to investigate the effect of compression and shearing on post-deformation particle and bonding structure.

The technique used includes scanning electron microscopy. The analyses were carried out using EDAX Quanta 600 scanning electron microscope as shown in Figure 3.16. Attempt were made to see the effect of cement content and confining pressure on the deformation characteristics of the material; both from microscopic and macroscopic approach.

A Scanning Electron Microscope (SEM) is essentially a high magnification microscope, which uses a focussed scanned electron beam to produce micrographs of the sample.

The SEM constructs a virtual image from the signals emitted by the sample. It does this by scanning its electron beam line by line through a rectangular (raster) pattern

on the sample surface. The scan pattern defines the area represented in the micrograph. At any instant in time the beam illuminates only a single point in the pattern. As the beam moves from point to point, the signals it generates vary in strength, reflecting differences in the sample.

The output signal is thus a serial data stream. Modern instruments include digital imaging capabilities that convert the analog data from the detector to a series of numeric values. These values are then manipulated as desired. The primary electron beam interacts with the sample in a number of key ways:-

- Primary electrons generate low energy secondary electrons, which tend to emphasize the topographic nature of the specimen.
- Primary electrons can be backscattered which produces micrographs with a high degree of atomic number (Z) contrast.
- Ionized atoms can relax by electron shell-to-shell transitions, which lead to either X-ray emission or Auger electron ejection. The X-rays emitted are characteristic of the elements in the top few μm of the sample.

The SEM instrument has many applications across different industry sectors. The extremely high magnification images together with localised chemical information mean the instrument is capable of solving a great deal of common industrial issues such as particle analysis, defect identification materials and metallurgical problems. Microscopic study of uncemented and cemented fibre reinforced specimens was carried out with the help of scanning electron microscopy (SEM). The specimens were investigated before and after the triaxial testing. Before triaxial testing,

particle shape, structure, sand-cement fibre bond interaction (for cemented sand), and homogeneity of the fibre reinforced sand-cement mix were examined.

After isotropic compression, consolidated drained shearing and consolidated undrained shearing, the specimens were investigated for subsequent deformations and change in the composite due to compression and shear.

(a)

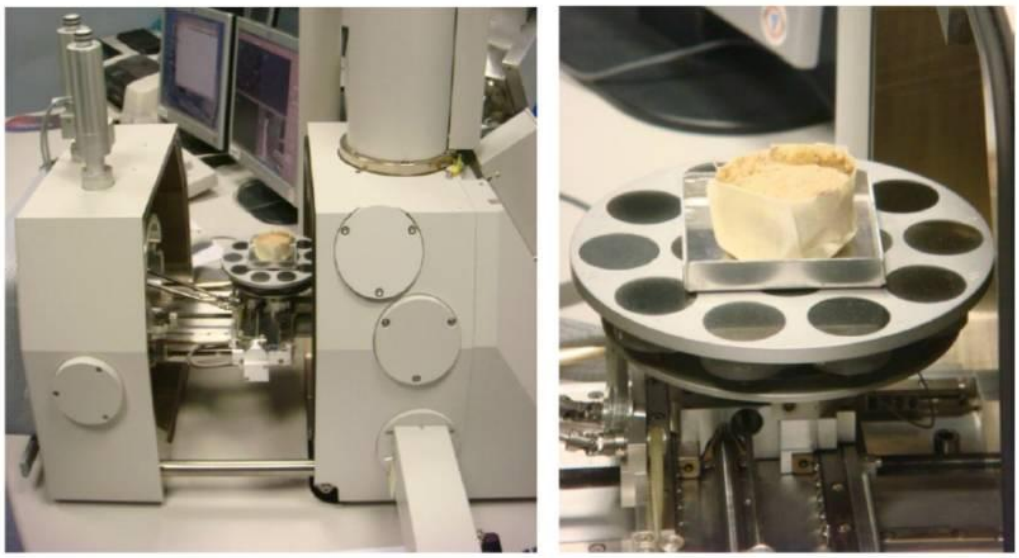

(b)

Figure 3.13 Scanning Electron Microscope: (a) outside views; (b) inside views.

3.5 Test procedures

The testing procedures and the computer controlled software usage for conventional and high-pressure triaxial system are similar except with slight differences in some of the steps. The detail procedure for both conventional and high-pressure testing is described below:

3.5.1 Saturation

1) Flushing

For a conventional triaxial testing system, the cell loading ram was raised to nearly the top so that during placing the cell it does not touch the top of the sample. The cell was placed on the base by taking care not to catch the top and bottom drainage tubes under the bottom of the cell. The screws were tightened and the top loading ram was then lowered so that it just touched the top of the sample.

The cell was filled with water through the cell pressure port, using the water tank and air pressure in order to provide lateral confinement to the sample. When the water started to flow out of the air bleeding valves the cell pressure port and the bleeding valves were closed. The bleeding valve at the end of the pipe was held in the air to ensure that the pipe was filled with water to avoid air interruption in the pipe.

The cell pressure port was opened and using the cell pressure wall panel, a small holding confining pressure of 10kPa was applied and the vacuum pressure was released. Water was fed into the specimen through the bottom drainage line under a small hydraulic head. A minimum of one litre of water in excess of the volume of

the voids in the specimen was percolated through the specimen. The back pressure tube was the connected to the top and bottom drainage tube and the saturation ramp was applied.

Water was flushed from the bottom of the sample with a low hydraulic head until the sample pores were filled and water exits from the top of the sample. In order to ensure the saturation of the sample, the saturation ramp was applied.

2) Saturation ramp

The objective of the saturation stage is to ensure that all the voids are filled with water. This is usually achieved by raising the pore pressure to a level, high enough for the water to absorb into solution all the air originally in the voids.

The GDS program was then set up for a saturation ramp to attempt to saturate the sample, maintaining the same effective holding confining pressure, the cell pressure and back pressure were increased. Saturated ramp was applied to the specimen for 12hours. All the specimens were back saturated at 700kPa for conventional pressure tests and at a back pressure of 2000kPa for high pressure tests by raising the cell pressure and back pressure simultaneously with a low difference. A B-value of 0.95 was achieved for uncemented samples and 0.90 for cemented samples.

3.5.2 Consolidation

After checking and obtaining the required B-value, the samples were isotropically consolidated. The specimens were isotropically consolidated to the desired confining pressures and the volume changes were measured exactly at the end of consolidation. In isotropic loading only one-way drainage was permitted and the

consolidation stage was continued until the back volume change approached to zero. The objective of the consolidation stage was to bring the specimen to the state of effective stress required for carrying out the compression test.

3.5.3 Drained shearing

During this stage, the cell pressure was maintained constant while the specimen was sheared at a constant deformation rate of 0.15 mm/min.

The GDS program was then set up for shearing. For consolidated drained, (CD) test, back volume, axial load, axial displacement were set at zero, before the start of the test. At the end of the test, cell and back pressures were manually set to zero. The cell was emptied and sample removed.

3.5.4 Undrained shearing

For standard triaxial undrained compression, shearing commenced at the end of isotropic consolidation. From triaxial acquisition, the consolidated undrained (CU) stage was created. Prior to starting the shear stage axial displacement and axial strain were set to zero. All the CU tests were carried out under a deformation-controlled loading mode at a constant rate of 0.15 mm/min. A GDS computer data logger was used throughout for test control and data acquisition.

3.6 Repeatability of test results

The repeatability of test results was verified by the results of experiments performed on Portaway sand. The isotropic compression tests were run under isotropic loading and unloading and drained compression tests were performed on dense fibre reinforced sand by "repeat tests" at selected effective confining pressures, σ'_3. Good agreement was obtained for both isotropic (Figure 3.14) and drained compression tests (Figure 3.15).

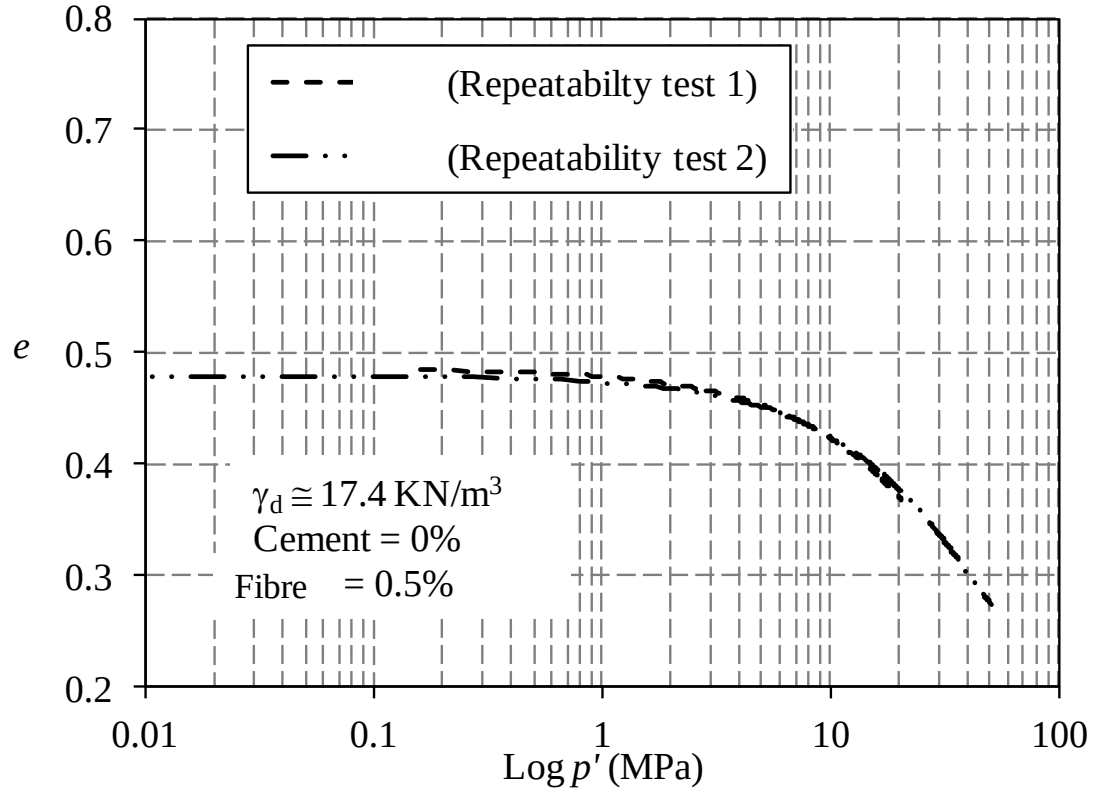

Figure 3.14 Repeat tests on Portaway sand for isotropic compression.

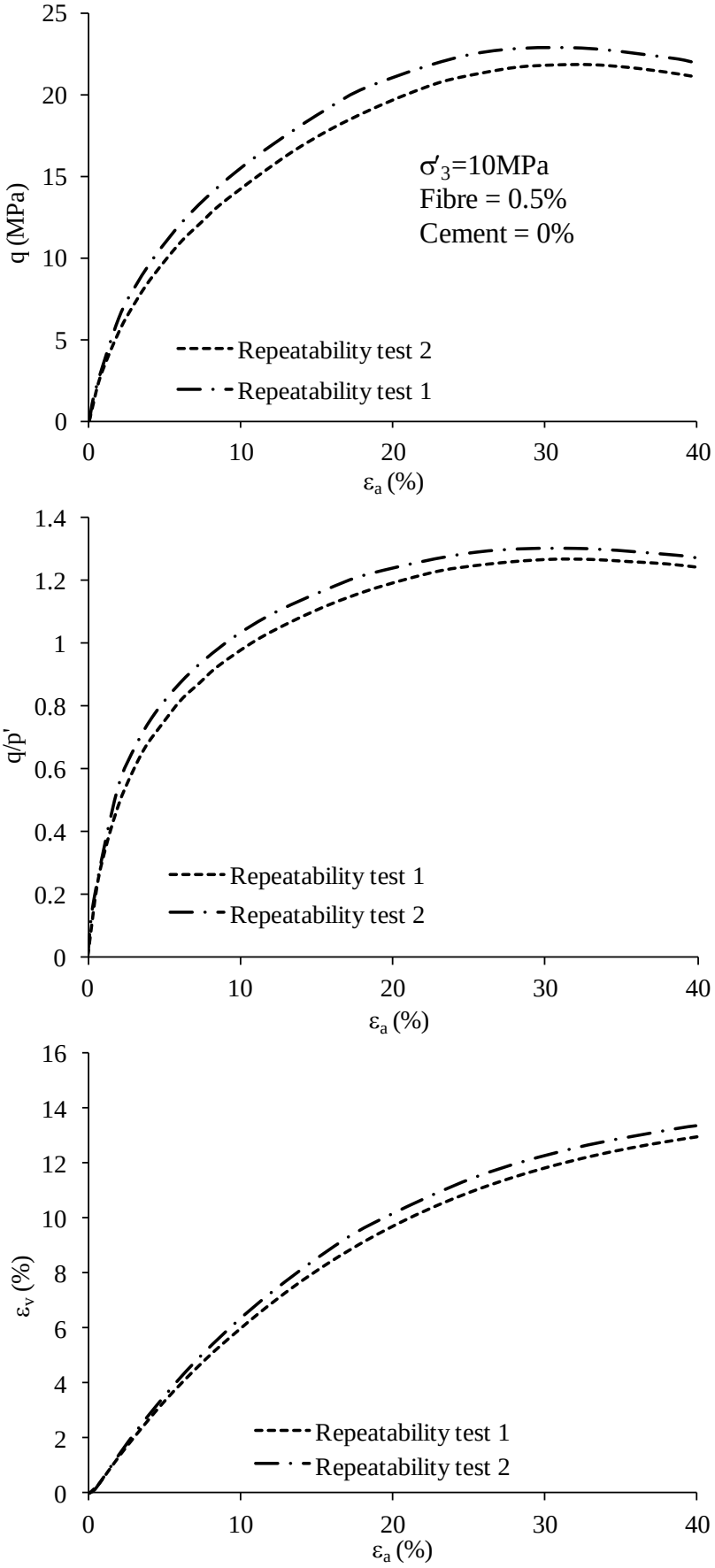

Figure 3.15 Repeat tests on fibre reinforced sand for drained comrpession tests.

3.7 Summary

Well-graded, medium quartz sand from Sheffield (England), known as Portaway sand was used as the base material for the cemented specimens. The index properties of Portaway sand were determined by British Standard methods (BS 1377). The sand grains were mainly sub angular and sub rounded in shape. Before the preparation of cemented specimens, the sand was passed through 2 mm sieve to remove gravel size particles and washed through 0.063 mm sieve under the running water to re-move fines. Ordinary Portland cement was used as cementing material. Its initial setting time is 80 to 200 minutes and its specific gravity was 3.15.

The method of undercompaction was adopted for the preparation of both cemented and uncemented fibre reinforced sand specimens to achieve varying degrees of initial relative densities, void ratios, and dry unit weights. Bishop-Wesley Conventional pressure and GDS high-pressure triaxial apparatus were used for conventional and high pressure triaxial testing respectively.

The first stage of each test was the sample saturation. This was done by applying a small positive effective stress and then raising simultaneously both the cell and backpressures keeping the effective stress constant. The backpressure was increased typically to around 700kPa, for uncemented sand and to around 2000kPa for cemented sand, when the pressures were kept constant and the sample was allowed to saturate for at least 24h or longer if required, until a B value of 95% was achieved.

An exploratory series of tests were run to identify and fix the problems before the commencement of investigatory testing. Specimen stratification and membrane punctures were noticed at high pressures. Suitable arrangements were made to avoid these errors.

A microscopic study of uncemented and cemented specimens of Portaway sand was carried out with the help of SEM. Particle shape, structure, sand-cement-fibre bond interaction (for cemented sand), mineralogy of sand and sand-cement composition and homogeneity of the sand-fibre mix were examined. Moreover, the specimens were investigated for subsequent deformations and changes in the structure due to compression and shear.

CHAPTER 4

ISOTROPIC COMPRESSION BEHAVIOUR

4.1 Introduction

Compression, i.e., more intimate packing of particles, promotes locking, including engaging surface roughness, among soil particles and increases the stiffness of a granular aggregate. During compression of granular materials, both unlocking and locking mechanisms operate simultaneously.

In recent years there has been significant utilization of fibre to improve the shear strength of geotechnical materials. However, little information related to the compression characteristics of fibre reinforced cemented materials is available in the literature. Also a review of literature reveals that there are different results reported regarding the isotropic compression characteristic of sand with the addition of fibres.

The effects of different initial void ratios and the addition of fibre and cement content on the compression characteristics of Portaway sand are investigated in this chapter. The list of isotropic compression tests discussed in this chapter is given in Table 4.1. The samples were carefully prepared to obtain the desired relative density values with the addition of the fibres and cement as discussed in section 3.3.2.

Table 4.1 Summary of results of istropic compression tests.

Test	p′ (MPa)	C (%)	F (%)	D_r (%)	e_0	e_c
IC-0F0C20M	20	0	0	90	0.495	0.383
IC-0.25F0C20M	20	0	0.25	90	0.495	0.364
IC-0.5F0C20M	20	0	0.5	90	0.495	0.363
IC-0.5F5C20M	20	5	0.5	80	0.529	0.449
IC-0.5F0C50M	50	0	0.5	89	0.495	0.272
IC-0.5F0CL50M	50	0	0.5	48	0.687	0.341
IC-0.5F5C50M	50	5	0.5	86	0.523	0.364
IC-0.5F5CMD50M	50	5	0.5	62	0.584	0.464
IC-0.5F5CL50M	50	5	0.5	40	0.657	0.453

4.2 Effect of initial void ratio

In order to observe the effect of initial void ratio on the isotropic compression characteristics of fibre reinforced cemented and uncemented sands, high pressure isotropic compression tests were carried out on samples of uncemented and cemented fibre reinforced Portaway sand at different initial void ratios (e_0). The cement contents of 0% and 5% were used with 0.5% of fibres and the resulting isotropic compression e-log (*p*′) curves are plotted.

State paths during isotropic compression may be plotted on a graph of specific volume, *v* versus logarithm of mean effective stress, ln(p'). For soils compressed for the first time, there is a unique relationship between specific volume and mean normal effective stress p', which is represented by a straight line on the graph of *v* against ln(p'), known as the Normal Compression Line (NCL).

$$\upsilon = 1 + e = \mathrm{N} - \lambda \ln p' \qquad 4.1$$

From the compression curves of fibre reinforced uncemented sand as shown in Figure 4.1, it can be noticed that by the progressive increase in the confining pressure there is a tendency for convergence of the compression curves of the specimens prepared with different initial void ratios. At the end of isotropic compression, the curves tend to approach to a unique void ratio at high pressures shown as dashed line. Similar observation were also reported by (Consoli et al., 2005b) for fibre reinforced sand. The values of λ and N obtained from NCL are 0.160 and 1.9 respectively. Dos Santos et al. (2010b) also reported similar value for the slope of NCL but N value is quite low as compare to the reported values of 3.09.

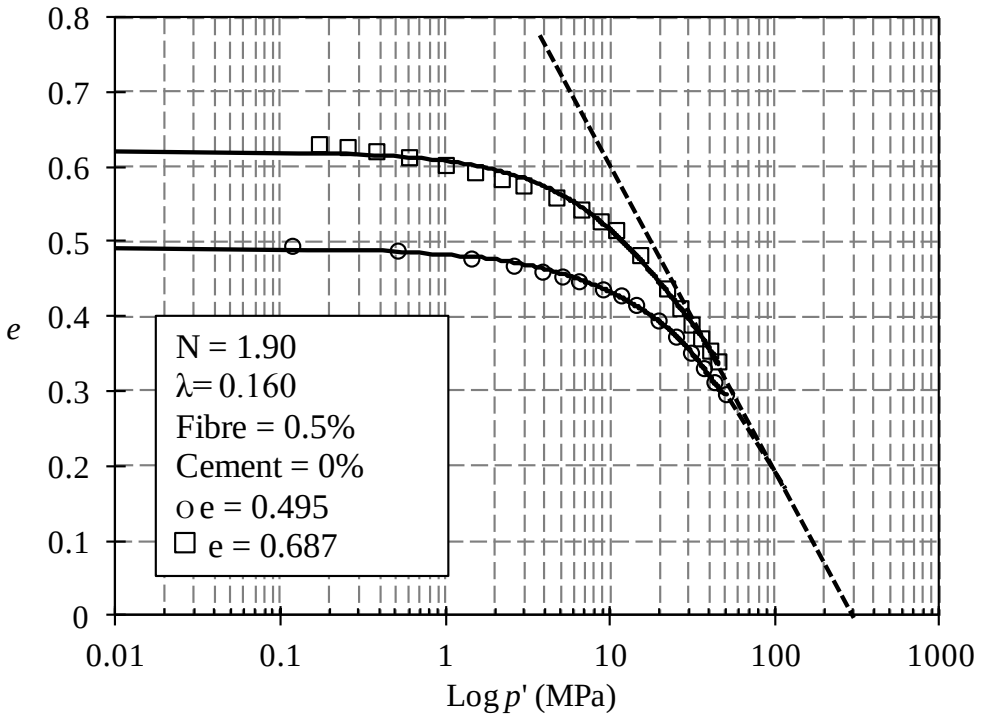

Figure 4.1 Isotropic compression curves of fibre reinforced sand at different initial void ratios.

Similarly, from Figure 4.2, which shows the e-log(p') curves of fibre reinforced cemented sand, it can be observed that the cemented sand also demonstrates similar trend of convergence in the compression curves having a tendency to

approach a unique void ratio at high pressures as is noticed for fibre reinforced uncemented sand. This suggests that by the increase in confining pressure during isotropic compression, there is tendency of convergence in the compression curves for both uncemented and cemented fibre reinforced sands, which are prepared at different initial void ratios. The only difference that can be noticed in the compression curves is the difference in the compression path and the compression index. For instance, at the end of compression the final void ratio for fibre reinforced uncemented sand is less than the final void ratio for fibre reinforced cemented sand, which suggests that fibre reinforced cemented sand, is relatively less compressible as compared to the fibre reinforced uncemented sand. The numerical values N and λ obtained for fibre reinforced cemented sands are 2.03 and 0.173 respectively. The final void ratio at the end of consolidation (e_c) are given in Table 4.1.

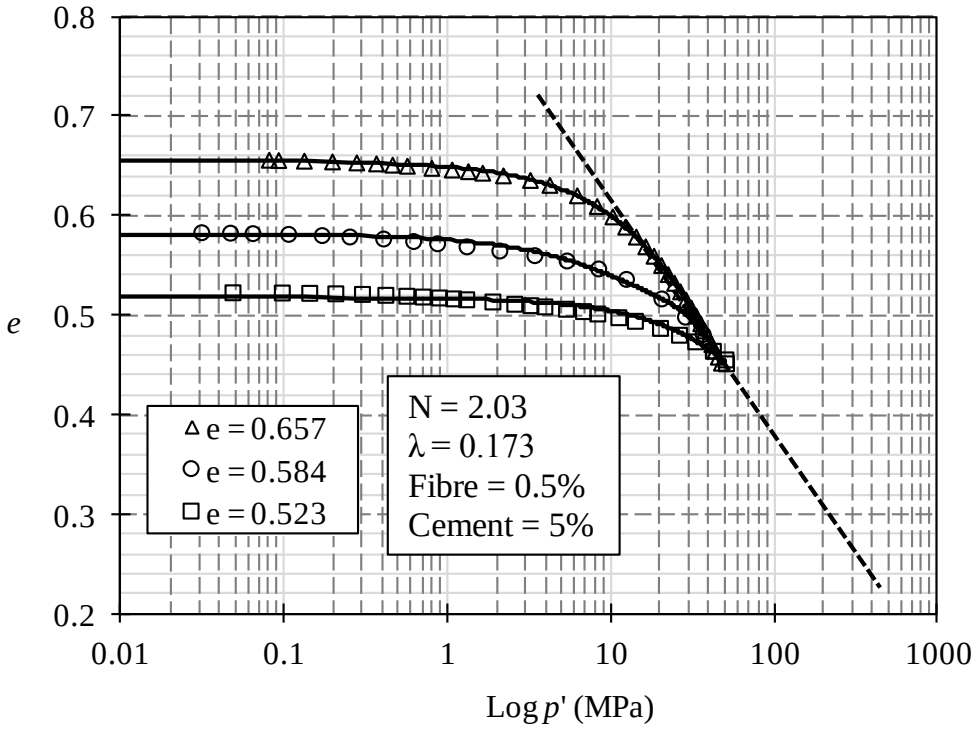

Figure 4.2 Isotropic compression curves of fibre reinforced cemented sand at different initial void ratios.

4.3 Effect of addition of fibre in sand

The effect of the addition of 0.25% and 0.5% fibre in sand at constant void ratio is shown in Figure 4.3. It can be seen that the addition of fibre has very little or no effect on the compression characteristic of sand and they follow the same compression line up to 2MPa. After this fibre reinforced sand samples tend to compress marginally more. During isotropic consolidation, the fibres are compressed in all directions, and therefore do not function as tensile reinforcement until a relatively large lateral tensile strain has occurred in the soil upon shearing. Ling and Tatsuoka, (1994) also pointed out that under isotropic compression reinforcement may not play any role in the initial phase of loading. Michalowski and Cermak, (2002) also reported that fibres in compression do not contribute to reinforcement, and may even have an adverse effect. Whereas, Ibraim and Fourmont, (2006) reported that the presence of reinforcement provides an extra resistance to the compaction, causing a less dense packing as the quantity of fibres is increased. This can result in more volumetric compression of fibre reinforced sand. It can also be seen that 0.25% and 0.5% fibre reinforced samples have the same compression throughout the test, which in turn suggest that varying fibre content has also no effect in isotropic compression. Fibre reinforced sand samples apparently seem to have more compression than sand. This might be due the slight variation in the initial void ratio and also may be due to the fact that fibres have a specific gravity, G_s, of 0.9 which results in lesser initial void ratio. As compression is achieved by interparticle slip and rotation, fibre could provide a smooth surface which facilitates more compact rearrangement of particle. This results in slightly

higher compression. It can also be concluded from the isotropic compression curves that fibres only contribute in triaxial shearing when they are subjected to tensile forces. There is negligible effect from the addition of fibre when they are subjected to compressive forces in isotropic compression. There are contradictory results reported in literature and this has been discussed in detail in literature review.

The volumetric strain curves of sand and fibre reinforced sand are also shown in Figure 4.4. It can be seen that the volumetric strain of fibre reinforced sand is high which in turn suggests that fibre reinforced sand is more compressible than sand only. Though this effect is not noticeable in e-Log(p') curve plotting the effective confining pressure, p' on a non-logarithmic scale shows fibre reinforced samples to be more compressible. Previously reported work showed that the addition of fibre in sand or cemented sand improves the isotropic compressive behaviour and fibres were reported to have both extended and broken. SEM analysis was carried out to see the microstructure of the sample to see any changes in fibre and sand. This is discussed in coming sections.

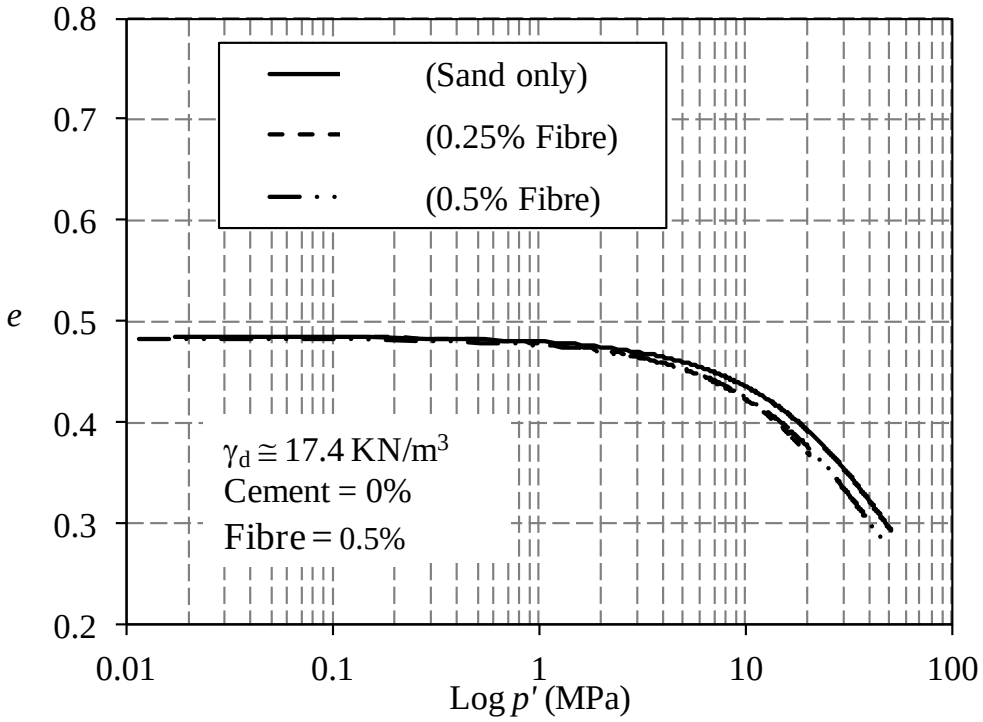

Figure 4.3 Effect of addition of fibre on isotropic compression behaviour of sand.

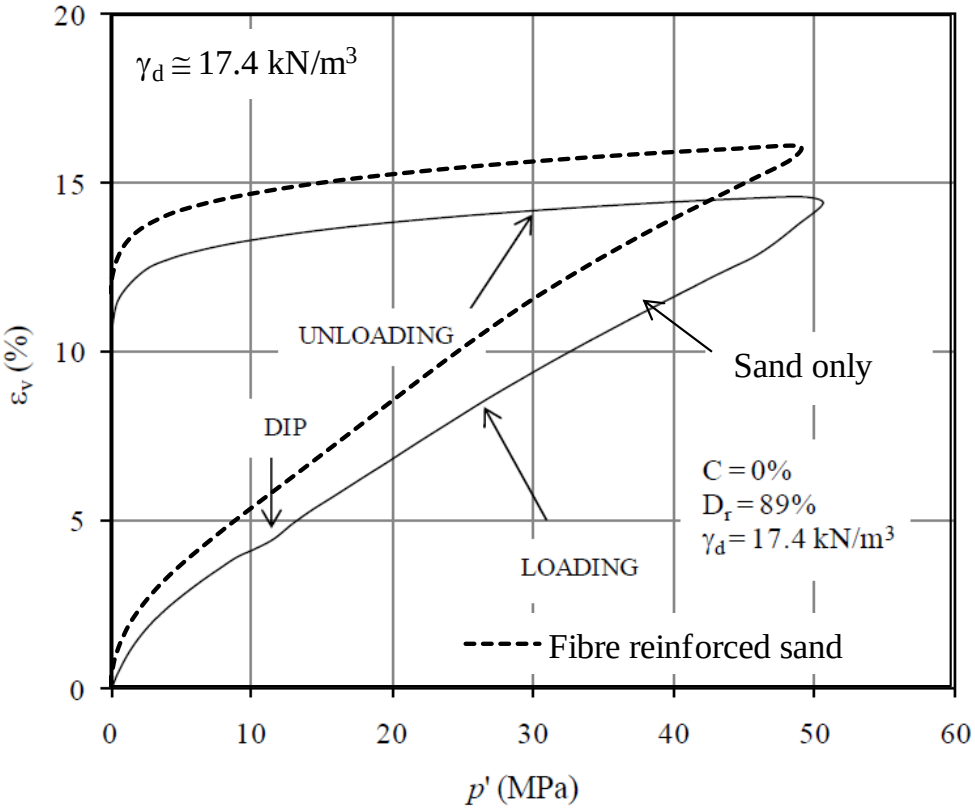

Figure 4.4 Effect of addition of fibre on volumetric strain curve in isotropic compression of sand (modified after Marri 2010).

4.4 Effect of addition of fibre in cemented sand

As it is seen that the addition of fibre in sand has not much effect, it is interesting to see the effect of fibres when added to cement. In order to investigate the effect of the addition of 0.5% fibre in 5% cemented sand, tests were carried out at constant initial void ratio and were consolidated to a confining pressure of 50MPa. The results of the tests are shown in Figure 4.5 and Figure 4.6. The void ratio, e, Vs Log (p') curve is shown in Figure 4.5. It can be seen that similar to the result of the addition of fibre in sand only, the addition of fibre in cemented sand has also not much effect in cemented sand. Both the cemented and fibre reinforced cemented samples follow nearly the same line of compression. It can be seen that similar to the effect observed in fibre reinforced sand, the fibre reinforced cemented sample compresses more at higher pressures above 8MPa. Figure 4.6 (b) shows the ε_v-p' curve in which, similar to the behaviour of fibre reinforced sand, fibre reinforced cemented sand shows more compression after 8MPa. This might be due to the effect of the cement bonding until the pressure reaches such a high value that the fibre cement bond resisted the compression and thereafter particle crushing and bond breakage caused the fibre reinforced cemented sample to compress quickly. Thus after looking at the results of fibre reinforced cemented and uncemented samples it can be concluded that effect of the addition of fibre is negligible in isotropic compression where they are subjected to compression.

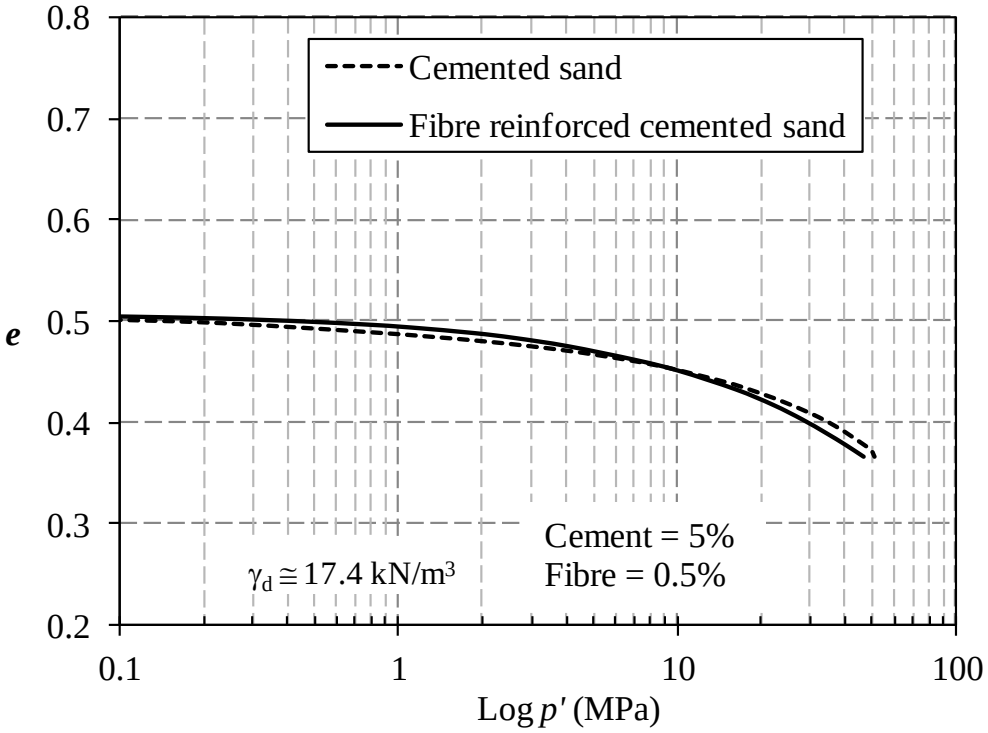

Figure 4.5 Effect of addition of fibre on isotropic compression behaviour of cemented sand.

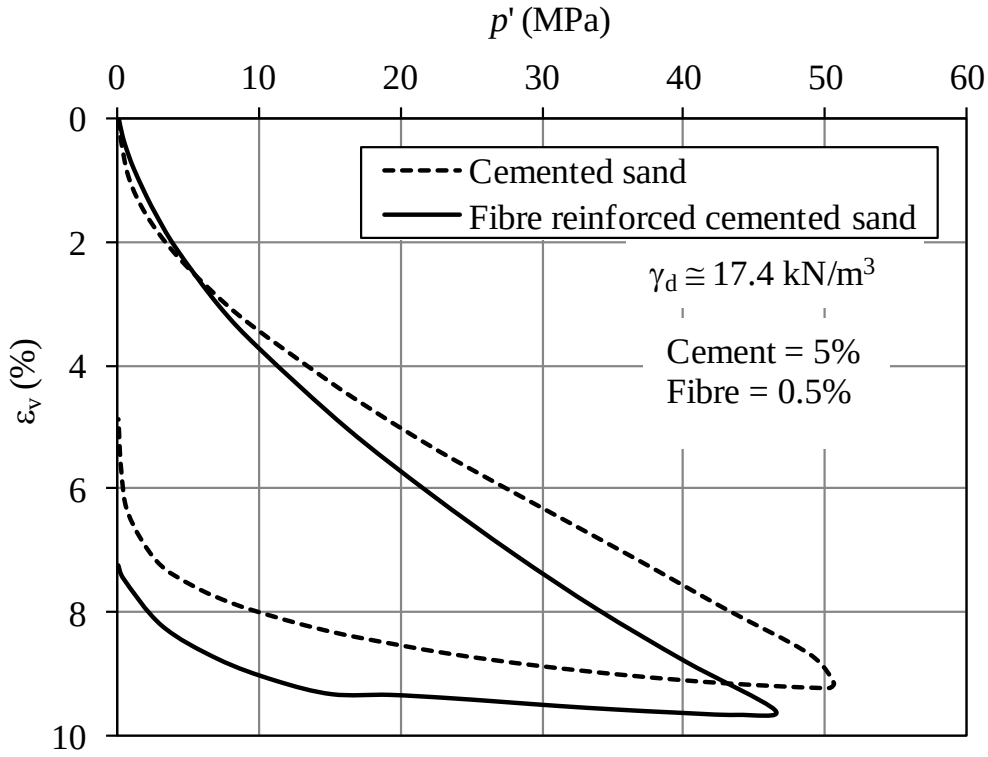

Figure 4.6 Effect of addition of fibre on volumetric strain curve in isotropic compression of cemented sand.

4.5 Scanning Electron Microscope analysis

Soil is a particulate material and the shear stress is mostly transferred through particle contacts. Thus, the soil microstructure has very important role in understanding soil behaviour. Microstructure can be observed under electron microscopes (e.g. Environmental Scanning Electron Microscope (ESEM) and SEM) to understand the particle arrangement and interaction in soils.

It is widely recognized that mechanical behaviour of fibre reinforced cemented sands can be directly related to microstructure, i.e. the geometrical arrangement of the grain particles, fibre distribution and bonding. It is generally known that the amount and type of cement and fibre are primary factors influencing the strength of the composite. The amount of cement and uniform distribution of fibre can have profound effects on bulk mechanical behaviour of the material. However, the micro scale interactions between individual constituents of grain-cement-fibre network subjected to differential stresses are not fully understood. Detailed experimental characterization of these systems would improve the predictive information for the geomechanical phenomenon.

In this study, SEM analysis was carried out on fibre reinforced cemented and uncemented samples. The selected specimens were investigated before and after isotropic compression.

4.5.1 Fibre distribution

The distributed discrete fibres act as a spatial three dimensional network to interlock soil grains, help grains to form a unitary coherent matrix and restrict the

displacement. Macroscopic observations of the samples were showing a reasonably homogeneous mixture of the composite. To investigate the mixing, distribution and homogeneity of fibres microscopically in cemented and uncemented samples, SEM analysis was carried out on samples before and after isotropic testing. It was important to analyse the sample after testing as well because it could not have been possible to see the mixing of fibres inside the sample after testing. Figure 4.7 shows SEM micrograph of fibre reinforced cemented and uncemented soil samples before testing showing mixing and distribution of fibres in sand and cemented sand. It is important to note that SEM micrographs represent the qualitative information regarding the distribution of the fibres. The area of investigation is always very small and limited to a specific horizontal or to a plane of failure. The SEM analysis cannot be carried out at different planes. The distribution of fibres at this micro level is shown to be uniform and consistent. It is also worth mentioning that SEM micrograph shown is of about a 1mm to 2mm diameter part of the whole sample surface. In the fibre reinforced cemented sample shown in Figure 4.7(a), the sample was analysed untested and shows only the top surface of the specimen. There can be seen very proper consistent bonding of the grains in their natural bedding plane, some poor bonding and cement deposition on the surface of the sand grains and fibres as well. Figure 4.7(b) shows the SEM micrograph of fibre reinforced uncemented sample. It can be seen that fibres are distributed reasonably uniformly and making a network of fibre with sand grains. Similar distribution has also been shown by Tang et al., (2007) has been discussed in the literature review.

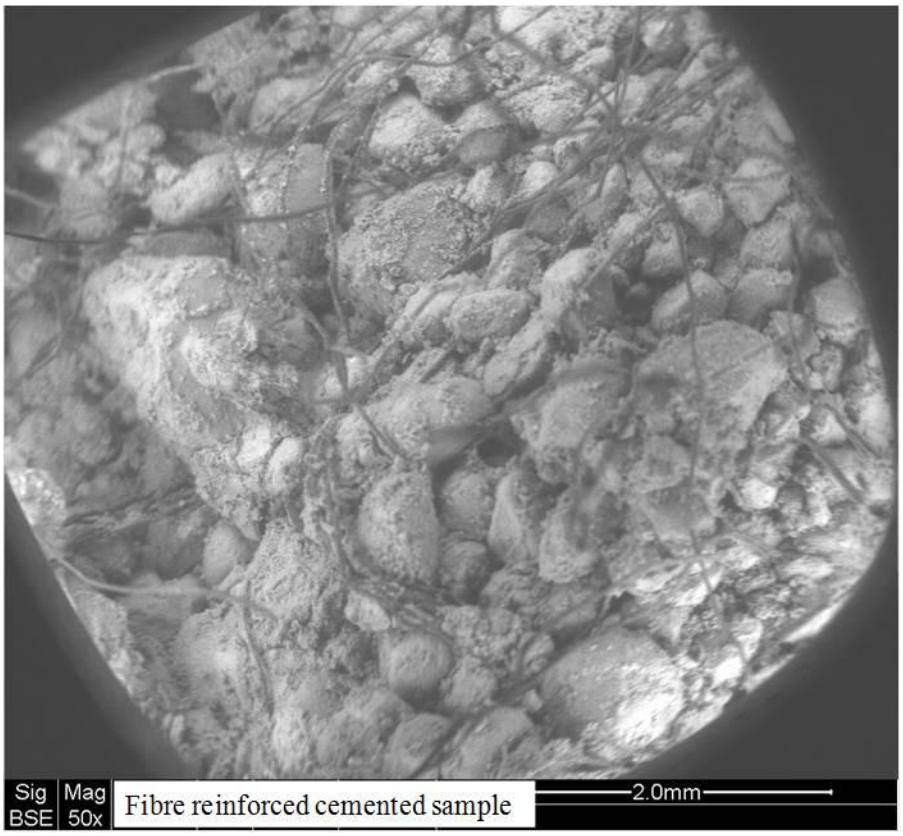

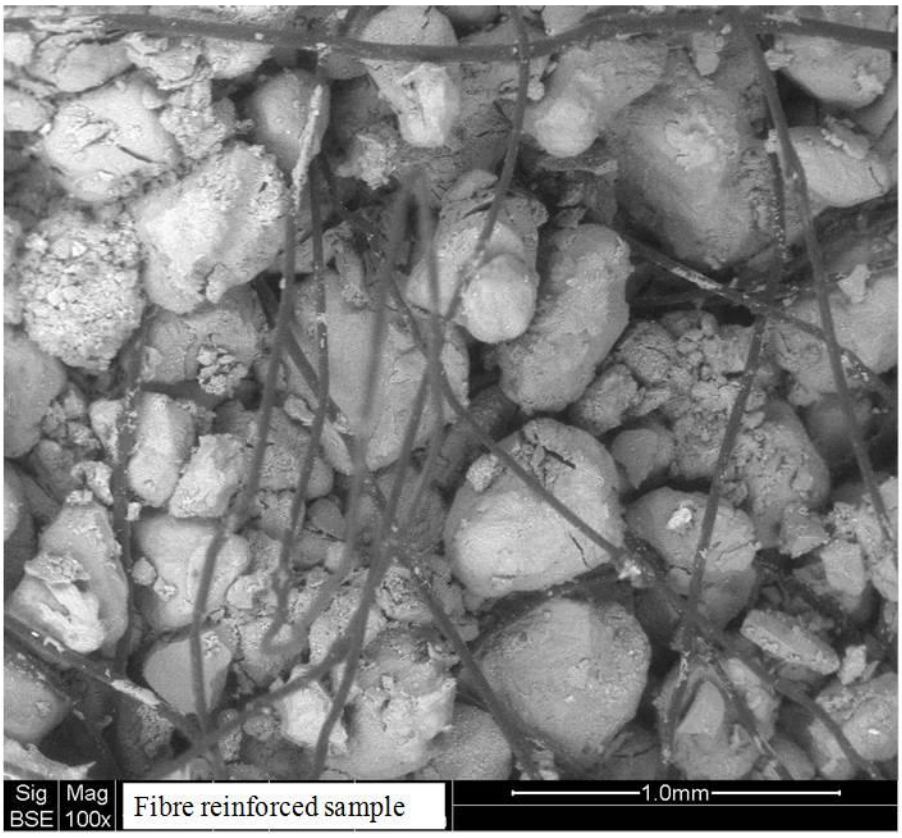

Figure 4.7 Fibre reinforced samples showing distribution of fibre before testing; a) 0.5% fibre and 5% cemented reinfroced sample and b) 0.5% fibre reinfroced sample.

4.5.2 Particle crushing and fibre breakage

In order to investigate the effect of isotropic compression on fibre reinforced cemented and uncemented sand, the isotropically compressed specimens were further investigated with the help of the SEM microscope. For this purpose, both cemented and uncemented samples were taken. In all soils, particle rearrangement into a more compact configuration is achieved by overcoming interparticle friction through interparticle slip and rotation. In some soils, particle rearrangement is also facilitated by overcoming particle strength through particle damage as in granular soils.

The results of isotropic compression tests carried out on cemented and uncemented sand samples showed the negligible effect of fibres as discussed in this chapter. SEM micrograph shown in Figure 4.8 and Figure 4.9 verify the above stated results as these micrographs show very little effect in terms of fibre breakage. Fibres were mostly found pinched and twisted. It can be seen that particle crushing is very significant and readily noticeable while fibres are seen distorted in shape but are not seen broken suggesting they were not subjected to tensile stresses.

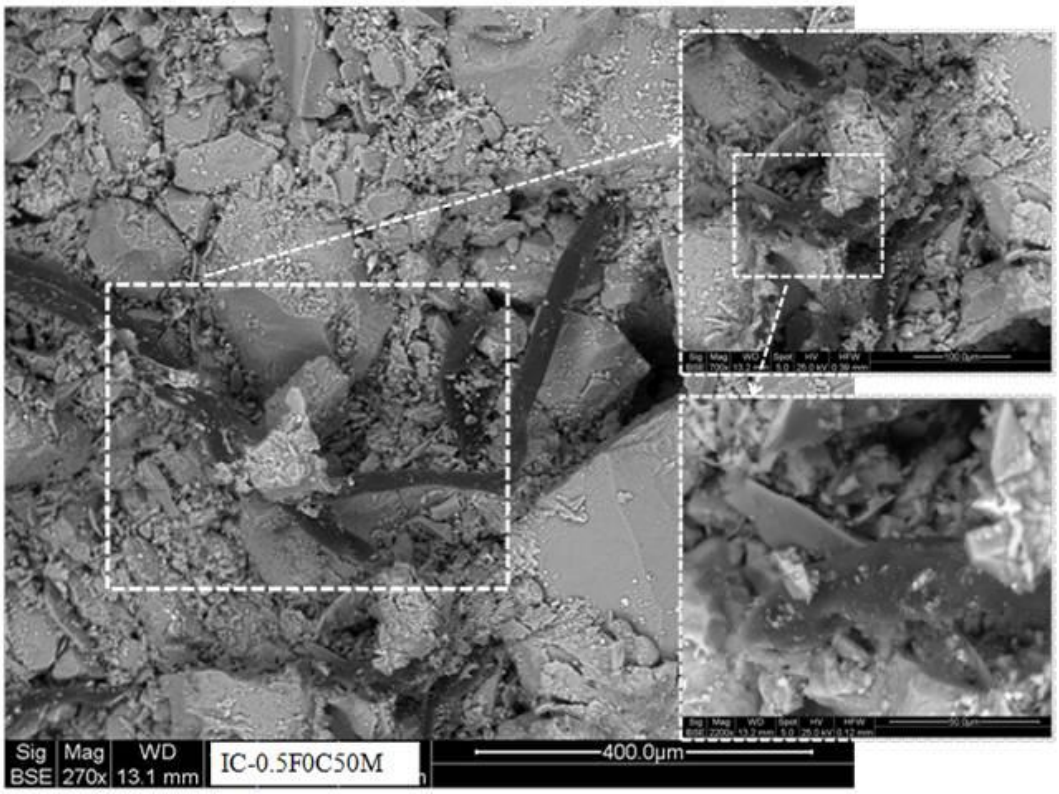

Figure 4.8 SEM micrograph of 0.5% fibre reinforced sample analysed after isotropic compression showing fibre twisting and particles crushing at horizontal plane.

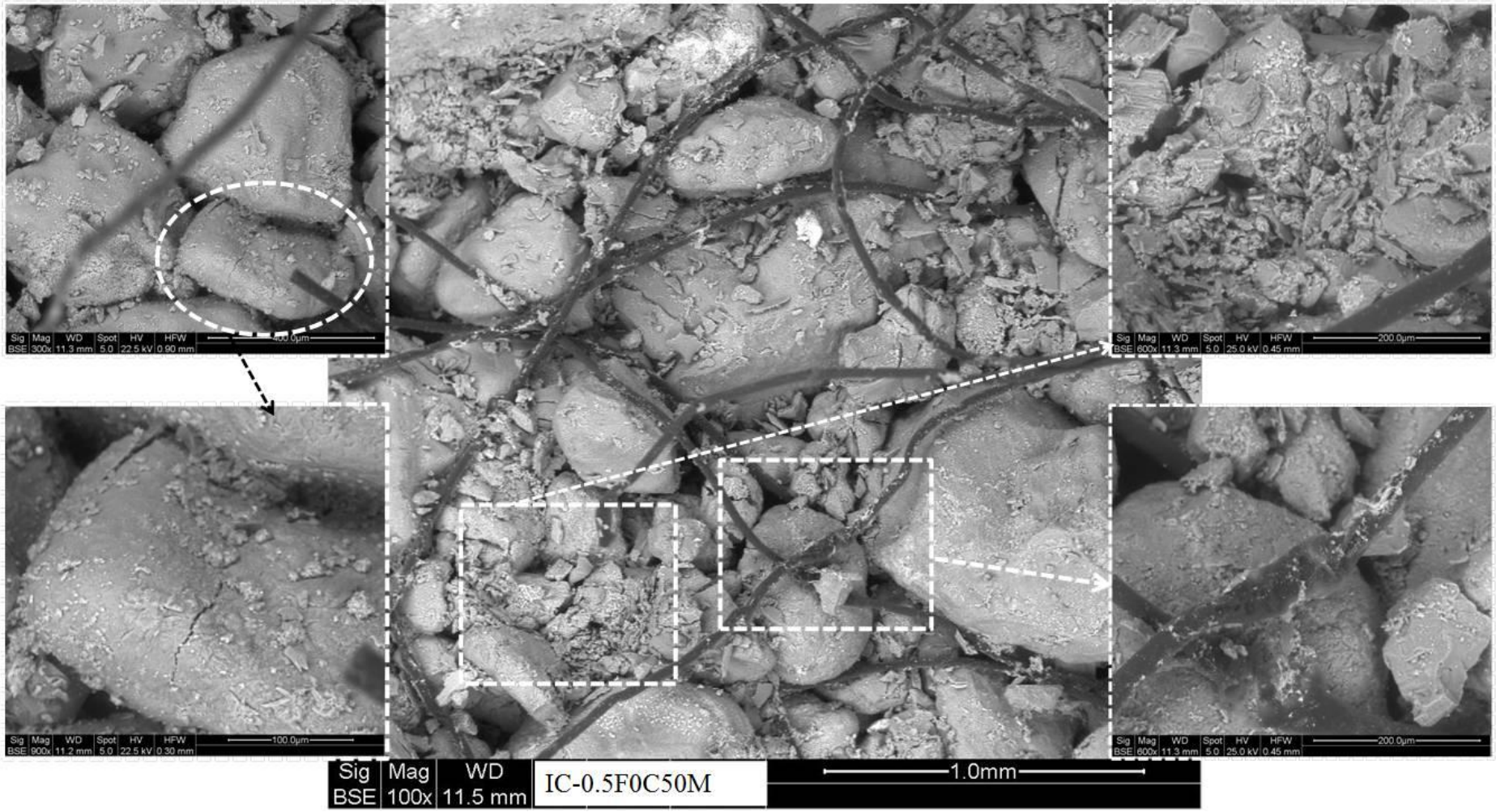

Figure 4.9 SEM micrograph of 0.5% fibre reinforced sample showing particle crushing and fibre pinching.

4.6 Summary

This chapter was aimed at a fundamental understanding of the behaviour of fibre reinforced cemented and uncemented sand under isotropic compression, when compared with sand. High pressure isotropic compression tests were carried out on samples of uncemented and cemented Portaway sand at different initial void ratios, different fibre and cement contents.

1) From the experimental investigations, it was observed that the effect of initial void ratio for both cemented and uncemented fibre reinforced sands appear to diminish at high pressures and there is convergence in the isotropic compression curves. Similar to uncemented sand, the cemented sands with different initial void ratios converge towards a unique final void ratio. Therefore, the variation of initial void ratio has less significance at high confining pressures.
2) Keeping the initial void ratio constant the effect of the addition of fibre in sand and cemented sand was also examined and it could be seen that the effect of fibre is either very nearly negligible or the addition of fibre increases the overall compression of both sand and cemented sand.
3) The value of λ and N for sand and fibre reinforced sand is 0.160 and 1.88 respectively while for cemented and for fibre reinforced cemented sand the values are 0.173 and 2.03. Therefore, no effect of fibre was seen in isotropic compression tests for both cemented and uncemented sand samples.
4) Regarding the particle crushing and fibre breakage, fibre/cement content was not found to resist the deformation due to higher confining pressures.

For instance, for both uncemented and cemented fibre reinforced sand, SEM micrographs indicated significant particle crushing, fibre twisting and punching. However, for fibre reinforced sand, only fibre twisting and pinching was seen and there was hardly any fibre breakage. This verifies the results seen in e-log (p') curves that fibres did not contribute in resisting the isotropic compression due to only being subjected to compressive stresses.

CHAPTER 5

STRESS-STRAIN BEHAVIOUR

5.1 Introduction

The stress–strain and volume change behaviour of cemented sand can be well understood from triaxial compression tests. The shear strength of cemented soils under varying drainage conditions has been a topic of significant interest. A wealth of experimental data has been published in the literature for behaviour of cemented sand (e.g. Clough et al. 1981, Coop and Atkinson 1993, Abdulla and Kiousis 1997a, Abdulla and Kiousis 1997b, Consoli et al. 2000, Dano et al. 2004, Haeri et al. 2006, Consoli et al. 2007). There is also literature available for fibre reinforced uncemented sand. These experimental data have contributed significantly to the understanding of the important factors that control the shear strength behaviour of cemented and uncemented fibre reinforced sands under drained conditions. There is also some experimental work available for fibre reinforced cemented sand.

The present work evaluates the mechanical behaviour of fibre reinforced cemented and uncemented Portaway sand using triaxial drained and undrained compression tests. Some typical tests are presented in Table 5.1. Drained and undrained triaxial compression tests were performed with initial confining pressures between 50kPa and 20MPa. The tests consisted of drained isotropic compression followed by drained and undrained shearing under axial strain control. The total confining

pressure was maintained constant throughout shearing. In present study the effects of varying fibre and cement content, addition of fibre and cement, and effect of varying confining pressure are considered, keeping the density of the material constant (17.4kN/m^3).

5.2 Drained behaviour

In order to understand the drained behaviour of fibre reinforced cemented and uncemented, isotropically consolidated drained (CD) tests were conducted on Portaway sand reinforced with varying (0%, 0.25% and 0.5%) fibre and (0%, 2%, 5% and 10%) cement contents. The specimens were isotropically consolidated to mean effective stresses, σ'_3 = 50kPa to 20MPa and sheared under drained conditions with σ'_3 maintained constant. The deviatoric stress (q), the effective stress ratio (q/p′), and the volumetric strain (ε_v) were plotted versus the axial strain (ε_a).

5.2.1 Effect of fibre and cement

The results of consolidated drained compression tests (CD) are presented in Figure 5.1 and Figure 5.2 to illustrate the effect of the addition of 0.5% fibre and/or 5% cement in sand at effective confining pressures of 300kPa and 4MPa. The effect of the addition of fibre and cement is shown at 300kPa and 4MPa to show the effect at lower and higher pressures. It can be seen in Figure 5.1 (a) that the addition of fibres has increased the initial stiffness, peak deviatoric stress and ultimate strength of both the sand and cemented sand. The peak deviatoric stress is shown by black circles.

Table 5.1: Summary of isotropically consolidated drained compression tests

Test	σ'_3 (MPa)	C (%)	F (%)	γ_d (kN/m^3)	e_0	e_c	p'_f (kPa)	q_f (kPa)	ϕ'_f (°)
CD-0.25F0C0.5M	0.5	0	0.25	17	0.529	0.526	108.7	179.9	40.4
CD-0.25F0C1M	1	0	0.25	17.4	0.523	0.518	205.1	317.5	38.1
CD-0.25F0C4M	4	0	0.25	17.4	0.523	0.51	411	623.7	37.3
CD-0.25F0C10K	10	0	0.25	16.9	0.538	0.517	591.6	881.2	36.6
CD-0.25F2C0.5M	0.5	2	0.25	17.4	0.523	0.492	965.2	1397.2	35.7
CD-0.25F2C1M	1	2	0.25	17	0.524	0.492	1836.2	2363.4	32.4
CD-0.25F2C4M	4	2	0.25	17.1	0.519	0.4641	7778.9	8673.9	31.9
CD-0.25F2C10M	10	2	0.25	17.1	0.523	0.467	18450.3	22505.3	30.6
CD-0.25F5C0.5M	0.5	5	0.25	16.7	0.553	0.4427	32923.6	38944.5	29.4
CD-0.25F5C 1M	1	5	0.25	17.3	0.519	0.516	331	778.8	58.2
CD-0.25F5C4M	4	5	0.25	17.3	0.515	0.508	444.9	954.1	52.5
CD-0.25F5C10M	10	5	0.25	17.3	0.513	0.497	763.1	1384.8	44.2
CD-0.25F10C0.5	0.5	10	0.25	17.3	0.514	0.504	1387.1	2395	42
CD-0.25F10C1M	1	10	0.25	17.4	0.509	0.495	2288	3800	40.6
CD-0.25F10C4M	4	10	0.25	17.4	0.511	0.483	7537.1	10636	34.8
CD-0.25F10C10M	10	10	0.25	17.4	0.511	0.456	17775.2	23360	32.6
CD-0.5F0C0.5M	0.5	0	0.5	17.4	0.511	0.433	33282.3	39895.6	29.7

Table 5.1(continued): Summary of isotropically consolidated drained compression tests

Test	σ'_3 (MPa)	C (%)	F (%)	γ_d (kN/m^3)	e_0	e_c	p'_f (kPa)	Q_f (kPa)	ϕ'_f (°)
CD-0.5F0C1M	1	0	0.5	17.4	0.495	0.471	153	282.6	45.8
CD-0.5F0C4M	4	0	0.5	17.4	0.491	0.446	236.8	405.3	41.9
CD-0.5F0C10M	10	0	0.5	17.4	0.495	0.407	460.1	779.9	41.3
CD-0.5F2C0.5M	0.5	2	0.5	17.4	0.496	0.502	666.8	1101.3	40.4
CD-0.5F2C1M	1	2	0.5	17.4	0.523	0.499	1045.6	1638.9	38.4
CD-0.5F2C4M	4	2	0.5	17.4	0.523	0.471	2004.3	2881.5	35.4
CD-0.5F2C10M	10	2	0.5	17.4	0.495	0.446	7023.7	9203.4	32.5
CD-0.5F5C0.5M	0.5	5	0.5	17.4	0.536	0.522	17595	22917.3	32.4
CD-0.5F5C1M	1	5	0.5	17.4	0.510	0.498	34994	44219	31.8
CD-0.5F5C4M	4	5	0.5	17.4	0.517	0.488	363.5	939.8	65
CD-0.5F5C10M	10	5	0.5	17.4	0.507	0.459	449.4	1050.1	57.5
CD-0.5F10C0.5	0.5	10	0.5	17.4	0.510	0.481	749.2	1644	53.5
CD-0.5F10C1M	1	10	0.5	17.4	0.515	0.455	970.9	2021.7	50.7
CD-0.5F10C4M	4	10	0.5	17.4	0.522	0.431	1517.6	2721.1	47.3
CD-0.5F10C10M	10	10	0.5	17.4	0.51	0.402	2497.5	4375.5	43.1

The addition of fibres has also increased the axial strain corresponding to the peak strengths at σ'_3 = 300kPa but at σ'_3 = 4MPa the addition of fibre has reduced the axial strain corresponding to the peak strength. This might be due the high confining pressure. The addition of fibre in cemented sand also results in less pronounced brittle behaviour. The stress ratio (q/p') vs. axial strain curve is also shown in Figure 5.1(b). it can be seen that after achieving the peak strength, sand and fibre reinforced sand axial strains increase with very little loss in deviatoric strength while post peak behaviour of cemented and fibre reinforced cemented sand shows a rapid decrease in deviatoric stress up to 10% axial strain and thereafter achieves nearly a perfect plastic state until the end of test. No strain hardening could be seen with the addition of fibres as reported by other researchers. Addition of fibre increases the initial compression followed by strong expansion with a maximum dilation rate taking place immediately after the peak strength Volumetric strain, ε_v and axial strain, ε_a curve shown in Figure 5.1 (c). Similar results were reported by Ibraim et al., (2010), and Diambra et al., (2007b) but Consoli et al., (1998) reported that the addition of fibre reduces volumetric expansion. It can be seen that the dilation rate decreases as the composites reach final stages and does not reach a constant volume state i.e. critical state.

The effect of the addition of fibre in sand and cemented sand is also shown at higher confining pressure i.e. σ'_3 = 4MPa in Figure 5.2. It can be seen that the addition of fibres increased the peak deviator stress for both clean and cemented sand. However, the fibre reinforcement did not cause any significant difference in ultimate state. It is seen that q/p' versus ε_a curve converge to a unique stress ratio

of 1.3. The ε_v-ε_a curve shows a continuous compression in all the composites throughout the tests and does not reach to constant volume state. The addition of fibre reduces the compression of sand and cemented sand. It can be concluded from the results that the effect of the addition of fibre in sand and cemented sand is also dependent on confining pressures and the behaviour varies with the increase in confining pressure. It would be interesting to see how varying the confining pressure affects the behaviour of the composites and this has been discussed in next section.

It has been seen that the addition of fibre changes the behaviour of cemented and uncemented sand. How changing the fibre content affect the behaviour of the material is presented here at low and high confining pressures i.e. at σ'_3 = 500kPa and 10MPa. Lower and higher confining pressures have been shown as it was observed that material behaviour is also dependent on confining pressure.

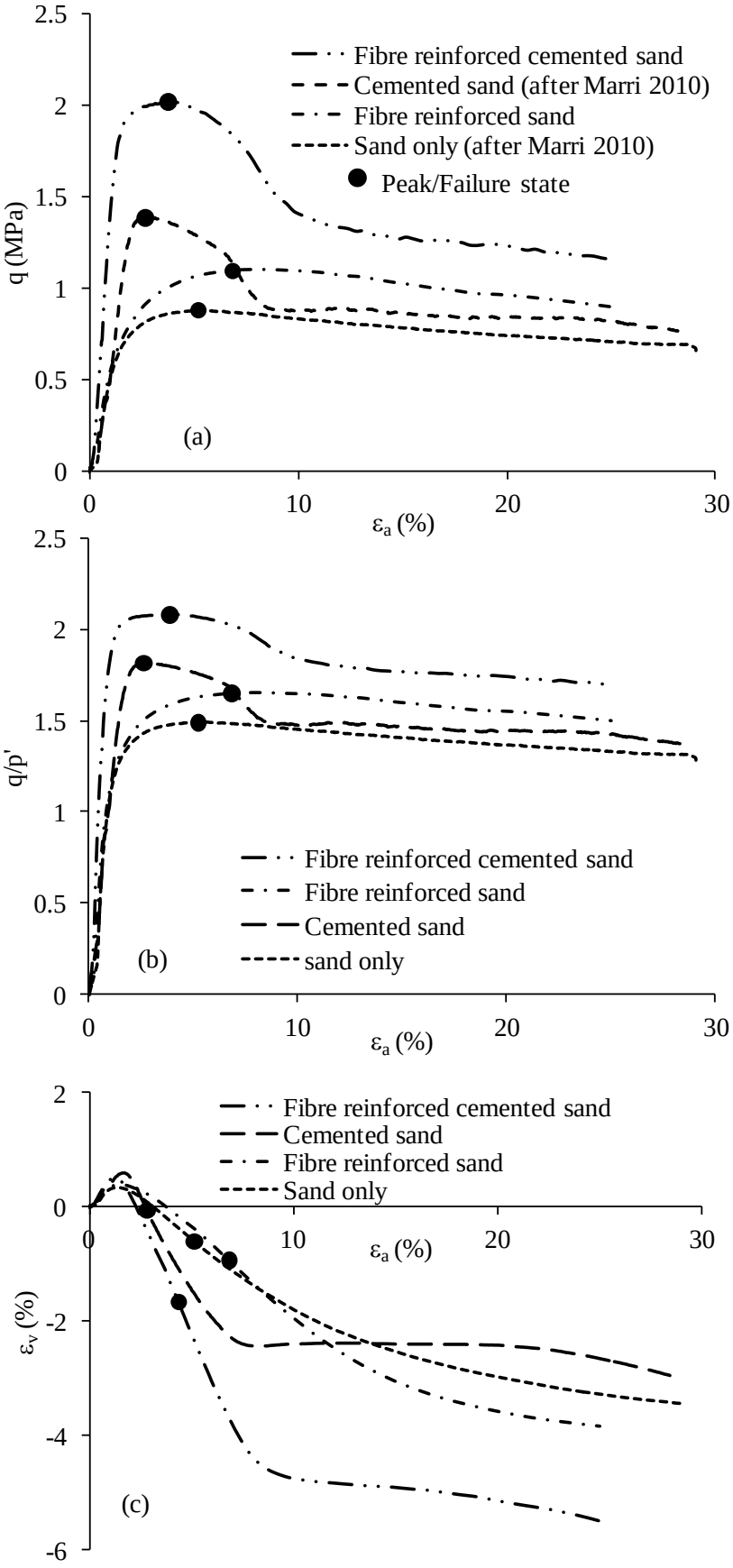

Figure 5.1 Effect of 0.5% fibre and 5% cement on the stress-strain behaviour of Portaway sand at σ'_3= 300kPa, (a) q-ε_a; (b) q/p'-ε_a; and (c) ε_v-ε_a curves.

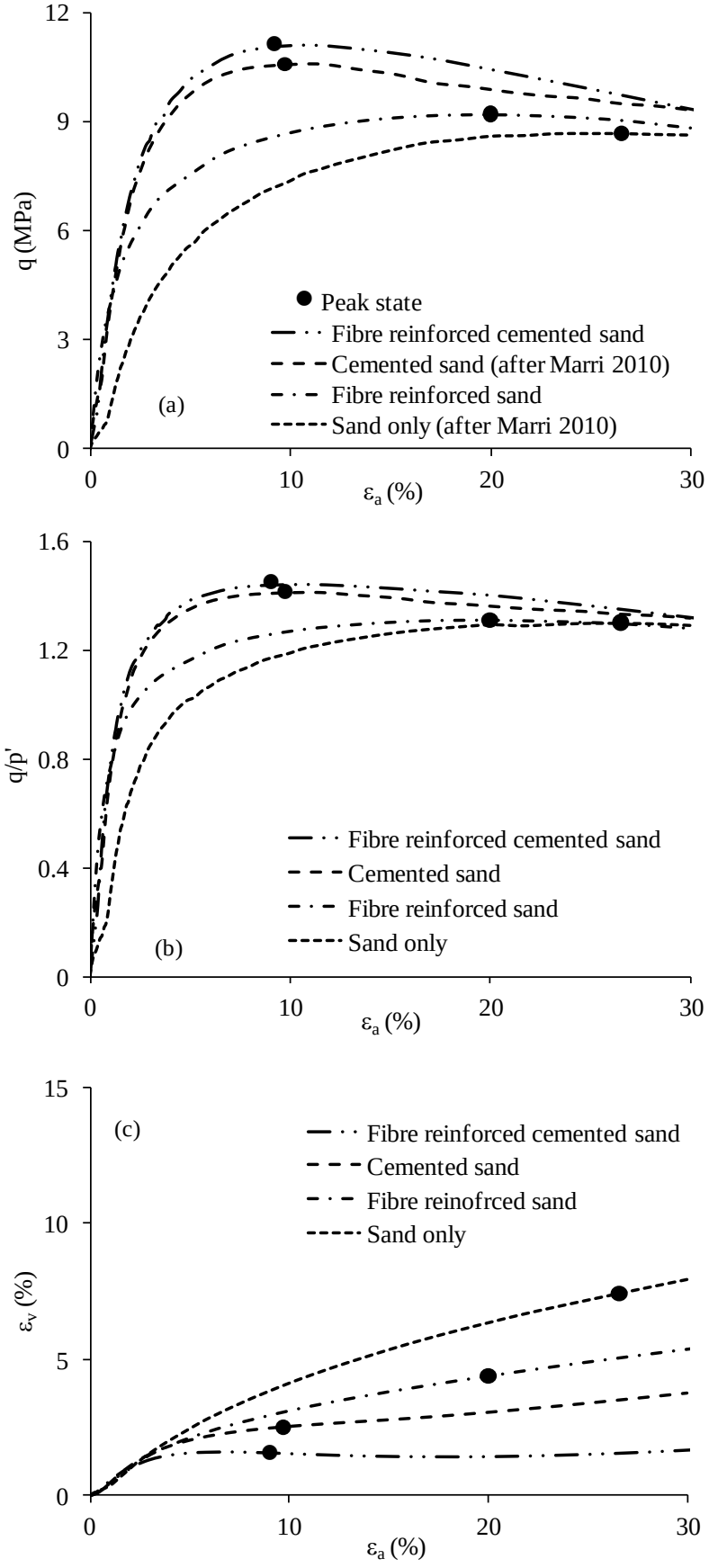

Figure 5.2 Effect of 0.5% fibre and 5% cement on the stress-strain behaviour of Portaway sand at σ'_3= 4Mpa, (a) q-ε_a; (b) q/p'-ε_a; and (c) ε_v-ε_a curves.

Figure 5.3 shows the behaviour of fibre reinforced sand at 0.25% and 0.5% fibre content. The behaviour of unreinforced sand is also shown for comparison. It can be seen in Figure 5.3(a) that increasing the fibre content increases the peak strength but has shown very little effect on initial stiffness. Michalowski and Cermak, (2002) reported that in randomly distributed fibres, a part of the fibres is compressed and a part is subjected to extension, therefore, the fibres in compression do not contribute to strength. Therefore increase in strength due to increase in fibre content depends on fibre orientation as well. Varying the fibre content has also increased the axial strain corresponding to peak strength, as well as the ultimate strength of material. The deviatoric stress reduces after achieving peak strength depicting strain softening. Increasing fibre content increases the interlock between the sand particles and provides more resistance during shearing. The (q/p')-ε_a curve in Figure 5.3(b) shows that the stress ratios continuously decrease until the end of the test and do not reach a unique stress ratio. The volumetric behaviour of fibre reinforced sand with varying fibre content demonstrate that adding fibre content reduces the initial compression and increases the dilatancy with maximum dilatancy achieved at peak deviatoric stress. As was observed the material behaviour is confining pressure dependent as well, and a similar trend was observed here with varying fibre content. The increase in strength with increase in fibre content as seen at σ'_3= 500kPa was hindered at a higher confining pressure i.e. σ'_3= 10MPa as shown in Figure 5.4 showing that the effectiveness of the addition of fibre or increasing fibre content is more at low confining pressure and that with the gradual increase in confining pressure reduces the effectiveness of fibre. It can also be seen by comparing the behaviour at two different confining pressures that post peak

softening reduces with a gradual increase in confining pressure and higher confining pressure materials deform with a gradual increase in deviatoric stress until end of the test. It can be seen that the fibre effect is in between 5% and 10% axial strain which suggests that the effect of the fibre becomes mobilised after some shearing. At higher confining pressure the affect of varying fibre content could not be seen and 0.25% and 0.5% fibre content reinforced material showed approximately the same response until they reached the peak state at the same axial strain at the end of test.

The effect of varying cement content (0%, 2% and 5%) at constant fibre content (0.5%) is shown in Figure 5.5. The q-ε_a curve in Figure 5.5 (a) shows that with increasing cement content not only peak deviatoric stress increases but also initial stiffness increased and post peak, the material depicts strain softening behaviour because of the inclusion of fibres. The axial strain corresponding to peak deviatoric stress reduced due the fact that the addition of cement increases the initial stiffness which results in higher peak stress at less axial strain. It can also be observed that composites converge to a unique stress ratio of approximately 1.4 at the end of the tests as shown in Figure 5.5(b). The volumetric behaviour with increasing cement content shows more initial compression and strong expansion at higher cement content. It can also be seen that with 2% and 5% cement, the material deforms at constant volume at 15% and 10% axial strain respectively suggesting the critical state. This constant volume state was not seen for fibre reinforced uncemented sand specimen.

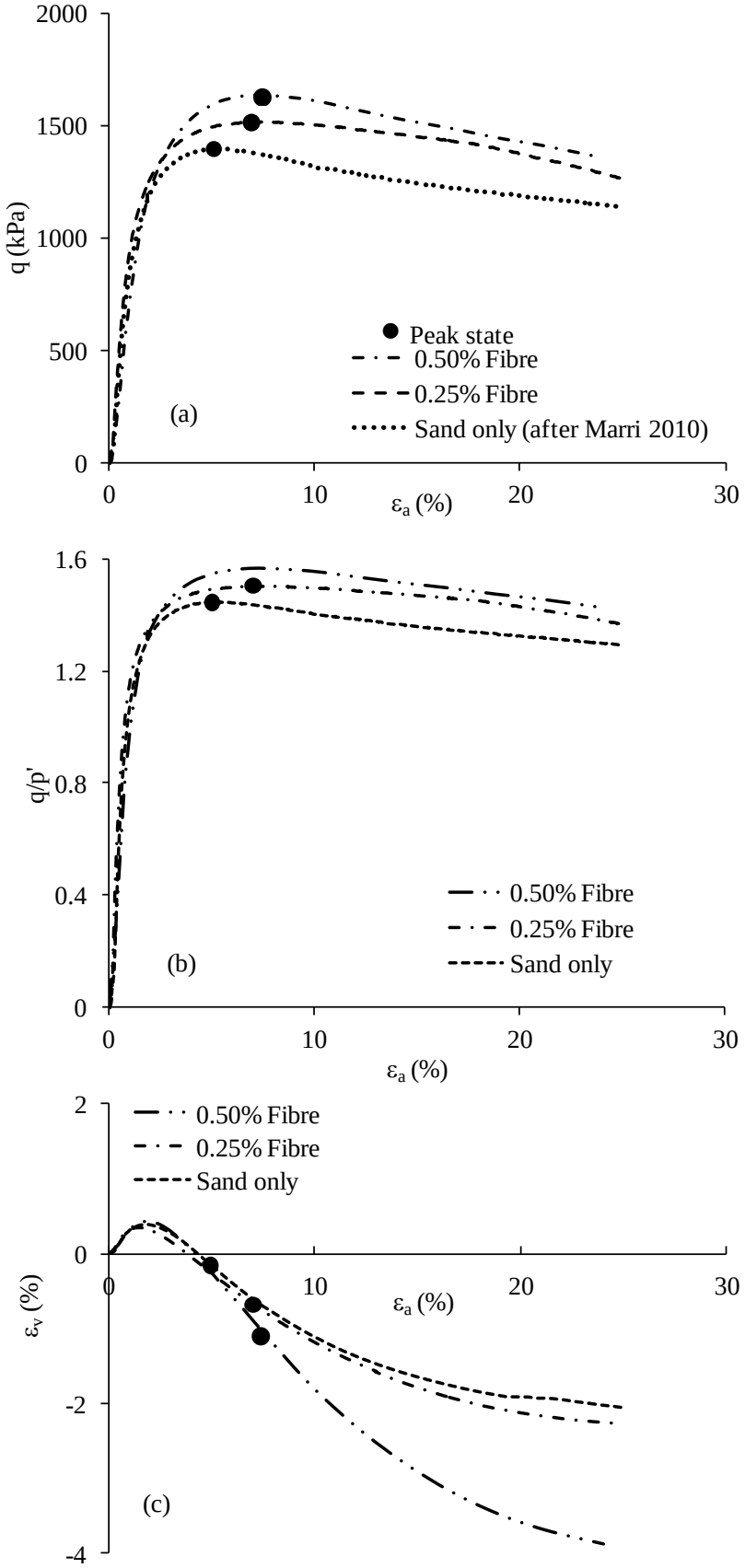

Figure 5.3 Effect of varying fibre on the stress-strain behaviour of Portaway sand at σ_3' = 500kPa, (a) q-ε_a; (b) q/p'-ε_a; and (c) ε_v-ε_a curves.

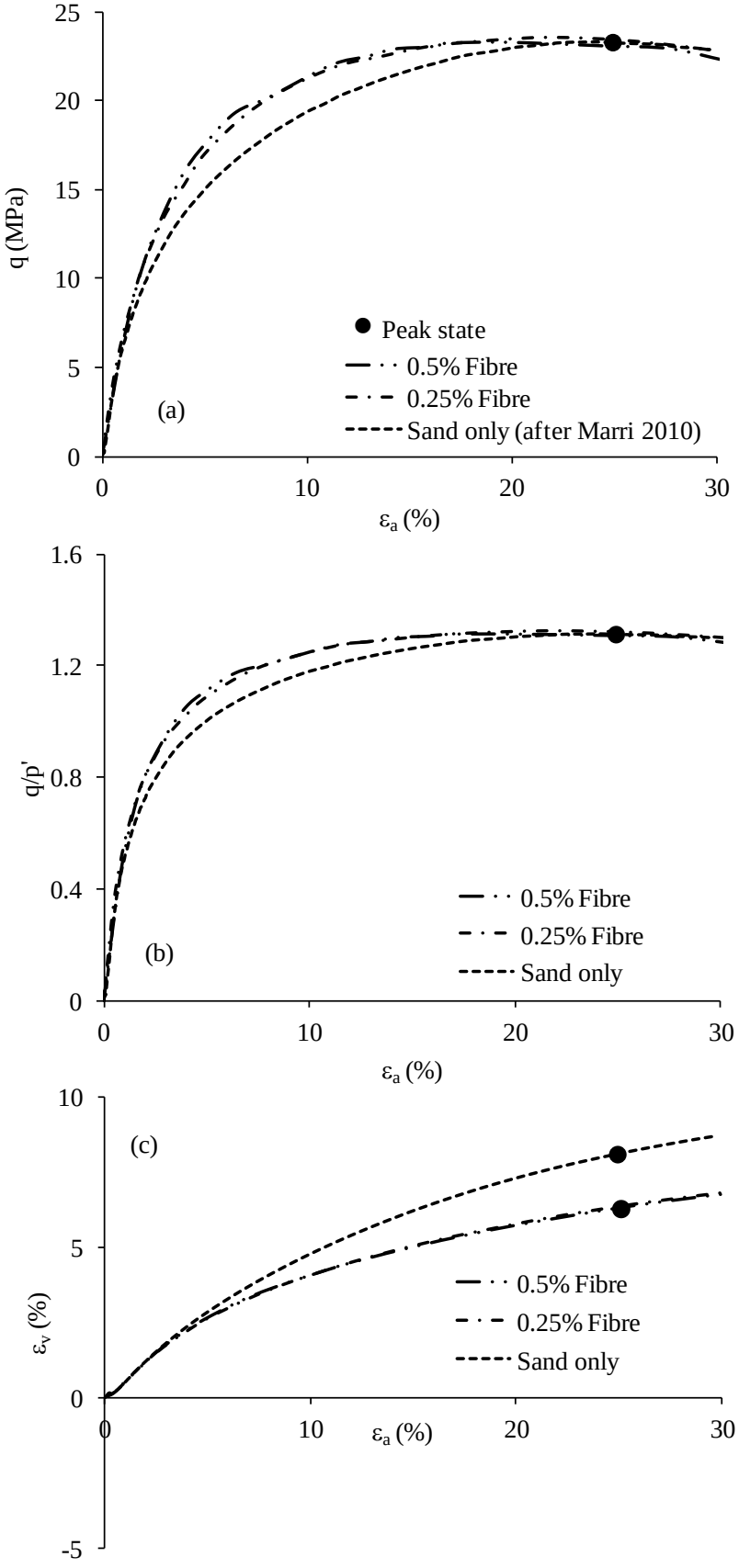

Figure 5.4 Effect of varying fibre on the stress-strain behaviour of Portaway sand at σ_3' = 10MPa, (a) q-ε_a; (b) q/p'-ε_a; and (c) ε_v-ε_a curves.

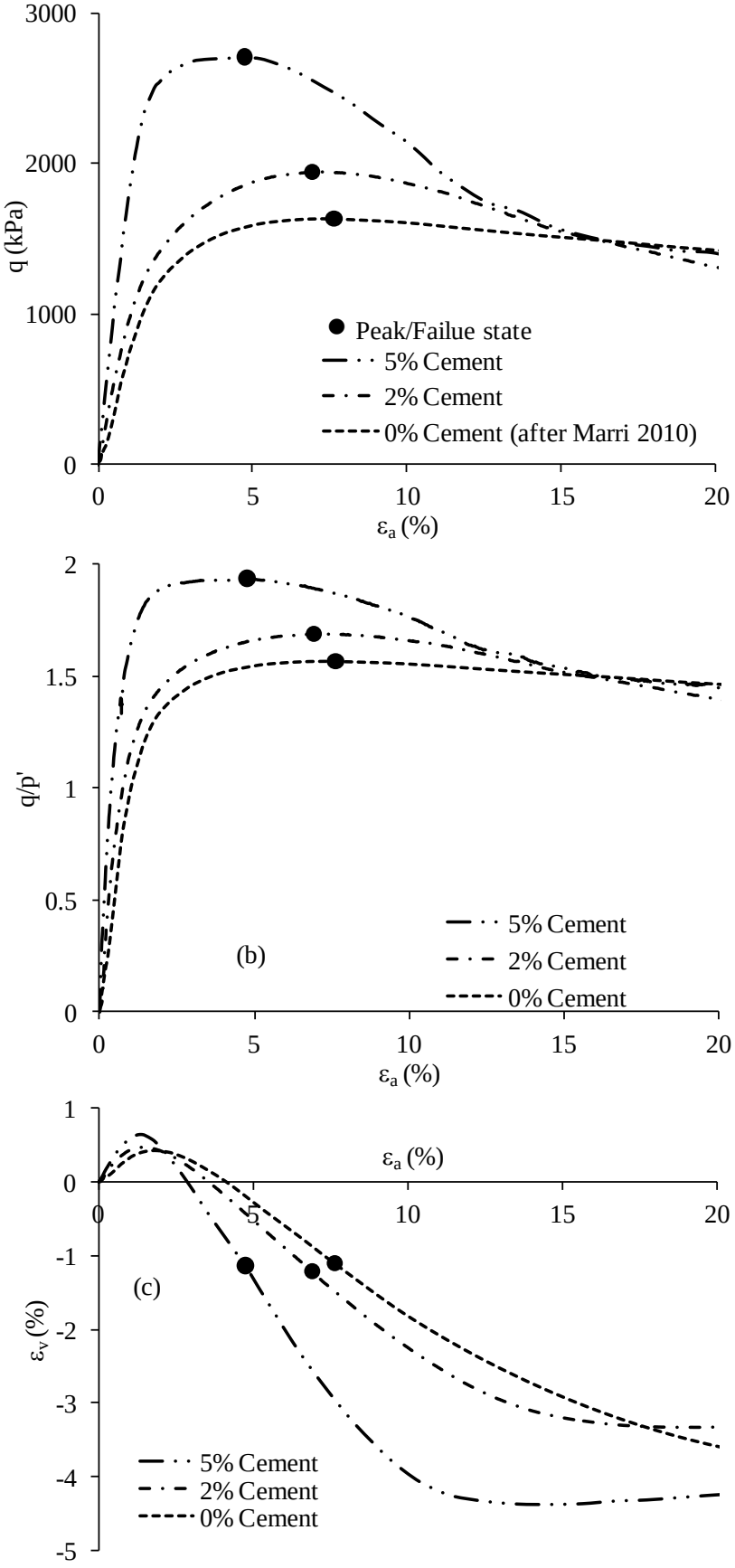

Figure 5.5 Effect of varying cement content on the stress-strain behaviour of 0.5% fibre reinforced sand, (a) q-ε_a; (b) q/p'-ε_a; and (c) ε_v-ε_a curves.

5.2.2 Effect of confining pressure

The stress-strain curves obtained from CID tests on clean Portaway sand are shown in Figure 5.6. For the clear demonstration of the wider range of confining pressures, the stress-strain curves are presented in two groups, confining pressure ranging from 100kPa to 1MPa (shown in Figure 5.6(a)) and from 4MPa to 10MPa (shown in Figure 5.6(b)). The stress-strain curves shown in the figure reveal that, by the increase in confining pressures there is an increase in the initial linear elastic stiffness of the material for both conventional and high-pressure ranges. By the progressive increase in the axial deformation during shear, it can be noticed that at relatively lower confining pressures there is a tendency in the stress-strain curves to reach a peak stress level prior to subsequent post peak softening. However, by the gradual increase in the confining pressures it is observed that the tendency to attain peak in the stress-strain curves is being suppressed and the post peak softening is plunging to a continuous hardening phenomenon. This transition from strain softening to hardening with a gradual increase in effective CP occurs at 1MPa where it can be seen that material is deforming at constant deviator stress after the peak. Moreover, it can be noticed that the peak stress is delayed by the gradual increase in the confining pressures. For instance, at conventional pressures the majority of peak stresses are reached within 5% of axial strain. On the contrary a high pressure, the maximum deviator stress continues to increase with the progression of axial strain. The ultimate strength also seems to increase with increase in CP.

The volumetric strain behaviour of sand is illustrated in Figure 5.6(c). From the figure, it can be observed that there is initial compression irrespective of the

magnitude of confining pressure. The initial compression is followed by the commencement of dilation at lower confining pressures up to 500kPa. However, the dilation is significantly pressure dependent. For instance, at low pressures, there is a higher rate of dilation and at high pressures there is a decrease in the rate of dilation. By the continuous increase in the confining pressure the dilation is suppressed and there the compression phenomenon can only be seen. From Figure 5.6(c) these trends can easily be noticed. For instance, from 100kPa to 1MPa, there is initial compression followed by the dilation, however, from 4MPa to 20MPa there is continual compression.

It can also be seen that there is no clear tendency in the material to reach critical state i.e. deform at no volume change. As only at 1MPa there is negligible volumetric change in the material but at $p' \leq$ 500kPa material continues to dilate and at $p' \geq$ 4MPa there is clear trend of the material to compress continuously with the increase in axial strain. It is to be noted that at p'= 20MPa test terminated at an axial strain of approximately 20% due to the load cell reaching its maximum capacity.

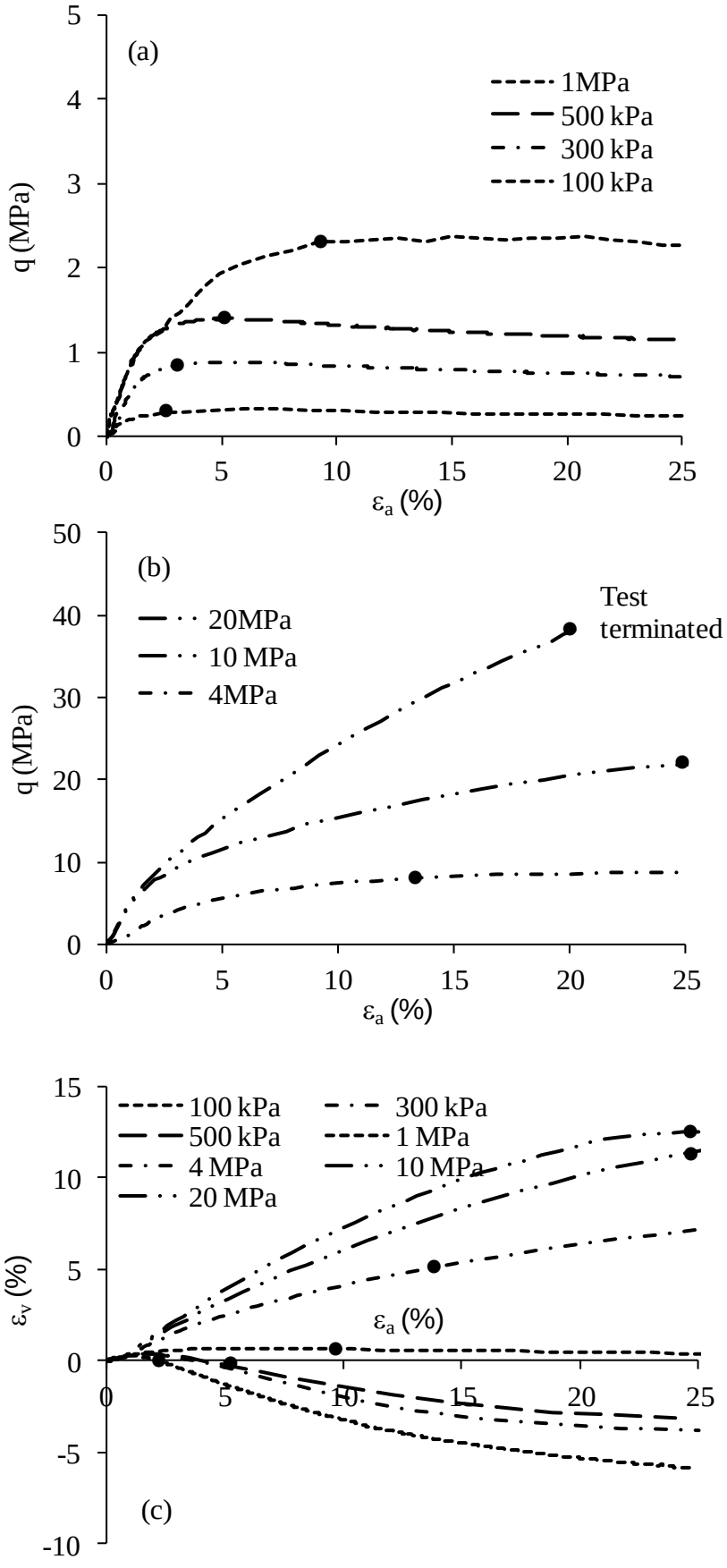

Figure 5.6 Effect of confining pressure on unreinforced sand, (a) q-ε_a; (b) q/p'-ε_a; and (c) ε_v-ε_a curves (after Marri 2010).

The effect of confining pressure on fibre-reinforced sand is illustrated in Figure 5.7. From Figure 5.7(a) and (b), it can be observed that the general response of fibre-reinforced sand against confining pressure is consistent with that of uncemented sand. However, an increase in confining pressure has resulted in an increase in the peak deviator stress, initial stiffness, and ultimate strength similar to the response observed for the parent sand. Stress-strain response changes from strain softening to strain hardening with the increasing confining pressure. It can be seen that the material deforms with decreasing stress level after reaching the peak deviator stress up to 1MPa and deformed continuously at the same stress after attaining peak stress at CP of 4MPa. It can also be seen that at CP of 10MPa & 20MPa the material has strain hardened and there is no definite peak. This suggests that up to 1MPa the material behaviour was consistent with the response of dense sand and at $\geq$ 4MPa the material behaviour changed to that of loose material. The transition from softening to hardening in fibre reinforced sand occur at p'= 4MPa. In contrast, Dos. Santos et al. 2010 reported that all fibre-reinforced specimens were found to strain-harden to reach a steady strength, irrespective of the initial void ratio. This might be due to the density effect as denser specimens show post peak softening. The void ratios used by Santos et al. ranged between 0.7-0.8 while in the current study these are approximately 0.5.

Gray and Alrefeai, (1986) also mentioned a critical confining stress and reported that the failure mechanism of fibre reinforced soil was found to be dependent on confining stress. Up to a threshold value referred to as the critical confining stress, failure occurs by frictional slipping of the reinforcement. For stresses greater than

the critical stress, failure is governed by the tensile strength of the fibre where soil normally fails before the fibres.

Volumetric strain behaviour of the fibre-reinforced sand is shown in Figure 5.7(c) and it was observed that the behaviour was similar to that of unreinforced parent sand. The only difference that can be observed is that with the addition of fibre at 1MPa, the clean sand behaviour is purely compressive but with the addition of fibre, it showed dilation. Hence, it can be said that the addition of fibre reduces the rate of compression, which can also be clearly seen at other higher confining pressures. Similar to the response observed in clean sand the fibre reinforced sand also tends to either dilate continuously at low confining pressures or compress till the end of the test at higher effective confining pressures. Hence, no critical state condition i.e. zero volume change was achieved in the volumetric response of fibre reinforced sand.

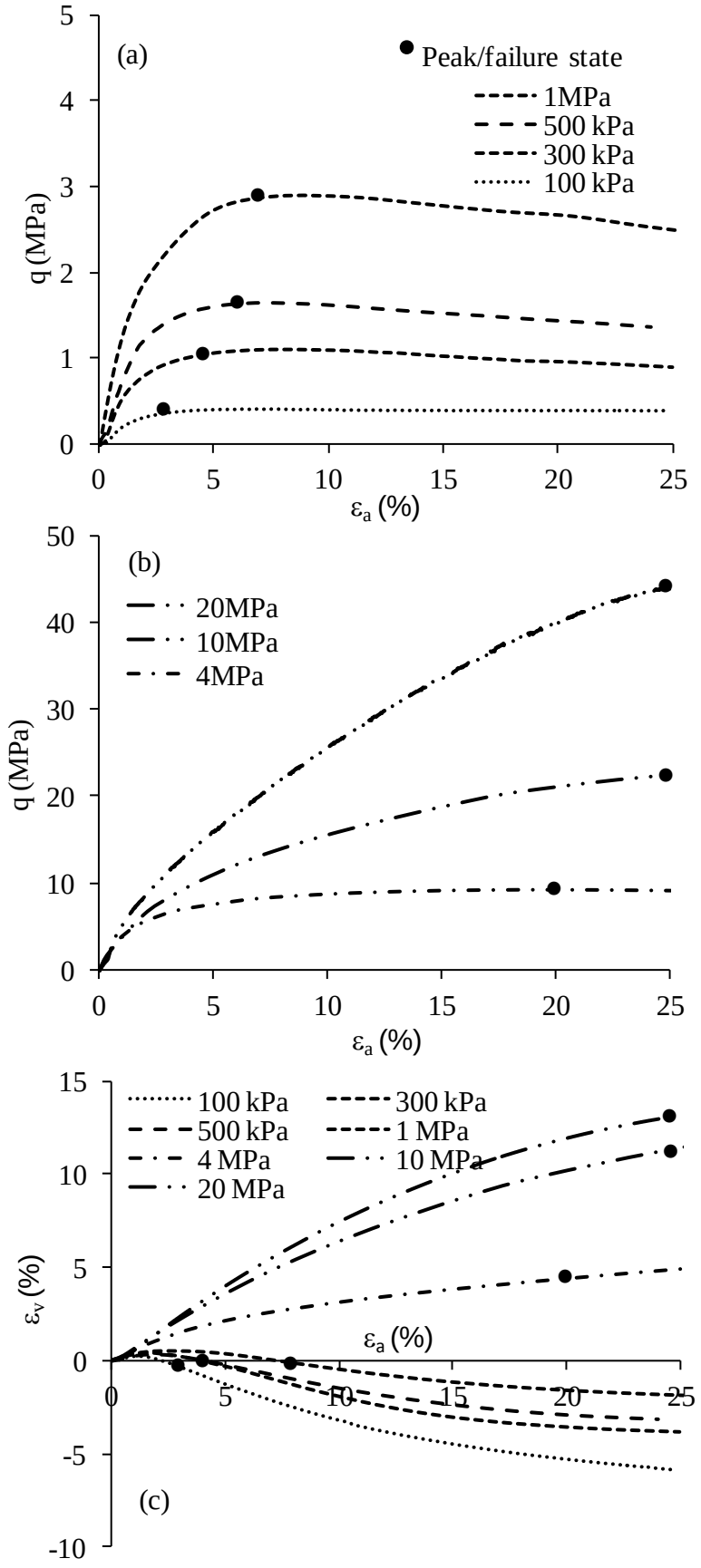

Figure 5.7 Effect of confining pressure on 0.5% fibre reinforced sand, (a) q-ε_a; (b) q/p'-ε_a; and (c) ε_v-ε_a curves.

The effect of confinement on the behaviour of fibre reinforced cemented sand is presented in Figure 5.8, in which the deviator stress, q and the volumetric strain, ε_v have been plotted against axial stain ε_a. As expected, the confining pressure has increased the peak deviator stress, initial stiffness (initial linear portion of the curve), and ultimate strength of the composites. It can be observed that peak deviator stress has increased with an increase of confining pressure and the axial strain at which peak strength is attained has increased as well. After reaching the peak stress, the stress-strain curves tend to softened at a comparatively higher rate in fibre reinforced cemented sand up to CP of 1MPa, thereby softening was slow until only hardening could only be seen at 20MPa where the deviator stress increased continuously with shearing. Past work by Clough*, et al.* (1981) and Rad and Clough, (1982) have also shown that both weakly and moderately cemented sands demonstrate a failure mode that is brittle under low confining stresses and ductile under higher pressures. The reason for the change from brittle to ductile failure modes was shown to be related to the relative contributions to sand response by the cementation and frictional components of the deformation resistance mechanism. The frictional component is further augmented by the activation of friction due to fibre as well. Thus, for the change of the mode of failure from brittle to ductile there seems to be a contribution of both confining pressure and fibre reinforcement. It is to be noted that at 20MPa, the test was terminated at an axial strain of 20% since the load cell reached it maximum capacity.

The volumetric response shows that with the increase in confining pressure the rate of dilation decreases and at a higher confinement, the dilative behaviour

changed into pure compression as shown in Figure 5.8(c). It can also be observed that at low CP up to 500kPa, fibre reinforced cemented sand dilated at a higher rate and reached a maximum value of volumetric strain and thereafter, expansion or dilation within the material was less pronounced. However, the rate of dilation before reaching to a maximum value also reduced with increasing p′ until at 1MPa there was no definite peak value and material expanded continuously with the increasing axial strain. The striking response that can be observed in volumetric behaviour of all the three material combinations is that at a particular confining pressure in each combination, the volumetric strain nearly gets constant and the material deform at more or less no volumetric change. This critical confining pressure was observed to be 1MPa for clean sand and 4MPa for fibre reinforced cemented sand. However, for fibre reinforced sand, it was expected to be between 1MPa and 4MPa but this needs to be verified.

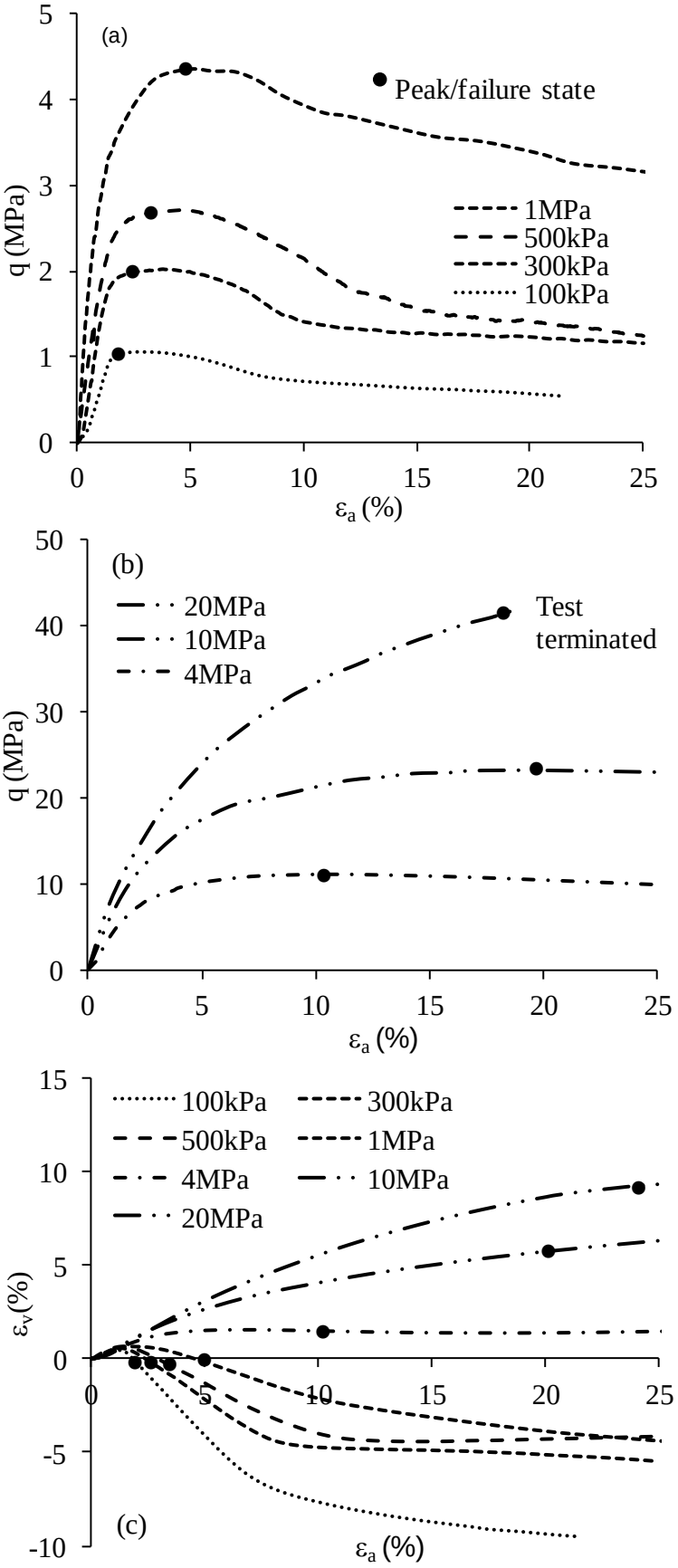

Figure 5.8 Effect of confining pressure on 0.5% fibre and 5% cemented reinforced sand.

5.2.3 Drained shear strength

The confining pressure also affects the shear strength parameters, i.e., the cohesion, and friction angle. The failure envelopes of the sand, fibre reinforced sand, cemented sand and fibre reinforced cemented sand in q_f-p_f' plane are shown in Figure 5.9. There is some diverse opinion in the literature regarding the shape of failure envelopes. For instance, Asghari, et al. (2003), Haeri, et al. (2005) have reported curved envelopes for cemented sand and on the contrary, failure envelopes have also been reported as straight lines Consoli, et al. (2009) and bilinear Consoli, et al. (2007). The failure envelopes in the current study are based on the best-fit curves of the data points. These envelopes appear to be straight lines at lower pressures as shown in the enlarged figure at low confining pressure but with the gradual increase in confining pressure there could be noticed a slight tendency of convergence of the reinforced material curves toward the parent material. From the extrapolation of these best-fit curves it could be presumed that at further higher confining pressures these curves might reach to a constant value.

Nevertheless, a linear approximation was used for calculating the shear strength parameters. The results were extrapolated to zero confining pressure to get the approximate values of the cohesion intercept. The values of the cohesion intercept were 176kPa, 287kPa and 940kPa for the non-reinforced sand, fibre reinforced sand, and fibre reinforced cemented sand respectively, as can be seen in Figure 5.10. As a result, the addition of fibre and cement has the effect to increase the cohesion of uncemented sand.

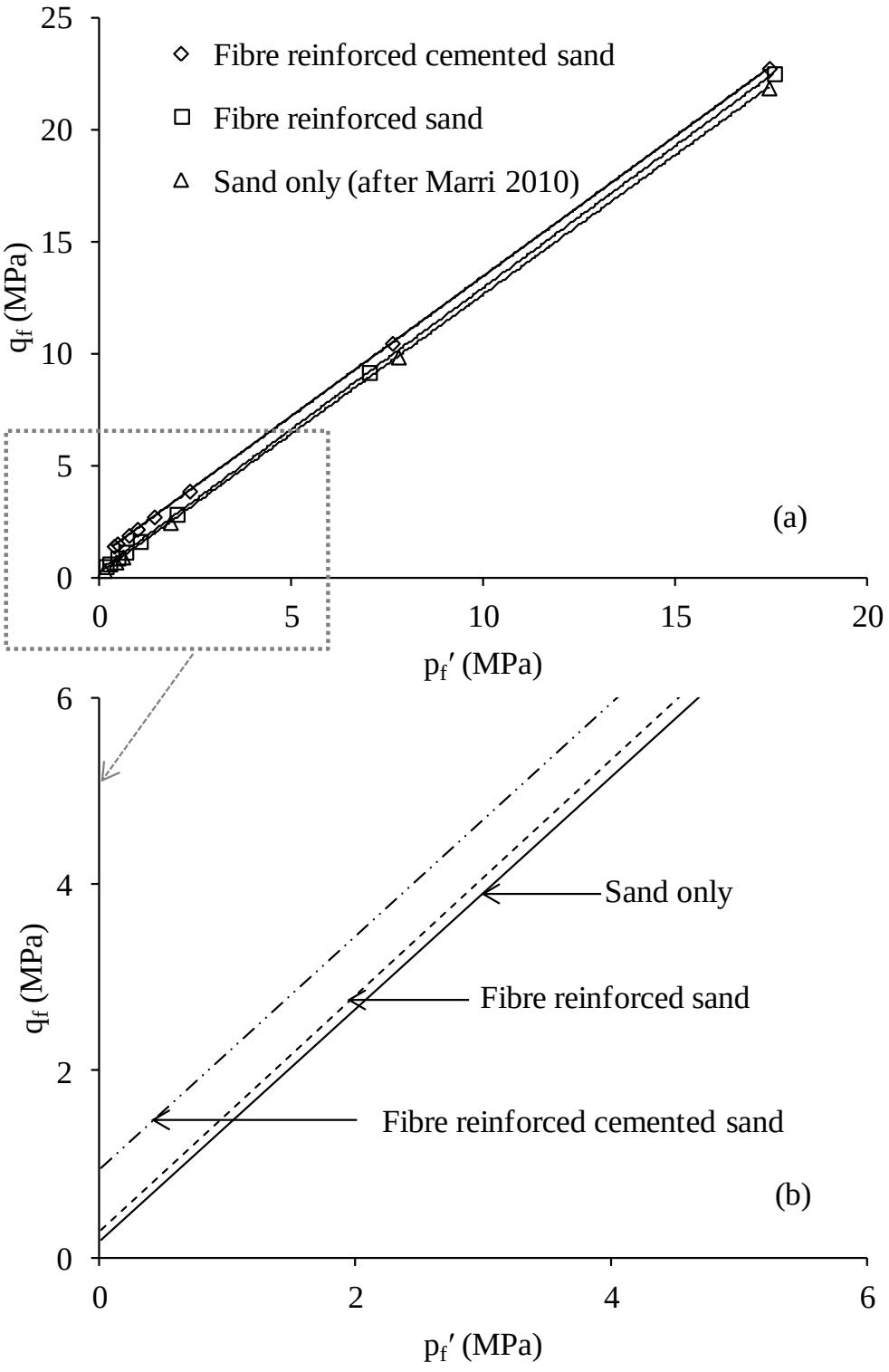

Figure 5.9 Effect of fibre and cement on the failure envelopes of Portaway sand.

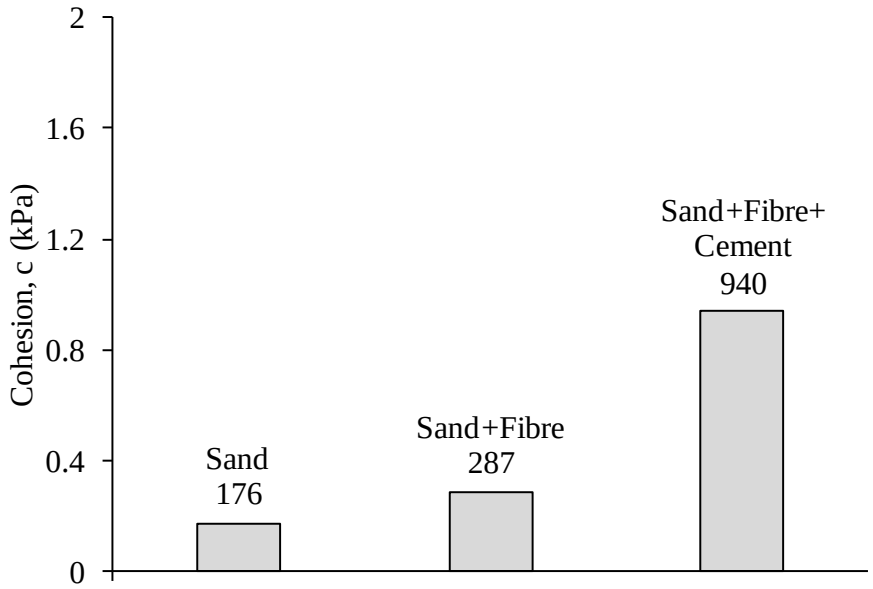

Figure 5.10 Effect of fibre and cement content on cohesion.

Plots of the effective stress ratios at failure $(q/p')_f$ for all the materials are given in Figure 5.11. It is clear that the addition of fibre and/or cement content and varying confining pressure affects the failure state of the composites. The $(q/p')_f$ increases with the addition of fibre and cement content but reduces with increasing confining pressure. Therefore, the differences between the peak strength of specimens are large at low confining pressures and reduce significantly at high pressures. In other words, the influence of the addition of fibre and cement content is greater at low confining stresses and this effect reduces with an increase in confining stress. It can also be observed at higher confining pressure the stress ratio converges to a unique stress ratio of 1.3.

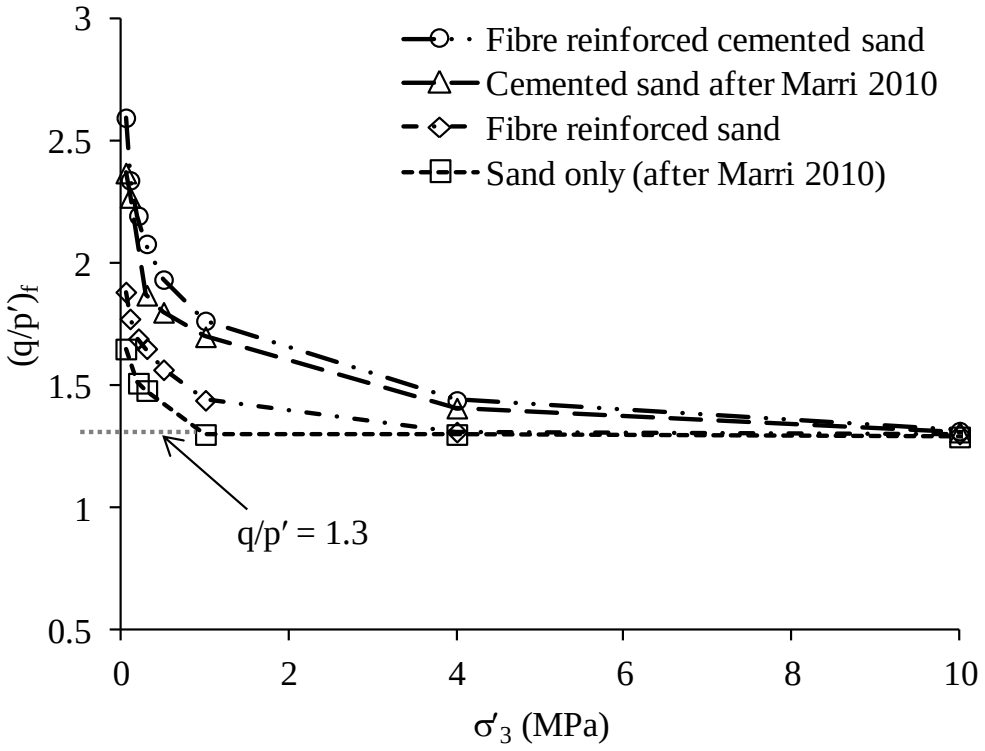

Figure 5.11 Effect of fibre and cement on the peak stress ratio of Portaway sand.

From Figure 5.12, it can be observed that with the increase in confining pressure there is decrease in the friction angle and at a confining pressure of 10MPa the difference in friction angle is hardly noticeable and at 20MPa the curves show a tendency of approaching to a constant value.

The addition of fibre and cement considerably influences the shear strength parameters. Figure 5.12 shows the effect of the addition of fibre and cement on the peak friction angle of sand, fibre reinforced sand and cemented sand. It can be observed that there is an increase in the ϕ_f of the sand by the addition of cement, fibre, or both and a decrease in the friction angle with increasing confining pressure. However, this increase in friction angle is more pronounced at low confining pressures as shown in the magnified figure. With increasing confining pressure above 1MPa this effect appears to diminish gradually and at 20MPa, the effect

appears to be unnoticeable. Therefore, at and above 10MPa there is a negligible effect of fibre and confining pressure on the friction angle. Moreover, it attains a nearly constant value for all the combinations.

It was previously reported in the literature that the friction angle significantly increases with the increase in cement and fibre contents at conventional pressures. For instance, Consoli et al. (1988) reported the increase in frictional angle from 35 to 46 degree because of fibre inclusion to the sand, and Consoli et al. (2004) reported an increase in the frictional angle due to the increase in cement content. In the present study, it was further extended to the high pressures.

Thus, it can be concluded that the friction angle of sand depends not only on the reinforcement but also on the effective confining pressure. For instance the frictional angle of clean sand, fibre reinforced sand, cemented sand, and fibre reinforced cemented sand at 50kPa is 40.4°, 45.8°, 58.2°, and 65° respectively. However, beyond 10MPa the frictional angles for all compositions approach to 32°.

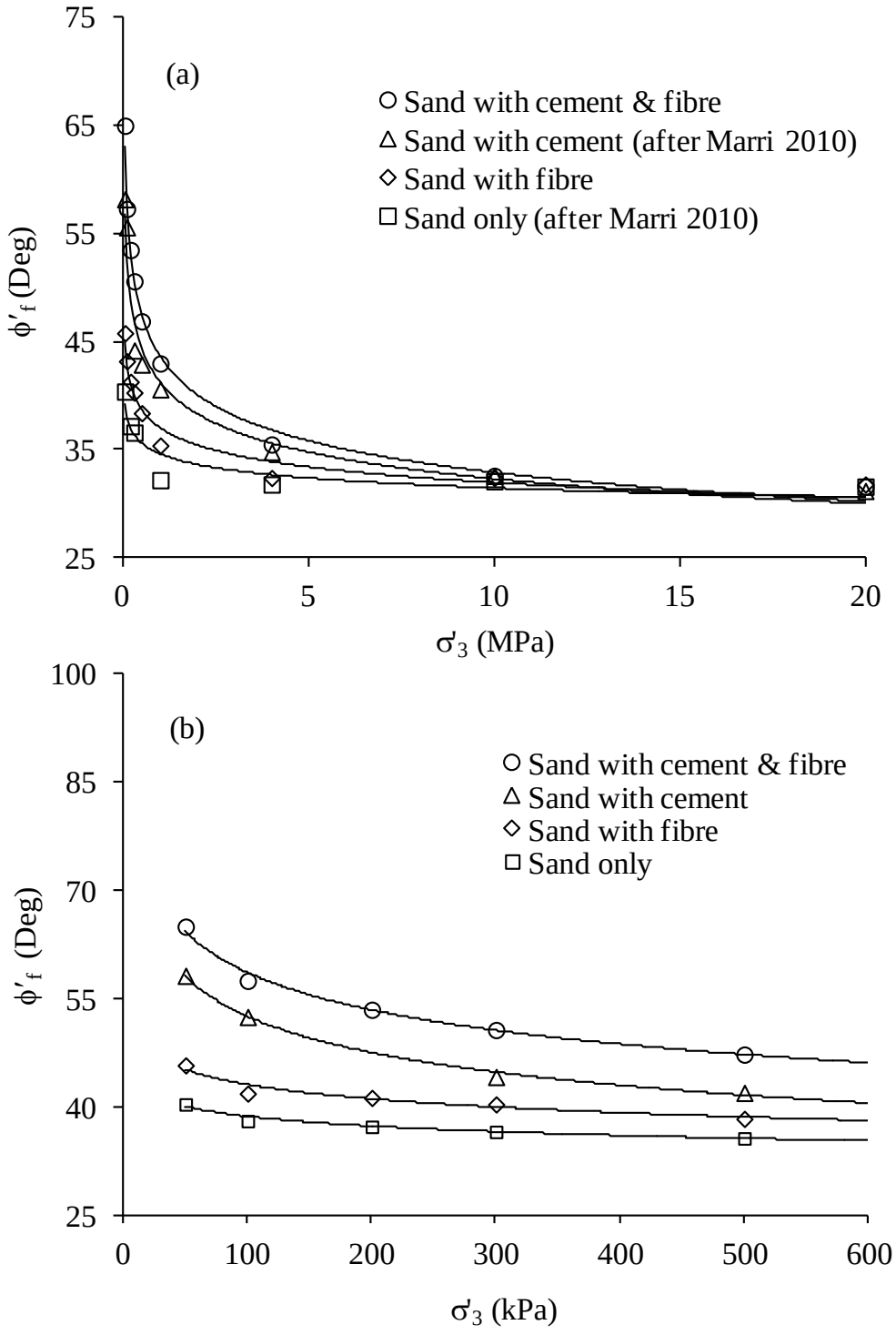

Figure 5.12 Effect of fibre and cement on the peak/failure friction angle of Portaway sand.

The increase in q_{max} in terms of percentage when compared with the strength of clean sand is greater at low confining pressures and decreases with the increase in

confining pressure as shown in Figure 5.13. The fibre effect on cemented and uncemented samples is also higher at low confining pressure and it gradually decreases with increasing confining pressures

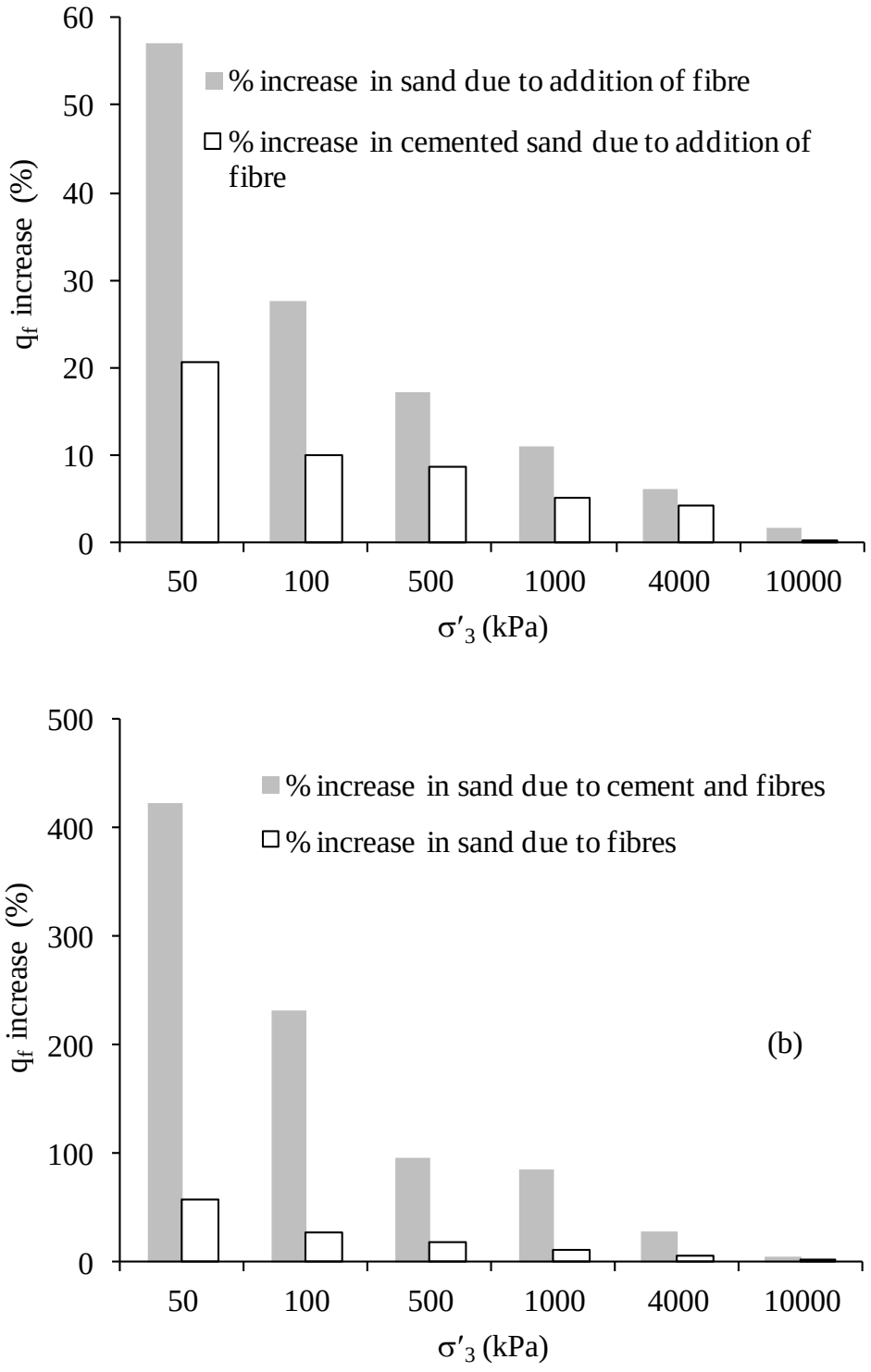

Figure 5.13 Effect of fibre and cement content on percent increase in strength: (a) addition of fibre; (b) increase due to fibre and/or cement.

5.3 Undrained behaviour

The behaviour of granular materials can normally be accurately characterized for practical applications from the results of drained tests, since in many problems the material can usually be considered fully drained. However, if the permeability of the material is relatively low, as in cemented sands, undrained conditions can exist. The undrained behaviour is of utmost importance for strength and deformation analyses under short-term conditions. Consideration of how the undrained shear strength of sand is related to changes in pore pressure provides a more useful and practical framework for understanding the undrained strengths of these materials, and for characterizing undrained strengths for practical purposes. An attempt to illustrate the typical engineering characteristics of fibre reinforced cemented and uncemented sand, undrained triaxial compression tests were performed with initial confining pressures between 100kPa and 20MPa. The role of fibre and cement content and confining pressure on the mechanisms controlling the undrained shear behaviour was investigated. The tests consisted of drained isotropic compression followed by undrained shearing under strain control. The total confining pressure was maintained constant throughout shearing. The specimens were sheared at a strain rate of 0.15mm/min. Induced pore pressure was measured with a pressure transducer attached to the base of the triaxial cell.

5.3.1 Effect of fibre and cement

The effect of the addition of fibre and cement on undrained triaxial behaviour is presented in Figure 5.14 in which q-ε_a, Δu-ε_a and q-p' curves are shown. It can be

seen q-ε_a curve in Figure 5.14(a) that initial stiffness in undrained triaxial tests is unaffected by the addition of fibre, contrary to the behaviour observed in drained triaxial tests, although fibre has increased the maximum deviatoric stress and ultimate strength. Sariosseiri and Muhunthan, (2009) reported similar observation for cemented soil.

Drained specimens tend to dilate more than undrained ones, inducing a greater desire for radial strain and therefore greater potential tensile stresses in the fibres which create an increased confinement on the sand in the drained specimens and hence a much larger increase in strength than observed for undrained specimens.

The generation of pore water pressure, Δu, is plotted against axial strain in Figure 5.14(b). It can be seen that pore pressure of the sand after reaching the maximum value remains the same until the end of the test while pore pressure for the fibre reinforced sample reduces after attaining peak value. It can also be seen that there is strong reduction in pore pressure for cemented and fibre reinforced cemented sand samples. Because of the high confining pressure there is no negative pore pressure developed consistent with the no dilatancy observed in drained triaxial tests.

The effective stress paths presented in Figure 5.14(c) is also used for further analysis of undrained behaviour. For all four tests, the effective stress path has an initial very small straight segment. This segment corresponds to the initial region of the q-ε_a curve which shows very high stiffness. The effective stress path bends to the left thus implying the significant pore pressure generation. This can be viewed

as the onset of significant bond breakage and yielding. Eventually the phase transformation state, PT, defined as the state when dp' changed from negative to positive, is reached. After the PT state, the stress path for cemented and fibre reinforced cemented samples traced along the direction of dp'>0 and appeared to approach closely the failure line from drained triaxial test and fibre reinforced uncemented samples traced along the direction of dp'<0.

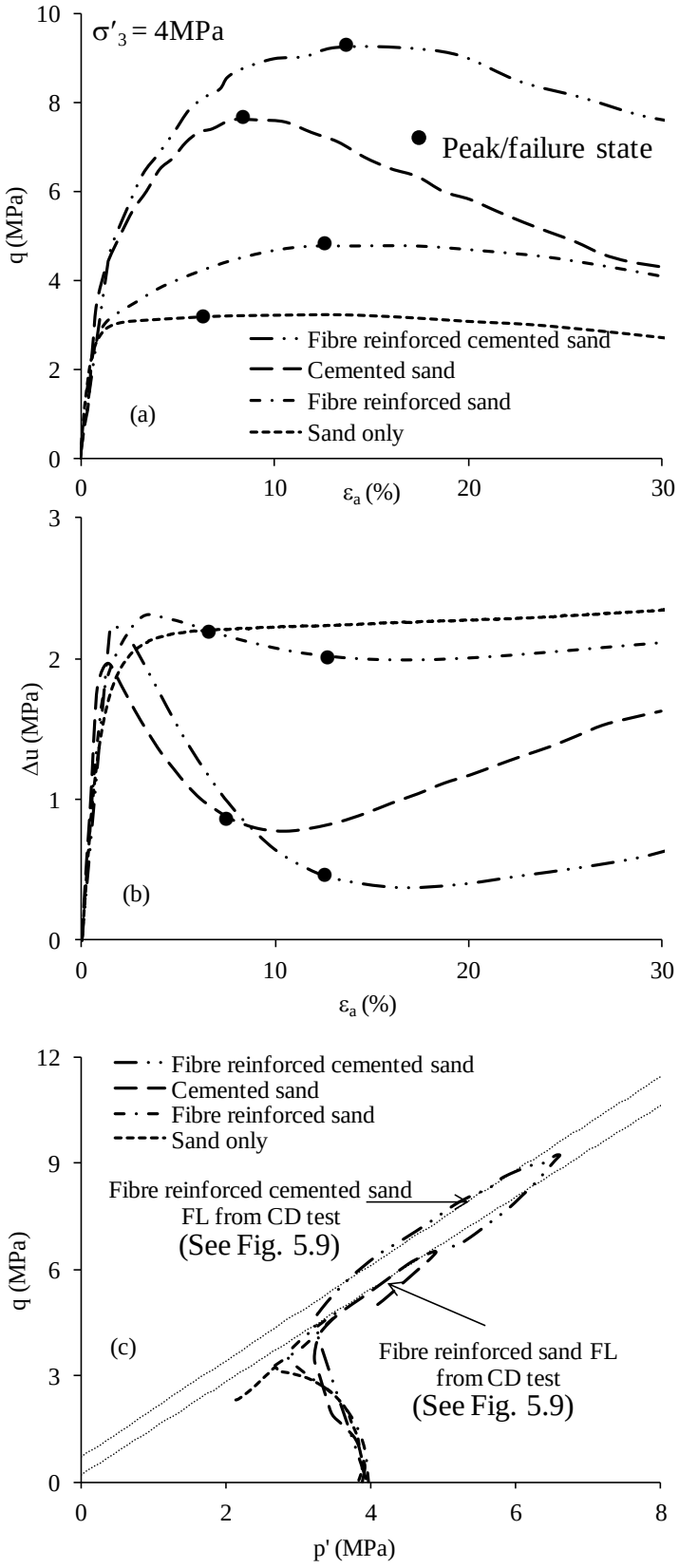

Figure 5.14 Effect of fibre and cement content on the undrained triaxial behaviour of Portaway sand at σ'_3= 4MPa: (a)stress strain curve; (b) pore pressure-axial strain; and (c) stress paths.

5.3.2 Effect of confining pressure

The effect of confining pressure on undrained triaxial behaviour of fibre reinforced uncemented and cemented sand is presented in Figure 5.15 and Figure 5.16.

The results of CIU tests carried out on fibre reinforced Portaway sand are presented in Figure 5.15. The q-ε_a curves show an increase in peak deviator stress and residual strength with the increase in confining pressure. It can also be seen that with increasing confining pressure the material attains higher peak strength but the axial strains corresponding to these peaks are decreasing. At higher confining pressure after reaching peak strength, material deforms with continuously decreasing deviatoric stress showing the tendency of strain softening. The ultimate strength of the composite has also increased with the increasing confining pressure. Similar to behaviour observed in clean sand there is the effect of confining pressure at the initial stiffness of the material while in drained tests CP has the trend of increasing the initial stiffness.

The excess pore water pressure versus axial strain curves are also shown in Figure 5.15 (b). The excess pore water pressure remained positive (consistent with a tendency for the sample to contract) at higher confining pressure but at 1MPa, after a first stage of positive excess pore water pressure, negative excess pore water pressure was produced (consistent with a tendency for the sample to dilate). In general, the higher the confining pressure the higher the pore pressure measured in the test. It can also be seen that the excess pore water pressure increased and approached a constant value throughout shearing until the end of test. The Δu-ε_a

curves obtained from the specimens consolidated to p' of 1MPa and 4MPa showed an initial excess pore water pressure and a distinct peak (i.e. u_{max}). After that, a reduction in the excess pore water pressure was observed in the two tests until the peak deviator stresses were reached and the shear bands were developed.

The stress paths are shown in Figure 5.15(c), it can be seen that at 4MPa and 10MPa the curves after initial straight line segment of high stiffness bends to the left implying the onset of yielding. At confining pressures of 1MPa and 4MPa after PT state the stress paths appeared to approach closely to the failure line obtained in drained triaxial tests.

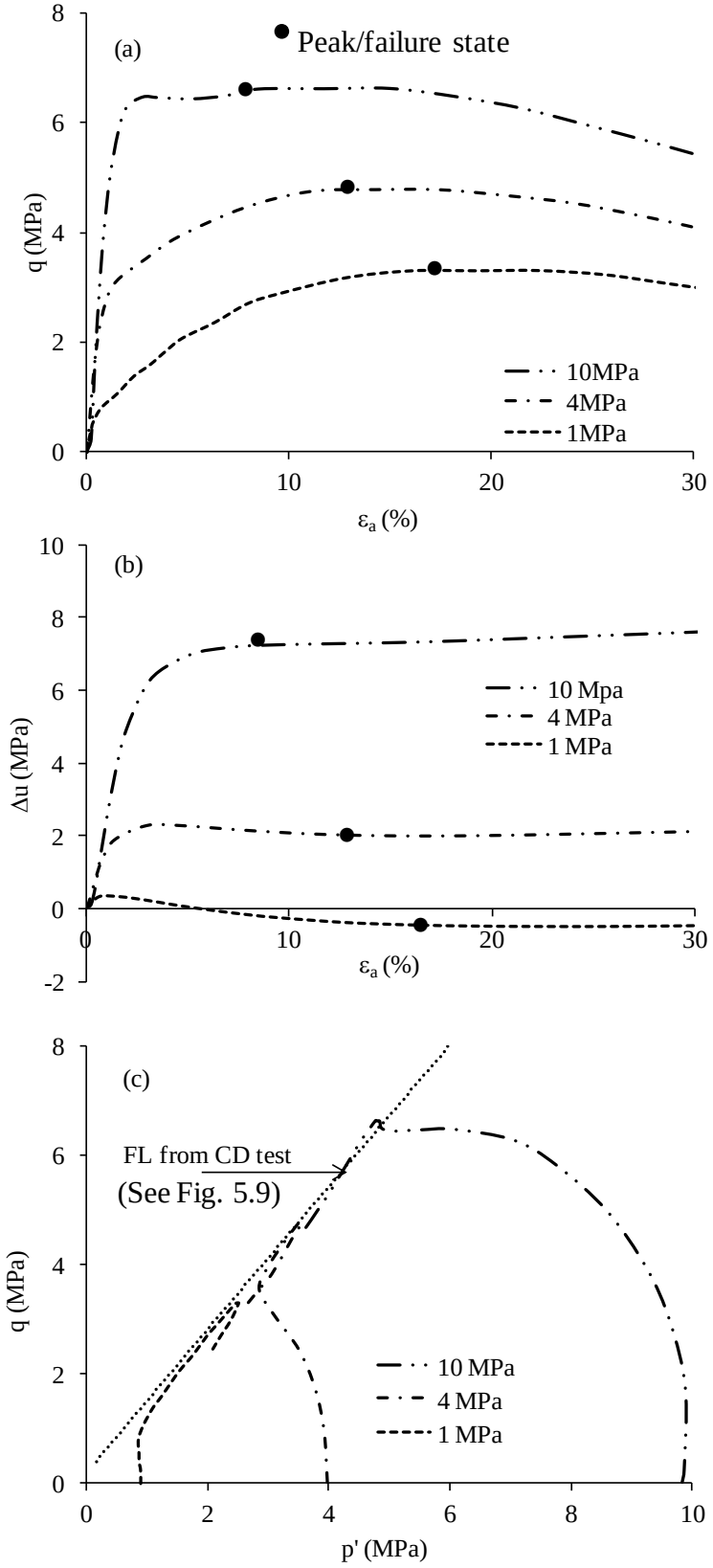

Figure 5.15 Effect of confining pressure on the undrained triaxial beahviour of 0.5% fibre reinforced sand: (a) stress-strain behaviour; (b) pore pressure response; and (c) stress paths.

The results of CIU triaxial tests carried out on fibre reinforced cemented specimens with 5% cement and 0.5% fibre contents are presented and discussed in this section. The specimens were isotropically consolidated to different mean effective stresses, p′ of 1, 4, 10, and 20MPa.

The q-ε_a curves show a increase in peak deviator stress with the increase in confining pressure. The stiffness and residual strength also seems to increase with increment in *p*′. It can also be seen that with increasing CP the material attains higher peak strength at decreasing axial strains. At higher CP after reaching peak strength, material deforms with continuously decreasing deviatoric stress showing the tendency of strain softening but at CP of 1MPa, it deforms at nearly the same stress level. The ultimate strength of the composite has also increased with the increasing confining pressure.

The excess pore water pressure versus axial strain curves are also shown in Figure 5.16 (b). The excess pore water pressure remained positive (consistent with a tendency for the sample to contract) at higher confining pressure but at 1MPa, after a first stage of positive excess pore water pressure, negative excess pore water pressure was produced (consistent with a tendency for the sample to dilate). In general, higher the confining pressure higher the pore pressure measured in the test. It can also be seen that in the specimen sheared at p′ of 20MPa the excess pore water pressure increased continuously throughout shearing and approached a constant value at the end of test. The Δu-ε_a curves obtained from the specimens consolidated to p′ of 1MPa and 4MPa showed an initial excess pore water pressure and a distinct peak (i.e. u_{max}). After that, a reduction in the excess pore water

pressure was observed in the two tests until the peak deviator stresses were reached and the shear bands were developed.

For the uncemented fibre reinforced material, the stress paths from undrained tests define a similar failure envelope to that defined by the drained tests. However, in the fibre reinforced cemented material (see Figure 5.16 (c)), the undrained tests cross the failure surface defined by the q_{max} points from drained tests, showing that the material can attain higher stress ratios when sheared in an undrained condition. However, the q_{max} points for the undrained tests agree quite well with the drained tests in terms of stress ratio. The difference between limiting stress ratios from undrained and drained tests is likely to be due to the fact that volumetric straining (as happens in the drained tests) will contribute to breakdown of the cemented bonds (Malandraki and Toll, 2001). When volume strains are prevented (in undrained tests) a higher stress ratio can be sustained before the bonds break down (Asghari et al., 2003).

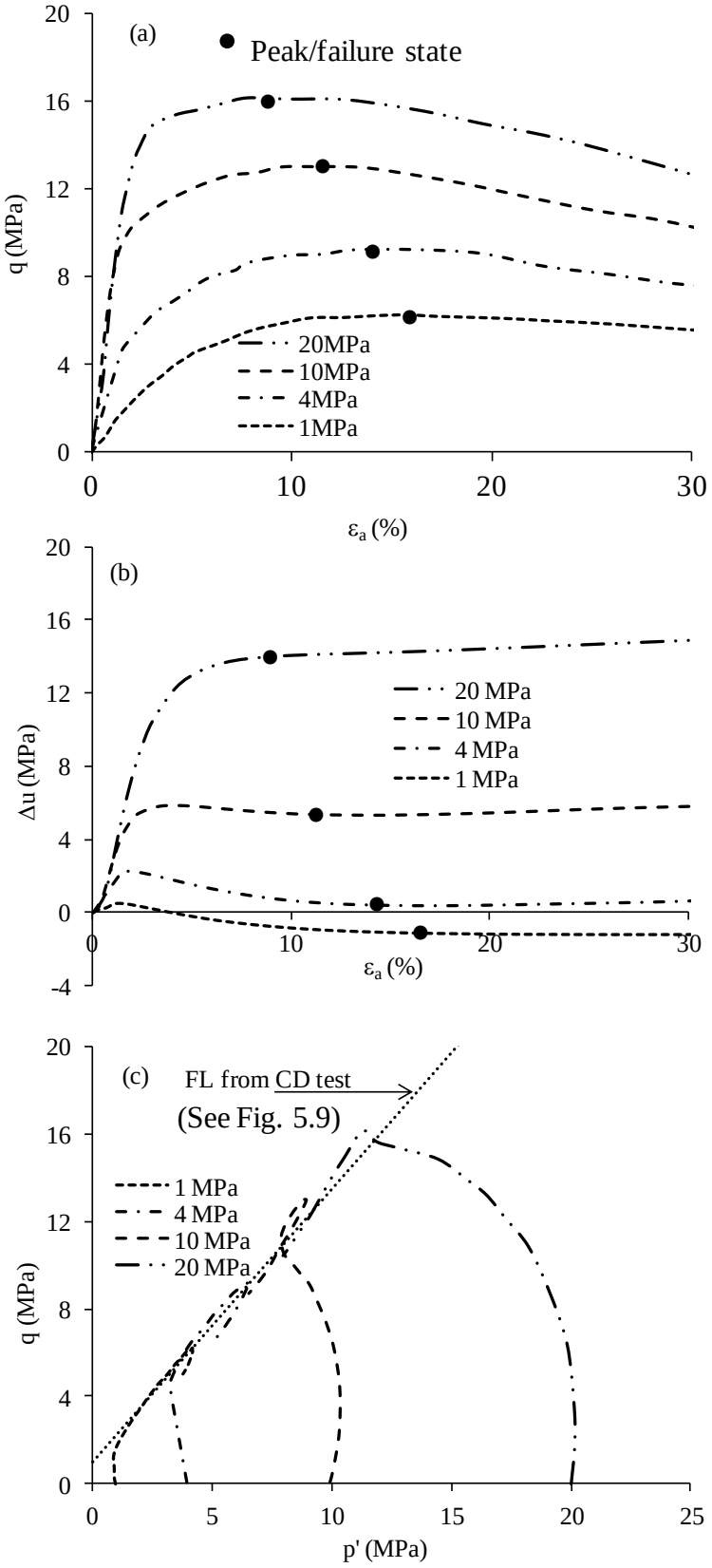

Figure 5.16 Effect of confining pressure on the undrained triaxial beahviour of 0.5% fibre and 5% cemented sand: (a) stress-strain behaviour; (b) pore pressure response; and (c) stress paths.

5.4 Comparison of drained and undrained behaviour

To investigate the effect of drainage condition on the stress-strain response of fibre reinforced material, the data for both drained and undrained tests at 4MPa is presented in Figure 5.17 for fibre reinforced sand, cemented sand and fibre reinforced cemented sand. The q-ε_a curves are shown in Figure 5.17 (a) for all the different compositions. It can be observe that all the materials show the same initial stiffness for both types of tests but in undrained tests fibre reinforced sand yields while in drained triaxial tests, deviatoric stress increases until it reaches a maximum value at about 10% axial strain. In both the tests after achieving peak stress the samples continue to deform with rapid increase in axial strain and very little increase in deviatoric stress. Similar behaviour can be seen in cemented and fibre reinforced cemented sand samples that after attaining peak deviatoric stresses follow nearly parallel lines until the end of the test.

The stress paths are also shown in Figure 5.17 (b), these stress paths show many of the features commonly associated with uncemented and cemented samples. The stress path for the drained test is a straight line with a slope 3/1 in q-p' space. The highest point on that line is the failure point for uncemented and cemented samples. However, for cemented samples the test continues with strain softening behaviour where the stress condition decreases along the same stress path to reach a lower ultimate stress. Effective stress paths of undrained tests are also shown.

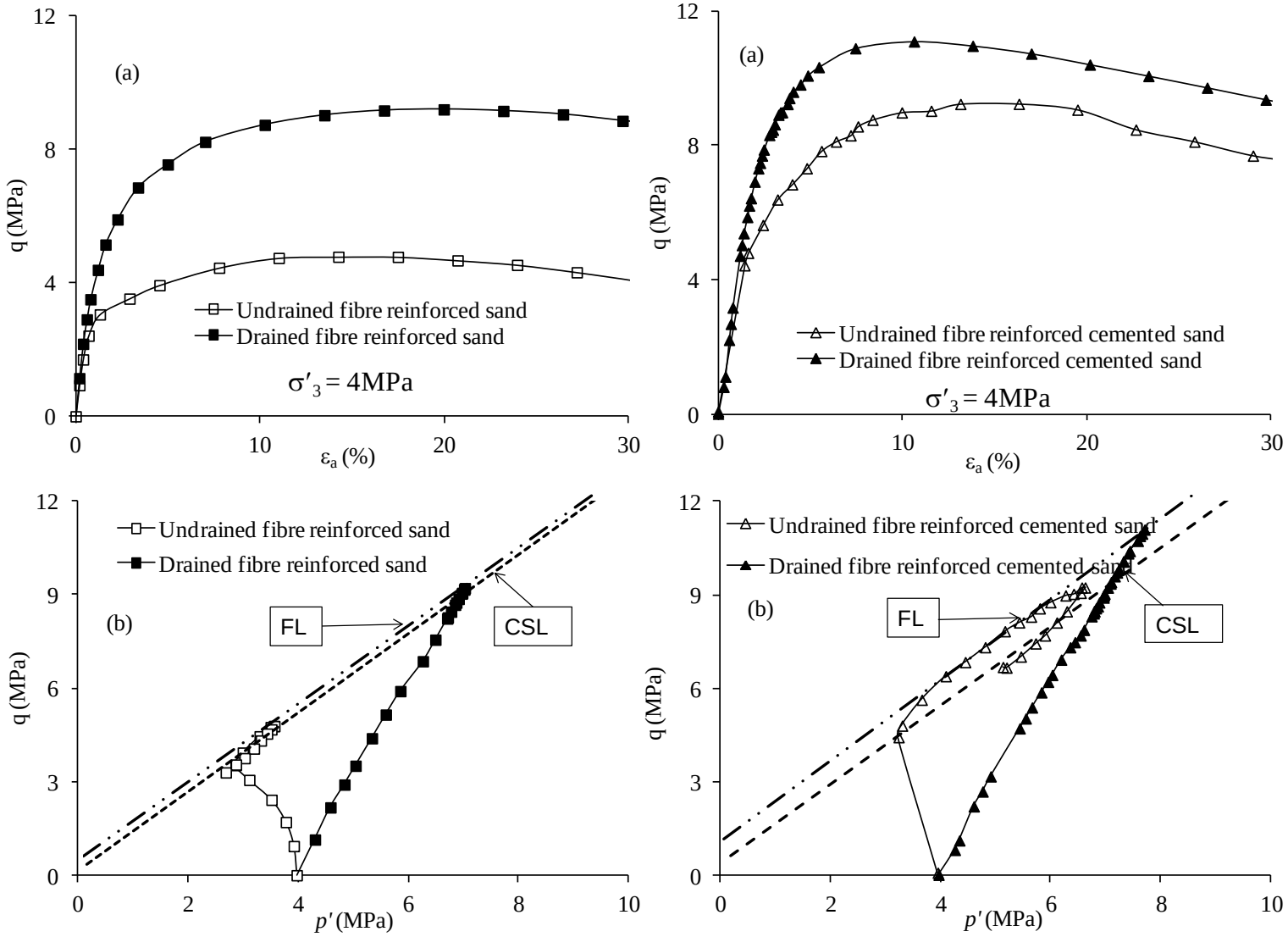

Figure 5.17 Effect of drainage condition on the stress-strain behaviour of fibre reinforced cemented and uncemented sand.

5.5 Summary

The stress-strain behaviour of Portaway sand with the addition of fibre and cement in a wide range of confining pressure was investigated in both drained and undrained conditions. From the experimental results, it could be seen that the addition of fibre and varying confining pressures significantly influences the mechanical response of sand. From the triaxial compression behaviour of cemented sand the following conclusions can be drawn:

1) The addition of fibre and/or cement content in the sand can markedly augment the strength. The results show strength enhancement and volumetric dilation. These features become more pronounced with increasing fibre content and prevail only under low confining pressure. However, at high pressures strain-hardening behaviour is observed. Greater volumetric contraction, identical to the loose sand can be measured.
2) In any case, by the addition of fibres, cement and/or varying confining pressures there is an increase in the peak strength of the sand. The position of peak stress changes with the change in fibre and cement content and confining pressure. The addition of cement content results in a brittle behaviour causing the peak strength to occur at smaller strain levels. However, the addition of fibre reduces brittleness. On the other hand, an increase in confining pressures induces ductility and causes the peak strength to occur at larger strain levels depending upon the magnitude of confining pressure.

3) The addition of fibre also increases the peak friction angle of both cemented and uncemented sand while increasing confining pressure reduces the friction angle and at confining pressures 4MPa and above no effect of either confining pressures or fibres could be seen.
4) Addition of fibres also induces cohesion in sand and increases the cohesion of cemented sand. The strength envelopes appear to be straight lines at low confining pressures while with the increasing confining pressure become slightly curved.
5) The results of the triaxial tests performed on cemented and uncemented fibre reinforced sand show that the addition of the cement content could improve the strength of soils under undrained and drained loading conditions. Shear strength parameters of effective stress cohesion intercept and friction angle increase in the CU and CD tests, due to the addition of fibre and cement.

CHAPTER 6

STRESS-DILATANCY BEHAVIOUR

6.1 Introduction

The phenomenon for dense granular materials to expand in volume is usually called dilatancy. This usually takes place after a small initial compression. Zero rate of dilatancy corresponds to the critical state of soil. The dilatancy can be identified in either the volumetric strain versus axial strain or the dilatancy versus stress ratio curves as recorded during laboratory testing and is discussed in the literature.

Various researchers for instance Consoli et al., (2009c), Dos Santos et al., (2010a), Bolton, (1986), Yu et al., (2007) have suggested evaluating dilatancy using the parameter, D which is equal to the negative of the ratio of the increments in volumetric strain $d\varepsilon_v$ to the increments in shear strain $d\varepsilon_q$ i.e. Dilatancy, $D= -d\varepsilon_v/d\varepsilon_q$. The detail review of the literature, regarding the dilation of fibre reinforced granular materials (see Section 2.5 in Chapter 2) reveals that the previous studies lack detail information on stress dilatancy behaviour and the dilation angle of fibre reinforced soils.

The past research also did not investigate in detail the influence of condition factors; such as the varying fibre content, cement content, and confining pressures. How dilatation and high peak friction angles at low stresses are gradually

suppressed by increasing higher stresses would be one of the interesting aspects of the study of dilatancy characteristics.

To capture the dilative properties, specimens with varying degrees of fibre and cement contents were prepared and tested for a wider range of confining pressures. The investigations were mainly based on the effect of the addition of fibre and cement, the effect of varying fibre and cement contents, and confining pressures. A number of experiments were run to capture the dilative behaviour of uncemented and cemented fibre reinforced sand. A summary of tests data used in this chapter is given in Table 6.1. In this table the effective confining stress (σ'_3), cement content (C %), fibre content (F%), initial void ratio(e_0), void ratio at the end of consolidation (e_c), peak/failure frictional angle (ϕ'_f), ultimate/critical frictional angle (ϕ'_{cr}) and maximum dilatancy angles (ψ'_p) are given.

Table 6.1 Summary of isotropically consolidated drained compression tests (dilatancy parameters).

Test	σ'_3 (MPa)	C (%)	F (%)	e_0	e_c	ϕ'_f (°)	ϕ'_{cr} (°)	Ψ'_p (°)
CD-0.5F0C50K	0.05	0	0.5	0.523	0.518	45.8	45.1	25.3
CD-0.5F0C100K	0.1	0	0.5	0.523	0.516	41.9	41.9	20.4
CD-0.5F0C200K	0.2	0	0.5	0.523	0.509	41.3	39.8	21.3
CD-0.5F0C300K	0.3	0	0.5	0.523	0.502	40.4	36.8	15.1
CD-0.5F0C500K	0.5	0	0.5	0.523	0.499	38.4	35.1	14.3
CD-0.5F0C1M	1	0	0.5	0.523	0.471	35.4	30.1	9.5
CD-0.5F0C4M	4	0	0.5	0.495	0.446	32.5	30.7	-4.3
CD-0.5F0C10M	10	0	0.5	0.495	0.407	32.4	31.6	-5.5
CD-0.5F2C500K	0.5	2	0.5	0.541	0.518	41.2	31.4	22.6
CD-0.5F0C20M	20	0	0.5	0.495	0.362	31.8	31.6	-7.7
CD-0.5F5C50K	0.05	5	0.5	0.501	0.498	65	53.4	55.1
CD-0.5F5C100K	0.1	5	0.5	0.501	0.494	57.5	46.7	52.6
CD-0.5F5C200K	0.2	5	0.5	0.501	0.481	53.5	45.1	46.5
CD-0.5F5C300K	0.3	5	0.5	0.501	0.494	50.7	41.3	41.1
CD-0.5F5C500K	0.5	5	0.5	0.536	0.522	47.3	34	34.1
CD-0.5F5C1M	1	5	0.5	0.51	0.498	43.1	36.7	22.3
CD-0.5F5C4M	4	5	0.5	0.517	0.488	35.5	31.1	-2.7
CD-0.5F5C10M	10	5	0.5	0.507	0.459	32.6	30.9	-3.3
CD-0.5F5C20M	20	5	0.5	0.514	0.435	31.2	30.7	-3

Where:

C= cement content; **F**= fibre content, ψ'_p= angle of dilation= $\tan^{-1}(-d\varepsilon_v/d\varepsilon_q)$

6.2 Effect of the addition of fibre and cement

The dilative behaviour of sand is significantly influenced by the addition of cement and fibre as shown in Figure 6.1 and Figure 6.2, in which the stress ratio-axial strain, volumetric strain-axial strain and stress ratio-dilatancy curves obtained for a constant confining pressure of 300kPa and 1MPa are plotted. Lower and higher confining pressures are selected to show the effect of confining pressure as well, as it was found in previous chapters that the effect of the addition of fibre and cement varies with change in confining pressures. The dry density of all the samples were kept constant to explore the effect of the addition of fibre and cement separately as well as the combined effect of the addition of fibre and cement. It can be seen in Figure 6.1(a) that addition of fibre has increased the stress ratio of both sand and cemented sand. The axial strains corresponding to maximum stress ratio $(q/p')_{peak}$, seem to have increased with the addition of fibres. The maximum dilation occurs at $(q/p')_{peak}$ for both fibre reinforced cemented and uncemented sand. The points of maximum rate of dilation were selected from stress ratio (q/p') vs. dilatancy (D) relationship and located on the stress-strain and volumetric strain curves. It was noted that maximum dilatancy occurs at maximum stress ratio. However, Dos Santos et al., (2010a) reported that at lower confining stresses, the inclusion of fibres increases the peak stress ratio, but unlike for pure sand, this peak stress ratio does not correspond to the maximum dilatancy, and rather seems to be reached at the end of dilation. All the samples compress initially until reaching at a point of instant zero dilation and then dilate till the end of the tests. The tendency of dilation was found to be more in fibre reinforced composites as it can be seen in

Figure 6.1(b) that sand and cemented sand without fibres dilates less and tends to reach very close to zero volumetric change at the end of the tests. The (q/p')-(D) plot is shown in Figure 6.1(c) and it can be seen that fibre has move the plot to the left and upward which suggests that the inclusion of fibre increases both dilation and stress ratio of sand and cemented sand. These results suggest that the dilative response of the composite could be a outcome of an apparent densification mechanism of the sand matrix resulting from the presence of the fibres in the voids as reported by Ibraim et al., (2010). It is also interesting to see that the stress-dilatancy graphs are approximately linear in the (q/p')-D space between the low stress ratio initial part of the curve and the peak stress ratio.

Figure 6.2 shows the effect of the addition of fibre and cement to the dilatancy behaviour at an effective confining pressure of 1MPa. It can be seen that behaviour is consistent with that observed at 300kPa but the addition of fibre and/or cement has been shown to reduce dilatancy at 1MPa.

Consoli et al., (2009c) showed different results for stress dilatancy behaviour of fibre reinforced cemented and uncemented sand and reported that fibre reinforced sand samples showed a similar maximum dilatancy as that of unreinforced sand, but reached at a higher stress ratio, 2.0. In addition, after reaching the maximum dilatancy, the value of the maximum stress ratio is seen to continuously increase with decreasing dilatancy until reaching zero at critical state at a stress ratio of about 2.4 on the vertical axis.

The addition of cement has also the effect of increasing dilation because of bonding while the combined effect of fibre and cement render the maximum dilation in all three different compositions. The change in volume associated with dilation of fibre reinforced cemented sand implies that after bond breakage, the behaviour of the fibre reinforced cemented sand degenerates to that of the fibre reinforced uncemented sand and at this stage fibres should have increased the dilation as they increased the dilation in the case of clean sand.

A typical SEM micrograph of 0.5% fibre reinforced sample sheared at initial confining pressure of 10MPa is shown in Figure 6.3. A SEM micrograph of the fibre reinforced cemented sample is also shown in Figure 6.4. The sample is of 0.5% fibre and 5% cement sheared at effective confining pressure of 1MPa. It can be seen that the cement bond has broken as well as the particles have crushed. After this particle and bond breakage the fibres could have resisted the shearing until the fibres have failed in extension. The fibre damage was also observed in SEM analysis of both the cemented sand and fibre reinforced cemented sand.

A possible reason for an increase in dilatancy due to addition of fibre could be that fibres fill the voids present in dense sand, which could provide a platform to the sand and cemented sand particle for rolling over when sheared, hence increasing dilation. However, Consoli et al. (2005) provided opposite reasoning for isotropic compression behaviour.

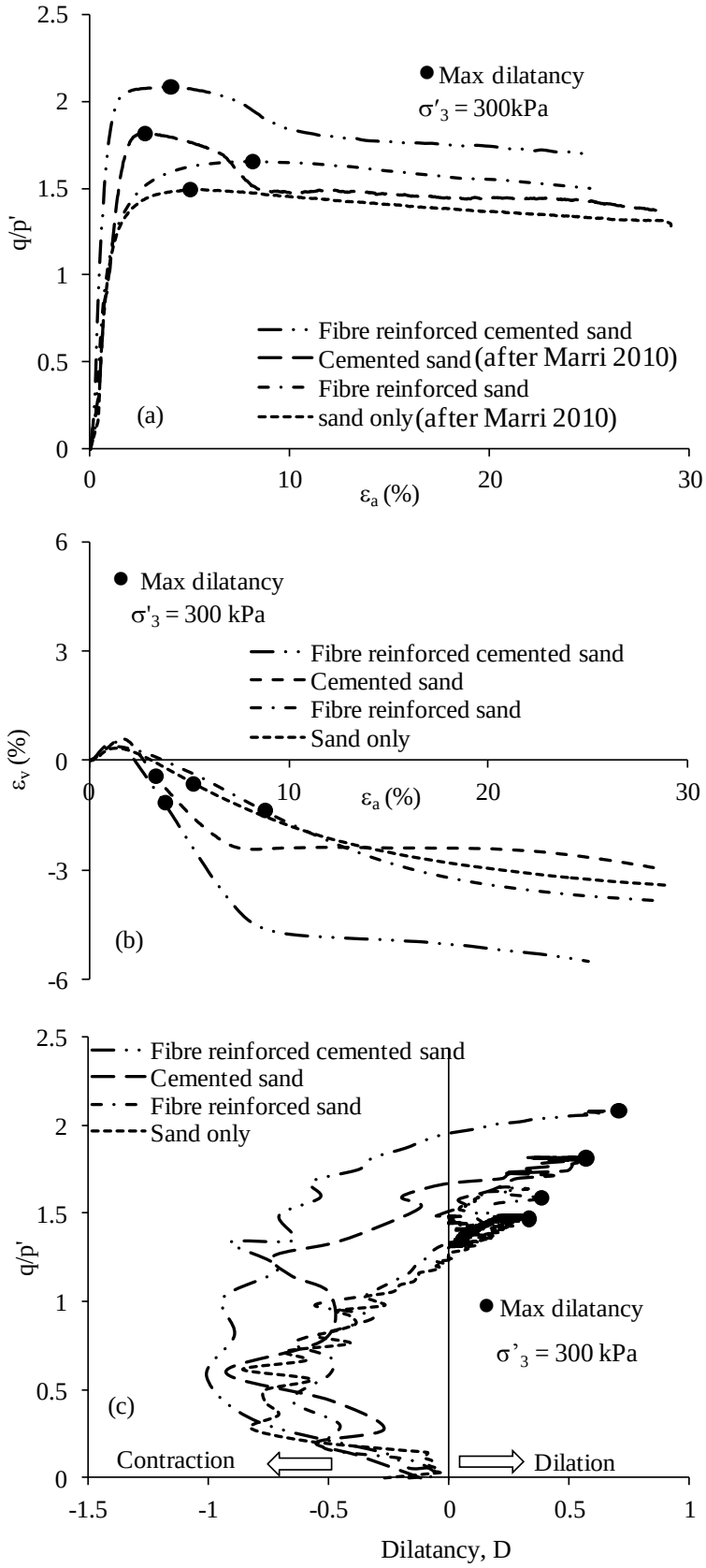

Figure 6.1 Location of point of maximum dilation and effect of fibre and cement content in the (a) stress-strain; (b) volumetric respone; and (c) stress-dilatancy behaviour of Portaway sand.

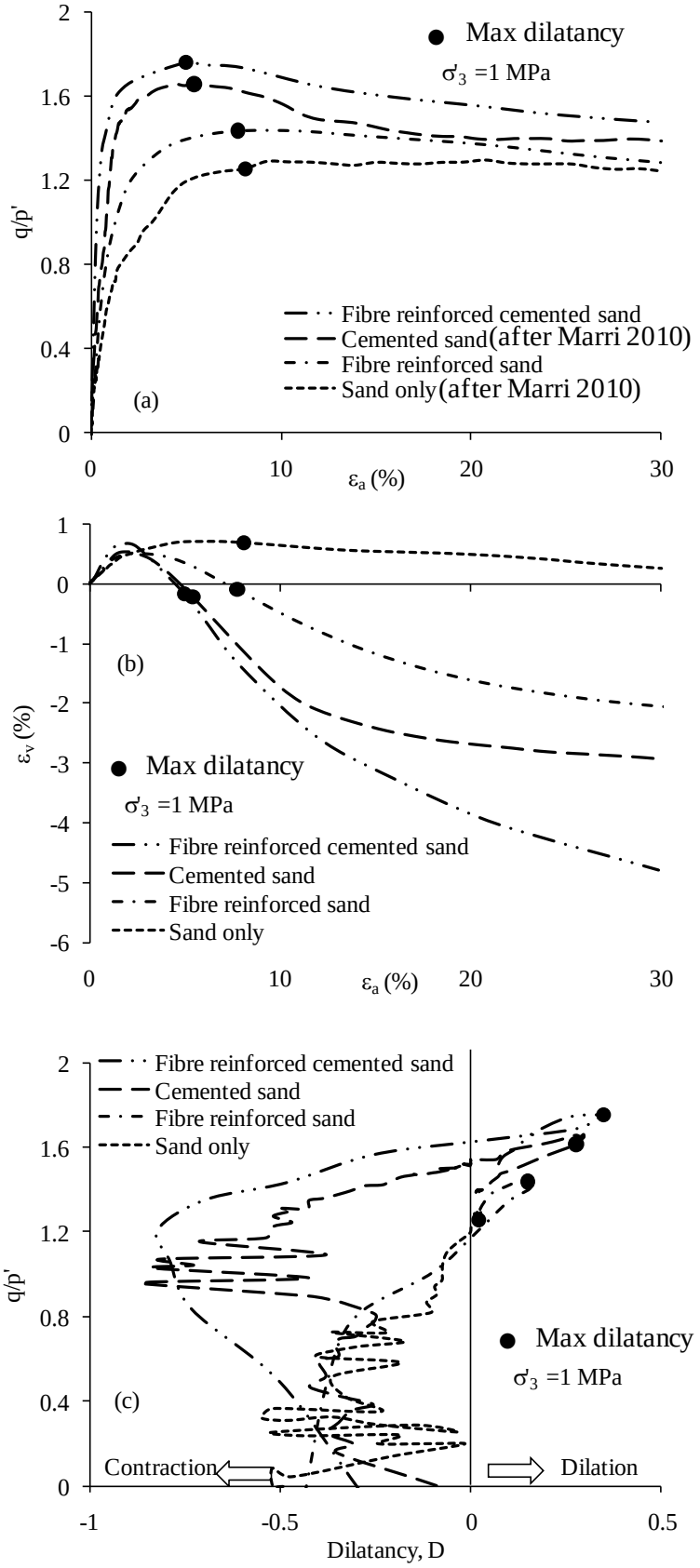

Figure 6.2 Location of point of maximum dilation and effect of fibre and cement content in the (a) stress-strain; (b) volumetric respone; and (c) stress-dilatancy behaviour of Portaway sand.

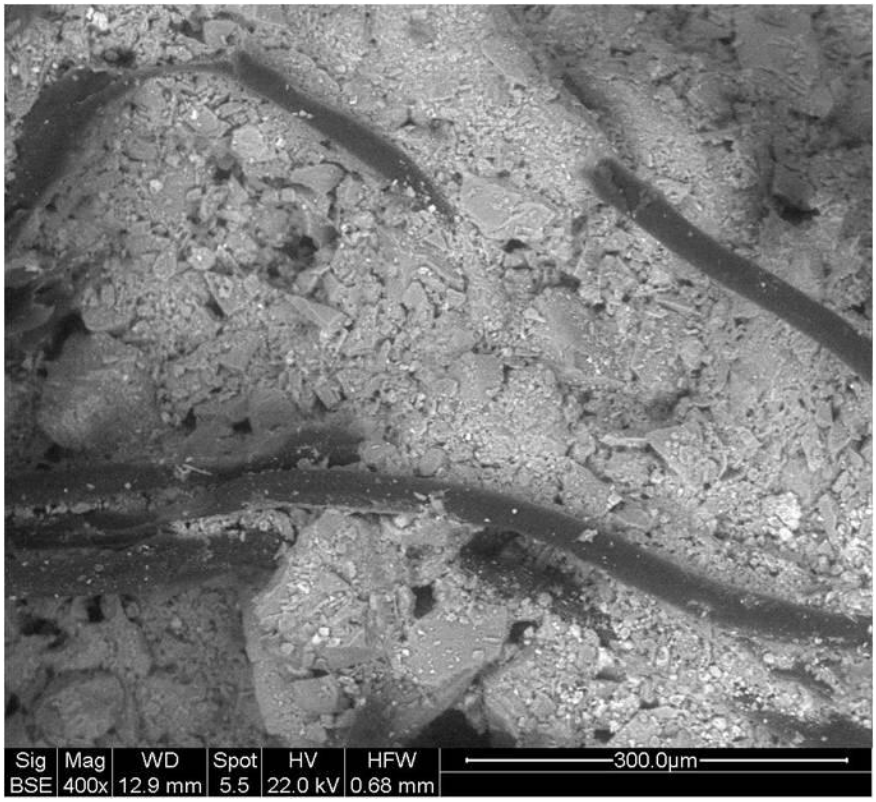

Figure 6.3 Typical SEM micrograph demonstrating the particle crushing & fibre breakage of 0.5% fibre reinforced sample sheared at 1MPa.

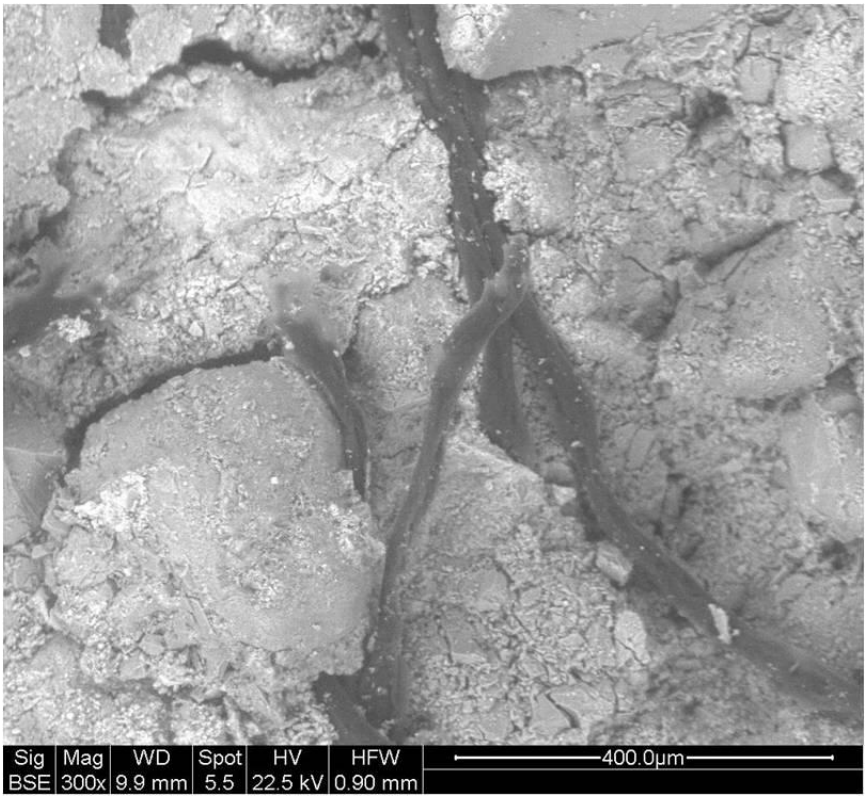

Figure 6.4 Typical SEM micrograph demonstrating the particle and bond break & fibre damage of 5% cemented & 0.5% fibre reinforced sample sheared at 1MPa.

6.3 Effect of confining pressure

The effect of the addition of fibre has a considerable effect on stress-dilatancy response of sand and cemented sand as reported in previous section. It would be interesting to investigate how the varying confining pressure affects dilatancy behaviour of fibre reinforced sand and fibre reinforced cemented sand in a wide range of confining pressures. The effect of an increase in confinement on the behaviour of fibre reinforced sand and fibre reinforced cemented sand is presented in this section. Specimens were prepared at constant dry unit weight of 17.4kN/m^3. The dry unit weight was kept the same for uncemented and cemented fibre reinforced sand specimens. The specimens were isotropically compressed and sheared at confining pressures ranging from 50 kPa to 20 MPa.

6.3.1 Fibre reinforced sand

The effect of confining pressure was investigated on the dilatational behaviour of the material in Figure 6.5. The ε_v vs. ε_a plot in Figure 6.5a, shows that dilative behaviour is being suppressed with gradual increase in confining pressure. At effective confining pressures above 1MPa the material shows complete compression characteristics similar to the behaviour usually observed for loose sand. From these experimental results, it is obvious that at high pressures the effect of dilation is diminishing. It can be presumed that the application of increasing confining pressure causes both the propagation of micro cracks and the opening of voids within the material to be suppressed, and so as the confining pressure increases, the deformation reduces. This suppression of dilatancy behaviour with

increasing confining pressure can also be observed in the stress-dilatancy curve as shown in Figure 6.5(b). It can be seen that dilatancy is at a maximum at lower confining pressure and reduces gradually with the increase in confining pressure. It is to be noted that dilatancy is diminished completely after 1MPa i.e. showing complete compression at 4MPa. This suggests that the shift from dilative behaviour to compressive behaviour in fibre reinforced sand occurs at a confining pressure between 1MPa to 4MPa. It was also mentioned in the preceding section that the effect of fibre gradually diminishes with increasing confining pressures. This suppression of dilatancy with increasing confining pressures has been reported by most of the researchers for sand and cemented sand. Reported work for fibre reinforced composites is scarce and there is a lack of consensus as Consoli et al., (2009b) reported that there is no effect of confinement in the range of 100kPa to 500kPa on dilatancy behaviour of sand and fibre reinforced sand and only the stress ratio is reduced.

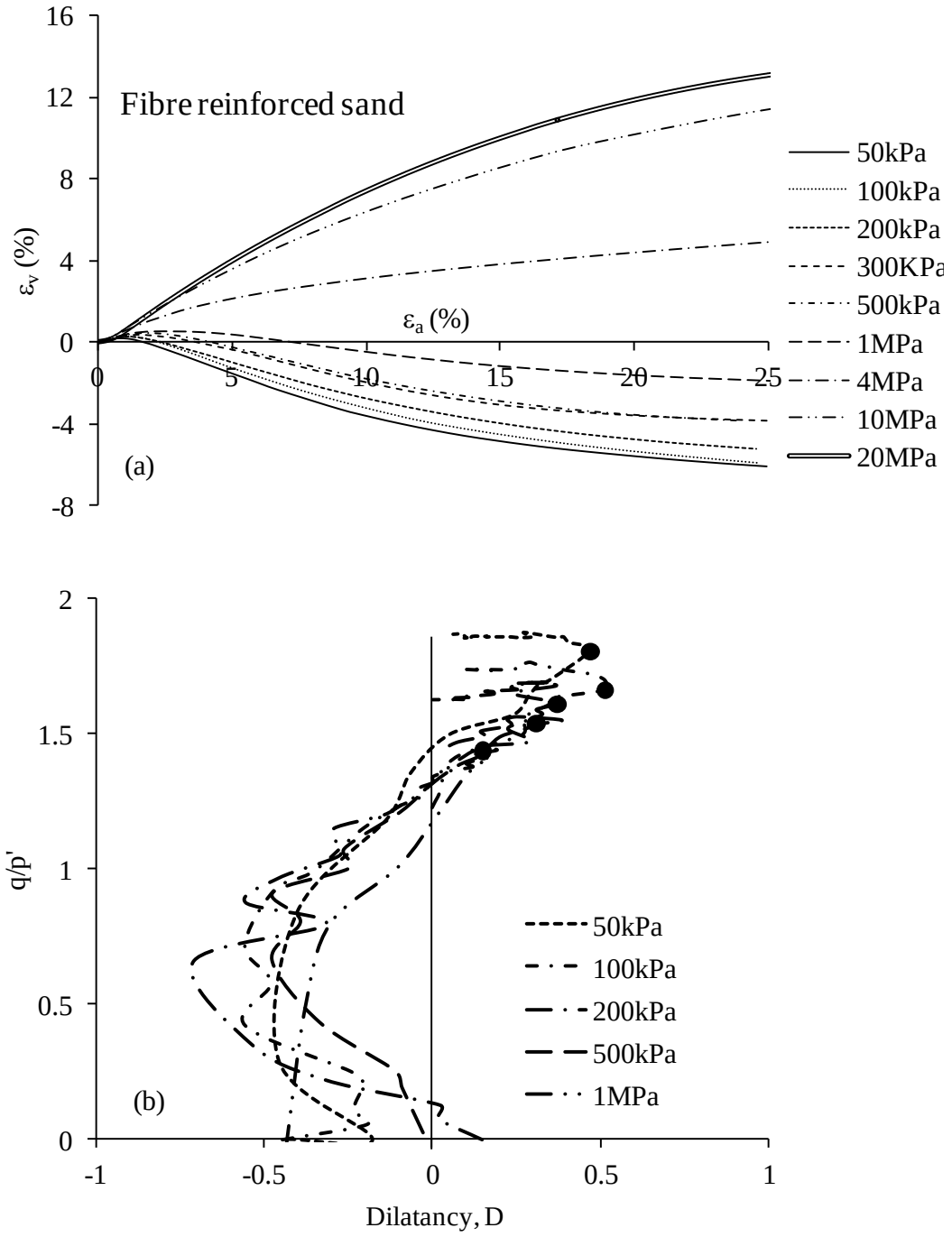

Figure 6.5 Dilatancy behaviour under varying confining pressure of fibre reinforced sand on a) ε_v-ε_a , and b) q/p'-D.

6.3.2 Fibre reinforced cemented sand

The effect of confining pressure on the dilatational behaviour of the fibre reinforced cemented sand is shown in Figure 6.6. The ε_v vs. ε_a plot in Figure 6.6a, shows similar results as that observed for fibre reinforced sand. The dilatancy decreases with

increasing confining pressure and axial strain to this point of maximum dilatancy increases with increasing confining pressures. The ε_v-ε_a curve shows that dilation is gradually suppressed with increasing confining pressure until 1MPa where confining pressure overcomes the dilative behaviour and total compressive behaviour can be seen at σ'_3= 4MPa and above. It can be concluded after comparing the responses of sand and fibre reinforced sand, as well as cemented sand and fibre reinforced cemented sand, that they follow the same trend but here is more dilation and compression in fibre reinforced materials. This additional dilation and compression observed in fibre reinforced materials suggests that this might only be due to the effect of the addition of fibre.

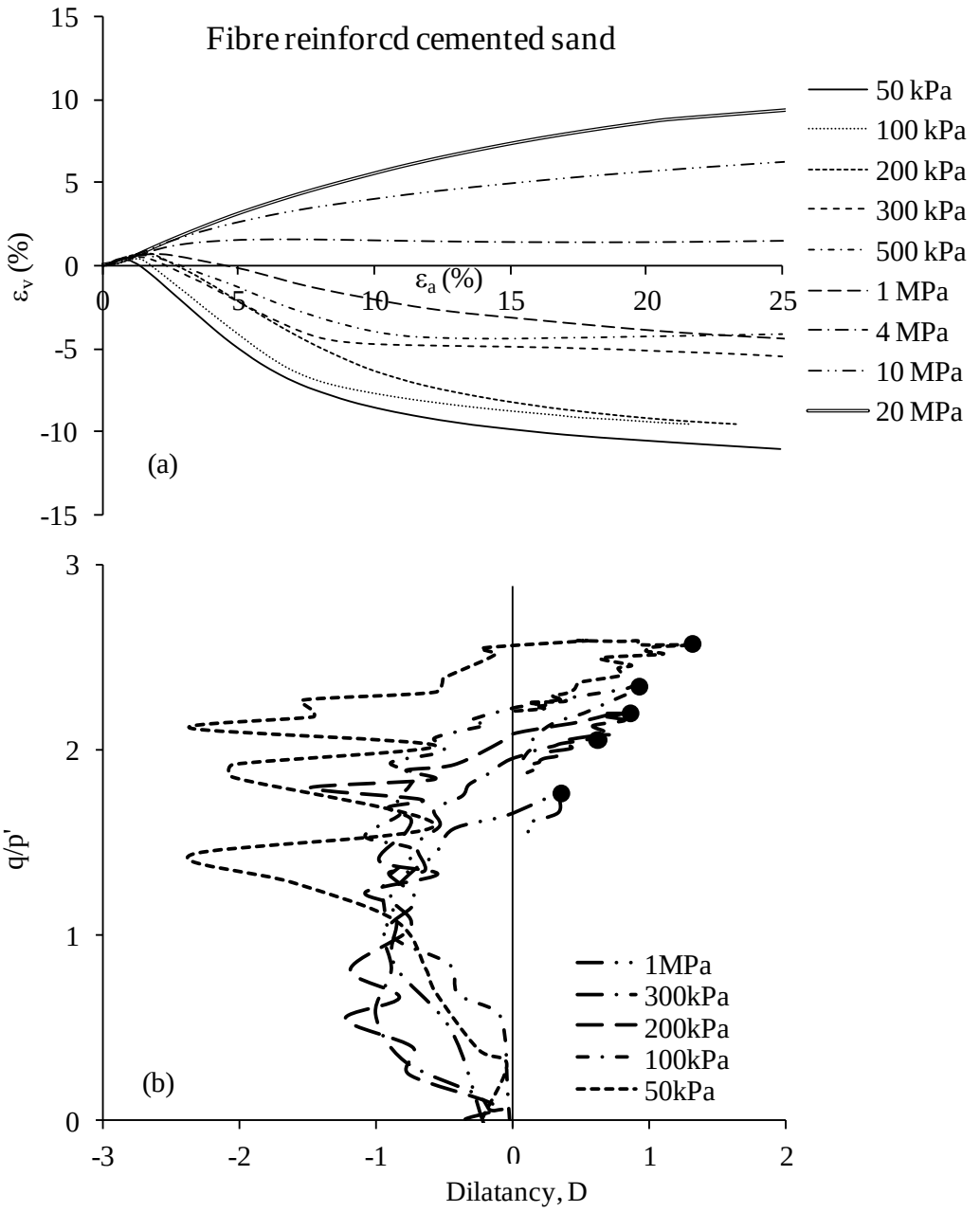

Figure 6.6 Stress dilatancy behaviour under varying confining pressure of fibre reinforced cemented sand on a) ε_v-ε_a , and c) q/p'-D.

6.4 Effect of the fibre content

The effect of varying fibre content is investigated at 0% and 5% cement content and is shown in Figure 6.7. The effect is first shown for uncemented sand at the effective confining pressure of 500kPa. It can be observed that at 0.25% fibre content the effect is not appreciable and there is very little difference between the

volumetric response of unreinforced and 0.25% fibre reinforced sand but the effect of fibre is considerable at 0.5% fibre content.

The effect of varying fibre content for 5% cemented sand is shown at low and high pressure to elaborate the effect of confinement as well. It can be seen that there is very little effect of varying fibre content from 0.25% to 0.5% and volumetric response of 0.25% and 0.5% fibre reinforced cemented sand is nearly same at both low and high pressures. It is interesting to note that for sand there was little effect of 0.25% fibre and the effect was only noticeable at 0.5% fibre but contrary to the behaviour of clean sand the effect of fibre is the same at 0.25% and 0.5% fibre content.

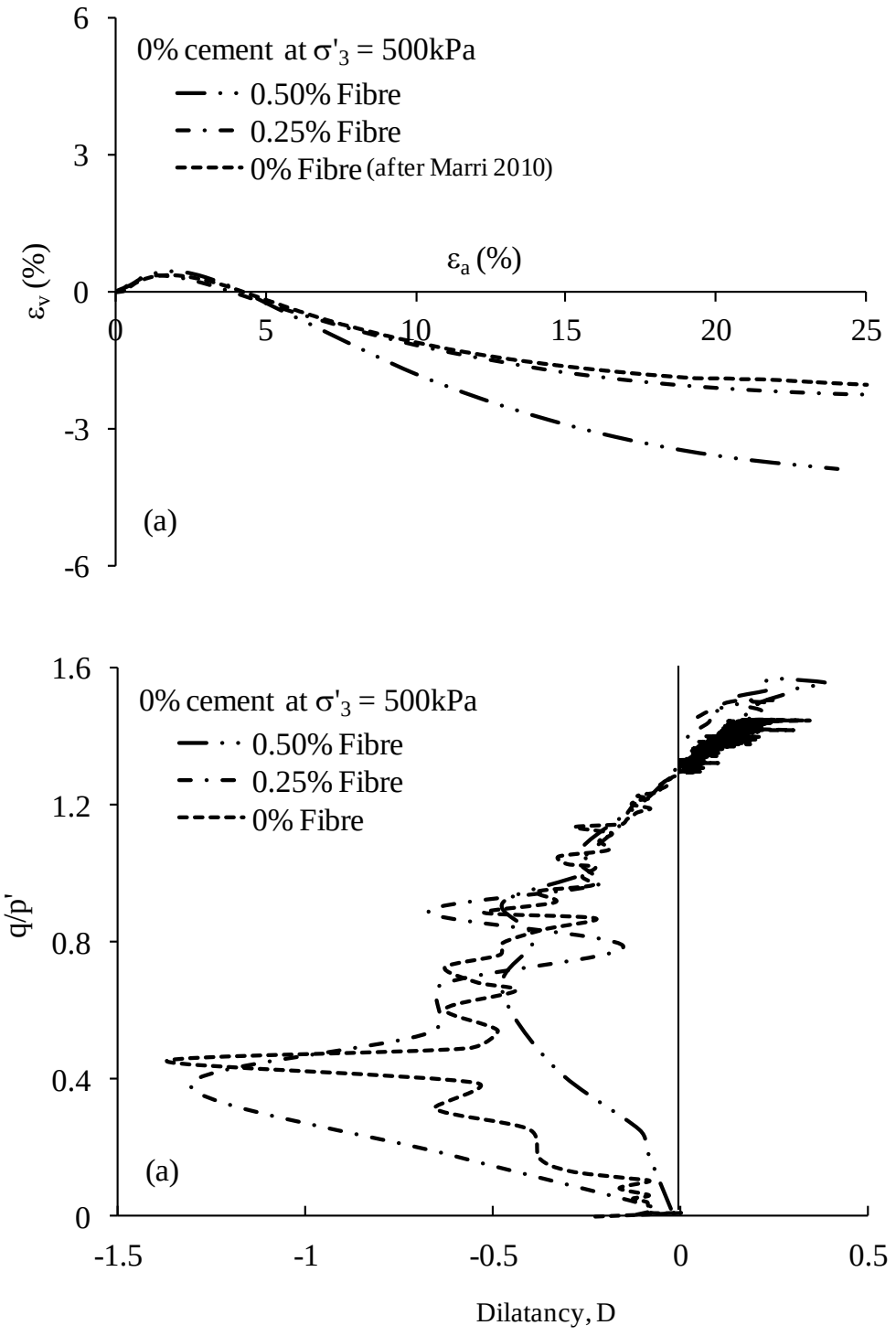

Figure 6.7 Dilatancy behaviour of cemented sand under varying fibre content, a) ε_v-ε_a , and c) q/p'-D.

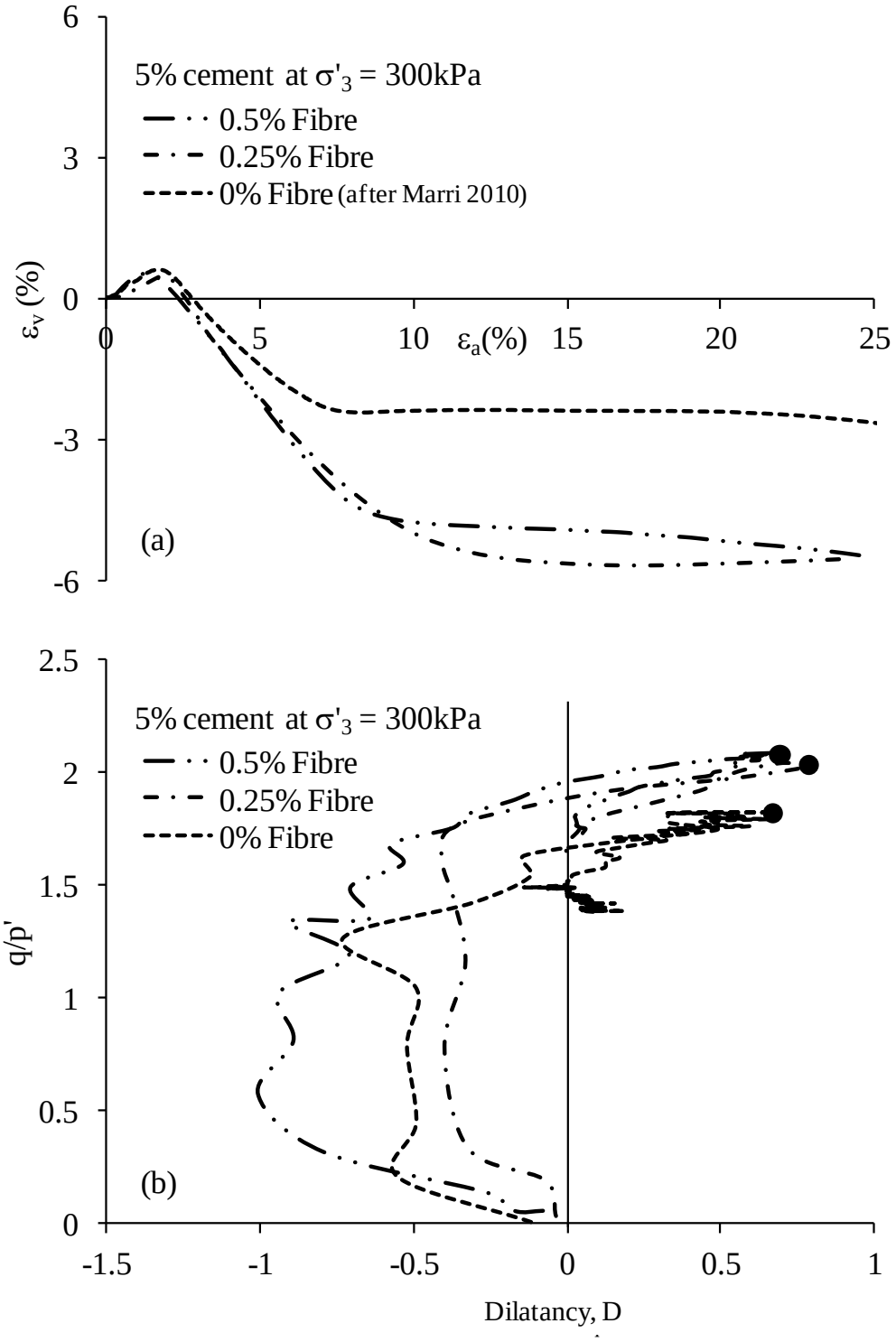

Figure 6.8 Dilatancy behaviour of cemented sand under varying fibre content, a) ε_v-ε_a , and c) q/p'-D.

6.5 Effect of the cement content

It has been observed that the addition of fibre and cement sand inhibits dilatancy and increase in confining pressure suppresses dilatancy. How varying cement content in fibre reinforced sand effect the stress-dilatancy behaviour of fibre reinforced sand is explored in this section. The stress dilatancy behaviour of 0.5% fibre reinforced sand is investigated by increasing the cement content from 0% to 2% and 5% at a constant confining pressure of 500kPa. The results are shown in Figure 6.9. The ε_v-ε_a plot shows that material at 2% and 5% cement content tend to deform at zero volume change but uncemented fibre reinforced sand dilates continuously until the end of the test. The q/p' vs. D curve is also shown in Figure 6.9. It can be observed that increasing cement content moves the plots to the left. The maximum dilatancy points are marked with filled circles and have also been marked on ε_v-ε_a curves. It can also be seen that all the three curves meet at a stress ratio of 1.4 at zero dilatancy line.

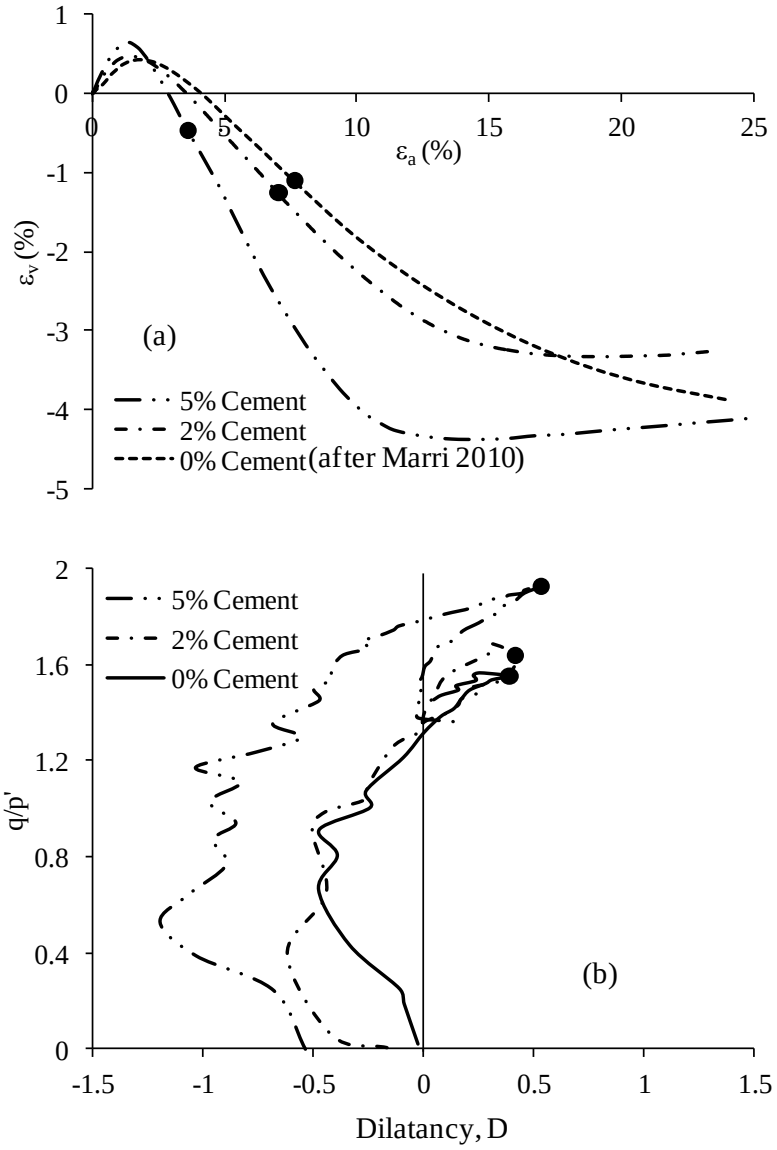

Figure 6.9 Stress dilatancy behaviour at σ'_3=500kPa confining pressure of 0.5% fibre reinforced cemented sand, a) ε_v-ε_a , and b) q/p'-D

6.6 Dilatancy angle

The angle of dilation controls an amount of plastic volumetric strain developed during plastic shearing and is assumed constant during plastic yielding. The value of zero dilatancy angles corresponds to the volume preserving deformation while in shear. The peak friction angle of sand depends on its critical state friction angle and on dilatancy.

To capture the overall effect of the addition of fibre, cement and confining pressure in sand on stress-dilatancy behaviour the dilation angles of the composite are shown in Figure 6.10, which shows dilatancy angle of sand, fibre reinforced sand and fibre reinforced cemented sand with increasing confining pressures. It can be seen that the dilatancy angle decreases with increasing confining pressures. The dilation angle is positive i.e. dilative up to 1MPa and at 4MPa the dilation angles are negative showing total compression. The effect of reinforcement on dilation angle is highest at lower confining pressure and reduces with increasing confining pressures. It can also be observed that overall compression increases with increasing confining pressures. Comparing all the curves, it can be seen that the addition of both cement and fibres increases the higher dilatancy as compare to the increase in dilatancy due to the addition of fibres alone.

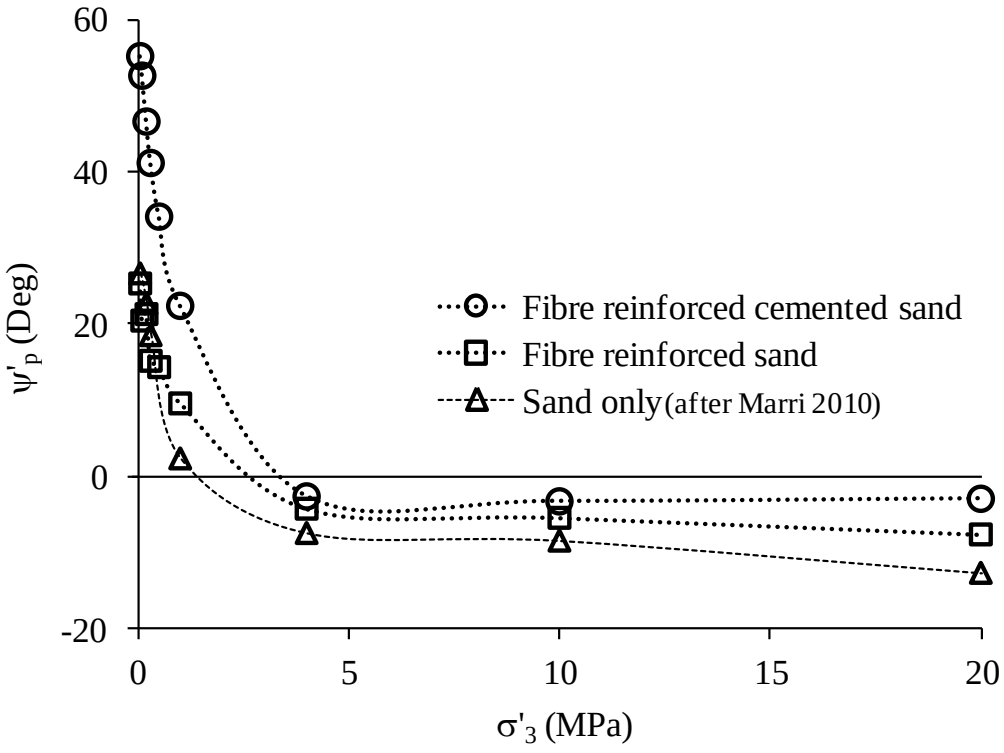

Figure 6.10 Effect of fibre and cement on dilatancy angle of sand.

To develop an empirical relationship between the angles of shearing and dilation, triaxial compression test data for fibre reinforced cemented and uncemented sand is plotted between ψ_p vs. ϕ_f as shown in Figure 6.11. The slopes of the lines for fibre reinforced cemented and uncemented sand are 0.4 to 0.5 respectively, the lines crosses zero dilatancy angle at 34°, suggesting critical angle for both cemented and uncemented fibre reinforced sand. Bolton, (1986) reported similar method of determination of ϕ'_{cr}, from extrapolation of a series of values of ϕ'_{max} recorded in compression tests on soil samples, in which the rate of dilation at failure was observed, so that a value consistent with zero dilation at failure could be determined. Therefore, the empirical relationship could be developed as given in Eq. (6.1) for the plane strain condition.

$$\phi'_{peak} - \phi'_{cr} = (0.4\ to\ 0.5)\ \psi_{peak} \qquad 6.1$$

For triaxial compression of sand, Bolton (1986) established the relationship given in Eq. (6.2), which is re-reported by Chakraborty and Salgado (2010).

$$\phi'_{peak} - \phi'_{cr} = 0.5\ \psi_{peak} \qquad 6.2$$

The comparison of Eq. (6.1) and (6.2) suggests that there is close approximation to the empirical relations.

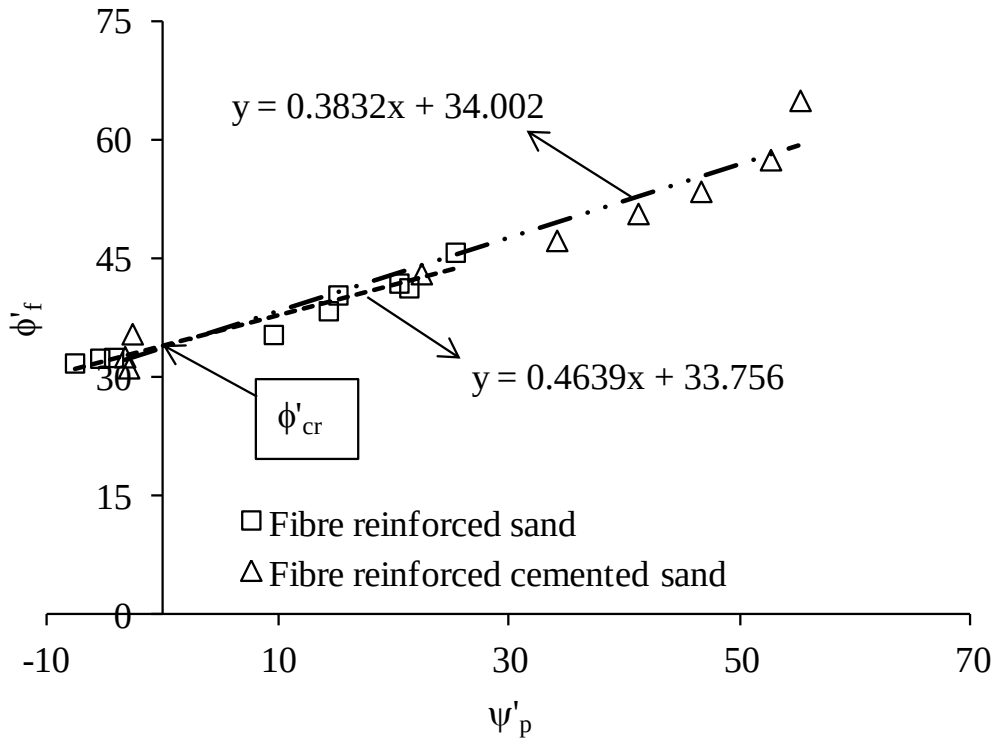

Figure 6.11 Relationship between ϕ'_f and ψ'_p.

Figure 6.12 shows the triaxial test data of increasing effective stress at failure of fibre reinforced cemented and uncemented sand with initial relative density of 85%. It can be seen that Eq. 6.3 proposed by Bolton, (1986) taking into account the affect of initial relative density, I_D and effective confining pressure, p' for sand is in between fibre reinforced sand and fibre reinforced cemented sand.

$$\phi'_{peak} - \phi'_{cr} = 0.3\, I_R \qquad 6.3$$

Where

$$I_R = D_R\,(10 - \ln p') - 1$$

The best interpretation of I_R values which are calculated to be negative at high confining pressure is that considerable contraction in volume and consequent increase in I_D will take place before ϕ'_{cr} is mobilised.

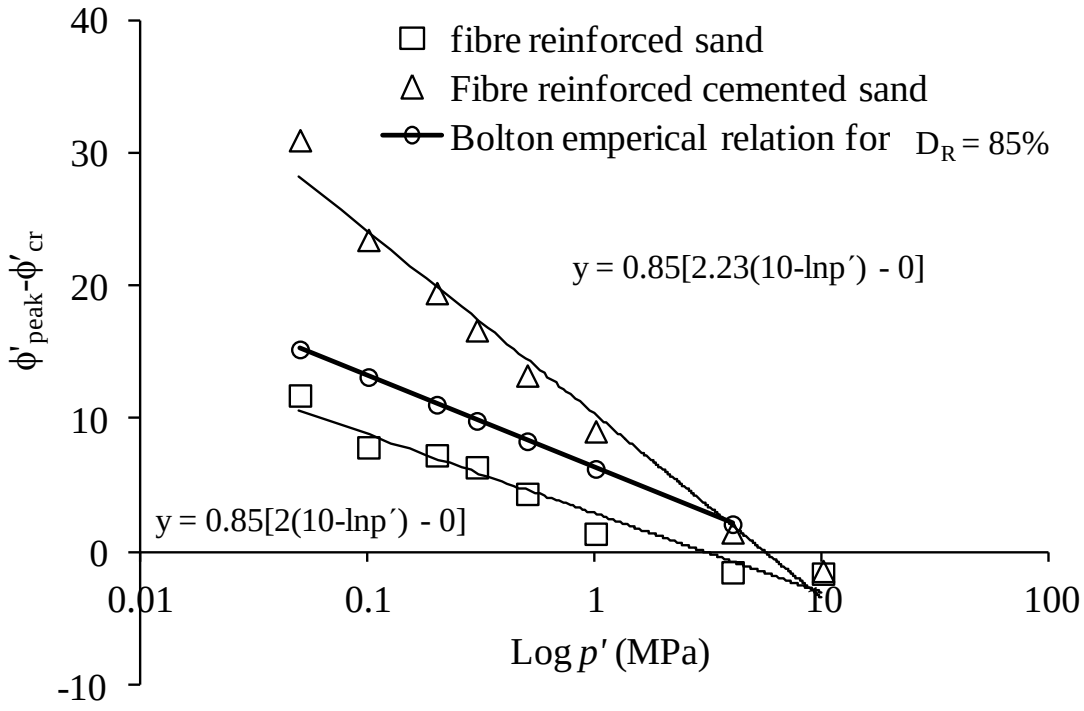

Figure 6.12 Illustration of proposed mechanism of dilation in fibre reinforced materials.

Diambra et al., (2009) also proposed an equation with the inclusion of fibres as

$$I_R = a_0(D_R\,(Q - \ln p') - \gamma) \qquad 6.4$$

Where a_0 = 0.3, γ = 0 and Q = 6.4. The best fit values of γ and Q obtained from the plot of experimental data shown in Figure 6.12 are 0 and 10 respectively, whereas a_0 value differs for cemented and uncemented fibre reinforced sand as 2 for uncemented fibre reinforced sand and 2.23 for fibre reinforced cemented sand.

The plots of mobilisation of friction and dilatancy angles with shearing have also been plotted and are shown in Figure 6.13 and Figure 6.14. It can be observed that peak friction angles decrease with increasing confining pressures. The maximum friction angles also get mobilised at lowest axial strain at lowest confining pressure and with increasing pressure the axial strain corresponding to the peak are increases. At pressures above 4MPa the peak friction angles are not achieved until

the end of the tests suggesting the compressive response due the effect of high confining pressure. It is interesting to note that at lower confining pressures in the range of 50kPa to 300kPa there is not much change in the value of friction angle after reaching at peak friction angle and from 500kPa to 1MPa the friction angles decrease after reaching a peak. This trend corresponds to softening and above 4MPa the trend is that of hardening.

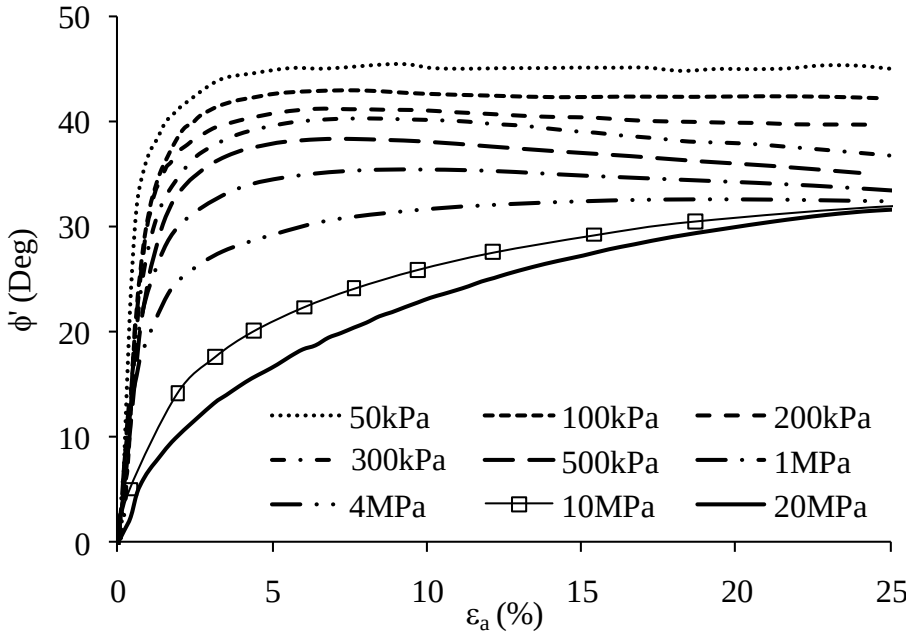

Figure 6.13 Effect of confining pressure on mobilised friction angle of fibre reinforced sand.

The variation of dilatancy angle with increasing axial strain is shown in Figure 6.14 which shows that dilatancy angle reduces to a certain negative value depicting the compressive behaviour and after reaching to maximum compression the negative value decreases. With the increasing axial strain the dilation angle reduces and tends to reach zero dilation toward the end of all the tests. All the curves seem to converge at zero dilatancy angle at the end of the test at an axial strain of about

30%. This suggests that the material tends to reach critical state at the end of the test.

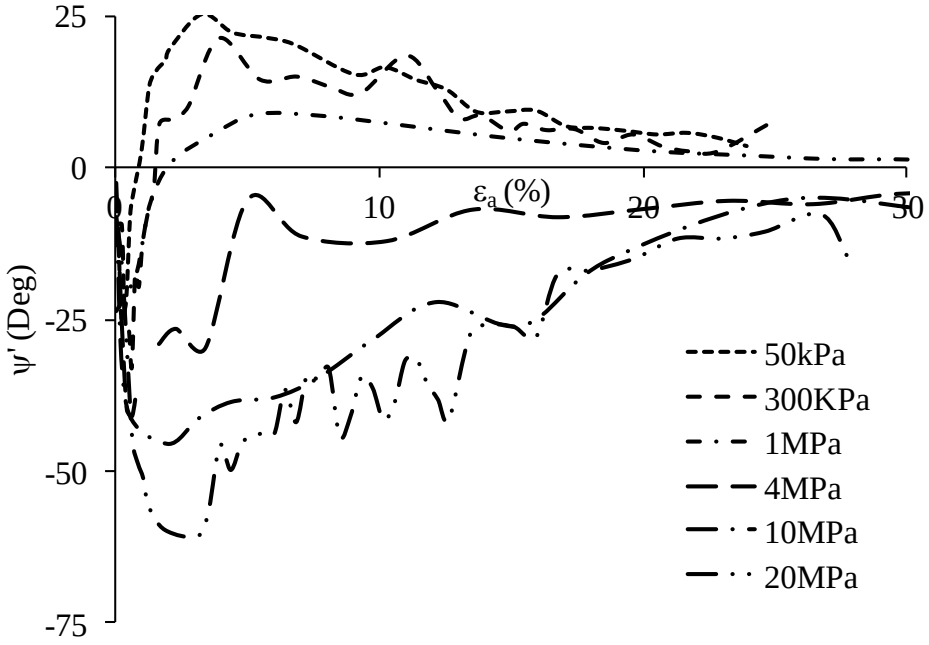

Figure 6.14 Effect of confining pressure on mobilised dilatancy angle of fibre reinforced sand.

The effect of addition of fibre in sand and cemented sand can also be observed in Figure 6.15 in which dilatancy angles are plotted for all the composites. The fibres have increased the peak dilatancy angle of sand from 1.5° to 10.17° and from 15.95° to 18.9° of cemented sand. It can be seen the effect of fibre is more significant in sand than its effect in cemented sand.

The dilatancy angles of fibre reinforced cemented sand with varying cement content is shown in Figure 6.16 which shows the increase in dilatancy angle with increasing cement content. It can be seen that the dilatancy angle of fibre reinforced sand has increased with the increase in cement content.

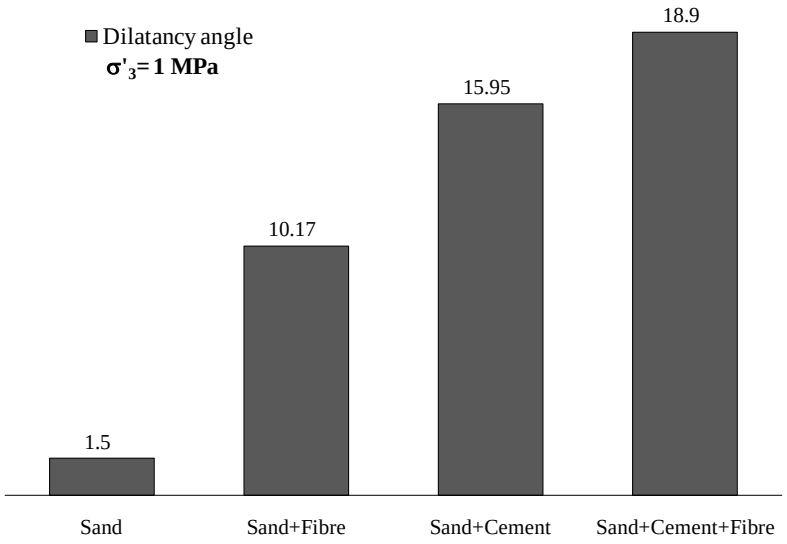

Figure 6.15 Effect of addition of fibre and cement content on dilatancy angle of Portaway sand.

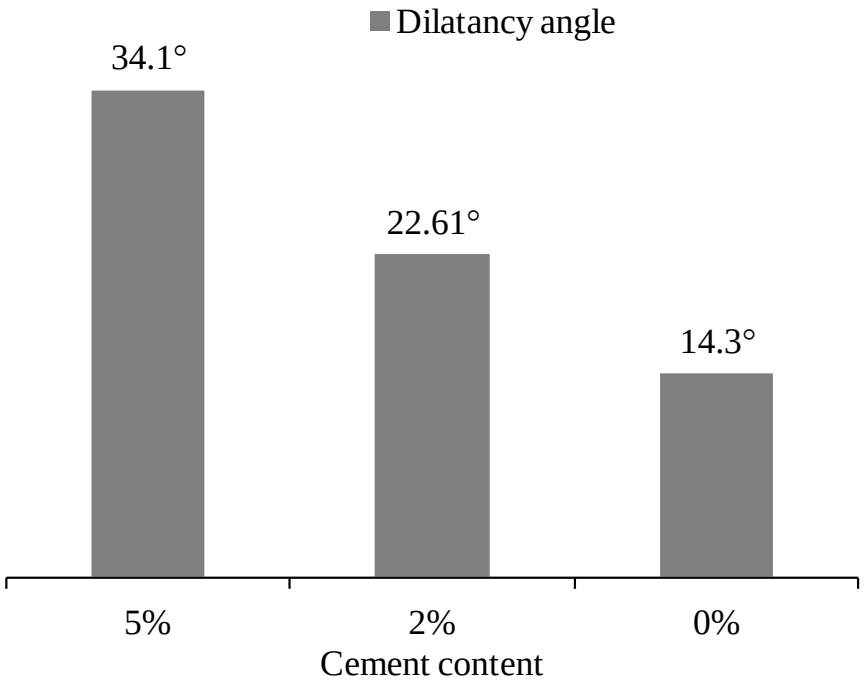

Figure 6.16 Effect of varying cement content on dilatancy angle of 0.5% fibre reinforced sand at σ'_3 = 500kPa.

6.7 Summary

Triaxial drained compression tests were carried out on uncemented and cemented fibre reinforced sands with different fibre and cement contents and at a wide range

of confining pressures. The mechanism of dilatancy, its significance and dependence on fibre and cement content and confining pressures were investigated.

From the analysis of the experimental data presented in the chapter it can be concluded that stress dilatancy behaviour of the all the composites discussed is influenced by the parameters investigated. The results are summarised in the following points:

1) The commencement (point of initiation of dilatancy), maximum dilatancy, and post-peak dilatancy are fibre content, cement content, and confining pressure dependent. There is a significant effect of the addition of fibre on the response of both cemented and uncemented sand. The addition of fibres increases the dilative behaviour of the composites.
2) The addition of fibre increases the dilatancy while increasing confining pressures reduces dilatancy.
3) The dilatancy angle increases from 1.5° to 10.17° in sand and from 15.95° to 18.9° of cemented sand due to the addition of fibres. Thus the effect of addition of fibre is more in sand than in cemented sand.
4) Increasing the cement content also increases the dilatancy angle from 21.23° to 22.16° and 28.18° for 0%, 2% and 5%.
5) The stress ratio, volumetric strain and dilation increase due to the individual or combined addition of fibre and cement. Varying confining pressure, fibre content and cement content all seem to have affected the dilative response of the materials. Increasing confining pressure decreases the dilation and it

was observed that the effect of fibre and/or cement was highest when confining pressure was the lowest.

6) At higher confining pressures the effect of confinement was so dominant that there was no dilation observed at pressure above 4MPa.

CHAPTER 7

FURTHER CHARACTERISTICS

7.1 Introduction

The general isotropic compression, stress-strain and dilatancy behaviour has been discussed in previous chapters. The present chapter examines the stiffness, yielding, failure modes and criteria, deformation at micro level and critical state behaviour of fibre reinforced cemented and uncemented sand.

7.2 Stiffness and stiffness degradation

Stiffness is the resistance to deformation by an applied force. Accurate determination of soil stiffness is difficult to achieve in routine laboratory testing. Conventionally, the determination of the axial stiffness of a triaxial sample is based on external measurements of displacement, which include a number of extraneous movements. The present method of soil strain measurement with external load measurement devices has a certain limitation particularly where the soil exhibits high stiffness at small strains but still this could give a reasonable approximation to the real values for measuring the stiffness of cemented sand at high pressures.

The stiffness degradation curves of sand and cemented sand in drained triaxial tests with the addition of fibres are shown in Figure 7.1. Samples with 0.5% fibre and 5% cement were tested at effective confining pressure of 4MPa.

From the figure, it can be seen that the effect of the addition of fibre in sand increases the stiffness but as it can be seen this effect of addition of fibres is very significant in clean sand. This suggests that fibre in clean sand provide more resistance to any deformation which could be due to fibres in clean sand becoming active first in resisting any deformation compare to cemented sand as the cementing effect dominates in fibre reinforced cemented sand samples. However, after reaching to a maximum stiffness there is sudden drop in the stiffness magnitude by the increase in shear strain. At large strain levels of about 10%, the effect of fibres on stiffness modulus is diminishing. The characteristic variation of stiffness with strain is similar in all tests.

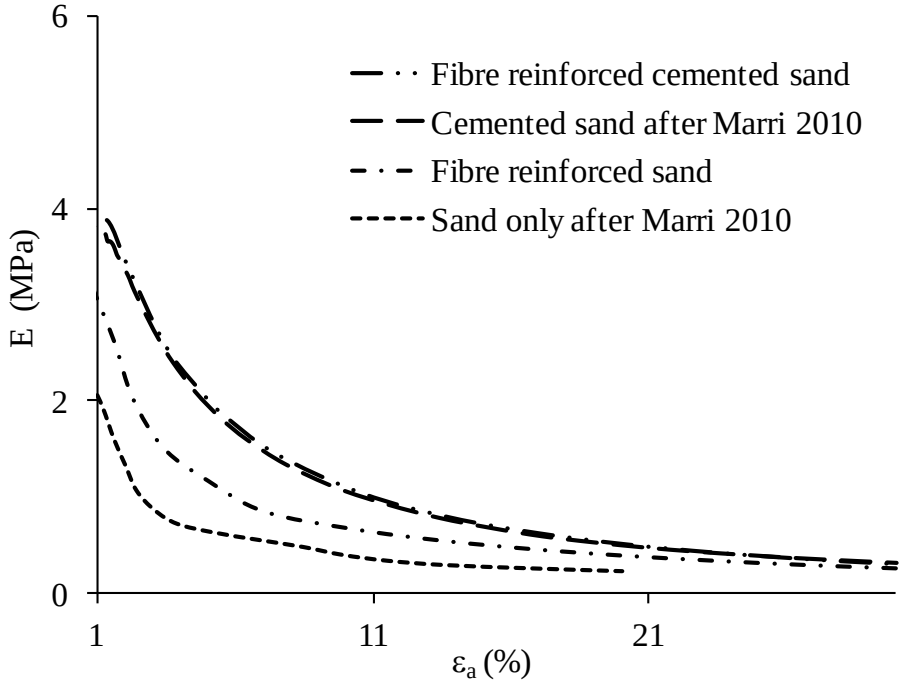

Figure 7.1 Effect of addition of fibre and/or cement on stifness degradation during drained triaxial tests at σ'_3=4MPa.

As it has been observed that addition of fibre has the effect on the initial stiffness of the samples, it is worth investigating how increasing the effective of confining pressures affect the pattern of stiffness degradation with strain during shearing. To

examine this, curves of stiffness degradation with strain are plotted for fibre reinforced sand at different effective confining pressures in Figure 7.2. It can be seen that increasing the confining pressure increases the stiffness of fibre reinforced sand but contrary to the result observed with the addition of fibre the degradation curves do not converge at an axial strain of 10% but continue to degrade with different values until the very high axial strain. Similar degradation patterns were also reported by Sharma and Fahey, (2004) for clean sand.

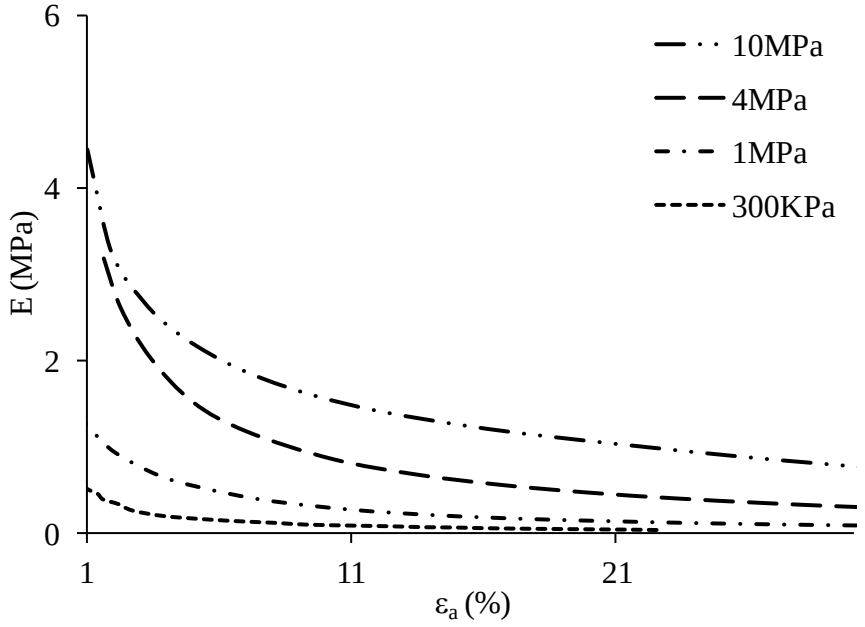

Figure 7.2 Effect of confining pressure on stifness degradation of fibre reinforced sand during drained triaxial tests.

The stiffness degradation curves for undrained triaxial tests are also presented for the effect of the addition of fibre in cemented and uncemented sand and also for the effect of increasing effective confining pressures in Figure 7.3 and Figure 7.4 respectively. From the figure, it can be seen that, similar to the drained compressions the fibre content and confining pressure effects are profound in the start of the deformation and then degrading quickly to a small and stable state. At large strain levels the effect of cement and confining pressure still persists.

Moreover, comparing the effect during drained and undrained compression tests, it can be seen that at large strain levels the magnitude of the drained deformation modulus is relatively higher than that of undrained tests.

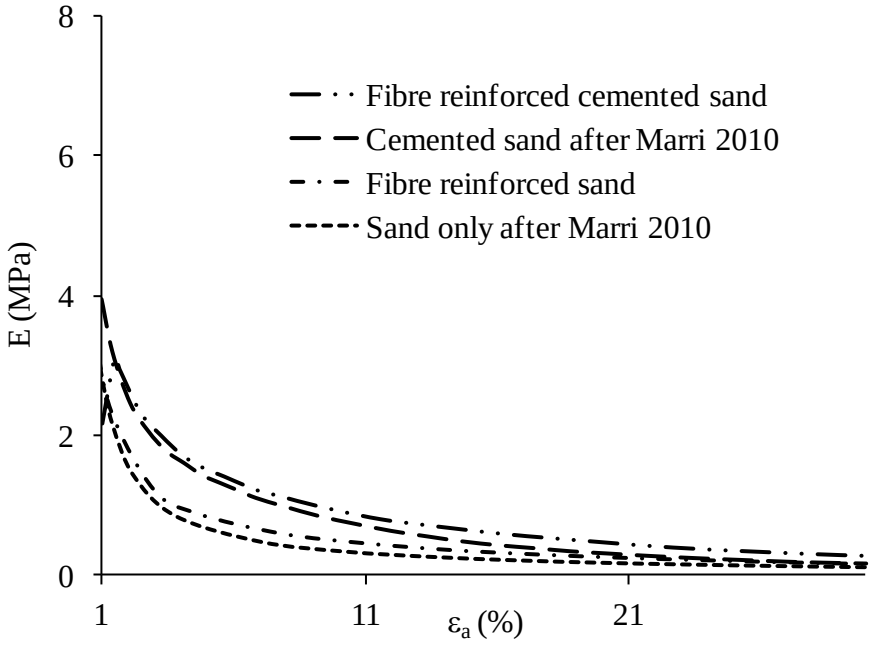

Figure 7.3 Effect of addition of fibre and/or cement on stifness degradation during undrained triaxial tests at σ'_3=4MPa.

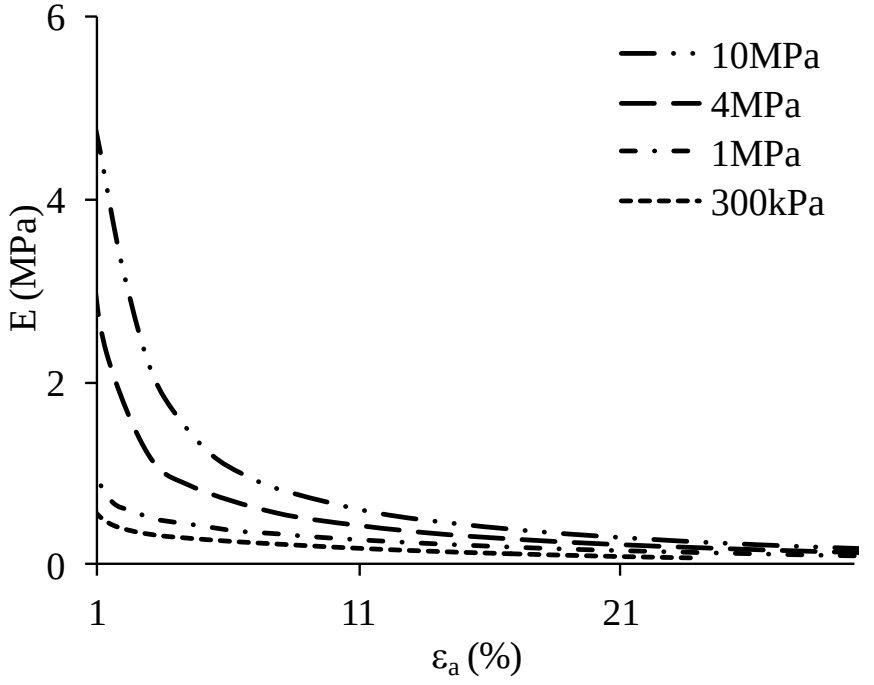

Figure 7.4 Effect of confining pressure on stifness degradation of 0.5% fibre reinforced sand during undrained triaxial tests.

7.3 Yielding characteristics

Classically, the term yielding refers to the transition from elastic to plastic behaviour, and is associated with sharp curvature developing in the stress-strain curve during triaxial shear (Kuwano and Jardine 2007). Wang and Leung (2008) simply determined the yield point as the starting point of the transition from a stiff to a less stiff response. Following the Wang and Leung (2008) procedure, the primary yield is taken as the point where stress-strain curves deviates from the initial linear portion on the q/p'-ε_a curve. Summary of the test results with corresponding parameters are shown in Table 7.1.

Table 7.1 Summary of test data used (elastic parameters).

Test	σ'_3 (MPa)	C (%)	F (%)	q_y (MPa)	p_y (MPa)	E (MPa)
CD-0F0C0.3M	0.3	0	0	0.23	0.372	0.40
CD-0F0C1M	1	0	0	0.27	1.06	1.12
CD-0F0C4M	4	0	0	2.34	4.2	2.59
CD-0F0C10M	10	0	0	5.21	11.45	4.61
CD-0F0C20M	20	0	0	4.24	21.14	5.20
CD-0.5F0C0.3M	0.3	0	0.5	0.306	0.4	0.51
CD-0.5F0C1M	1	0	0.5	1.05	1.31	1.31
CD-0.5F0C4M	4	0	0.5	2.91	4.834	4.80
CD-0.5F0C10M	10	0	0.5	6.318	11.85	3.26
CD-0.5F0C20M	20	0	0.5	8.2	22	4.41
CD-0F5C0.3M	0.3	5	0	1.21	0.704	0.67
CD-0F5C1M	1	5	0	0.159	1.02	3.38
CD-0F5C4M	4	5	0	0.5	4.174	6.48
CD-0F5C10M	10	5	0	4.2	11.40	6.72
CD-0F5C20M	20	5	0	1.8	20.58	4.49
CD-0.5F5C0.3M	0.3	5	0.5	1.46	0.782	1.39
CD-0.5F5C1M	1	5	0.5	1.67	1.4	3.75
CD-0.5F5C4M	4	5	0.5	5.4	5.66	4.01
CD-0.5F5C10M	10	5	0.5	9.2	12.8	5.71

The yield point is located at starting point of the transition from a stiff to a less stiff response (i.e. deviation from linearity). These yield points of different material composition at increasing confining pressures are plotted as shown in Figure 7.5. It can be seen that addition of fibre increases yield stress in both sand and cemented sand at all the different confining pressures.

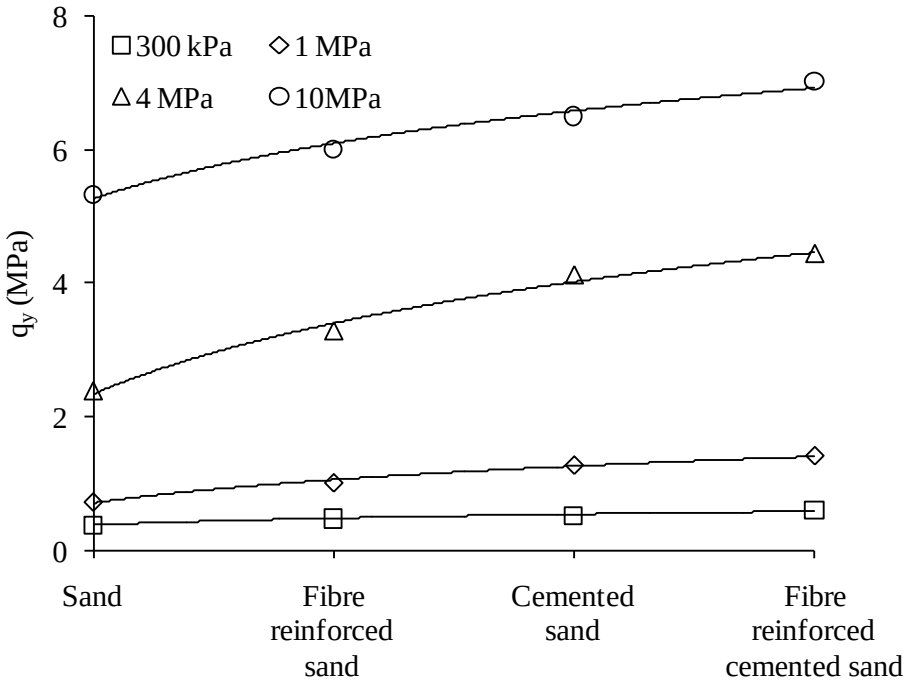

Figure 7.5 Effect of addition of fibre in sand and cemented sand on yield stress at different confining pressures.

The effect of confining pressures on the primary yield stress of sand and cemented sand with and without fibre reinforcement is shown in Figure 7.6. The results show that the confining pressure has a significant effect on the yield strength q_y, during triaxial compression. The relationship between the yield stress q_y and effective confining pressure σ'_3 follows a curve pattern with convex shape and the yield curves expand with increasing cement.

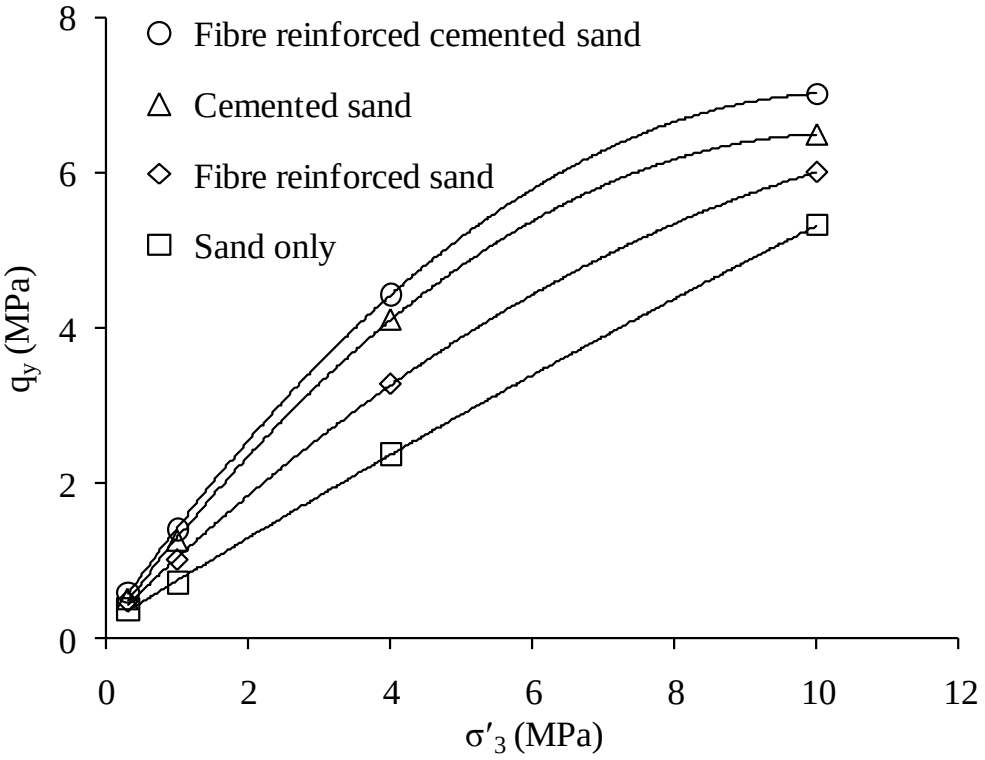

Figure 7.6 Effect of confining pressure on the yield stress.

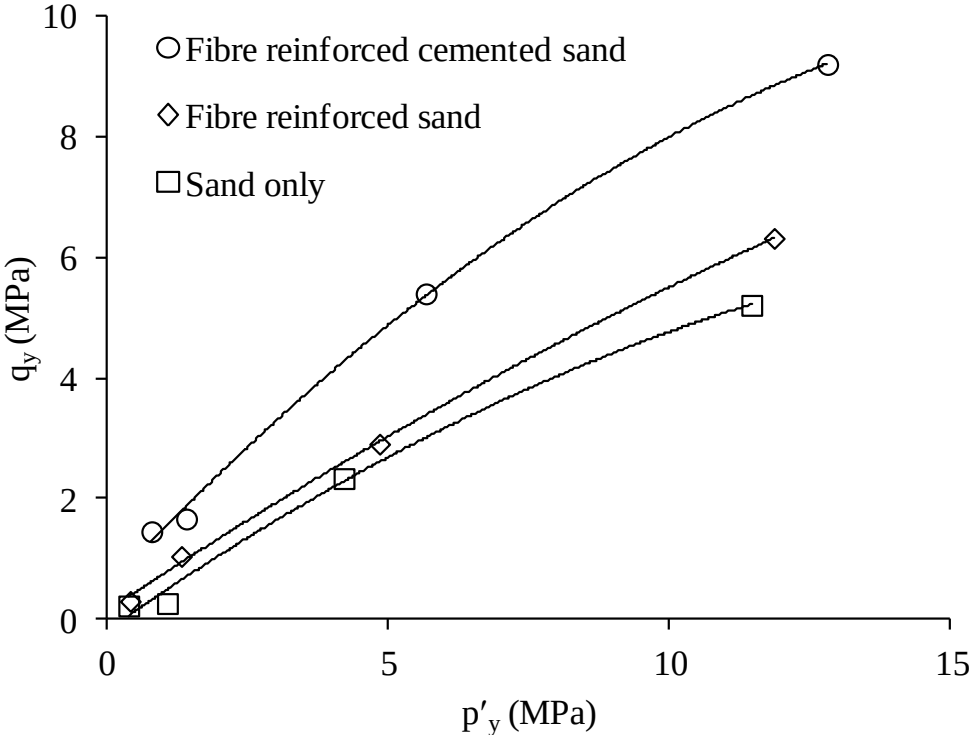

Figure 7.7 Yield curves for different compositions.

7.4 Failure criteria and modes of failure

There are different criteria for defining failure. The maximum deviatoric stress, q_{max}, has often been used as a failure criterion. An alternative failure criterion is the effective stress ratio defined as $(q/p')_{max}$. In an undrained test, the maximum deviatoric stress and maximum effective stress ratio may not occur at the same stress state and axial strain. The maximum effective stress ratio is a function of the pore-water pressure measured during the undrained test. On the other hand, the maximum deviatoric stress is not a direct function of the pore pressures. The limiting strain failure criterion is also sometimes used when large deformations are required in order to mobilize the maximum shear stress.

In an attempt to understand the failure mechanism of fibre reinforced cemented sand, triaxial drained and undrained compression tests were carried out. Considering the effect of the addition of fibres content, cement content and confining pressures, the failure conditions were examined on the bases of the laboratory investigations. From the drained compression tests (see Figure 5.1 to Figure 5.5 Page 125-131) it can be seen that for a varying range of fibre contents, cement contents and confining pressures the maximum deviatoric stress q_{max} and the maximum stress ratio defined as $(q/p')_{max}$ occurs at the same axial strain. This experimental evidence validates the assumption of co-occurrence of q_{max} and $(q/p')_{max}$. However, by the increase in confining pressure it is evident that the cited failure criteria occur at very large strains, as large as 25% (see Figure 5.2 and Figure 5.4), while such large strains are rarely tolerable for various geotechnical structures. For such a case, the limiting strain failure condition could be an alternative criterion.

In the case of undrained triaxial compression tests, it is noticeable that the maximum stress difference, q_{max} does not coincide with maximum effective stress ratio $(q/p')_{max}$. It can be observed that by the addition of fibre the maximum deviatoric stress position shifts towards the right i.e., at larger axial strain (see Figure 5.14(a)) and by the increase in confining pressure its position shifts towards the left i.e., it occurs at small axial strains (see Figure 5.15 and Figure 5.16). However, in either case it is limited with 15% of axial strain.

A failure mode is the manner whereby the failure is observed. Generally, it describes the way in which the failure happens. Traditionally failure in compression is categorized in two modes. In the first, a sample may show strain localization and fail by strain softening and brittle failure under relatively low confining pressure. Moreover, in the second, it may show barrelling and fail by strain hardening under elevated confining pressure. While at intermediate pressures, a transitional regime is sometime observed, with failure modes involving complex localized features such as conjugate shear bands.

The transition from the brittle to the ductile mode of failure was observed from 0.1MPa to 20MPa. It was observed that the brittle behaviour increased with increasing cement content and decreased with the addition of fibres and an increase in confining stress. This is consistent with observations made for cemented gravelly sand by Asghari et al. (2003).

Figure 7.8 shows the modes of failure observed at different confining pressures and material compositions in consolidated drained triaxial tests.

(a) (b) (c)

Figure 7.8 Mode of failure: (a) brittle at 0.5% fibre, 5% cement at 50kPa; (b) transiltional at 0.5% fibres 0% cement at 1MPa ; and (c) ductile modes at 0.5% fibre 0% cement at 4MPa.

The mode of failure, which indicates clear shear banding during consolidated drained compression, can be seen in Figure 7.8(a), having a cement content of 5% and shearing at an effective confining pressure of 50kPa. Sand and fibre reinforced sand without the addition of cement does not show appreciable brittleness.

An interesting feature of the fibre reinforced cemented sand as shown in Figure 7.8(b) is that over a broad range of intermediate pressures the failure mode cannot be unambiguously categorized as strictly "brittle" or "ductile". Moreover, instead of a single shear band, the cylindrical surface of the failure sample is marked by several conjugate shears. This type of transitional failure mode is referred as "quasi-brittle" by Klein et al. (2001).

The brittleness index above the confining pressure range of 4MPa for cemented and fibre reinforced cemented sands specimen can be characterised by ductile attributes with an overall strain-hardening trend. However, sand with and without the addition of fibre shows a ductile mode of failure even at low confining

pressures. The mode of failure for a specimen with a fibre content of 0.5% and an effective confining pressure of 4MPa is shown in Figure 7.8 (c), which is showing a bulging pattern during consolidated drained shearing.

Overall, in cemented samples, the peak strength and the associated strain-softening response become more distinct with the addition of fibres or increasing confining pressure. Adding cement is markedly increasing the strength and altering the stress-strain behaviour. Increase of confinement reduces the softening tendencies, and generally results in a more ductile response. These findings are in accordance with previously published results, for example, Wang and Leung (2008), Ismail et al. (2002), Schnaid et al. (2001), and Clough et al. (1981).

The mechanical properties of the materials are essential for understanding the behaviour of fibre reinforced materials to provide a useful method of predicting failure mode. An absolute measure of such behaviour is provided by the brittleness index (I_B) defined by the following expression given by Consoli et al. (1998).

$$I_B = \frac{q_f}{q_u} - 1 \tag{7.3}$$

Where q_f is failure/maximum deviator stress and q_u is the ultimate deviator stress.

From Figure 7.11, it can be observed that the brittleness index is high at relatively lower confining pressure and with the addition of cement contents. This indicates a stronger, stiffer, and more brittle material. As the index decreases, approaching zero, the failure behaviour becomes increasingly ductile.

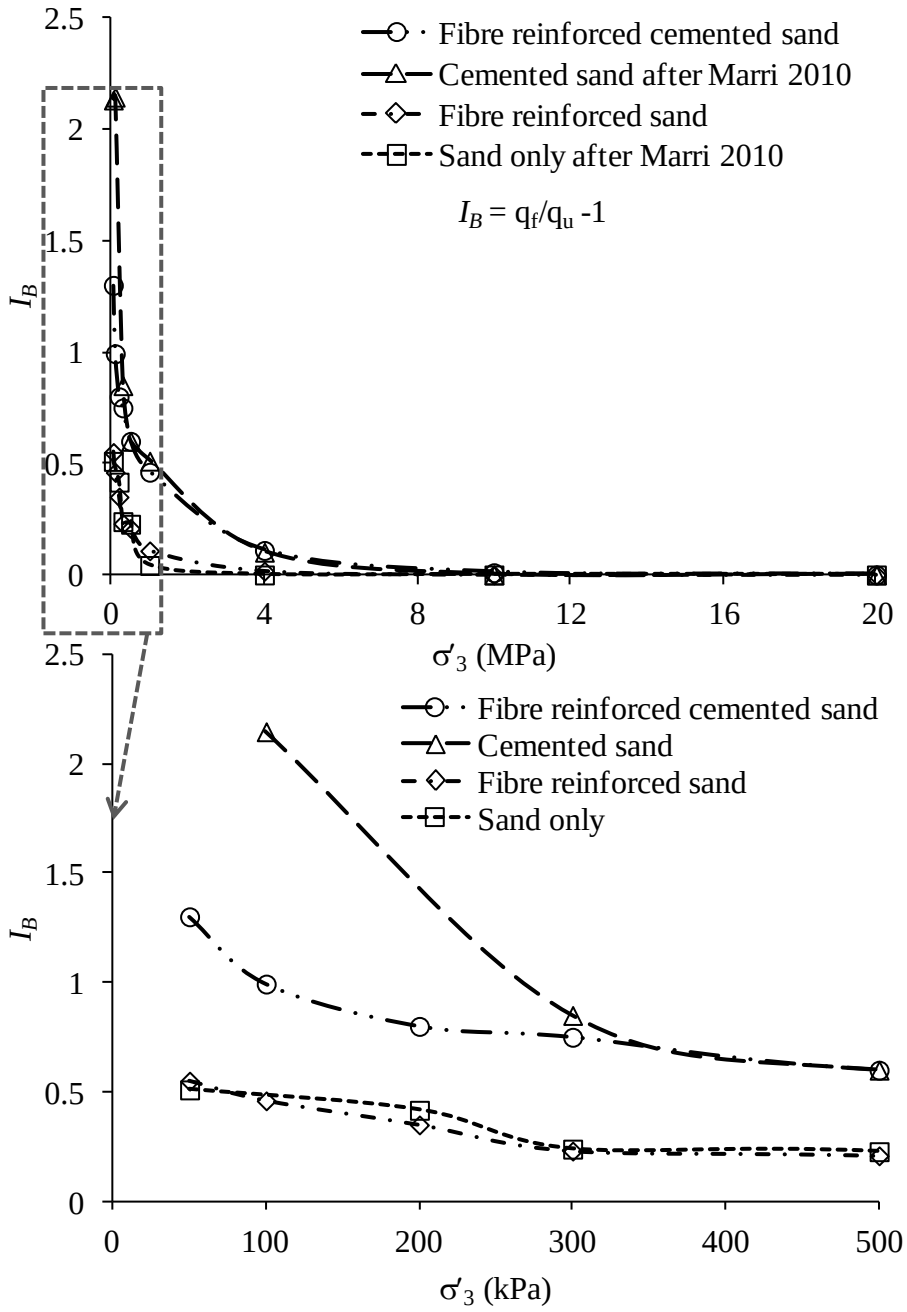

Figure 7.9 Effect of addition of fibre/cement and confining pressure on brittleness index.

7.5 SEM analysis

In order to see the effect of shearing on particle crushing, cement bond breakage and fibre damage, uncemented and cemented samples were investigated after shearing. Figure 7.10 shows the microstructure of fibre reinforced uncemented

sand after shearing at the confining pressure of 10MPa. It can be seen that there is significant crushing of sand particles. Lumps of crushed particles and fibre breakage are clearly visible. The amount of particle crushing is affected by the stress level, particle size, the stress magnitude and the stress path (Lade et al., 1996).

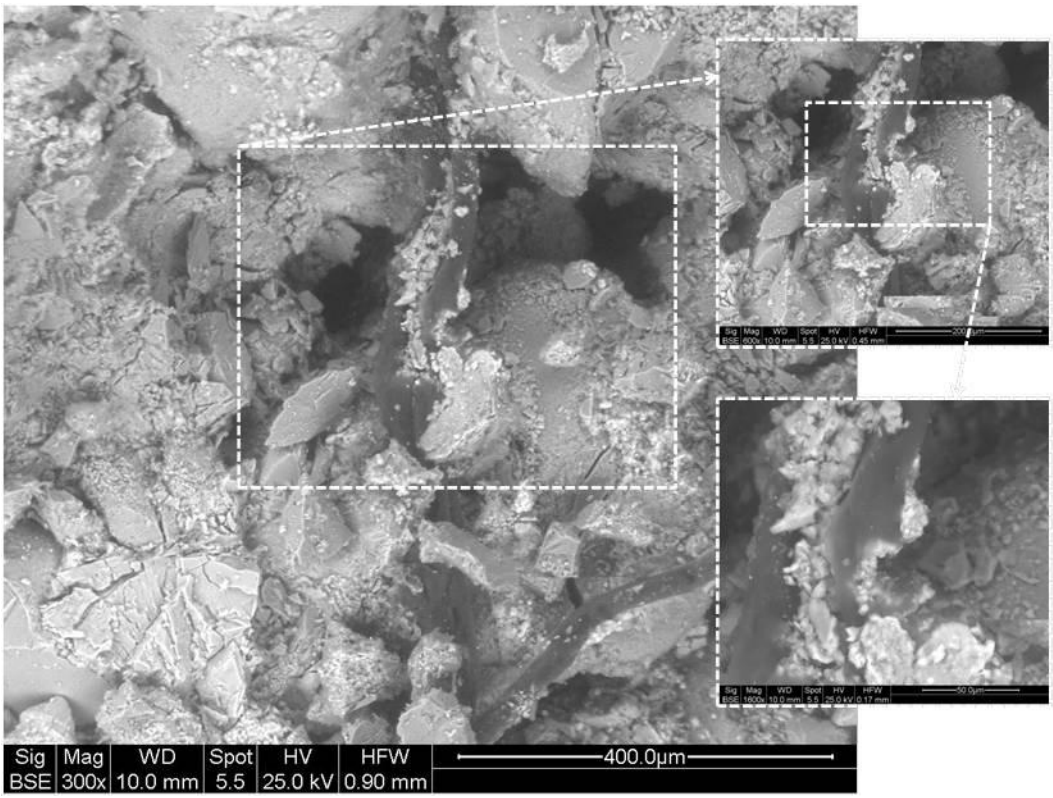

Figure 7.10 Particle crushing and fibre breakage in 0.5% fibre reinforced uncemented sand at horizontal plane after shearing at 10MPa.

Figure 7.11 shows the SEM micrograph of fibre reinforced cemented sand with 0.5% fibre and 5% cement content sheared at 10MPa. The amount of particle crushing in the fibre reinforced cemented sample as compared to uncemented sand was observed to be more.

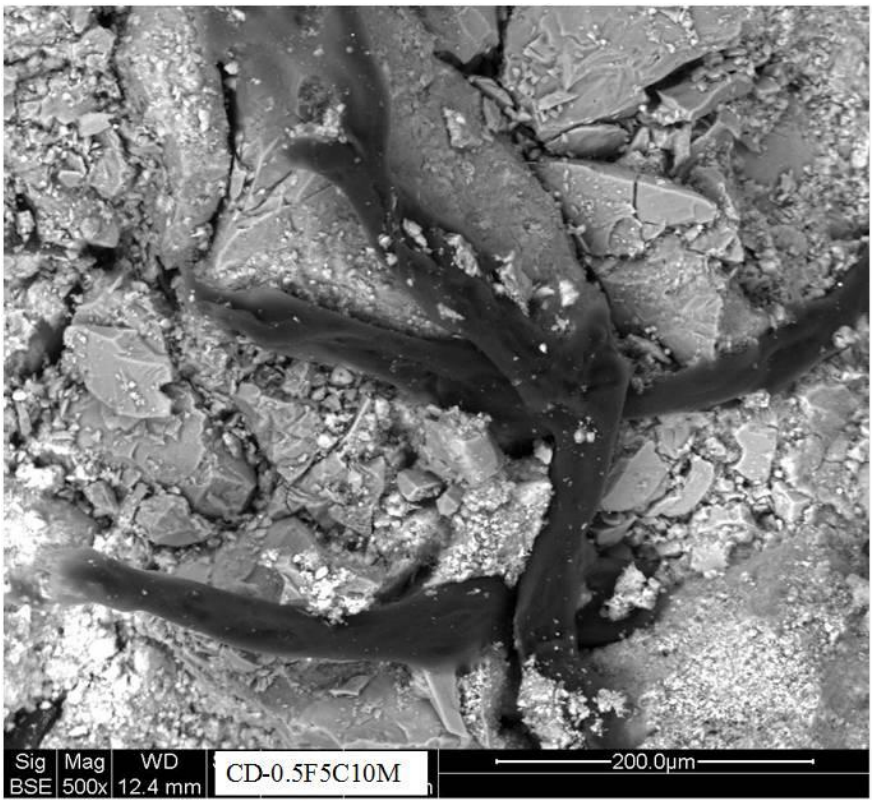

Figure 7.11 Particle crushing, bond and fibre breakage in 0.5% fibre and 5% cemented sand sheared at 10MPa at failure plane after testing.

The SEM micrographs of the subsections of bulging (tested at 10MPa) and shear band (tested at 500kPa) are shown in Figure 7.11 and Figure 7.12 respectively. From Figure 7.11 it can be seen that along with bond breakage there is particle crushing as well. On the other hand, from Figure 7.12 it is evident that during shear at 500kPa of confining pressure, cement bonds were broken along the shear plane; however, there is no significant particle breakage. Only a few fractures on the surface of the sand grains can be seen along with fractured particles.

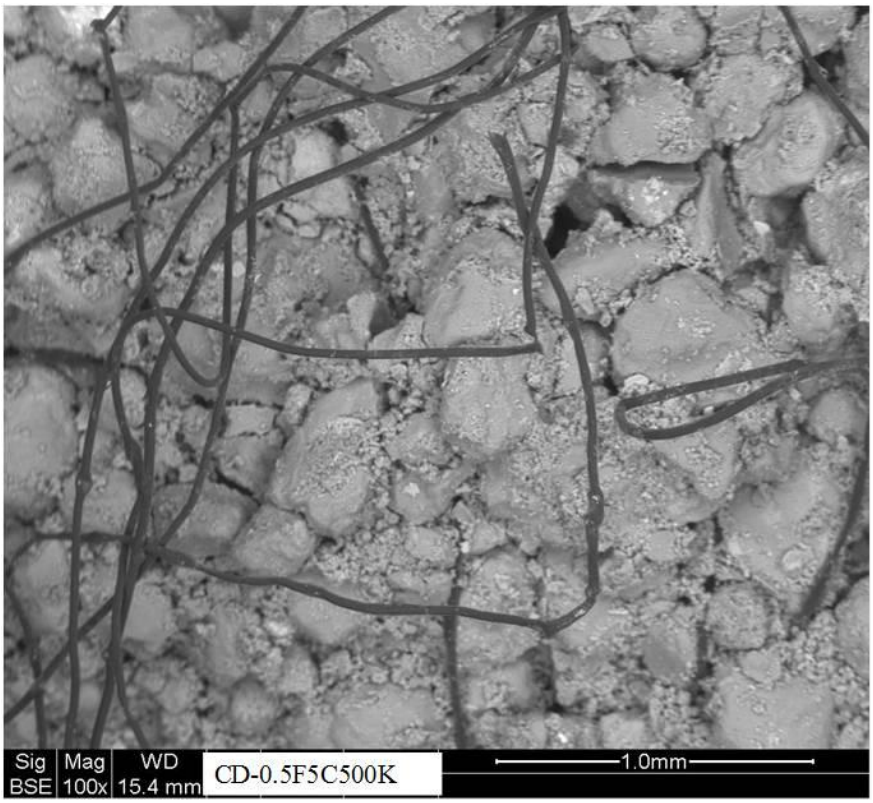

Figure 7.12 Bond and fibre breakage in 0.5% fibre and 5% cemented sand sheared at 500kPa.

In order to investigate the effect of undrained shearing, fibre reinforced cemented samples were also analysed under SEM. Figure 7.13 shows the microstructure of 0.5% fibre and 5% cement reinforced sand after undrained shearing at an effective confining pressure of 10MPa. It can be seen that there is less significant crushing of sand particles and fibre damages. One reason for less deformation during undrained conditions as compared to the drained conditions might be due the fact that during undrained shearing pore water pressure increases with the increase in deviatoric stress.

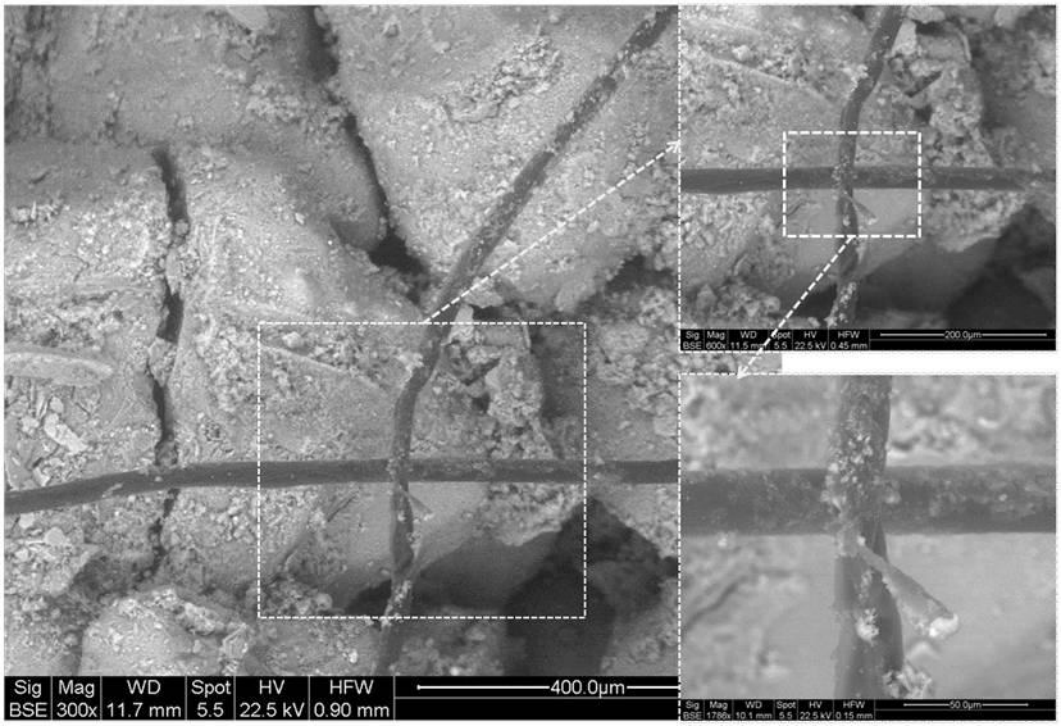

Figure 7.13 Particle crushing, bond and fibre breakage in undrained shearing of 0.5% fibre and 5% cemented sand after shearing at 10MPa.

7.6 Critical/ultimate state behaviour

There are quite a number of papers and case studies available in literature regarding the critical state concepts in sandy soil. The existence of a critical state wherein indefinite shear occurs is a major feature of the family of elastic-plastic models known as critical state soil mechanics (Schofield and Wroth, 1968). However, it should be noted that the majority of these studies are associated with fine and uniform sands and are at conventional pressures. There is a lack of data for the fibre reinforced uncemented or cemented sands. Studies reported in the literature (e.g. Gray & Ohashi, 1983; Gray & Al-Refeai, 1986; Maher & Ho, 1993; 1994; Consoli et al., 2009a) have generally been conducted independently and have not always been consistent. For a topic so wide it has been difficult to build a

unified framework that could be linked to other recognised frameworks, for example, the critical state framework (Consoli et al. 2010).

For the purpose of developing a useful framework, in the analyses presented here it has been necessary to identify representative lines at large strains, where reasonably constant stress and volume were found with continuous shearing. The end points for the triaxial tests of fibre reinforced cemented and uncemented sand have been plotted in a q-p' and e-ln(p') graphs in Figure 7.14 and Figure 7.15 respectively. The end points for these tests provided reliable points to derive a critical state line in the stress plane, though the volumetric strain had not stabilised at the end of all tests. The deviatoric stress was, however found to be reasonably constant at the end of the tests (see Figure 5.7 and Figure 5.8).

The summary of the triaxial compression test data stating the critical/ultimate state parameters is shown in Table 7.2.

Table 7.2 Summary of test data used in critical state analysis.

Test	σ'_3 (kPa)	e_0	e_c	e_{cr}	q_{cr} (kPa)	p_{cr} (kPa)	$(q/p')_{cr}$	ϕ'_{cr} (Deg)
Fibre reinforced sand	50	0.523	0.518	0.611	271.6	146.5	1.853	45.1
	100	0.523	0.516	0.600	356	235.5	1.511	41.9
	200	0.523	0.509	0.600	711	437	1.63	39.78
	300	0.523	0.502	0.560	895	597	1.50	36.82
	500	0.523	0.500	0.560	1356	952	1.424	35.15
	1000	0.495	0.471	0.500	2422	1848	1.31	32.54
	4000	0.495	0.446	0.373	9052	6975	1.3	32.24
	10000	0.495	0.407	0.246	22562	17488	1.3	32.07
	20000	0.495	0.362	0.185	43790	34570	1.27	31.52
Fibre reinforced cemented sand	50	0.501	0.498	0.663	408	186	2.2	53.5
	100	0.501	0.494	0.636	527	275	1.92	46.58
	200	0.501	0.481	0.623	963	520	1.86	45.1
	300	0.501	0.495	0.577	1155	682	1.7	41.3
	500	0.536	0.522	0.585	1240	910	1.4	33.7
	1000	0.510	0.498	0.563	3141	2082	1.51	37.0
	4000	0.517	0.488	0.465	9716	7207	1.35	33.40
	10000	0.507	0.459	0.368	23074	17629	1.31	32.5
	20000	0.529	0.448	0.310	44418	35000	1.27	30.71

In the failure state of geomaterials with reinforcement, the effect of the addition of fibre and/or cement ought to make the strength of soil increase and extends the domain in which the soil can exist. In order to introduce the reinforcement effect, two assumptions have been suggested by Kasama et al. (2004) as 1) the failure line with reinforcement on q-p' space is shifted but parallel to that of geomaterials without reinforcement and 2) the failure line of soils with reinforcement on e-ln(p')

space is represented by a linear relationship and the slope of this line is steeper than that of soils without the addition of reinforcement.

It can be seen that the critical state lines for all the composites are almost close to each other at the large scale. The only difference that can be seen is in the enlarged figure shown where the addition of fibres and cement has shown to increase the cohesion of sand and fibre reinforced sand, though the M value for the materials remains nearly the same. The values of ultimate state stress ratio obtained from the test data as shown in Table 7.2 match reasonably well with (q/p') ≈1.3 for tests run at high CP, but at low CPs, the values of stress ratios are high but it should be kept in mind that tests at low confining pressures were terminated at axial strains of 25%, whereas at high confining pressure they were continued untill 40% axial strain.

Dos Santos et al., (2010a) reported a curved line for fibre reinforced sand and reported that the critical state ratio, M is dependent on effective confining pressure and has been discussed in detail in the literature review.

The critical state data has also been analysed in e-ln(p') space and the curve obtained are shown in Figure 7.15. It can be seen that CSL appears to be curved to reach maximum void ratio at low stresses, as at these stresses samples were dilating at the end of the tests. At higher stresses, the data points define a straight line parallel to NCL of fibre reinforced cemented and uncemented sand. Similar results were reported by Dos Santos et al. (2010a). The specimen tested at the high confining pressure of 4MPa which reached stable stress and volume at the end of the test, could be assumed to have reached a critical state. The data point for that

sample and others tested at CP above 4MPa plots closely to the data points of the NCL and form CSL parallel with NCL.

It is not at all certain that the specimens would have reached a critical state anyway even at an axial strain of 40%. Thus a true CSL for the reinforced soil cannot be defined, and the CSLs can only be regarded as representative of large strain behaviour.

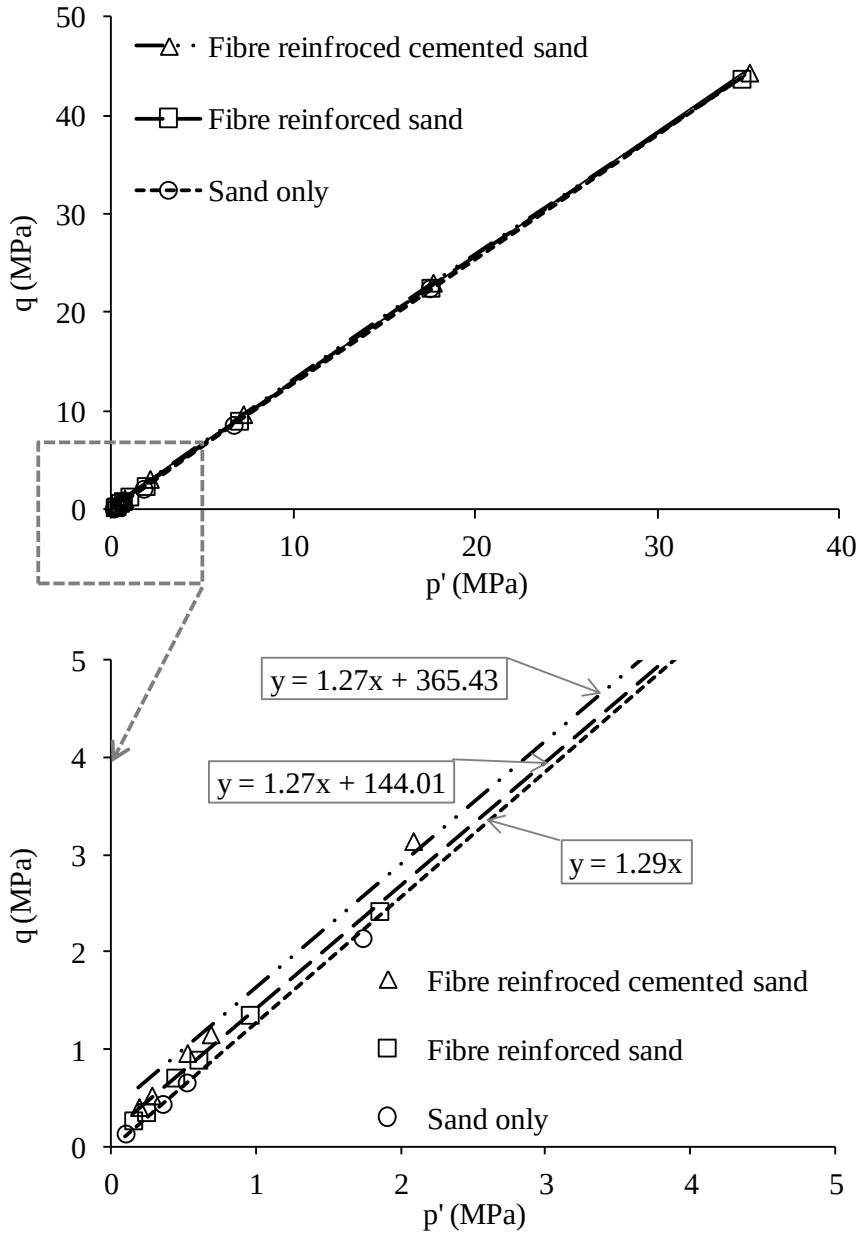

Figure 7.14 Critical state lines of fibre reinforced cemented and uncemented sand in q-*p'* space.

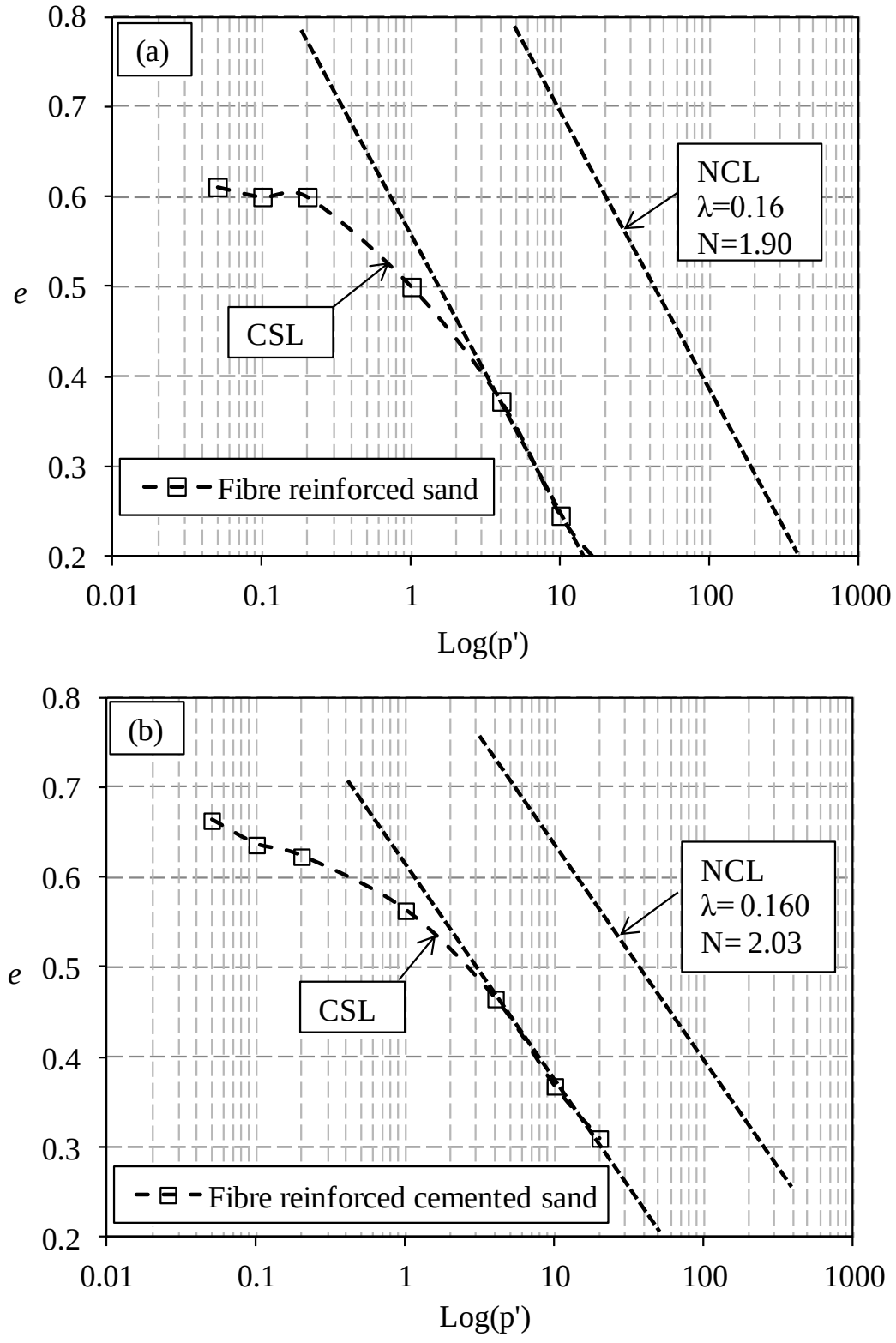

Figure 7.15 Critical state lines in e-ln(p') space, (a) fibre reinofrced sand and (b) fibre reinforced cemented sand.

7.7 Summary

The effects of the addition of fibre and confining pressures were investigated on the deformation characteristics, stiffness, yielding, failure modes, micromechanics and critical state through laboratory testing. The brief summary of the experimental results is described as follow:

1. The addition of fibres and increasing confining pressure affect the deformation pattern of the composites. The addition of fibres reduces the particle breakage at low confining pressures but at high confining pressures both particle crushing and fibre breakage were significant. Varying the drainage conditions also alter the deformation of the composites as in undrained tests the extent of particle crushing and fibre twisting and breakage were less significant.
2. The addition of fibre and increasing confining pressure also affect the initial stiffness of the composites. Similarly, the addition of fibres and increasing confining pressure increases the yield stress of the sand and cemented sand.
3. Failure modes are also significantly affected by the addition of fibre and the changing confining pressure. The addition of cement causes the materials failure mode to be brittle. However, the addition of fibre has been observed to reduce the brittleness of cemented sand. Increasing confining pressure also changes the material behaviour from brittle to ductile and from strain softening to strain hardening.
4. The specimens exhumed after shearing showed brittle, transitional and ductile modes of failure, depending upon the percentage of fibre and/or

cement content and the amount of confining pressure applied. The quantitative analysis of the mode of failure was made with the help of a brittleness index (I_B). High values correspond to brittle mode and low values to transitional mode and values close to zero shows a ductile mode of failure. The values of I_B increase with the addition of fibres in both cemented and uncemented sand and decreases with the increase in confining pressures. The value was as high as 2.1 for fibre reinforced cemented sand at 100kPa and reduces gradually to approximately zero at and above 4MPa. The addition of fibre reduces the brittleness and at 100kPa the values decreased from 2.1 to 1. At and above 4MPa, all samples showed a ductile mode of failure with I_B values very close to zero.

5. The state of the soil at which axial deformation occurs without any change in volumetric strain (constant volume strain) i.e. critical state for fibre reinforced cemented and uncemented samples could not be reached at the terminal axial strain of 40%, although deviatoric stress was almost stable. Therefore, the end points for these tests provided reliable points to derive a critical state line in the stress plane.
6. The CSLs in q-p’ space for fibre reinforced cemented and uncemented sand are parallel. The value of M for both fibre reinforced cemented and uncemented sand remains 1.3. The critical state line in e-ln(p’) space appears to be curved and at low pressures curved to maximum void ratio and at high pressures follows line parallel to NCL of fibre reinforced cemented and uncemented sand obtained in isotropic compression tests.

CHAPTER 8

CONCLUSIONS AND RECOMMENDATIONS

8.1 Introduction

From the detailed literature review it can be concluded that a lot of work has been done on effects of fibre and cement on the behaviour of sand. There is general consensus that fibre improves the soil behaviour at a conventional range of pressures. However, the behaviour of sand and cemented sand has not been studies at high pressures with the addition of fibre. Therefore, more data is needed to understand fundamental mechanisms and to develop and modify existing or new constitutive soil models for increased confining pressures.

Also the review of the literature reveals that there are areas in the behaviour of fibre reinforced sand which have not been dealt with in detail which lack consensus and therefore needs further exploration. For example isotropic compression behaviour, stress-dilatancy behaviour and micromechanics of fibre reinforced cemented and uncemented sand. An attempt has been made to explore the effect of varying and/or the addition of fibres on sand and cemented sand on the aforementioned parameters at conventional to high confining pressures.

It should also be noted that nearly all previous studies carried out on fibre reinforced cemented or uncemented materials have not considered the effect of fibre reinforcement on the yielding and critical state behaviour of the

materials. In the present research in this regard some features of the behaviour of fibre reinforced uncemented and cemented granular materials have been investigated at wide range of confining pressures.

8.2 Conclusions

8.2.1 Problems in triaxial tests

During the sample preparation and testing there is a likelihood of certain errors due to several reasons, some of these can be avoided by careful handling, and some are unavoidable. Therefore, for good quality results it is important to be cautious about such types of error and apply necessary corrections for unavoidable errors before subsequent investigations and analysis. Some of the problems and the solution adopted were:

1) The samples, stuck to the sides in the moulds and therefore it was found very difficult to extract samples from the mould. To overcome this problem transparent sheet used for overhead projectors were laid inside the periphery of the mould. It was also used at the bottom of the mould to prevent sticking. This proved to be very useful in overcoming this problem.
2) The Bishop-Wesley triaxial tests apparatus was found not capable of testing cemented samples with effective confining pressures higher than 300kPa due to the insufficient capacity of the load cell used. For conventional and high pressures a uniform size of samples (100mm height by 50mm diameters) was initially used. To overcome this problem it was required to reduce the size of the samples to 38mm diameter.

8.2.2 Isotropic compression

High pressure isotropic compression tests were carried out on samples of uncemented and cemented Portaway sand at different initial void ratios and different fibre and cement contents.

1) From the experimental investigations, it was observed that the effect of initial void ratio for both cemented and uncemented fibre reinforced sands appeared to diminish at high pressures and there was convergence in the isotropic compression curves. Similar to uncemented sand, the cemented sands with different initial void ratios converge towards a unique final void ratio. Therefore, the variation of initial void ratio has less significance at high confining pressures.
2) Keeping the initial void ratio constant, the effect of the addition of fibre in sand and cemented sand was also examined and it could be seen that the effect of fibre is either very nearly negligible or the addition of fibre increases the overall compression of both sand and cemented sand.
3) The value of λ and N for sand and fibre reinforced sand is 0.160 and 1.88 respectively while for cemented and for fibre reinforced cemented sand the values are 0.173 and 2.03. Therefore, no effect of the inclusion of the fibre was seen in isotropic compression tests for both cemented and uncemented sand samples.
4) Regarding the particle crushing and fibre breakage, fibre/cement content was not found to resist the deformation due to higher confining pressures. For instance, for both uncemented and cemented fibre reinforced sand, SEM

micrographs indicated significant particle crushing, fibre twisting and punching. However, for fibre reinforced sand, only fibre twisting and punching was seen and there was hardly any fibre breakage. This verifies the results seen in e-log (p') curves that fibres did not contribute in resisting the isotropic compression due to only being subjected to compressive stresses.

8.2.3 Stress-strain behaviour

The stress-strain behaviour of Portaway sand with the addition of fibre and cement in a wide range of confining pressure was investigated in both drained and undrained conditions. From the experimental results, it could be seen that the addition of fibre and varying the confining pressure significantly influences the mechanical response of sand. From the triaxial compression behaviour of cemented sand the following conclusions can be drawn:

1) The addition of fibre and/or cement content in the sand can markedly augment the strength. The results show strength enhancement and volumetric dilation. These features become more pronounced with increasing fibre content and prevail only under low confining pressure. The percent increase in peak strength in sand due to the addition fibre is 56% whereas fibre increased the peak strength of cemented sand by 20%. This increment in strength due to the addition of fibre gradually reduced and at a CP of 10MPa the effect was almost zero. The combined effect of the addition of cement and fibres is found to be very significant and the strength increase observed at 50kPa was 410% when compared with the strength of sand at the same effective confining pressure. The combined effect also

reduced with increasing confining pressures and at 10MPa the increase was almost zero. However, at high pressures strain-hardening behaviour was observed. Greater volumetric contraction, identical to the loose sand could be measured.

2) In any cases the addition of fibres, cement and/or varying confining pressures there was an increase in the peak strength of the sand. The position of peak stress changed with the change in fibre and cement content and confining pressure. The addition of cement content resulted in a brittle behaviour causing the peak strength to occur at smaller strain levels. However, the addition of fibre reduced brittleness. On the other hand, an increase in confining pressures induced ductility and caused the peak strength to occur at larger strain levels depending upon the magnitude of confining pressure.

3) The addition of fibre also increased the peak friction angle of both cemented and uncemented sand while increasing confining pressure reduced the friction angle. At confining pressure of 4MPa and above, no effect of either confining pressures or fibres could be seen. For instance at 50kPa the friction angle of sand, fibre reinforced sand, cemented sand and fibre reinforced cemented sand are 40.4°, 45.8°, 58.2° and 65° and hence reduced gradually to 32° for all the composites at 10MPa and above.
4) The addition of fibres also induced cohesion in sand and increased the cohesion of cemented sand. The cohesion increased from 176kPa in sand to 287kPa in fibre reinforced sand and 940kPa in fibre reinforced cemented

sand. The strength envelopes appeared to be straight lines at low confining pressures and with the increasing confining pressure become slightly curved. Linear assumption showed the friction angle of the failure envelopes to be approximately 51.3°.

5) The results of the triaxial tests performed on cemented and uncemented fibre reinforced sand show that the addition of the cement content could improve the strength of soils under undrained and drained loading conditions. Shear strength parameters of effective stress cohesion intercept and friction angle increased in the CU and CD tests, due to the addition of fibre and cement.

8.2.4 Stress-dilatancy behaviour

From the analysis of the experimental data it can be concluded that the stress dilatancy behaviour of the all the composites is influenced by the parameters investigated. The results are summarised in the following points:

1) The commencement (point of initiation of dilatancy), maximum dilatancy, and post-peak dilatancy are fibre content, cement content, and confining pressure dependent. There was a significant effect from the addition of fibre on the response of both cemented and uncemented sand. The addition of fibres increases the dilative behaviour of the composites.
2) The addition of fibre increases the dilatancy while increasing confining pressures reduces dilatancy.
3) The dilatancy angle of sand increased from 1.5° to 10.17° due to the addition of fibres and from 15.95° of cemented sand to 18.9° in fibre reinforced

cemented sand. Thus the effect of the addition of fibre is more in sand than in cemented sand.

4) Increasing the cement content also increased the dilatancy angle from 21.23° to 22.16° and 28.18° for 0%, 2% and 5% cement content respectively.
5) The stress ratio, volumetric strain and dilation increased due to the individual or combined addition of fibre and cement. Varying confining pressure, fibre content and cement content all seem to have affected the dilative response of the materials. Increasing confining pressure decreases the dilation and it was observed that the effect of fibre and/or cement was highest when confining pressure was the lowest.
6) At higher confining pressures the effect of confinement was so dominant and there was no dilation observed at pressure above 4MPa.

8.2.5 Stiffness and yielding characteristics

The effect of the addition of fibre and changes confining pressures were investigated for changes in stiffness and yielding characteristics. Key effects of the addition of fibre and increasing confining pressure are;

1. The addition of fibres and increasing confining pressure increased the yield stress of the sand and cemented sand. With the increase in confining pressure the yield stress of fibre reinforced sand increased from 471kPa 1MPa, 3.3MPa and 6.01MPa at CPs of 300kPa, 1MPa, 4MPa and 10MPa respectively.
2. The addition of fibres and increasing confining pressures also affected the stiffness of the composites. The stiffness was observed to be slightly higher

in undrained test. The addition of fibre increased the stiffness of clean sand in drained triaxial tests carried out at a CP of 4MPa from 3MPa to 3.2MPa and in cemented sand increases in stiffness there was hardly any noticeable effect.

8.2.6 Strength and deformation

1. The addition of fibres and increasing confining pressure affected the micromechanics of the composites. The addition of fibres reduced the particle breakage at low confining pressures but at high confining pressures both particle crushing and fibre breakage were significant. Varying the drainage condition also alter the deformation of the composites as in undrained tests the extent of particle crushing and fibre twisting and breakage were less significant.
2. The specimens exhumed after shearing showed brittle, transitional and ductile mode of failure, depending upon the percentage of fibre and/or cement content and the amount of confining pressure applied. The quantitative analysis of the mode of failure was made with the help of brittleness index (I_B). High values correspond to brittle mode and low values to transitional mode and values close to zero show ductile mode of failure. The values of I_B increased with the addition of fibres in both cemented and uncemented sand and decreased with the increase in confining pressures. The value was as high as 2.1 for fibre reinforced cemented sand at 100kPa and reduced gradually to approximately zero at and above 4MPa. The addition of fibre reduced the brittleness and at 100kPa the values decreased

from 2.1 to 1. At and above 4MPa all samples showed a ductile mode of failure with I_B values very close to zero.

8.2.7 Critical state behaviour

1. The state of the soil at which axial deformation occurs without any change in volumetric strain (constant volume strain) i.e. critical state for fibre reinforced cemented and uncemented samples could not be reached at terminal axial strain of 40%, although deviatoric stress was almost stable. Therefore, the end points for these tests provided reliable points to derive critical state lines in the stress plane.
2. The CSLs in q-p' space for fibre reinforced cemented and uncemented sand are parallel. The value of M for both fibre reinforced cemented and uncemented sand remains 1.3. The critical state line in e-ln(p') space appears to be curved and at low pressures curved to a maximum void ratio. At high pressures it follows the line parallel to NCL of fibre reinforced cemented and uncemented sand obtained in isotropic compression tests.

8.3 Practical implications

The addition of fibres in sand improves the behaviour and this beneficial effect has been quantified by various parameters. Today, soil reinforcement has practically invaded the civil engineering industry the world over, as viable and economical construction materials with diverse uses particularly in concrete structures. However, there is very little effect of fibres at high pressures. Therefore its use in

structures which are subjected to high pressures can be very limited, hence, potential applications are limited to shallow depths.

Construction of building and other civil engineering structures on weak or soft soil is highly risky on geotechnical grounds because such soil is susceptible to differential settlements, poor shear strength and high compressibility. Improvement of load bearing capacity of the soil may be undertaken by a variety of ground improvement techniques like stabilisation of soil, adoption of reinforced earth technique etc. The reinforced earth technique is considered as an effective ground improvement method because of its cost effectiveness, easy adaptability and reproducibility.

Soil mass reinforced with randomly distributed discrete fibres resembles the conventional earth reinforcement in many of its properties. The preparation of fibre reinforced soil is quite similar to that of conventional soil stabilisation. Mostly the discrete fibres are simply added and mixed with the soil, much the same as cement, lime or any other additives.

Presently, the soil reinforcement technique is well established and is used in variety of applications same as the improvement of bearing capacity, reinforced retaining walls, pavement rehabilitation, filter and drainage control, etc.

From the laboratory investigations and subsequent test data, it is possible to extract fundamental material parameters, such as cohesion (c), frictional angle (ϕ), dilatancy angle (ψ), void ratio (e), deformation modulus (E) etc. These parameters can be used in predicting material's behaviour and in computer models to predict how the material will behave in larger scale engineering applications. The materials real behaviour can be useful for any numerical modelling and designing the geotechnical structures.

8.4 Recommendations for future study

Due to time limit and other constraints current study was carried out by experimentally investigating the behaviour of Portaway sand with the addition of different content of 23mm long polypropylene fibres only. Therefore recommendations for future studies are;

1. Different fibre length may be investigated to see the effect of fibre length. Also different fibres other than polypropylene can provide useful information on the behaviour of Portaway sand at a wide range of confining pressures.
2. Detailed microscopic analysis could also provide significant information regarding the failure characteristics and deformation mechanism of fibre reinforced sand. Therefore, detailed SEM and/or X-ray analysis would be very valuable in understanding the behaviour of fibre reinforced soil at micro level.
3. Modeling the behaviour of fibre reinforced soils from experimental findings could also be undertaken to validate and extend further the mechanism of fibre reinforced soil.

REFERENCES

ABDULLA, A. & KIOUSIS, P. 1997. Behavior of cemented sands .1. Testing. *International Journal of Numerical and Analytical Methods in Geomechanics,* 21**,** 533-547.

ASGHARI, E., TOLL, D. G. & HAERI, S. M. 2003. Triaxial behaviour of a cemented gravely sand, Tehran alluvium. *Geotechnical and Geological Engineering,* 21**,** 1-28.

ATKINSON, J. 2007. *Mechanics of soil and foundations, Taylor and Francis,* London.

BARKSDALE, R. D. and BLIGHT, G. E. (1997). Compressibility and settlement of residual soils. In Mechanics of Residual Soils, (G. E. Blight Ed.) 95–154. Rotterdam: A. A. Balkema.

BEEN, K., and JEFFERIES, M. (2004). Stress-dilatancy in very loose sand, Canadian Geotechnical Journal, 41, 972-989.

BOLTON, M. 1986. The strength and dilatancy of sand. *Geotechnique,* 36**,** 65-78.

BOPP, P. A. & LADE, P. V. 2005. Relative density effects on undrained sand behavior at high pressures. *Soils and foundations,* 45**,** 15-26.

BOUKPETI, N. & DRESCHER, A. 2000. Triaxial behavior of refined Superior sand model. *Computers and Geotechnics,* 26**,** 65-81.

CHEN, C. Undrained and Drained triaxial tests of fibre-reinforced sand. *In:* LI, G., CHEN, Y. & TANG, X., eds. *4th Asian Regional Conference on Geosynthetics, 2008* Shanghai, China. Springer Berlin Heidelberg, 114-120.

CONSOLI, N., BASSANI, M. & FESTUGATO, L. 2010. Effect of fiber-reinforcement on the strength of cemented soils. *Geotextiles and Geomembranes***,** 344-351.

CONSOLI, N., CASAGRANDE, M. & COOP, M. 2005a. Behavior of a fiber-reinforced sand under large shear strains. *Proceedings of the 16th International Conference on Soil Mechanics and Geotechnical Engineering, Vols 1-5***,** 1331-1334.

CONSOLI, N., CASAGRANDE, M. & COOP, M. 2005b. Effect of fiber reinforcement on the isotropic compression behavior of a sand. *Journal of Geotechnical and Geoenvironmental Engineering,* 131**,** 1434-1436.

CONSOLI, N., CASAGRANDE, M., PRIETTO, P. & THOME, A. 2003a. Plate load test on fiber-reinforced soil. *Journal of Geotechnical and Geoenvironmental Engineering,* 129**,** 951-955.

CONSOLI, N., CASAGRANDE, M., THOME, A., ROSA, F. & FAHEY, M. 2009a. Effect of relative density on plate loading tests on fibre-reinforced sand. *Geotechnique,* 59**,** 471-476.

CONSOLI, N., FESTUGATO, L. & HEINECK, K. 2009b. Strain-hardening behaviour of fibre-reinforced sand in view of filament geometry. *Geosynthetic International,* 16**,** 109-115.

CONSOLI, N., HEINECK, K. & CASAGRANDE, M. 2003b. Large strain behaviour of polypropylene fiber-reinforced sandy soil. *SOIL AND ROCK AMERICA-12th Panamerican Conference on Soil Mechanics and Geotechnical Engineering.*

CONSOLI, N., MONTARDO, J., DONATO, M. & PRIETTO, P. 2004. Effect of material properties on the behaviour of sand–cement–fibre composites. *Ground Improvement,* 8**,** 77-90.

CONSOLI, N., MONTARDO, J., PRIETTO, P. & PASA, G. 2002. Engineering behavior of a sand reinforced with plastic waste. *Journal of Geotechnical and Geoenvironmental Engineering,* 128**,** 462-472.

CONSOLI, N., PRIETTO, P. & ULBRICH, L. 1998. Influence of fiber and cement addition on behavior of sandy soil. *Journal of Geotechnical and Geoenvironmental Engineering,* 124**,** 1211-1214.

CONSOLI, N., VENDRUSCOLO, M., FONINI, A. & DALLA ROSA, F. 2009c. Fiber reinforcement effects on sand considering a wide cementation range. *Geotextiles and Geomembranes,* 27**,** 196-203.

COOP, M. & ATKINSON, J. 1993. The mechanics of cemented carbonate sands. *Geotechnique,* 43**,** 53-67.

DIAMBRA, A., IBRAIM, E., MUIR WOOD, D. & A, R., A. R. 2009. Fibre reinforced sands: Experiments and modelling. *Geotextiles and Geomembranes* [Online].

DIAMBRA, A., RUSSELL, A., IBRAIM, E. & WOOD, D. 2007a. Determination of fibre orientation distribution in reinforced sands. *Geotechnique,* 57.

DIAMBRA, A., RUSSELL, A., IBRAIM, E. & WOOD, D. 2007b. Determination of fibre orientation distribution in reinforced sands. *Geotechnique,* 57**,** 623-628.

DOS SANTOS, A., CONSOLI, N. & BAUDET, B. 2010a. The mechanics of fibre-reinforced sand. *Geotechnique***,** 791-799.

DOS SANTOS, A., CONSOLI, N., HEINECK, K. & COOP, M. 2010b. High-Pressure Isotropic Compression Tests on Fiber-Reinforced Cemented Sand. *Journal of Geotechnical and Geoenvironmental Engineering***,** 885-890.

GRAY, D. & ALREFEAI, T. 1986. Behaviour of fabric-reinforced versus fiber-reinforced sand. *Journal of Geotechnical Engineering-ASCE,* 112**,** 804-820.

GRAY, D. & OHASHI, H. 1983. Mechanics of fiber reinforcement in sand. *Journal of Geotechnical Engineering-ASCE,* 109**,** 335-353.

HAMIDI, A. & HAERI, S. 2008. Stiffness and Deformation Characteristics of a Cemented Gravely Sand. *International Journal of Civil Engineering,* 6.

HUANG, J. & AIREY, D. 1998. Properties of artificially cemented carbonate sand. *Journal of Geotechnical and Geoenvironmental Engineering,* 124**,** 492-499.

HUANG, W., SUN, D. & SLOAN, S. 2007. Analysis of the failure mode and softening behaviour of sands in true triaxial tests. *International Journal of Solids and Structures***,** 1423-1437.

IBRAIM, E., DIAMBRA, A., WOOD, D. & RUSSELL, A. 2010. Static liquefaction of fibre reinforced sand under monotonic loading. *Geotextiles and Geomembranes***,** 374-385.

IBRAIM, E. & FOURMONT, S. 2006. Behaviourof sand reinforced with fibres. *Soil Stress-Strain Behavior: Measurement, Modeling and Analysis, Geotechnical Symposium.* Roma.

KANIRAJ, S. & HAVANAGI, V. 2001. Behaviour of cement-stabilized fiber-reinforced fly ash-soil mixtures. *Journal of Geotechnical and Geoenvironmental Engineering,* 127**,** 574-584.

KASAMA, K., OCHIAI, H. & YASUFUKU, N. 1998. A constitutive model of cemented geomaterials based on critical state concept. *13th Southeast Asian Geotecnical Conference, 16-20 November.* Taipei, Taiwan.

LADE, P. 1989. Experimental observations of stability, instability and shear planes in granular materials. *Ingenieur Archiv,* 59**,** 114-123.

LADE, P. V. & YAMAMURO, J. A. 1996. Undrained sand behavior in axisymmetric tests at high pressures. *Journal of Geotechnical Engineering-ASCE,* 122**,** 120-129.

LADE, P. V., YAMAMURO, J. A. & BOPP, P. A. 1996. Significance of particle crushing in granular materials. *Journal of Geotechnical Engineering-ASCE,* 122**,** 309-316.

LANCELOT, L., SHAHROUR, I. & AL MAHMOUD, M. 2006. Failure and dilatancy properties of sand at relatively low stresses. *Journal of Engineering Mechanics-Asce,* 132**,** 1396-1399.

LATHA, G. & MURTHY, V. 2007. Effects of reinforcement form on the behavior of geosynthetic reinforced sand. *Geotextiles and Geomembranes,* 25**,** 23-32.

LEE, M.-J., HONG, S.-J., CHOI, Y.-M. & LEE, W. 2010. Evaluation of deformation modulus of cemented sand using CPT and DMT. *Engineering Geology,* 115**,** 28-35.

LING, H. & TATSUOKA, F. 1994. PERFORMANCE OF ANISOTROPIC GEOSYNTHETIC-REINFORCED COHESIVE SOIL MASS. *Journal of Geotechnical Engineering-ASCE,* 120**,** 1166-1184.

MAHER, M. & GRAY, D. 1990. Static response of sand reinforced with randomly distributed fibers. *Journal of Geotechnical Engineering-ASCE,* 116**,** 1661-1677.

MAHER, M. & HO, Y. 1993. Behaviour of fibre reinforced cemented sand under static and cyclic loads. *Geotechnical Testing Journal,* 16**,** 330-338.

MALANDRAKI, V. & TOLL, D. 2001. Triaxial tests on weakly bonded soil with changes in stress path. *Journal of Geotechnical and Geoenvironmental Engineering***,** 282-291.

MARRI, A. 2010. *The mechanical behaviour of cemented granular materials at high pressures.* PhD Thesis, University of Nottingham.

MARRI, A., WANATOWSKI, D. & YU, H. S. 2010. Drained Behaviour of Cemented Sand at High Pressures. *The 17th Southeast Asian Geotechnical Conference.* Taipei, Taiwan.

MESRI, G. & VARDHANABHUTI, B. 2009. Compression of granular materials. *Canadian Geotechnical journal,* 46**,** 369-392.

MICHALOWSKI, R. 2008. Limit analysis with anisotropic fibre-reinforced soil. *Geotechnique,* 58**,** 489-501.

MICHALOWSKI, R. & CERMAK, J. 2002. Strength anisotropy of fiber-reinforced sand. *Computers and Geotechnics,* 29**,** 279-299.

MICHALOWSKI, R. & CERMAK, J. 2003. Triaxial compression of sand reinforced with fibers. *Journal of Geotechnical and Geoenvironmental Engineering,* 129**,** 125-136.

MICHALOWSKI, R. & ZHAO, A. 1996. Failure of fiber-reinforced granular soils. *Journal of Geotechnical Engineering-ASCE,* 122**,** 226-234.

MOFIZ, S., TAHA, M. & SHARKER, D. 2004. Mechanical stress-strain charecteristic and model behaviour of geosynthetic reinforced soil composites. *17th ASCE Engineering Conference.*

MOONEY, M., FINNO, R. & VIGGIANI, M. 1998. A unique critical state for sand? *Journal of Geotechnical and Geoenvironmental Engineering,* 124**,** 1100-1108.

PRABAKAR, J. & SRIDHAR, R. 2002. Effect of random inclusion of sisal fibre on strength behaviour of soil. *Construction and Building Materials,* 16**,** 123-131.

ROTHENBURG, L. & KRUYT, N. 2004. Critical state and evolution of coordination number in simulated granular materials. *International Journal of Solids and Structures,* 41**,** 5763-5774.

ROTTA, G., CONSOLI, N., PRIETTO, P., COOP, M. & GRAHAM, J. 2003. Isotropic yielding in an artificially cemented soil cured under stress. *Geotechnique,* 53**,** 493-501.

SARIOSSEIRI, F. & MUHUNTHAN, B. 2009. Effect of cement treatment on geotechnical properties of some Washington State soils. *Engineering Geology,* 104**,** 119-125.

SAXENA, S. & LASTRICO, R. 1978. Static properties of lightly cemented sand. *Journal of Geotechnical Engineering,* 104 (GT12)

SCHNAID, F., PRIETTO, P. & CONSOLI, N. 2001. Characterization of cemented sand in triaxial compression. *Journal of Geotechnical and Geoenvironmental Engineering,* 127**,** 857-868.

SHARMA, S. & FAHEY, M. 2004. Deformation characteristics of two cemented calcareous soils. *Canadian Geotechnical Journal,* 41**,** 1139-1151.

SHENG, D., YAO, Y. & CARTER, J. 2008. A volume-stress model for sands under isotropic and critical stress states. *Canadian Geotechnical Journal,* 45.

SMITH, G. 1990. *Elements of soil mechanics*, BSP professional Books.

SUZUKI, K. & YAMADA, T. 2006. Double Strain Softening and Diagonally Crossing Shear Bands of Sand in Drained Triaxial Tests. *International Journal of Geomachanics,* 6.

SWAMI, S. 2005. *Reinforced soil and its engineering applications,* New Delhi, India, I.K International Pvt. Ltd.

TANG, C., SHI, B., CHEN, F. & Y, A. C. 2007. STrength and mechanical behaviour of short polypropylene fibre reinforced and cement stabilized clayey soil. *Geotextile and Geomembranes,* 25**,** 194-202.

VERMEER, P. & DE BORST, R. 1984. Non-associated plasticity for soils, concrete and rock. *Heron,* 29**,** 1-64.

VIDAL, H. 1969. The principle of reinforced earth. *Highway Research Record, Highway Research Board,* 282**,** pp 1-16.

WANG, Y. H. and LEUNG, S. C. (2008). A particulate-scale investigation of cemented sand behaviour, Canadian Geotechnical Journal, 45(1), 29-44.

WOOD, D. 1990. *Soil behaviour and critical state soil mechanics*, Cambridge university Press.

YAMAMURO, J. A. & LADE, P. V. 1996. Drained sand behavior in axisymmetric tests at high pressures. *Journal of Geotechnical Engineering-ASCE,* 122**,** 109-119.

YU, H. S., TAN, S. M. & SCHNAID, F. 2007. A critical state framework for modelling bonded geomaterials. *Geomechanics and Geoengineering,* 2**,** 61-74.